UTS UNIVERSITY OF TECHNOLOGY SYDNEY

Optimal planning and operational strategy for biogas power generation system design in wastewater plant

by Derick Rudson Goncalves de Lima - 13699638

Thesis submitted in fulfilment of the requirements
for the degree of

Doctor of Philosophy

under the supervision of
A/Prof. Li Li
Prof. Jahangir Hossain
A/Prof Jiangfeng Zhang

University of Technology Sydney
Faculty of Engineering and IT

September 2025

Certificate of Original Authorship

I, Derick Rudson Goncalves de Lima, declare that this thesis is submitted in fulfilment of the requirements for the award of Doctor of Philosophy, in the School of Electrical and Data Engineering at the University of Technology Sydney.

This thesis is wholly my own work unless otherwise referenced or acknowledged. In addition, I certify that all information sources and literature used are indicated in the thesis.

This document has not been submitted for qualifications at any other academic institution.

This research was supported by an Australian Government Research Training Program (RTP) Scholarship doi.org/10.82133/C42F-K220.

Signature: 

Date: September 30, 2025

Abstract

Municipal wastewater treatment plants (WWTPs) are energy-intensive facilities with high operational costs, often heavily dependent on electricity supplied by the main grid. In response to the global shift towards sustainable development, there has been a growing focus on integrating renewable energy recovery technologies into WWTPs as environmentally friendly strategies aimed at enhancing energy efficiency, improving sustainability, and reducing operating costs.

Renewable energy technologies offer multiple benefits, including reductions in both carbon footprint and dependence on grid-supplied electricity, while also supporting WWTPs in meeting their sustainability targets. By adopting renewable energy sources, WWTPs can significantly reduce overall energy demand, achieve energy self-sufficiency and, in some cases, even become net energy producers. Among the available renewable energy technologies, anaerobic digestion is one of the most widely adopted due to its effectiveness in treating sewage sludge and its capacity to generate biogas. The use of biogas produced can offset a significant portion of a plant's energy needs, contributing to the reductions in operating costs and dependence on electricity supply from the main grid.

To effectively maximise the potential of renewable energy in WWTPs, particularly through anaerobic digestion and biogas utilisation, there is a need to explore new strategies, including operating and planning optimisation. This can include the development of both short-term operational strategies and long-term energy system planning, incorporating various types of renewable technologies to ensure energy reliability, economic efficiency, and minimal reliance on the main grid. In this context, this thesis presents three integrated models designed to address these challenges: (i) a biogas forecast model, (ii) an operation model, and (iii) a planning model. The biogas model aims to estimate the biogas production from sewage sludge, taking into consideration the semi-continuous sludge feeding process of the anaerobic digester, and its outputs serve as inputs for both operation and planning models. The operation model aims to minimise the energy operating costs for the WWTP under two scenarios: (a) utilisation of current power generation assets, and (b) implementation of a microgrid system. Finally, the planning model determines the optimal configuration of the power generation system, supporting long-term infrastructure decisions for the WWTP.

Acknowledgements

This project is part of the RACE for 2030 Industry PhD Program (Project Number: 21.B5.P.0217), funded by the RACE for 2030 CRC, Sydney Water Corporation, and the University of Technology Sydney. I would like to acknowledge them for their technical and financial support.

Firstly, thanks to God for everything and for giving me strength and guidance in times of difficulties.

I would like to express my immense and sincere gratitude to my primary supervisor, Professor Li Li, and my co-supervisors, Professor Jiangfeng Zhang and Professor Jahangir Hossain, for their unlimited support and extraordinary guidance. I cannot translate into words how blessed I feel to have been supervised by them during my Ph.D. journey. Thanks to them for providing valuable feedback, reviewing my progress constantly, being easily accessible at all times, providing numerous challenges to make me grow as a researcher, and also for always being like friends, willing to listen to any concerns about research or personal life, and motivating me to boost mental and physical health.

Special thanks to Gregory Appleby, who has been involved in this project since the beginning, sharing technical expertise and valuable industry insights on the subject.

I would like to thank the team at Sydney Water Corporation, including Brendan Galway, Michael Young, Glenda Stowell, Manav Kaur, and the broader team, for their support in providing access to historical data and technical information. I also would like to thank the RACE for 2030 CRC team for their support, guidance throughout my studies, and the opportunity to participate in workshops and events. I must thank the Industry Reference Group which supported me during my studies, sharing industry knowledge and expertise. A special thanks to Robert May and Jason West from SA Water, and Lauren Randall from Hunter Water.

To all my PhD friends, including Amin who really helped me at the beginning, but also Moj, Ali, Sahand, Dilip, Forrest, Jiwei, Saheb, Tony, Ahmed and all others. They warmly and patiently accompanied me in discussing and solving the problems encountered in the study.

Lastly, but most importantly, I would like to thank my family. Thanks to my mother Dolores, father Rud, brother Diego and sister Rayanne for their unconditional support throughout this Ph.D. journey and my entire life. Finally, I would like to dedicate a special thank you to my friend and ex-wife, Fernanda. Without her, I would not have even considered pursuing a PhD. She was the inspiration behind the start of this journey and offered incredible support throughout for many years.

And a big thank you to my grandma Isabel, who always dreamed of me becoming a medical doctor, but in the end, I became a doctor in electrical engineering instead.

List of Publications

Journal:

1. D. Lima, G. Appleby, and L. Li, "A scoping review of options for increasing biogas production from sewage sludge: Challenges and opportunities for enhancing energy self-sufficiency in wastewater treatment plants," Energies, vol. 16, no. 5, p. 2369, 2023, issn: 1996-1073
2. D. Lima, L. Li, and G. Appleby, "A review of renewable energy technologies in municipal wastewater treatment plants (WWTPs)", Energies, vol. 17, no. 23, p. 6084, 2024, issn: 1996-1073
3. D. Lima, L. Li, and G. Appleby, "Biogas production modelling based on a semi-continuous feeding operation in a municipal wastewater treatment plant", Energies, vol. 18, no. 5, p. 1065, 2025

Conference:

1. D. Lima, L. Li, and J. Zhang, "Minimizing electricity costs using biogas generated from food waste," in 2021 31st Australasian Universities Power Engineering Conference (AUPEC), IEEE, 2021, pp. 1–6

Journal (To Submit)

1. D. Lima, L. Li, and J. Zhang, "Minimising operation costs in a wastewater treatment plant (WWTP) – Part 1: Traditional power generation assets".
2. D. Lima, L. Li, and J. Zhang, "Minimising operation costs in a wastewater treatment plant (WWTP) – Part 2: Microgrid system".
3. D. Lima, L. Li, and J. Zhang, "Optimal planning and operation of a microgrid-based power system in a WWTP".

Contents

List of Publications **iv**

1 Introduction **2**
1.1 Background . . . 2
1.2 Research Aims and Objectives . . . 3
1.3 Research Questions . . . 4
1.4 Significance and Contributions . . . 4
1.5 Research Methodology . . . 5
1.6 Thesis Organisation . . . 6

2 Literature Review **8**
2.1 Introduction . . . 8
2.1.1 WWTP Overview . . . 10
2.1.2 Sewage Sludge . . . 11
2.2 Energy Resources in WWTPs . . . 11
2.2.1 Site-Specific Sources . . . 11
2.2.2 Non-Site-Specific Sources . . . 33
2.2.3 Challenges and Opportunities . . . 36
2.3 Research Gaps . . . 37
2.4 Summary . . . 37

3 Biogas Model **39**
3.1 Introduction . . . 39
3.2 Background . . . 39
3.3 Related Works . . . 40
3.4 Model Framework and Design . . . 42
3.4.1 FIFO Methodology . . . 42
3.4.2 Semi-Continuous Operation . . . 42
3.4.3 Model Formulation . . . 44
3.5 Model Validation . . . 46
3.5.1 Data Inputs . . . 46
3.5.2 Simulation Results . . . 47
3.5.3 Batch and Semi-Continuous Operation Modes . . . 51
3.5.4 Biogas Model Limitations . . . 54
3.6 Summary . . . 54

4 Operation Model: Current Assets **56**
4.1 Introduction . . . 56
4.2 Background . . . 56
4.3 Model Framework and Design . . . 58

4.3.1 Biogas Components . . . 60
4.3.2 Current Power Generation Assets . . . 61
4.4 Simulation Results . . . 63
4.4.1 Inputs and Assumptions . . . 63
4.4.2 Case Studies . . . 65
4.5 Summary . . . 81

5 Operation Model: Microgrid 83
5.1 Introduction . . . 83
5.2 Background . . . 83
5.3 Model Framework and Design . . . 85
5.3.1 Microgrid Configuration . . . 85
5.4 Simulation Results . . . 87
5.4.1 Inputs and Assumptions . . . 87
5.4.2 Case Studies . . . 88
5.5 Summary . . . 104

6 Optimal Planning and Operation 106
6.1 Introduction . . . 106
6.2 Background . . . 106
6.3 Microgrid Planning . . . 107
6.4 Model Framework and Design . . . 108
6.4.1 Biogas Components . . . 109
6.4.2 Microgrid Components . . . 109
6.5 Simulation Results . . . 112
6.5.1 Inputs and Assumptions . . . 112
6.5.2 Case Studies . . . 113
6.5.3 Discussions . . . 125
6.5.4 Sensitivity Analysis . . . 126
6.6 Summary . . . 133

7 Conclusion 135
7.1 Summary of Outcomes . . . 135
7.2 Recommendations and Future Work . . . 137

List of Figures

Figure 2.1 - WWTP diagram (sludge, primary and secondary wastewater treatments) 10
Figure 2.2 - Site-specific sources of renewable energy in a WWTP. 11
Figure 2.3 - Thermochemical processes applied to sewage sludge for energy recovery. . 18

Figure 3.1 - FIFO methodology representing a semi-continuous feeding mode of sewage sludge flow into an anaerobic digester 42
Figure 3.2 - Retention time changing behaviour 43
Figure 3.3 - Sewage sludge flow fed into the anaerobic digester 47
Figure 3.4 - Biogas production in 2020 (historical data vs. proposed model) 48
Figure 3.5 - Biogas production in 2021 (historical data vs. proposed model) 48
Figure 3.6 - Biogas production in 2022 (historical data vs. proposed model) 49
Figure 3.7 - Retention time and sewage sludge flow in 2020 52
Figure 3.8 - Retention time and sewage sludge flow in 2021 52
Figure 3.9 - Retention time and sewage sludge flow in 2022 53
Figure 3.10 - Retention time and sewage sludge flow from 2020 to 2022 53

Figure 4.1 - System configuration (Current Power Generation Assets) 58
Figure 4.2 - Biogas and natural gas components (Current WWTP configuration) . . . 59
Figure 4.3 - Biogas generation per day (in m^3) and sewage sludge volume that feeds the anaerobic digester per day (in m^3) 64
Figure 4.4 - Electricity consumption of the WWTP 64
Figure 4.5 - Breakdown of electricity components - Base Case (Current generation assets) 68
Figure 4.6 - Biogas production and utilisation - Base Case (Current generation assets) 68
Figure 4.7 - Biogas, biomethane and natural gas components (Case 1 - Operation model) 69
Figure 4.8 - Breakdown of electricity components - Case 1 (Current generation assets) 73
Figure 4.9 - Biogas production and utilisation - Case 1 (Current generation assets) . . 73
Figure 4.10 - Breakdown of electricity components - Case 2 (Current generation assets) 77
Figure 4.11 - Biogas production and utilisation - Case 2 (Current generation assets . . 77
Figure 4.12 - Breakdown of electricity components - Case 3 (Current generation assets) 80
Figure 4.13 - Biogas production and utilisation - Case 3 (Current generation assets . . 80

Figure 5.1 - WWTP system configuration (Microgrid - Operation model) 85
Figure 5.2 - Forecasted and actual gas prices in NSW, Australia, from 2020 to 2022 . 88
Figure 5.3 - Effluent flow from a large-scale WWTP in 2021 88

Figure 6.1 - WWTP system configuration (Planning model) 108
Figure 6.2 - Microgrid configuration (Case 2 - Planning model) 115
Figure 6.3 - Biogas, biomethane and natural gas components (Case 2 - Planning model) 116
Figure 6.4 - Microgrid configuration (Case 3 - Planning model) 120

Figure 6.5 - Biogas, biomethane, hydrogen and natural gas components (Case 3 - Planning model) . . . 121
Figure 6.6 - Microgrid capacity for different unit costs and weighting factors (Case 1 scenarios) . . . 130
Figure 6.7 - CAPEX and 1-year OPEX for different unit costs and weighting factors (Case 1 scenarios) . . . 131
Figure 6.8 - Microgrid capacity for different unit costs and weighting factors (Case 3 scenarios) . . . 132
Figure 6.9 - CAPEX and 1-year OPEX for different unit costs and weighting factors (Case 3 scenarios) . . . 133

List of Tables

Table 2.1 - Co-digestion of sewage sludge with different feedstocks 14
Table 2.2 - Pre-treatment methods applied on sewage sludge 15
Table 2.3 - Biogas upgrading technologies' characteristics 17
Table 2.4 - Studies focused on sewage sludge gasification 19
Table 2.5 - Types of pyrolysis and their characteristics 21
Table 2.6 - Studies focused on sewage sludge pyrolysis 21
Table 2.7 - Characteristics of HTC, HTL and HTG 23
Table 2.8 - Studies that applied hydrothermal treatments using sewage sludge 23
Table 2.9 - Studies related to supercritical water gasification on sewage sludge 26
Table 2.10 - Studies on biodiesel production from sewage sludge 27
Table 2.11 - Studies on MEC technology applied to municipal wastewater 28
Table 2.12 - Studies related to MFC technology using municipal or domestic wastewater 29
Table 2.13 - Hydropower plants installed in WWTPs 30
Table 2.14 - Studies on hydropower technologies applied in WWTPs 31
Table 2.15 - Studies exploring the electrolysis technology utilisation in WWTPs . . . 33
Table 2.16 - Solar, wind and hybrid system generation in WWTPs 34
Table 2.17 - Large-scale renewable energy projects in WWTPs 35
Table 2.18 - Renewable energy projects in WWTPs in Australia 36

Table 3.1 - Average biogas production (historical data vs. proposed model) 50
Table 3.2 - Performance metrics to assess the proposed biogas model 51

Table 4.1 - Historical data components of the WWTP 65
Table 4.2 - Electricity and network prices 65
Table 4.3 - Result summary for 1-year and 3-year optimisation horizons - Base case (Current generation assets) 66
Table 4.4 - Result summary for 1-month optimisation horizon - Base case (Current generation assets) 67
Table 4.5 - Result summary for 1-year and 3-year optimisation horizons - Case 1 (Current generation assets) 71
Table 4.6 - Result summary for 1-month optimisation horizon - Case 1 (Current generation assets) 71
Table 4.7 - Result summary for 1-year and 3-year optimisation horizons - Case 2 (Current generation assets) 74
Table 4.8 - Result summary for 1-month optimisation horizon - Case 2 (Current generation assets) 75
Table 4.9 - Result summary for 1-year and 3-year optimisation horizons - Case 3 (Current generation assets) 78
Table 4.10 - Result summary for 1-month optimisation horizon - Case 3 (Current generation assets) 78

Table 5.1 - Result summary for 1-year and 3-year optimisation horizons - Case 1 (Microgrid system) . . . 90
Table 5.2 - Result summary for 1-month optimisation horizon - Case 1 (Microgrid system) . . . 91
Table 5.3 - Result summary for 1-year and 3-year optimisation horizons - Case 1a (Microgrid system) . . . 93
Table 5.4 - Result summary for 1-month optimisation horizon - Case 1a (Microgrid system) . . . 94
Table 5.5 - Result summary for 1-year and 3-year optimisation horizons - Case 2 (Microgrid system) . . . 96
Table 5.6 - Result summary for 1-month optimisation horizon - Case 2 (Microgrid system) . . . 97
Table 5.7 - Result summary for 1-year and 3-year optimisation horizons - Case 3 (Microgrid system) . . . 100
Table 5.8 - Result summary for 1-month optimisation horizon - Case 3 (Microgrid system) . . . 101
Table 5.9 - Result summary for 1-year and 3-year optimisation horizons - Case 4 (Microgrid system) . . . 103
Table 5.10 - Result summary for 1-month optimisation horizon - Case 4 (Microgrid system) . . . 103

Table 6.1 - Unit costs for different technologies . . . 113
Table 6.2 - Proposed microgrid configuration - Case 1 (Planning model) . . . 114
Table 6.3 - Result summary for 1-year operation - Case 1 (Planning model) . . . 114
Table 6.4 - Proposed microgrid configuration - Case 2 (Planning model) . . . 119
Table 6.5 - Result summary for 1-year operation - Case 2 (Planning model) . . . 119
Table 6.6 - Proposed microgrid configuration - Case 3 (Planning model) . . . 124
Table 6.7 - Result summary for 1-year operation - Case 3 (Planning model) . . . 124
Table 6.8 - Unit cost ranges for different technologies . . . 127
Table 6.9 - Microgrid configuration - Case 1 scenarios (1a-1d) . . . 127
Table 6.10 - CAPEX, 1-year OPEX and payback period - Case 1 scenarios (1a-1d) . . . 127
Table 6.11 - Unit costs of each tecnology - Case 3 scenarios (3a-3d) . . . 128
Table 6.12 - Microgrid configuration - Case 3 scenarios (3a-3d) . . . 128
Table 6.13 - CAPEX, 1-year OPEX and payback period - Case 3 scenarios (3a-3d) . . . 128
Table 6.14 - Case 1 scenarios (1-1d) - Different weighting factors . . . 129
Table 6.15 - CAPEX, 1-year OPEX and payback period (Scenarios 1–1d and Sub-scenarios i-iv) . . . 130
Table 6.16 - Case 3 scenarios (3-3d) - Different weighting factors . . . 131
Table 6.17 - CAPEX, 1-year OPEX and payback period (Scenarios 3–3d and Sub-scenarios i-iv) . . . 132

Nomenclature

Biogas model

ϵ_{biogas} biogas production estimation error between model predictions and historical data

b_{ad} acidogen endogenous respiration rate

$c_{m_{ad}}$ average methane concentration in the biogas

E_{ch4} fraction of biodegradable COD removed and converted to methane

E_s biodegradable COD fraction removed and converted to sludge

$f_{ss_{rem}}$ sludge fraction removed from the sedimentation tank

$f_{ss_{unb,raw}}$ raw wastewater unbiodegradable fraction

$f_{ss_{unb,set}}$ settled wastewater unbiodegradable fraction

$f_{ss_{unb}}$ sewage sludge unbiodegradable fraction

$i_{b_{new}}$ least index parcel of sewage sludge

i_b index of the bottom parcel of sewage sludge

K_m michaelis dissociation constant

K_s substrate dissociation constant

n retention time

P_{ad} pressure inside the anaerobic digester

$P_{ad}^{\max}$ maximum pressure inside the anaerobic digester

$P_{ad}^{\min}$ minimum pressure inside the anaerobic digester

P_{amb} ambient pressure

Q_m final methane production volume

r_h volumetric hydrolysis/acidogenesis rate

S_{bpi} influent biodegradable particulate

S_{bp} residual biodegradable organic concentration

S_{bsai} influent volatile fatty acid concentration

S_m methane production concetration

S_{te} total effluent concentration

S_{ti} total influent concentration

t time

T_{ad} temperature inside the anaerobic digester

$T_{ad}^{\max}$ maximum temperature inside the anaerobic digester

$T_{ad}^{\min}$ minimum temperature inside the anaerobic digester

T_{amb} ambient temperature

$V_{ad}^{\max}$ maximum volume of the anaerobic digester

$V_{biogas_{ad}}$ volume of biogas inside the anaerobic digester

$V_{biogas_{ad}}^{\max}$ maximum volume of biogas inside the anaerobic digester

$V_{biogas_{ad}}^{\min}$ minimum volume of biogas inside the anaerobic digester

$V_{biogas_{amb}}$ volume of biogas at ambient temperature

$V_{biogas_{hist,ave}}$ average biogas production from historical data

$V_{biogas_{model,ave}}$ average biogas production from the proposed biogas model

$V_{m_{ad}}$ total volume of methane generated

$V_{ss_{ad}}$ sewage sludge inside the anaerobic digester

$V_{ss_{in}}$ volume of sewage sludge that enters the digester

$V_{ss_{out}}$ volume of sewage sludge that leaves the digester

Y_{ad} pseudo acidogen yield coefficient

Z_{ad} acidogen biomass concentration

Operation model

Δt time interval

η_{ch} battery charging efficiency

η_{dis} battery discharging efficiency

$\eta_{e_{chp}}$ electrical efficiency of the CHP system

$\eta_{th_{boiler}}$ thermal efficiency of the boiler

$\eta_{th_{chp}}$ thermal efficiency of the CHP system

η_{turb} turbine efficiency

λ_{dlf} distribution loss factor for the load

c_{bil} electricity price from bilateral contracts

$c_{ch4_{biogas}}$ methane concentration in the raw biogas

$c_{ch4_{biomet}}$ methane concentration in the biomethane

$c_{ele_{cap}}$ electricity price associated with network capacity charges

$c_{ele_{exp}}$ price for exporting electricity to the grid

$c_{ele_{imp}}$ price for importing electricity from the grid

$c_{ele_{other}}$ electricity price associated other charges

$c_{ele_{use}}$ electricity price related to network usages

c_{fog} cost associated with collecting and transporting FOG to the WWTP

$c_{gas_{exp}}$ price for exporting biomethane the grid

$c_{gas_{imp}}$ price for importing natural gas from the gas grid

$c_{gas_{market}}$ gas market price for the biomethane injected into the gas network

$c_{gas_{use}}$ price related to gas network usages

$c_{p_{biogas}}$ biogas calorific power

$c_{p_{gas}}$ natural gas calorific power

c_{spot} electricity spot market price

$c_{ts_{ss}}$ total solids concentration in the sludge

d_{ss} sewage sludge density

$E_{b_{ini}}$ initial state of energy level for the battery storage system

E_b energy stored in the battery storage system

$E_b^{\max}$ maximum energy level of the battery system

$E_b^{\min}$ minimum energy level of the battery system

g gravitational acceleration

H net head

h_{ds} specific heat capacity of digested sludge

h_{ss} specific heat capacity of sludge

h_w specific heat capacity or water

k_{jw} conversion factor from MJ to kWh

k_{up} conversion factor from raw biogas to biomethane

m_{ss} sludge mass flow into the digester

n_d number of days of the optimisation horizon

$P_{b_{ch}}$ battery charging power

$P_{b_{dis}}$ battery discharging power

P_{bil} power purchased from bilateral contracts

$P_{bil}^{\max}$ maximum power purchased from bilateral contracts

P_{chp} electrical power generated from the CHP system

$P_{chp}^{\max}$ maximum electrical power generated from the CHP system

P_{grid} power imported from the main grid

$P_{grid}^{\max}$ maximum power imported from the main grid

P_{hyd} power generated for the hydro turbine system

$P_{hyd}^{\max}$ maximum power generation of the micro-hydro system

P_{pv} Power generation from the PV system

P_{sold} power exported to the main grid

$P_{sold}^{\max}$ maximum power exported to the main grid

P_{spot} power purchased from electricity spot market

$P_{spot}^{\max}$ maximum power purchased from electricity spot market

P_{up} power used in the biogas upgrading system

$P_{up}^{\max}$ maximum power consumed by the biogas upgrading system

$P_{wwtp_{cap}}$ demand capacity of the WWTP

P_{wwtp} power consumption from the WWTP

p_w water density

$Q_{ad_{loss}}$ thermal losses power in the anaerobic digesters

Q_{ad} total thermal power required from the anaerobic digester system

Q_{boiler} thermal power generated from the boilers

$Q_{boiler}^{\max}$ maximum thermal power generated from the boilers

Q_{chp} thermal power generated from the CHP system

$Q_{chp}^{\max}$ maximum thermal power generated from the CHP system

Q_{ss} total thermal power required to heat sewage sludge

$r_{b_{ch}}$ maximum discharging rates for the battery system

$r_{b_{dis}}$ maximum charging rates for the battery system,

$r_{biogas_{ch}}$ maximum charging rate for the biogas operation

$r_{biogas_{dis}}$ maximum discharging rate for the biogas operation

r_{up} power rate of the biogas upgrading system

T_1 sludge temperatures in the sedimentation tank

$T_{ad_{ss}}$ sludge temperature in the anaerobic digester

u_{ad} binary variable to control the charging or discharging of biogas

u_b binary variable to control if the battery system is charging or discharging

u_{gas} binary variable to control whether natural gas is imported or not from the network

u_{grid} binary variable to control whether grid is supplying power for the WWTP or not

$V_{biogas_{ad_{ini}}}$ initial state of volume of biogas in the anaerobic digester

$V_{biogas_{boiler}}$ total volume of biogas used in the boilers

$V_{biogas_{boiler}}^{\max}$ maximum volume of biogas can be used in the boilers

$V_{biogas_{chp}}$ total volume of biogas used in the CHP system

$V_{biogas_{chp}}^{\max}$ maximum volume of biogas can be used in the CHP system

$V_{biogas_{ch}}$ volume of biogas stored in the anaerobic digester

$V_{biogas_{dis-boiler}}$ portion of biogas discharged and used in the boilers

$V_{biogas_{dis-chp}}$ portion of biogas discharged and used in the CHP system

$V_{biogas_{dis-flare}}$ portion of biogas discharged which is flared

$V_{biogas_{dis-up}}$ portion of biogas discharged and used in the upgrading system

$V_{biogas_{dis}}$ volume of biogas discharged from the anaerobic digester

$V_{biogas_{flare}}$ total volume of biogas flared

$V^{\max}_{biogas_{flare}}$ maximum volume of biogas can be flared

$V_{biogas_{gen-boiler}}$ portion of biogas generated used in the boilers

$V_{biogas_{gen-chp}}$ portion of biogas generated used in the CHP system

$V_{biogas_{gen-flare}}$ portion of biogas generated which is flared

$V_{biogas_{gen-up}}$ portion of biogas generated used in the upgrading system

$V_{biogas_{gen}}$ total volume of biogas generated

$V^{\max}_{biogas_{gen}}$ maximum volume of biogas generated

$V_{biogas_{up}}$ total volume of biogas used in the upgrading system

$V^{\max}_{biogas_{up}}$ maximum volume of biogas can be used in the upgrading system

V_{biomet} total volume of biomethane converted

V_{ef} effluent volumetric flow rate

V_{fog} volume of FOG collected and transported to the WWTP

$V_{gas_{grid}}$ volume of natural gas imported from the gas grid

$V^{\max}_{gas_{grid}}$ maximum volume of natural gas can be imported from the gas grid

$V^{\max}_{gas_{inj}}$ upper limit for gas injection into the gas network

Planning model

$\eta_{e_{fc}}$ electrical efficiency of the fuel cell system

$\eta_{th_{dryer}}$ thermal efficiency of the drying system

$\eta_{th_{fc}}$ thermal efficiency of the fuel cell system

a_1 weighting factor applied to the investment cost function

a_2 weighting factor applied to the total operating cost function

a_3 weighting factor applied to the payback period function

$c_{b_{unit}}$ cost of a battery system unit

$c_{boiler_{unit}}$ cost for boilers unit

$c_{chp_{unit}}$ cost of a CHP system unit

$c_{dryer_{unit}}$ cost of a drying system unit

$c_{fc_{unit}}$ cost of a fuel cell system unit

$c_{gasi_{unit}}$ cost of a gasification system unit

$c_{hyd_{unit}}$ cost for a micro-hydro system unit

$C_{op_{hd}}$ operating costs based on the current historical data when no microgrid is adopted

$c_{p_{biomet}}$ biomethane calorific power

$c_{p_{h2}}$ hydrogen calorific power

$c_{p_{syn}}$ syngas calorific power

$c_{pv_{unit}}$ cost for a PV system unit

$c_{ss_{disp}}$ price related to sewage sludge disposal

$c_{storage_{unit}}$ cost of the biogas storage system unit

$c_{up_{unit}}$ cost of a biogas upgrading system unit

$c_{we_{unit}}$ cost of a water electrolyser system unit

$E^{\max}_{b_{unit}}$ maximum energy levels of a battery system unit

$E^{\min}_{b_{unit}}$ minimum energy levels of a battery system unit

f_{inv} investment cost function

f_{mo} multi-objective cost function

$f_{op_{1y}}$ 1-year operating cost function

f_{op} total operating cost

f_{pb} payback period function

h_{vap} water latent heat of vaporization

$k_{dew_{dry}}$ conversion factor from sludge into syngas

$k_{dss_{dew}}$ conversion factor from digested sludge to dewatered sludge

$k_{h2o_{h2}}$ conversion factor fom water to hydrogen

$k_{ss_{syn}}$ conversion factor from digested sludge to dewatered sludge

N number of years in the microgrid's operational lifetime

n_{boiler} number of boiler units

n_b number of BESS units

n_{chp} number of CHP system units

n_{dryer} number of dryer units

n_{fc} number of fuel cell units

n_{gasi} number of gasification system units

n_{hyd} number of micro-hydro units

n_{pv} number of PV system units

$n_{storage}$ number of biogas storage units

n_{up} number of biogas upgrading system units

n_{we} number of water electrolysis units

$P^{\max}_{chp,unit}$ maximum electrical power generated from a CHP system unit

P_{dew} power consumption required to dewater digested sewage sludge

$P^{\max}_{fc_{unit}}$ maximum electrical power generated from the unit fuel cell system

P_{fc} electrical power generated from the fuel cell system

$P^{\max}_{gasi_{unit}}$ maximum power consumption from the gasification system

P_{gasi} power consumption from the gasification system

$P^{\max}_{hyd_{unit}}$ maximum power generation of the micro-hydro system unit

$P^{\max}_{pv_{unit}}$ maximum power generation of the PV system unit

$P^{\max}_{up_{unit}}$ maximum power used in a unit of biogas upgrading system

$P^{\max}_{we_{unit}}$ maximum power consumption from the unit water electrolysis system

P_{we} power consumption from the water electrolysis system

$Q^{\max}_{boiler,unit}$ maximum thermal power generated from a boiler unit

$Q^{\max}_{chp,unit}$ maximum thermal power generated from a CHP system unit

$Q^{\max}_{dryer_{unit}}$ maximum thermal power required for the drying system unit

Q_{dryer} thermal power required in the drying system

$Q^{\max}_{fc_{unit}}$ maximum thermal power generated from the unit fuel cell system

Q_{fc} thermal power generated from the fuel cell system

$Q_{ss_{dry}}$ total thermal power required for drying dewatered sewage sludge

r discount rate

$r_{b_{ch,unit}}$ discharging rating for the battery system unit

$r_{b_{dis,unit}}$ charging rating for the battery system unit

$r_{biogas_{ch,unit}}$ maximum charging rate for a single biogas unit in the anaerobic digestion system

$r_{biogas_{dis,unit}}$ maximum discharging rate for a single biogas unit in the anaerobic digestion system

$r_{dss_{dew}}$ power consumption rate for the sludge dewatering process

r_{gasi} gasifier electrical consumption rate

r_{we} power consumption rate of the whole electrolyser system

$s_{ad_{min}}$ lower bound scaling factor for biogas storage in the anaerobic digester

T_{ev} temperature of the water evaporation

$V^{\max}_{ad_{unit}}$ maximum limit for a single biogas storage unit

$V_{biogas_{dis-dryer}}$ portion of biogas discharged and used in the drying system

$V_{biogas_{dryer}}$ total volume of biogas used in the drying system

$V_{biogas_{gen-dryer}}$ portion of biogas generated used in the drying system

$V_{biomet_{fc}}$ volume of biomethane used in the fuel cell system

$V_{biomet_{sold}}$ volume of biomethane sold to the gas grid

$V^{\max}_{boiler_{unit}}$ maximum volume of gas can used in a unit of boiler

$V^{\max}_{chp_{unit}}$ maximum volume of biogas can be used in a unit of CHP system

$V^{\max}_{dryer_{unit}}$ maximum volume of gas used in the drying system unit

$V_{dss_{dew}}$ total volume of dewatered sludge

$V_{gas_{boiler}}$ volume of natural gas used in the boilers

$V_{gas_{dryer}}$ volume of natural gas used in the drying system

$V_{h2_{boiler}}$ volume of hydrogen used in the boilers

$V_{h2_{chp}}$ volume of hydrogen used in the CHP system

$V_{h2_{dryer}}$ volume of hydrogen used in the dyring system

$V_{h2_{fc}}$ volume of hydrogen used in the fuel cell system

$V_{h2_{sold}}$ volume of hydrogen sold to the gas grid

$V_{h2_{unit}}^{\max}$ upper limit of the water electrolysis system unit

V_{h2o} volume of water used in the water electrolysers

V_{h2} total volume of hydrogen generated

$V_{ss_{dry}}$ total volume of dried sludge

$V_{syn_{boiler}}$ portion of syngas used in the boilers

$V_{syn_{chp}}$ portion of syngas used in the CHP system

$V_{syn_{dryer}}$ portion of syngas used in the drying system

V_{syn} total volume of syngas generated

$V_{up_{unit}}^{\max}$ maximum volume of biogas can be used in a unit of biogas upgrading system

x_{h2} upper limit for blending hydrogen and biomethane for grid injection

List of Abbreviation

AD	Anaerobic digester
ADM1	Anaerobic digestion Model No. 1
ASM	Activated sludge model
ATW	Advanced treated water
b	Batch mode
BDM	Bligh and dyer method
BESS	Battery energy storage system
BMP	Biomethane potential
BOD	Biological oxygen demand
CaSA	Cathode surface area
CAPEX	Capital expenditure
CA	Chemical absorption
Cb	Corncob
CGE	Cold gas efficiency
CHP	Combined heat and power
C/N	Carbon-to-nitrogen ratio
COD	Chemical oxygem demand
CS	Cryogenic separation
CSBR	Conical spouted bed reactor
CST	Concentrating solar thermal
db	Dry weight basis
DERs	Distributed energy resources
Dlm	Dolomite
DS	Dry solids
DSS	Digested sewage sludge
EMWD	Eastern municipal water district
EqR	Equivalence ratio
ER	Energy recovery
ERqd	Energy required
FA	Free ammonia
FAME	Fatty acid methyl esters
FBR	Fluidised-bed reactor
FC	Fuel cell
FIFO	First-in, first-out
FIT	Feed-in tariff
FOG	Fat, oil, grease
FW	Food waste
fxc	Fixed Carbon
G	Glycerol
GT	Gas turbine
GTW	Grease trap waste
GW	Gigawatt
GWh	Gigawatt hour
HHV	Higher heating value
HRT	Hydraulic retention times
HSW	High-strength waste
HTC	Hydrothermal carbonisation
HTG	Hydrothermal gasification
HTL	Hydrothermal liquefaction
ICE	Internal combustion engine
IWA	International water association
JRDWRF	James R. Dilorio water reclamation facility
kW	Kilowatt
kWh	Kilowatt-hour
LCOE	Levelised cost of electricity
LCOH	Levelised cost of heating
LHV	Lower heating Value
LTCFB	Low temperature circulating fluidised bed
MAE	Mean absolute error
MC	Moisture
Ma	Microalgae
M	Microwave

MG	Microgrid
MGD	Mega gallons per day
MH	Micro-hydropower
MEC	Microbial electrolysis cell
MFC	Microbial fuel cell
MG	Microgrid
MJ	Megajoule
ML	Megalitre
mL	mililitre
MS	Membrane separation
MSE	Mean squared error
MW	Megawatt
MWh	Megawatt-hour
NI	Not informed
NPV	Net present value
O&M	Operation and maintenance cost
OPEX	Operating expenditure
OFMSW	Organic fraction of municipal solid waste
OLR	Organic loading rate
OM	Organic matter
OMP	Organic micropollutant
OPS	Organic physical scrubber
OT	Operation time
Oz	Ozonation
P	Pyrolysis
pb	Payback period
PEf	Primary effluent
PL	Point Loma
PM	Pig manure
PMS	Paper-mill sludge
PoM	Poultry manure
PSA	Pressure swing adsorption
PSS	Primary sludge
PV	Photovoltaic
QLD	Queensland
RES	Renewable energy source
RMSE	Root mean squared error
R^2	R-squared
RR	Recovery rate
RWW	Raw wastewater
SA	South Australia
SBBGR	Sequencing batch biofilter granular reactor
SCWG	Supercritical water gasification
SCWO	Supercritical water oxidation
SD	Sawdust
SEC	Specific energy consumption
SM	Swine manure
SMER	Specific moisture extraction rate
sp	Straw pellets
SOFC	Solid Oxide fuel cell
SS	Sewage sludge
SSRB	Solid residue biochar
SSS	Secondary sludge
SW	Surface water
Th	Thermal
TN	Total nitrogen
TOU	Time-of-Use
TS	Total solids
TDS	Total dissolved solids
TVS	Total volatile solids
TWh	Terawatt-hour
Uc	Ultrasonic
Ud	Ultrasound
UF	Ultrafiltration
VM	Volatile matter
WAS	Waste activated sludge
WE	Water electrolyser
WW	Wastewater
WWTP	Wastewater Treatment Plant
wt	Wet basis

Chapter 1

Introduction

This chapter presents an overview of the context in which this study is fitted. The research questions are defined along with the aims and objectives. The significance and contribution of this study are presented, and the methodology used for accomplishing the research objectives is described. Finally, the organization of the thesis is outlined at the end of the chapter.

1.1 Background

Wastewater treatment plants (WWTPs) are among the largest energy consumers in the municipal sector, primarily due to the energy-intensive nature of sewage treatment processes [1]. In Australia, WWTPs consume approximately 1 terawatt-hour (TWh) of electricity annually, accounting for about 0.4% of the country's total electricity usage. Treating 1 megalitre (ML) of sewage typically requires between 150 and 1,400 kilowatt-hours (kWh), depending on factors such as treatment level, plant capacity, energy efficiency, and regulatory requirements [2]. As wastewater volumes grow and effluent standards become more stringent globally, energy demands in WWTPs continue to rise. Paradoxically, municipal wastewater can contain up to ten times more energy than what is required for its treatment [3], [4]. While only a portion of this energy is recoverable, the potential exists for WWTPs to become net energy producers, thereby turning a major operational cost into a sustainability opportunity [5].

One of the main challenges in WWTPs is the treatment and disposal of sewage sludge, which is a by-product of the wastewater treatment process. Although it represents only 1–2% of the total wastewater volume, sludge treatment is both complex and costly. Anaerobic digestion (AD) is the most widely adopted technology for sludge treatment due to its environmental and economic benefits. In AD, microorganisms consume the organic matter in the sludge and, as a co-product, biogas and digested sludge are generated. This process significantly reduces the volume and mass of sludge, lowering disposal and sludge management costs. Additionally, it helps with sludge stabilisation, reducing odor and improving the safety of the treated sludge for further use or disposal to meet the disposal standards and regulatory requirements. The adoption of AD is often encouraged by regulatory policies and sustainability goals aligned with circular economy principles and renewable energy targets. It is a well-established, technically mature technology with proven scalability and adaptability for different plant sizes [6], [7].

In response to rising energy costs and sustainability goals, many WWTPs are seeking to both reduce energy consumption and increase renewable energy production [8]. Biogas produced

through AD is currently the primary renewable energy source in WWTPs, and plants with sludge digestion technology usually consume up to 40% less net energy than those without [9]. Additionally, the combination of anaerobic digestion and combined heat and power is considered one of the most effective energy alternatives, capable of reducing a plant's energy requirements by up to 35%. Depending on site needs and production volumes, biogas can be used on-site for heating purposes or power generation, exported to the grid, or upgraded for gas grid injection. All of these options can improve plant economics through revenue generation and reduced operational costs. Techniques such as co-digestion (using additional organic waste) and sludge pre-treatment can enhance biogas yields and provide additional benefits [3]. In Australia, approximately 55% of WWTPs currently capture biogas and generate bioenergy. However, there is significant opportunity to expand the use of biogas as renewable energy for existing and new facilities. Moreover, integrating biogas storage systems can help WWTPs manage supply and demand more flexibly, especially by offsetting peak electricity tariffs [1].

Beyond biogas, WWTPs are increasingly integrating other renewable energy technologies to support energy self-sufficiency [10]. A large number of renewable energy types are available for use in WWTPs, and by adopting these options, WWTPs can significantly decrease their overall energy demand and become energy self-sufficient or even energy positive [3], [11]. Renewable energy resources have become an essential component in the energy transition and energy management strategies and one of the most efficient and effective solutions for WWTPs. Some options can take advantage of a plant's specific sources, including heat recovery, biosolids gasification and pyrolysis, hydropower, biofuel, and hydrogen production, while others can be non-sector specific, such as solar photovoltaic, wind, and battery systems [11]. In 2018, the Australian water sector generated approximately 180 GWh (or 18%) on-site through renewables, with biogas contributing 69%, hydropower 30%, and solar PV 1% [12].

Although some studies have investigated the utilisation of renewable energy technologies in WWTPs, exploring the opportunities to optimise the integration of renewable energy technologies while reducing operating costs in these facilities is still a valid field of research. Studies on biogas production have often relied on lab-scale experiments, which may not fully replicate real-world and full-scale plant conditions. Others focus on empirical models with limited validation. Similarly, emerging technologies are often explored in isolation, with limited consideration of system-wide integration or scalability. Therefore, this research project aims to investigate operation and planning strategies to reduce operating costs in WWTPs by optimising biogas utilisation and the dispatch of power generation systems. It is expected that the insights gained will contribute to the long-term sustainability and cost-efficiency of WWTPs, supporting their transformation into energy-resilient infrastructure aligned with global energy transition goals.

1.2 Research Aims and Objectives

The aim of this thesis is threefold:

(i) to propose a biogas model for estimating biogas production from sewage sludge under a semi-continuous operation process;
(ii) to develop an operational model to minimise the operating costs of a large-scale wastewater treatment plant (WWTP), considering two scenarios: (a) existing generation assets, and (b) a microgrid system; and
(iii) to propose an optimal planning and operation model that minimises overall costs using a multi-objective optimisation approach.

The biogas model is designed to estimate on-site biogas production using a methodology that combines semi-continuous feeding of sewage sludge with a "First-In, First-Out" (FIFO) strategy. This biogas model serves as an input for both the operational and planning models.

The specific research objectives of this thesis are:

1. Develop a model that forecasts biogas production in a WWTP.
2. Develop an optimal operational strategy to minimise the energy operating costs of a WWTP under two scenarios: (a) existing generation assets, and (b) a microgrid system.
3. Develop a model to find the optimal configuration mix for the power generation system in a WWTP.

1.3 Research Questions

The research questions which this thesis aims to answer are:

1. What is the biogas potential in a WWTP? How can biogas production be forecasted in a large-scale WWTP?
2. What is the optimal operation strategy to minimise the energy operating costs of a WWTP under the following two scenarios: (a) existing generation assets, and (b) a microgrid system?
3. How should the power generation system be optimally planned considering renewable energy sources?

1.4 Significance and Contributions

The significance of this research lies in the need to address some of the key challenges faced by municipal WWTPs, which include exploring alternatives to reduce their high operating costs focused on both planning and operation optimisation for the generation system. With energy costs representing up to 60% of total operational expenses, and increasing demand driven by population growth and stricter effluent regulations, there is a critical need to explore innovative strategies to reduce energy consumption and associated costs. The study contributes by developing an integrated optimisation model that focuses on enhancing the efficiency of anaerobic digestion and leveraging its biogas output for on-site energy generation. By accurately modelling the semi-continuous AD process, the research enables an alternative methodology for estimating the biogas production for a large-scale WWTP, which is essential for improving energy planning and process control at those facilities.

Moreover, the study proposes a framework that integrates biogas modelling with microgrid energy systems, which is a relatively unexplored combination in existing literature, allowing for a dynamic and flexible energy strategy that balances generation and demand while reducing reliance on the external power grid. This approach supports the transition of WWTPs toward energy self-sufficiency, harnessing the latent energy potential in wastewater, which has been shown to be five to ten times greater than the energy required for its treatment. In doing so, the study contributes to broader sustainability and decarbonisation goals by promoting renewable energy utilisation and minimising greenhouse gas emissions.

This research also proposes an alternative option that explores optimisation approaches, offering a practical, data-driven framework that WWTP operators can adopt to reduce operating costs and better respond to operational variability. Additionally, the study incorporates a techno-economic analysis, providing decision-makers with a comprehensive tool to assess the feasibility and cost-effectiveness of deploying microgrid systems and optimised biogas utilisation strategies in real-world conditions. Finally, the interdisciplinary nature of this work makes a valuable contribution to both the academic and engineering communities by presenting a holistic, integrated methodology for improving energy efficiency and operational sustainability in wastewater treatment applications.

1.5 Research Methodology

This research work was conducted in a series of phases that are described in the following:

1. **Literature Review**
   The first phase of this research consisted of a comprehensive examination of the literature to understand the state of the art of anaerobic digestion models using sewage sludge as feedstock to estimate the biogas production in WWTPs. The methodologies and models followed by previous works, as well as their achievements, were analysed. Research gaps and needs were identified.

2. **Research questions, aims and objectives definition**
   After research gaps and needs were identified based on the literature review, the scope of this research was defined, including the research questions, aims and objectives.

3. **Data collection**
   Technical information and data from a large-scale WWTP located in Sydney, Australia, was collected. This phase was extremely important and essential to enable the model to be tested, validated and calibrated, providing a more accurate and reliable tool. The data to be collected on-site or provided by industry partner (Sydney Water Corporation) are listed below:
   • Sewage volume treated and organic composition: These data were essential to calculate the biogas generation potential. Biogas production and methane yield are related to the type of substrate used, and the organic compounds present in the effluent.
   • Biogas generation quantity and composition: This data was important to understand the anaerobic digestion operation performance, potential limitations, opportunities, and process efficiency. In addition, some of the parameters were required to estimate the caloric value of the biogas generated.
   • Electricity and gas data consumption: Understanding the WWTP electricity and gas demand was very important to design the best strategy for optimal planning and operation. Historical data are commonly used as input for simulations and optimisations. In addition, the energy and network tariff given to the WWTP were used to calculate the optimal operation scheduling.
   • Cogeneration system details: Knowing the current power generation capacity of the WWTP was essential to compare against the results of the planning and operation models. Moreover, historical data for the system efficiency, energy consumption, and operation time were also provided by Sydney Water Corporation. Some of these data were included in the models.

4. **Framework and Modelling**
   In this stage, the framework and modelling were designed. The modelling part included three main sections: (i) biogas forecast model, (ii) optimal operation of the power generation system in two scenarios: current assets, and microgrid system, and (iii) optimal planning of the power generation system. This phase included the mathematical formulation preparation for the three parts, starting with the biogas model, as its results are used as an input for both planning and operation models. Different case scenarios were proposed to investigate several aspects and potential alternatives for the WWTP.

5. **Optimisation and results checks**
   Different case scenarios were considered on both operation and planning models in order to maximise the benefits from the system potential. The optimisation problem aims to minimise the operation costs for the WWTP, following a control strategy which schedules the power generation dispatch for the plant and utilisation of biogas. Techno-economic analysis which includes optimal investment costs, payback period, levelised cost of electricity, system unit size, microgrid planning and operation was also investigated. The models were validated against historical data based on different case studies. The results were discussed and some technical papers with the obtained results have already been published, while others will be submitted in the near future.

6. **Thesis writing and future works**
   The last stage was the thesis writing and the proposal of future work directions to further explore this research topic.

1.6 Thesis Organisation

This thesis is organised as follows:

Chapter 2 provides a comprehensive review of the literature relevant to the overall aim. It explores different types of site-specific and non-site-specific energy technologies, including anaerobic digestion, thermochemical processes, solar, hydro, fuel cells, water electrolysers, and others.

This chapter leads to the following publications:

1. D. Lima, G. Appleby, and L. Li, "A scoping review of options for increasing biogas production from sewage sludge: Challenges and opportunities for enhancing energy self-sufficiency in wastewater treatment plants," Energies, vol. 16, no. 5, p. 2369, 2023, issn: 1996-1073

2. D. Lima, L. Li, and G. Appleby, "A review of renewable energy technologies in municipal wastewater treatment plants (wwtps)," Energies, vol. 17, no. 23, p. 6084, 2024, issn: 1996-1073

Chapter 3 proposes a novel methodology to forecast biogas production from sewage sludge in a large-scale WWTP. The model estimates the biogas production based on a semi-continuous feeding mode of sewage sludge. The results of the biogas model are used as an input for the following operation and planning models.

This chapter leads to the following publications:

1. D. Lima, L. Li, and G. Appleby, "Biogas production modelling based on a semi-continuous feeding operation in a municipal wastewater treatment plant," Energies, vol. 18, no. 5, p. 1065, 2025

Chapters 4 and 5 propose an optimal operation model which aims to optimise the anaerobic digestion operation process focusing in optimising the biogas production and utilisation while minimising the energy operating costs for the WWTP. The proposed operation model is divided into two parts based on the power generation infrastructure: (a) current generating assets (Chapter 4), and (b) microgrid system (Chapter 5). The first part (current assets) takes into account the current power generation system based on a large-scale WWTP used in this study. The second part (microgrid system) considers different types of renewable energy technologies, including photovoltaic, battery, micro-hydro, to investigate their contribution to electricity generation and energy supply. Different case studies are considered in both scenarios, and the results of the simulation are discussed in the end of each chapter.

This chapter leads to the following publications (To submit):

1. D. Lima, L. Li, and J. Zhang, "Minimising operation costs in a wastewater treatment plant (WWTP) – Part 1: Traditional power generation assets".
2. D. Lima, L. Li, and J. Zhang, "Minimising operation costs in a wastewater treatment plant (WWTP) – Part 2: Microgrid system".

Chapter 6 proposes a planning model which aims to find the optimal mix configuration of the power generation system for the WWTP. The proposed planning model is formulated based on a multi-objective function which includes both investment and operation costs. The results of the planning model are discussed and presented in the end of the chapter

This chapter leads to the following publications (To submit):

1. D. Lima, L. Li, and J. Zhang, "Optimal planning and operation of a microgrid-based power system in a WWTP".

Finally, Chapter 7 concludes this research by summarizing the key findings, main outcomes, and future research opportunities.

Chapter 2

Literature Review

The literature review of this thesis aims to comprehensively explore the significance of different renewable energy recovery technologies in municipal WWTPs, including site-specific and non-site-specific options, evaluating their impact on sustainability, energy efficiency, and overall operational effectiveness. Through a comprehensive review of current practices and emerging technologies, this study underscores the transformative potential of these innovations in advancing sustainable wastewater management.

2.1 Introduction

Wastewater treatment plants (WWTPs) are an essential component of a municipal system. These facilities receive raw municipal wastewater, treat it, and send the treated effluent back to the environment [13]. WWTPs are major energy consumers, requiring a significant amount of electricity for their operation. Treating municipal wastewater is a complex and costly process; for example, the energy costs can range from 2% to 60% of the total operating costs, depending on the level of treatment used [1]. On average, the energy required to treat 1,000 m^3 of sewage can be up to 1.4 MWh. The variation in energy use may be associated with several factors, such as treatment levels, facility capacity, energy efficiency, operational processes, and regulatory requirements [2]. In addition, due to more stringent effluent standards and rising wastewater volumes, energy demand at WWTPs has been increasing globally [5].

With rising electricity costs, sustainability targets, and efficiency goals, an increasing number of plants are looking for alternatives to minimise operating costs and reduce carbon emissions while increasing their energy efficiency [13]. A commonly used technology for treating wastewater in WWTPs is anaerobic digestion (AD), through which biogas is generated from sludge treatment. Although energy recovery from AD is a well-established and widely used option, other emerging renewable energy technologies are appearing as complementary sources to enhance energy production potential in WWTPs [2]. Renewable energy technologies can significantly decrease a plant's overall energy demand and, in some cases, help energy-intensive consumers move toward energy self-sufficiency or even energy positivity. For example, several WWTPs in the USA (i.e., East Bay Municipal Utility District, Gresham, Gloversville-Johnstown Joint, Point Loma, and Sheboygan Regional) and Europe (Aquaviva, Grevesmühlen, Strassim, Wolfgangsee-Ischl, and Zillertal) have implemented different strategies to reach self-sufficiency, including the adoption of renewable energy technologies and co-digestion [14].

Several studies have been conducted on this topic on renewable energy generation in WWTPs. Some studies have focused on a particular technology, including anaerobic digestion [15], fuel cells [16], combined heat and power (CHP) technologies [17], supercritical water gasification [18], hydrothermal liquefaction [19], thermochemical conversion processes [20], and hybrid systems [21]. Some works have examined new technologies not widely implemented in large-scale plants, including dark fermentation (DF), photocatalysis, photo-fermentation (PF), microbial photoelectrochemical cells (MPEC) [22], Microbial Electrolysis Cells (MECs) [23], microbial fuel cells (MFCs) [24], and biodiesel [25]. Other studies have explored different strategies and market opportunities for WWTPs, including energy spot markets [26]. Other studies have investigated methods for improving biogas generation from sewage sludge in WWTPs, including co-digestion [27]–[30], pre-treatment techniques [27], [28], [31], [32] and biological hydrogen methanation (BHM) [33], [34].

In this context, this literature review aims to summarise the main types of renewable energy technologies that can be used in WWTPs, including site-specific and non-site-specific sources. These technologies can help WWTPs reduce reliance on grid electricity, become more energy-sustainable, and reduce operating costs. In addition, this review also includes some alternatives that these facilities can explore to generate extra revenue and/or reduce operating costs, including providing grid services. This literature review aims to summeffluent is disposedarise the main types of renewable energy technologies that can be used in WWTPs, providing a comprehensive, balanced, and forward-thinking overview of this topic, drawing on related works in the academic literature, government, and industry reports.

The following research questions were considered to conduct this literature review:

1. Which types of site-specific and non-site-specific renewable energy technologies can be used in WWTPs?

2. What are the most common alternatives used to increase biogas generation from sewage sludge?

3. Which strategies and opportunities can be explored by WWTPs to increase revenues and benefits?

Based on the research questions, the following research objectives were developed:

1. Review different renewable energy technologies, including site-specific and non-site-specific options that can be adopted by WWTP

2. Review the most common techniques to improve biogas generation from sewage sludge in WWTPs

3. Investigate strategies and opportunities that WWTPs can consider to increase revenues and/or reduce operating costs

As the first step, the literature search was conducted primarily using three online databases (Scopus, IEEE Xplore, and ScienceDirect) for academic papers published in journals and conference proceedings. Despite limitations, this work aims to provide a comprehensive review of renewable energy generation technologies that can be used in WWTPs. Therefore, it is expected that the insights and results from this study will be useful in generating a clear, structured, and comprehensive understanding of the current state-of-the-art regarding renewable energy generation opportunities in WWTPs.

2.1.1 WWTP Overview

The main objective of a WWTP is to accelerate the natural process of purifying wastewater and return it back to the environment [15]. The wastewater treated by WWTPs, also known as effluent, must meet quality standards and regulatory requirements (i.e., solids, carbon, phosphorus, and nitrogen limits). The effluent's discharge standards can be defined by the state, territory, or national authorities. They can also vary from plant to plant depending on different factors, such as plant age, impact on waterways, and treatment capacity. WWTPs may differ in size, capacity, efficiency, effluent quality requirements, and types of treatment processes [5], [35]. In terms of treatment processes, wastewater plants can be composed of one (primary), two (secondary), or three (tertiary) stages. Figure 2.1 shows a schematic diagram of a facility with two stages, primary and secondary [7].

Preliminary and primary treatments are associated with the physical processes that are used to clean the wastewater. The objective of this stage is to remove solids from wastewater. In the preliminary stage, pollutants and large particles (i.e., rags, twigs, and stones), which can cause operational damage in treatment processes, especially to pumps, are removed from the wastewater. This stage usually uses screens, grit chambers, comminutors, and flotation. Primary treatment, also known as sedimentation, is where scum, suspended solids, and settled solids are removed by sedimentation on the primary clarifiers. In most facilities, the preliminary stage is considered part of the primary treatment [7]. Secondary treatment removes the organic matter that was not removed during the primary treatment. In this stage, biological mechanisms are able to remove up to 85% of the organic material contained in the wastewater. Usually, secondary treatment relies on biological reactors followed by a secondary clarifier with an activated sludge process. Some WWTPs are required to remove nutrients (i.e., nitrogen and phosphorus), and, in this case, additional tanks may be needed to meet the effluent quality standards in a process called nitrification–denitrification. Nutrient removal can be achieved by chemical or biological methods or a combination of both. Tertiary treatment aims to remove specific pollutants that were not removed from the previous treatment stages. It usually relies on chemical processes and filtration to provide the required polishing before the effluent is discharged. Additional treatment can be provided to extract nutrients and remove pathogens if required [7], [36]. Choosing the most appropriate effluent treatment technology for a WWTP involves considering various technical factors (i.e., effluent volume, water demand, and plant size), and some commercial software tools, such as Winflows, IMSDesign, and WAVE, can support the planning and design processes of a WWTP.

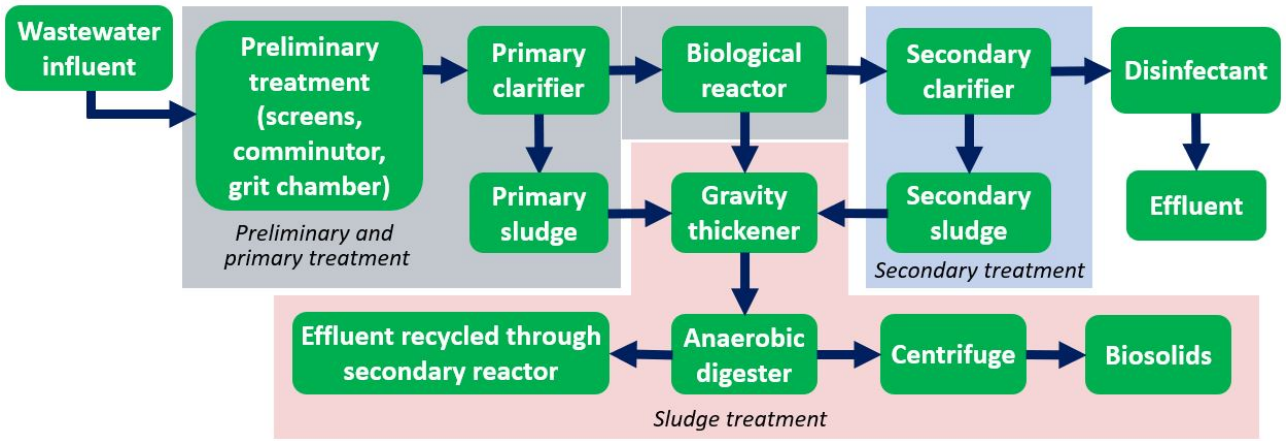

Figure 2.1: WWTP diagram (sludge, primary and secondary wastewater treatments)

2.1.2 Sewage Sludge

Sewage sludge is the solid material (organic and inorganic) removed from the raw wastewater during the treatment process. The amount of sludge produced in a WWTP is proportional to the quantity of wastewater treated by the plant and can be expressed in mass or volume. On average, the total sludge produced may range from 0.2 to 0.3 kg/m^3 of wastewater treated [7]. It contains a mixture of organic and inorganic matter and a high concentration of several pathogenic organisms that must be treated before disposal. Sewage sludge disposal is costly, and most WWTPs must follow regulatory requirements for waste management [37]. The energy recovery potential from sludge is directly related to three main components: (i) water content, (ii) organic (volatile) matter, and (iii) inorganic (inert) matter. Several methods are reported in the literature and industry, including anaerobic digestion (most common), co-digestion, composting, incineration, disposal in landfills, or utilisation in agriculture as a soil conditioner. However, due to the high costs of conventional treatment methods and the drive to improve sustainability targets and reduce operating costs of sludge disposal, WWTPs can recover energy from utilising sewage sludge using different methods [20], as shown in Figure 2.2. The energy content of dried sewage sludge, with 21–48% volatile matter, can range between 11.1 and 22.1 MJ/kg, and the calorific values for primary, secondary, and digested sludges were reported to be 16.2 MJ/kg, 12.2 MJ/kg, and 11.4 MJ/kg, respectively [38].

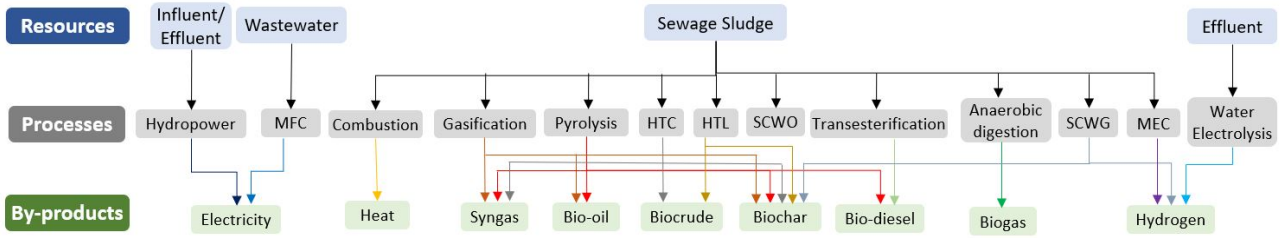

Figure 2.2: Site-specific sources of renewable energy in a WWTP.

2.2 Energy Resources in WWTPs

Renewable energy technologies have become an essential component of the energy transition and one of the most effective solutions for reducing costs and emissions from WWTPs. Several types of renewable energy sources can be adopted by a WWTP. Some options can take advantage of the site-specific resources, including energy recovery from wastewater and sewage sludge, influent/effluent flow, and treated water. In contrast, others can be non-site-specific, such as solar and wind. Although many technologies can be implemented in WWTPs, some are still in the research and development stages and have not been widely used in large-scale facilities [10].

2.2.1 Site-Specific Sources

Site-specific sources refer to the energy recovery embedded in the WWTP's resources, including wastewater, sewage sludge, influent/effluent flow, and treated water. In theory, the energy contained in municipal wastewater and sewage sludge can be five to ten times higher than the energy required for their treatment, and this energy is mainly found in three forms: chemical, hydraulic/kinetic, and thermal. Based on this huge potential, according to the Water Environment Federation, WWTPs have the potential to become energy-neutral facilities or even

net-energy producers [3]. Although many energy recovery methods can be used in WWTPs, each technology has its advantages, disadvantages, limitations, and potential benefits. Some of them are very widely used in large-scale plants (i.e., anaerobic digestion), and others are not as common (i.e., water electrolysis, MFC, and MEC). Figure 2.2 illustrates the energy resources that can be recovered from a WWTP and the conversion processes associated.

2.2.1.1 Anaerobic Digestion

Anaerobic digestion (AD) is the most common technology used to treat sewage sludge in WWTPs (48% of the total wastewater is treated through AD in the USA). The main objective of anaerobic digestion is to reduce the total and volatile solids load in sludge, reduce pathogens, and minimise odours. In this process, microorganisms consume the organic matter in the sludge and generate biogas as a by-product of the digested sludge. AD occurs in the absence of oxygen and is divided into four stages: hydrolysis, acidogenesis, acetogenesis, and methanogenesis. Anaerobic digestion and biogas production are influenced by several elements, including feedstock parameters, design, and operational conditions. Feedstock parameters are related to the biological, chemical, and physical characteristics contained in the sewage sludge, including total solids, suspended solids, volatile solids, chemical oxygen demand (COD), biological oxygen demand (BOD) and carbon-to-nitrogen ratio. Design and operational factors are related to operating parameters that influence the anaerobic digestion performance, including pH, alkalinity, temperature, retention time, organic loading rate (OLR), digestion volume, type of mixing and stages [15].

a. Optimising Biogas Generation in WWTPs

Improving anaerobic digestion efficiency enhances biogas production, and consequently, the facilities become less reliant on carbon-intensive electricity grid systems. However, optimising anaerobic digestion is a complex process, mainly due to the non-linear relationships among its parameters and variables. Because of its complexity, sub-optimal anaerobic digestion operations may be frequent in wastewater treatment facilities. The main issues faced during anaerobic digestion are low gas production, maintaining a stable process, and resuming biogas production after a process failure. In addition, limitations result from the first stage of the process (hydrolysis), which requires long retention times caused by the slow degradation of organic matter [15]. Biogas production through AD is limited to conversion of the readily biodegradable portion of the solids [3]. To overcome this limitation, some methods to improve biogas production include:

- Process optimisation: It involves operational conditions and parameters, such as temperature, organic loading rate (OLR), hydraulic retention time (HRT), and pH to enhance efficiency and biogas production. Models are classified as either steady-state or dynamic: steady-state models help design optimal system configurations by estimating HRT, reactor capacity, and gas output, while dynamic models focus on enhancing operational efficiency and adapting to changing parameters like feedstock composition, inhibition, and temperature. One of the most well-known and widely used models is the Anaerobic Digestion Model No. 1 (ADM1), developed by the International Water Association (IWA), which simulates both biochemical and physicochemical processes in AD systems. ADM1 has been validated across various scales and configurations. Additionally, IWA developed Activated Sludge Models (ASM1, ASM2, ASM2d, ASM3) to model the activated sludge process based on biokinetic rates. ASM1 is widely used for characterising organic matter in wastewater, while ASM2 and ASM2d add complexity by incorporating microbial behaviour in different environments. ASM3 introduces a storage component to model

particulate COD. These methods are commonly validated through mathematical modelling to replicate the AD process, and their integration into WWTPs offers advantages in monitoring, control, and energy efficiency [15].

- Co-digestion: The process of mixing two or more feedstocks to enhance biogas production, especially when the primary substrate, such as sewage sludge, has a low carbon-to-nitrogen (C/N) ratio and poor digestibility. The primary goal of co-digestion is to boost methane yield and biogas production to generate renewable energy (electrical, thermal, or mechanical), creating additional revenue for WWTPs. Depending on the type and quantity of feedstock used in the co-digestion, biogas production can increase significantly, resulting in less dependence on the electricity grid, a reduction in operating costs, and an increase in energy self-sufficiency. Adoption of co-digestion is recommended if there is spare generation capacity, gas storage, or even the capability to convert biogas into biomethane to accommodate the increased volume of biogas generation. Attractive feedstocks that can be combined with sewage sludge include fats, oils, and grease (FOG), food scraps and waste, food/beverage/dairy processing waste, the organic fraction of municipal solid waste (OFMSW), agricultural residues, livestock manure, biofuel by-products, and other high-strength waste (HSW). Depending on the feedstock and mixing ratio, co-digestion can increase biogas production between 25% and 400% compared to sludge-only digestion. For instance, while sludge alone may yield 0.9–1.1 m^3 biogas/day/m^3 digester, co-digestion can boost this to 2.5–4.0 m^3/day/m^3. Feedstock selection depends on factors like location, availability, and logistics costs (e.g., transport and storage). Several full-scale WWTPs worldwide have adopted co-digestion with significant success. For example, the East Bay Municipal Utility District earned $2 million in electricity revenues in 2012–2013, and the Des Moines WWTP trades 40–50% of its biogas for annual revenues of $460,000–800,000. Facilities in Germany (Grevesmühlen and Köhlbrandhöft) also reported energy surpluses and increased electricity generation from co-digestion [15].

- Pre-treatment techniques: These methods break down complex organic compounds in the sludge into simpler, more easily digestible molecules, thereby accelerating the hydrolysis step—the slowest phase in AD. This breakdown increases the solubility and bioavailability of substrates, making nutrients more accessible to microorganisms and boosting overall biogas yield. These processes can increase OLR, reduce HRT, and improve overall system efficiency, methane concentration and biogas production rates. Pre-treatment methods are generally classified into four main types: biological, chemical, mechanical, and thermal. Biological pre-treatment focuses on reducing organic matter and nutrients such as nitrogen and phosphorus to comply with effluent discharge regulations. Common biological techniques include aerobic digestion (used in an activated sludge process to stabilise and reduce the organic matter in the wastewater), dual-stage digestion (physical separation of hydrolysis and methanogenesis stages), enzyme addition (improves sludge's stabilisation, biodegradability, dewaterability, and methane yield), and temperature-phase systems. Chemical treatment involves the hydrolysis of organic compounds using chemical reagents. Alkaline and acid hydrolysis, ozonation, and oxidation are among the most widely used approaches. Alkaline treatment is popular due to its ability to adjust pH and solubilise organic compounds, while ozonation enhances biodegradability and contributes to sludge mass reduction. Mechanical pre-treatment aims to increase the surface area of sludge particles, making them more accessible to microorganisms. These methods include ultrasound, ultrasonic, microwave, high-pressure homogenisers, and pulse methods; among them, microwave and ultrasound are the most studied and applied in sewage sludge. These methods usually require moderate electricity consumption but also have low efficiency when not combined with other methods. Thermal pre-treatment uses both low and high temperatures (typically between 70–200 °C) and pressures (600–2500 kPa) to disrupt the sludge's

structure and improve solubility. Thermal hydrolysis is the most widely used method in the industry. These commercial systems have the capacity to increase biogas production by up to 150%, while also enabling higher OLR and reducing HRT, thereby enhancing the overall efficiency of the anaerobic digestion process [15].

Table 2.1 provides an overview of selected studies on the co-digestion of sewage sludge with different feedstocks. Across the reviewed studies, co-digestion consistently enhanced methane production compared with mono-digestion of sewage sludge. Food waste was the most frequently tested co-substrate, generally yielding higher methane production (up to 609 mL/g VS) and increased methane concentrations (up to ∼70%), depending on mixing ratios and retention times. Co-digestion with grease trap waste and fats, oils, and grease also produced substantial gains, with methane yields increasing two- to threefold under optimal conditions, although excessive loading sometimes reduced methane concentrations. The addition of glycerol showed strong synergistic effects, with methane yields exceeding 500–600 mL/g VS and concentrations above 70%. Animal manures feedstock (i.e., pig, poultry, and swine) provided moderate improvements in methane yield while maintaining stable methane concentrations. Co-digestion with microalgae also demonstrated potential, improving yields compared with sludge alone. In summary, the findings highlight that co-digestion enhances both methane yield and concentration, with the magnitude of improvement strongly influenced by the type of co-substrate, mixing ratios, and operating conditions.

Table 2.1: Co-digestion of sewage sludge with different feedstocks

Ref.	Substrate	System	CH_4 production	CH_4 concentration
[39]	SS and FW	6 × 5 L reactor, 37 °C, 22 days HRT, 10–50% FW:SS ratios	SS: 230–280 | FW:290–330 AcoD: 318–385	SS: 45–57 | FW: 49–57 AcoD: 53–55.7
[40]	SS and FW	2 L reactor, 30–38 °C, 22 days HRT, ratios (1:1, 1:2 and 1:3)	SS: 356–478 | FW: 511 AcoD: 453–609	SS: 53 | FW: 50.4 AcoD: 52–70.3
[41]	SS and FW	5 L reactor, 30–38 °C, 22 days HRT, different mixing ratios (1:1, 1.5:1, 2:1, 1:1.5 and 1:2)	SS: 625.4 | FW: 385.9–507.5 AcoD: 384.6–492	SS: 55.9–58.6 | FW: 58.8 AcoD: 53–60.4
[42]	SS and FW	6 L reactor volume, 35 °C, 8–30 days HRT and different SS:FW mixing ratio (2.4:1, 0.9:1, 0.4:1)	SS: 157–237 | FW: 377–465 AcoD: 215–400	SS: 63–65 | FW: 50–54 AcoD: 53–61
[43]	SS, GTS OFMSW	2 × 6 L reactor, 38 °C, 20 days HRT and 5–30% mixing ratio	SS: 300 | GTS: NI | OFMSW: NI | AcoD: 456–547	SS: 66 | GTS: NI | OFMSW: NI AcoD: 66–69
[44]	SS and GTW	6 L reactor, 35 °C, 15 days HRT, 1:1 mixing ration (PSS and WAS) + GTW 5% VS.	SS: 384 | GTW: NI AcoD: 641	SS: 61 | GTW: NI AcoD: 69
[45]	SS and FOG	For 55 °C: 10 L reactor, 20 days HRT. For 70 °C: 2 L reactor, and 2 days HRT. Mixing ratios: 20, 40, 60 and 80% FOG	SS: 138.3 | FOG: NI AcoD: 102–673	SS: 61.6–62.8 | FOG: NI AcoD: 49.7–67.3
[46]	SS and FOG	1 L reactor, 35 °C, 15 days HRT, 4 mixing ratios (14%, 24%, 43% and 39% GTW)	SS: 114–128 | FOG: 143–290 AcoD: 453–609	SS: 62.8–71.2 | FOG: 63.3 AcoD: 66.1–68.4
[47]	SS, FW and G	0.25 L reactor, 37 °C, 20 days HRT, 1:1 mixing ratio (SS:FW) with 1% and 3% glycerol.	SS: 138.3 | FW: NI | G: NI AcoD: 236–526	SS: 85.9% | FW: NI | G: NI AcoD: 77.4–79.4
[48]	SS and G	5.5 L reactor, 35 and 55 °C, 20 days HRT, 2 SS:G mixing ratios (99:1, 98.8:1.2 v/v%	SS: 296 (35 °C) & 354 (55 °C) | G: 277–475 (35 °C & 349–490 (55 °C) | AcoD: 250–660 (35 °C) & 230–530 (55 °C)	SS:NI | G:NI AcoD: 63–72 (35 °C) & 57–66 (55 °C)

Continued on next page

Table 2.1 – continued from previous page

Ref.	Substrate	System	CH_4 production	CH_4 concentration
[49]	SS and PM	0.16 L reactor, 35 °C, 47 days HRT, different SS:PM mixing ratios (21:1, 14:1, 7:1 VS)	SS: 182 | PM: 239 AcoD: 190–200	SS: 52–58 | PM: 52–58 AcoD: 52–58
[50]	SS, SM PoM	1 L (b) and 3 L (s-c) reactor, 35 °C, 15–30 days HRT, different mixing ratios	SS: 184 (b) | PoM: NI | SM: NI AcoD: 198–290 (b) & 186–273 (s-c)	SS: 67–68 | PoM: NI | SM: NI AcoD: 67–68
[51]	WAS and M	0.13 L reactor, 35 °C, 25–30 days HRT, 4WAS:M mixing ratio (3:1, 1:1, 1:3)	WAS: 362 | M: 318 AcoD: 354–442	WAS:NI | M:NI newline AcoD:NI

SS: Sewage sludge; AcoD: Co-digestion; NI: Not informed; GTW: Grease trap waste; G: Glycerol; PM: Pig manure; SM: Swine manure; Ma: Microalgae; FW: Food waste; PoM: Poultry manure; HRT: Hydraulic retention time; b: batch mode; OLR: Organic loading rate; s-c: semi-continuous mode; WAS: Waste activated sludge; PSS: Primary sludge

Table 2.2 provides a summary of studies that have examined the application of different pre-treatment techniques to sewage sludge. The main findings indicate that pre-treatment methods can enhance methane yields and biogas production compared with untreated sludge, although the extent of improvement and associated energy requirements vary across methods. Thermal treatments, particularly around 180 °C, consistently achieved significant improvements of 40–50% in methane yield, while ammonia-assisted thermal treatment also showed moderate gains. Microwave pre-treatments improved methane production by 17–45%, with results depending on energy input and digestion time. Ultrasound treatments delivered strong performance, achieving 20–50% yield increases and in some cases up to 80% higher methane production rates. Combined methods, such as ultrasonic–thermal–microwave or ultrasonic–ozonation, demonstrated synergistic effects with improvements ranging from 11% to 95%, although these often required high energy inputs that may limit their implementation. Generally, thermal and ultrasound methods appear to offer the most effective balance between yield enhancement and feasibility, while combined treatments can achieve higher gains but with higher energy costs.

Table 2.2: Pre-treatment methods applied on sewage sludge

Ref.	Type	Sludge	Treatment applied	AD process	Results
[52]	Th	WWTP in Valladolid, Spain	180–200 °C for 0.5h	Mesophilic, batch mode, and 25 days.	CH_4 yield can improve by up to 50% when compared with raw sludge.
[53]	Th	WWTP, in Korea.	Thermal process of 75–225 °C for 15 to 105 min.	Batch and continuous mode.	Optimal treatment conditions: 180 °C for 76 min to improve CH_4 roduction by 40% (from 194.5 to 72.9 mL CH_4/g COD).
[54]	Th	WAS from a WWTP in Changsha, China.	70 °C with ammonia (135.4 mg NH_3-N/L).	Mesophilic (35°C), batch mode, and 37 days.	CH_4 potential improved by 25% for ammonia treatment, 18% for thermal, and 16.5% for ammonia-thermal.
[55]	M	Qinghe WWTP in Beijing, China	Microwaved at 2450 MHz, 1 atm, and 55 rpm	Mesophilic, batch mode, and 25–30 days.	CH_4 yield increased by 20% (from 215 to 258 mL/g VS) for a 1-stage reactor, and a 2-stage reached 288 mL/g VS.
[56]	M	Copero urban WWTP in Spain.	400-700W, 30 kJ/g TS energy applied.	Mesophilic, batch mode, up tp 90 days.	CH_4 yield and production rate increased by 17% and 43%, respectively.
[57]	M	WWTP located in Leon, Spain.	Pre-treatment using 975 kJ/L was performed.	Mesophilic (34 °C), batch mode, and HRT up to 25 days.	CH_4 yield improved by 29%, 41%, 45%, and 43% for an HRT of 5, 10, 20, and 25 days, respectively.
[58]	Ud	Biobío WWTP, in Concepción, Chile.	26 kHz at 55 °C.	Mesophilic, batch mode up to 35 days.	Tests performed for 0.5, 15,500, and 30.5 MJ/kg TS under 3-13 hs. CH_4 yield increased by 50% and CH_4 rate by 30 80%.

Continued on next page

Table 2.2 – continued from previous page

Ref.	Type	Sludge	Treatment applied	AD process	Results
[59]	Ud and M	WWTP in of Mechelen-Noord, Belgium.	Specific energy used in both treatments was 96 kJ/kg sludge.	Mesophilic (37 CH_4), semi-continuous mode up to 67 d.	Biogas increased by 20% and 27% for the microwave and ultrasonic, respectively.
[60]	Uc	Full-scale WWTP in Antwerp-South, Belgium.	Specific energy ranged from 5 to 35 MJ/kg TS.	Mesophilic, batch mode, and 30 days.	Biogas production increased by 8.6%, 22.9%, and 31.4%, by applying 15, 25, and 35 MJ/kg TS, compared to raw sludge.
[61]	M, Ud and Th	Copero urban WWTP in Seville, Spain.	Th: 120 °C, 2 atm for 15 min. Uc: 25 °C, 1 atm, 150 W for 45 min. M: 100–900 W for 1.4 min.	Mesophilic (35 °C) and batch mode.	CH_4 production improved by 95%, 29%, and 20% by using sonication, thermal, and microwave. Ultrasonic, thermal, and microwave required 136, 36, and 20,145 kJ/g TS of specific energy.
[62]	Oz and Ud	Municipal WWTP, in Singapore.	Sequential treatment of ultrasonic and ozone	Mesophilic (35 °C), batch mode, and 30 days HRT.	Biogas production increased by 11% and 15.4% for ultrasonic and ultrasonic-ozone, respectively.
[63]	Th and Uc	Ulu Pandan municipal WWTP, in Singapore.	Uc treatment: 5 MJ/kg TS and th treatment at 65 °C.	Mesophilic (35 °C) and batch mode.	Biogas production increased by 20% with the combined treatment.

Th: Thermal, M: Microwave, Uc: Ultrasonic; Ud: Ultrasound; Oz: Ozonation; FA: Free ammonia; DS: Dry solids; OLR: Organic loading rate; WAS: Waste activated sludge

b. Biogas Opportunities in WWTPs

Biogas in WWTPs offers two main opportunities: reducing operational costs and generating additional revenue. It can be used on-site for heating anaerobic digesters, dewatering sludge, and in steam processes, with boilers being the most common method due to their efficiency and ability to handle low-quality biogas. CHP systems often provide primary heating, with boilers supplementing as needed. Biogas can also be used to generate electricity via fuel cells, gas turbines, or internal combustion engines. Additionally, hydrogen can be produced through steam methane reforming or water electrolysis powered by CHP-generated electricity. Some WWTPs flare unused biogas, a low-cost method that reduces methane emissions but does not recover energy [3], [64].

Biogas from sewage treatment plants typically has a lower heating value of 21.5–23.3 MJ/Nm^3 and mainly consists of methane (60–65%) and carbon dioxide (35–40%), with small amounts of other gases like nitrogen, oxygen, hydrogen sulfide, ammonia, and siloxanes. Methane contributes most to its energy content due to its high calorific value (42 MJ/kg). However, impurities reduce biogas's energy potential, damage equipment, and increase maintenance costs. The level of biogas treatment depends on its end use; for example, microturbines can tolerate up to 1,000 ppm of hydrogen sulfide, but fuel cells allow only up to 5.5 ppm. Common contaminants removed include water vapour, hydrogen sulfide, ammonia, siloxanes, halogenated hydrocarbons, and carbon dioxide. Upgrading biogas (raising methane content above 95%) is often required, particularly for fuel cell applications. Biogas can create additional revenue for WWTPs by either exporting electricity to the grid or injecting upgraded biogas into the gas grid. For gas grid injection, biogas must undergo an upgrading process to remove carbon dioxide, hydrogen sulfide, ammonia, and siloxanes [15]. Biomethane is widely used in Europe and other regions for transportation and electricity generation, and its injection into national gas grids requires strict quality standards. The standards required for biomethane injection into the gas grid can vary from country to country. For example, France and the Netherlands require a minimum concentration of methane of 86% and 85%, respectively, whereas Austria, Germany, and Switzerland require a minimum level of 96%, and Sweden even higher, at 97%. The maximum concentration of carbon dioxide allowed is 2.5% in France, 3% in Sweden and

Austria, and 6% in the Netherlands [65]. In addition, in the U.S. (California), the minimum methane concentration ranges from 93-96% [66]. In Australia, the gas calorific heating values should be between 37 MJ/m^3 and 42.3 MJ/m^3, and the maximum levels of hydrogen sulfide, water content, and sulphur are 5.2 mg/m^3, 73 mg/m^3, and 50 mg/m^3, respectively [67]–[69]. Table 2.3 compares the characteristics of biogas upgrading technologies [15]. Chemical absorption and cryogenic separation achieve very high methane purity, but both face challenges of high energy use and investment costs. Water scrubbing (WS) and membrane separation (MS) are the most widely implemented due to their lower energy demand, operational simplicity, and reliability, though each has limitations such as high water use (WS) or the need for multiple stages (MS). Overall, the choice of upgrading technology involves balancing methane recovery, cost, and resource requirements, with WS and MS emerging as the most practical options.

Table 2.3: Biogas upgrading technologies' characteristics

Type	ERqd (kWh/ m^3)	CH_4 RR (%)	CAPEX (£/ kWh)	OPEX (£/ kWh)	Plants (1)	Benefits	Drawbacks
CA	0.06∼ 0.17	99.9	264∼ 438	1.15∼ 1.92	104	Provide the highest biomethane purity; No need of biogas pressurized; No need for H_2S treatment;	Heat, water, and chemical required; Higher energy consumption; Problems with corrosion and precipitation
CS	0.18∼ 0.25	98∼ 99.9	394∼ 960	4.80∼ 7.10	9	No water and chemicals required; High biomethane purity;	Biogas and H_2S treatments required; High investment and O&M costs; Not very mature technology
PSA	0.16∼ 0.35	90∼ 98.5	255∼ 831	0.92∼ 6.50	81	Low energy consumption; Compact technology; No water and chemicals required; Widely used in small plants	Lower biomethane purity compared to others; H_2S treatment needed; High energy consumption and strict process control
WS	0.20∼ 0.30	98∼ 99.5	357∼ 731	0.47∼ 0.94	175	Low energy consumption; Simple, flexible, and low O&M costs; Remove NH_3 and H_2S; Most used method;	Dried process is needed; More strict process control; Chemicals may be required; High water demand
OPS	0.23∼ 0.33	96∼ 99	510∼ 969	0.92∼ 1.05	19	Remove NH_3, H_2S and other compounds; High biomethane purity;	High investment and O&M; Higher energy consumption; Heat and chemicals needed
MS	0.18∼ 0.35	85∼ 99	205∼ 367	0.79∼ 5.50	148	Simple, flexible, and low O&M costs; Compact and reliable; No chemicals, water, or heat required;	Require multiple stages; High investment costs; Not recommended for biogas composed of many impurities

CAPEX: Capital Expenditure; OPEX: Operating Expenditure; CA: Chemical Absorption; CS: Cryogenic Separation; MS: Membrane Separation; OPS: Organic Physical Scrubber; PSA: Pressure Swing Adsorption; WS: Water Scrubbing; ERqd: Energy required; RR: Recovery rate

(1) Total number of plants using upgrading technologies in some countries, including Germany, UK, Sweden, France, Switzerland, Denmark, the Netherlands, Austria, Finland, Canada, South Korea, Brazil, Estonia, and Ireland [70].

The decision to use biogas on-site or export it to the gas grid in WWTPs can depend on several factors, including biogas production rate, generation capacity, upgrade and storage capabilities, feed-in tariffs, and local regulations. While the technology for injecting biomethane into the grid is technically mature, economic feasibility remains a key barrier, largely due to the high capital, energy, and maintenance costs associated with upgrading systems. The economic feasibility of a biogas upgrading system can be challenging. The selection of the most suitable biogas upgrading technology requires an analysis of capital and operating costs. The operating and maintenance costs for these methods are associated with energy consumption, labour, and resources (water and/or chemicals used). Other factors to consider for technology selection include site-specific details, such as biogas production, regulations, and end-use purposes. The lowest-cost technology may not always be the most appropriate solution [15].

2.2.1.2 Thermochemical Processes

Thermochemical processes aim to recover the sludge energy content by changing its composition, including biological, chemical, and physical characteristics, based on thermal treatment to produce a valuable fuel, which can be solid, liquid, or gas renewable fuel. Additionally, it can reduce the operating costs related to sludge disposal and its negative impacts on the environment. These processes have been receiving significant attention over the last few decades, and they can be classified into incineration (also known as combustion), gasification, pyrolysis, and hydrothermal treatments [71]. Figure 2.3 illustrates different thermochemical methods that can be used to treat sewage sludge, producing valuable by-products, including hydrogen-rich gas, syngas, bio-oil, and biochar.

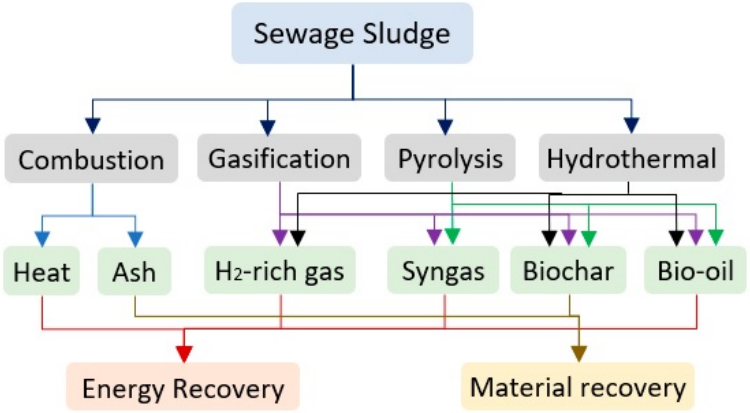

Figure 2.3: Thermochemical processes applied to sewage sludge for energy recovery.

a. Combustion

Also known as incineration, it occurs under high temperatures (between 800 °C and 1000 °C) and an excess of air. It is a very mature technology and one of the most traditional methods for converting biomass into energy. Its applications to sewage sludge have been widely studied, and the main benefits of using combustion include achieving complete oxidation of the organic elements in the biosolids, reducing the sludge volume, and ensuring pathogen destruction. In this process, heat and electricity can be recovered, and other co-products, such as ash (inert material), flue gas, and water, are generated [72]. Its main advantages include the ability to significantly reduce the sludge volume (up to 90%), destroy pathogens and toxic elements, being a mature technology, lower costs compared to other methods, odour control, and potential for energy recovery. However, this method also results in low energy efficiency, emission of toxic compounds, low economic viability, and usually requires additional fuel. Due to its high ash and water content, sewage sludge is typically mixed with other feedstocks (i.e., wood pellets) to achieve better performance (process known as co-combustion) [73].

Some commercial sludge treatment facilities have been reported in the literature, including plants in Belgium, China, Germany, Japan, the USA, the UK, and the Netherlands, which have used incineration to treat municipal sewage sludge [72]. For instance, a sludge treatment facility (STF) was constructed and started operations in 2015 in Hong Kong, China, to process 2000 tons/day of sewage sludge from the Stonecutter's Island WWTP. The STF is supplied by two generators capable of producing all the electricity needed to operate the plant. The STF is not only energy self-sufficient but also exports the electricity surplus (up to 2 MW) to the main grid [74].

b. Gasification

Gasification is a method in which the biomass (i.e., dried sludge) is exposed to a high temperature (about 1,000 °C) in a reduced air environment, generating syngas, heat, and ash. The syngas (synthetic gas) composition may include methane (CH_4), carbon monoxide (CO), carbon dioxide (CO_2), hydrogen (H_2), oxygen (O_2) and nitrogen (N_2), which can be cleaned to produce a higher quality fuel, whereas the heat can be further recovered to generate electricity. The high heating value (HHV) of syngas from sewage sludge gasification depends on different parameters, including gasification technology, operating conditions (i.e., temperature, pressure, and air-to-fuel ratio), and sewage sludge characteristics. On average, it may vary from 5.8 to 18 MJ/m^3. The benefits of gasification are related to the ability to deal with inorganic elements, generation of syngas and heat, low energy needs, being a mature technology, and combined feedstocks without quality/efficiency problems. However, issues related to low energy efficiency, emissions, economic viability, and additional fuel requirements are the main drawbacks [75]. Table 2.4 compiles studies investigating the gasification of sewage sludge, including dewatered sludge, paper-mill sludge, and mixtures with other biomass or coal. The feedstock properties varied widely in terms of moisture content (3–80%), volatile matter (9–67%), ash content (8–50%), and heating values (HHV 2.84–17.1 MJ/kg), which influenced gas yields and composition. Gasification was typically conducted in fluidized-bed or two-stage reactors at temperatures between 500–1,150 °C, with air or steam equivalence ratios ranging from 0.2 to 0.3. The resulting syngas generally contained 2–8% CH_4, 1–52% H_2, 4–19% CO, and 6–32% CO_2, with lower heating values (LHV) of 1.7–11.7 MJ/m^2 dry gas. Cold gas efficiency ranged from 35% to 92%, often improving when co-gasifying with additives (i.e.,sawdust, coal, dolomite, or activated carbon). In summary, higher gas yields and energy content were achieved using dry sewage sludge, co-gasification with high-volatile feedstocks, and two-stage gasifiers, demonstrating that feedstock composition, reactor type, and operational parameters critically affect syngas quality and process efficiency.

Table 2.4: Studies focused on sewage sludge gasification

Ref	Type	Feedstock composition	Operation parameters	Generated products
[76]	DEW	HHV 13.5 MJ/kg dry, 8.6% MC, 51.8% VM, 43.1% ash. UA: 51% C_4, 7.3% H_2, 7.9% N_2, 2.05% S_8, 31.8% O_2.	100 kW-th FBR, DEW feeding rate of 9.2-16 kg/h, temperature 790-815 °C, air flow 11-15 m^3/h,	Syngas LHV 3.6-4.5 MJ/m^3 dry, gas composition includes 4.6-6.6% CH_4, 8.4-10.2% H_2, 7.3-9.9% CO, 15.2-16.5% CO.
[77]	DEW + sp (mix ST)	HHV 13.2 MJ/kg dry, 30% MC, 67.7% VM, 9.8% ash. UA: 45.2% C_4, 5.8% H_2, 1.2% N_2, 0.4% S_8, 37.4% O_2.	100 kW-th LTCFB reactor, 45 kg of dry SS gasified for 28h, temperature 500-750 °C, Air eq. ratio of 0.2-0.3	Syngas LHV and HHV as 1.76 and 1.88 MJ/m^3 dry. Gas composition includes 2.5% CH_4, 1.6% H_2, 8% CO, 18% CO_2 and other gases.
[77]	SS +sp (mix BJ)	HHV 14.8 MJ/kg dry, 12.5% MC, 66.5% VM, 13.3% ash. UA: 43.5% C_4, 4% H_2, 1.2% N_2, 0.4% S_8, 36% O_2.	6 MW-th LTCFB reactor, 7.5 ton of dry SS gasified for 30h, temperature 500-750 °C, Air eq. ratio of 0.3	Syngas LHV and HHV as 3.84 and 4.2 MJ/m^3 dry. Gas composition includes 4.2% CH_4, 9% H_2, 11.8% CO, 19.4% CO_2 and other gases.
[77]	Dry SS (SLU BJ)	HHV 11.4 MJ/kg dry, 12.5% MC, 42.7% VM, 43.1% ash. UA: 27.6% C_4, 4.3% H_2, 3.9% N_2, 0.8% S_8, 19.8% O_2.	100 kW-th LTCFB reactor, 240 kg of dry SS gasified for 14h, temperature 500-750 °C, Air eq. ratio of 0.2-0.3	Syngas LHV and HHV as 1.88 and 2.05 MJ/m^3 dry. Gas composition includes 2.6% CH_4, 5% H_2, 4.5% CO, 18.5% CO_2.
[77]	Dry SS (SLU RA)	HHV 12.2 MJ/kg dry, 4.6% MC, 43.1% VM, 43.8% ash. UA: 28.7% C_4, 4.2% H_2, 3.9% N_2, 1.3% S_8, 18.1% O_2.	100 kW-th LTCFB reactor, 800kg of dry SS gasified for 40h, temperature 600-750 °C, Air eq. ratio of 0.2-0.3	Syngas LHV and HHV as 1.96 and 2.16 MJ/m^3 dry. Gas content: 2.4% CH_4, 6.6% H_2, 4.2% CO, 17% CO_2.
[78]	SS	SS: HHV 2.84 MJ/kg dry, 80.1% MC, 9.78% VM, 8.3% ash. UA: 6.27% C_4, 1.1% H_2, 0.77% N_2, 0.3% S_8, 3.2% O_2.	FBR operating under 784-822 °C with 0.3 air to fuel ratio. SS feeding rate of 25 kg/min,	Syngas LHV 2.3-2.6 MJ/m^3 dry. Gas content: 3-3.4% CH_4, 3.24-3.49% H_2, 5.6-6.9% CO, 23.2-27.8% CO_2. Gas yield: 28.5 m^3/min, CGE of 46.6-52.8%.

Continued on next page

Table 2.4 – continued from previous page

Ref	Type	Feedstock composition	Operation parameters	Generated products
[78]	SS and PMS	PMS: HHV 4.25 MJ/kg dry, 51.4% MC, 29.9% VM, 18.33% ash.UAs: 13.9% C_4, 2.03% H_2, 0.42% N_2, 0.15% S_8, 13.8% O_2.	FBR, SS:PMS ratio 1:2 and 1:1 at 816-858 °C and 0.3 air:fuel ratio. SS and PMS rate of 8.3-12.5 kg/min	Syngas LHV 1.7-2.42 MJ/m^3 dry. Gas content: 2.6-3.65% CH_4, 2.6-4.13% H_2, 3.95-4.7% CO, 17.4-25.42% CO_2. Gas yield: 29.4 m^3/min, CGE of 45-6-61.6%.
[79]	Dry SS	6.5% MC, 48% VM, 47.6% ash, 4.3% fxc. UA: 51% C_4, 7% H_2, 7.5% N_2, 2.4% S_8, 32% O_2.	20 kW bubbling FBR, temperature of 850 °C, air ratio of 0.25, fuel mass flow of 7kg/h.	Syngas yield of 1.3 m^3/kg. Gas composition in fraction mole: 6% CH_4, 40% H_2, 20% CO, 32% CO_2 and other gases.
[80]	Dry SS	HHV 11.7 MJ/kg dry. 6.8% MC, 37.9% VM, 50% ash, 12% fxc.UA: 29.7% C_4, 4.3% H_2, 4.6% N_2, 1.4% S_8, 59.9% O_2.	20 kW reactor operated for 12h daily with a 20 kg/h capacity (240 kg/day max.) at 1,000-1,150°C.	Gas composition in fraction mole: 1.2% CH_4, 23.3% H_2, 18.5% CO, 13.4% CO_2, 43.6% N_2. 1 kWh electrical power from 1.2 kg municipal sludge gasified could be achieved.
[81]	Dry SS	LHV 9.2 MJ/kg dry, 7.8% MC, 47.8% VM, 47.5% ash. UA: 48.8% C_4, 7.4% H_2, 7.1% N_2, 2.3% S_8, 34.2% O_2.	20 kW dual FBR at 800 °C. Parameters: 2.7 kg/h steam flow, 3.6-5.4 kg/h fuel flow, 1.5 mol/mol molar steam-to-carbon ratio.	Gas yield: 0.85 m^3/kg, CGE of 45-60%. Gas content: 0.1 CH_4 m^3/m^3, 0.46 H_2 m^3/m^3, 0.12 CO m^3/m^3, 0.3 CO_2 m^3/m^3.
[82]	Dry SS	SS: HHV 11 MJ/kg dry, 3.2% fxc, 55% VM, 41.8% ash. UA: 21.86% C_4, 3.4% H_2, 3.8% N_2, 0.64% S_8, and 28.5% O_2.	Reactor at 700-900 °C up to 1h reaction. Applied HTC to SS prior gasification. SS:SD mix ratio of 1:0, 1:3, 1:1, 3:1, and 0:1	At 900 °C, syngas yield was 0.93 m^3/kg, LHV 5.62 MJ/kg dry and gasification efficiency of 67.1%. Gas composition includes approx. 2% CH_4, 5% H_2, 35% CO and 58% CO_2.
[82]	Dry SS and SD	SD-SS: HHV 12-17 MJ/kg dry, 12.8-21.2% fxc, 46.2-6% VM, 13.8-4% ash. UA: 33.3-49.2% C_4, 3.6-5.4% H_2, 1.8-2.7% N_2, 0.2-0.5% S_8, 19-30% O_2.	Lab-scale tubular reactor at 700-900 °C temperature and 1 to 60 min reaction time. Applied HTC to SS prior gasification. SS:SD mix ratio of 1:0, 1:3, 1:1, 3:1, and 0:1.	At 900 °C and mix ratio of 3:1 (SS:SD), syngas yield was 1.04 m^3/kg, LHV 8.15 MJ/kg dry and gasification efficiency of 77.7%. Gas composition includes approx. 7% CH_4, 8% H_2, 45% CO and 40% CO_2.
[83]	SS	64.2% VM. UA: 41.2% C_4, 5.2% H_2, 3.2% N_2, 20.7% O_2, and HHV 14.1 MJ/kg.	Temperature around 750-850 °C, mass rate of sludge around 170–260 g/h.	Syngas yield: 0.45-1.13m^3/kg, LHV 6.5-9.73 MJ/m^3. Gas content: 20-23% H_2, 4-13% CH_4. Biochar HHV between 2.8-14.9 MJ/kg.
[84]	Dry SS	7.1% MC, 51.5% VM, 4% fxc, 37.4% ash. UA: 31.3% C_4, 4.6% H_2, 4.7% N_2, 1.3% S_8, 20.7% O_2. LHV 13.2 MJ/kg.	FBR at 813-817 °C, 60–260 min reaction time, and usage of additives (active carbon, Ni,and Fe)	Syngas LHV 5.04-6.52 MJ/m^3 dry with CGE of 67.5-88.87%. Gas composition: 4-6.5% CH_4, 13.4-28.13% H_2, 10-13.4% CO, 9.4-14.5% CO_2, 44-51.7% of N_2 and other elements.
[85]	Dry SS	LHV 13.1 MJ/kg dry, 8.7% MC, 51.3% OM, 41.7% ash. UA: 29.5% C_4, 4.9% H_2, 4.1% N_2, 1.6% S_8, 15.0% O_2.	FBR with 0.3 air to fuel ratio and 800 °C operating temperature. Sludge feeding rate around 1.2-3.7 g/min, and use DO as catalyst (10% mix with SS)	Without DO, Syngas LHV 2.9-3.6 MJ/m^3 dry, CGE of 35.7-43.2%, gas yield 2.7-3 m^3/kg. Gas: 2.3-3.3% CH_4, 8.5-10.3% H_2, 6.1-9% CO, 13.2-13.9% CO_2. With DO, Syngas LHV 2.9-3.9 MJ/m^3 dry, CGE of 35-48.8%, gas yield 2.8-3.2 m^3/kg. Gas: 2.2-3.2% CH_4, 9.6-14% H_2, 5.3-9.7% CO, 12.6-15.1% CO_2.
[86]	Dry SS	LHV 17.1 MJ/kg dry, 5.3% MC, 61.56% VM, 26.14% ash, 7% fixed. C UA: 39.46% C_4, 5.8% H_2, 5.35% N_2, 0.9% S_8, 24.4% O_2.	Two-stage gasifier (bubbling and fixed FBR) in series. 2 kg/h SS feeding rate, and use AC and CaO as additives (up to 1.5kg). EqR of 0.25 at 785-820 °C.	Products: 52-66% syngas, 19-23% char, 14.3-20.3% condensate liquid and tar. Syngas LHV: 9.22-11.7 MJ/m^3 dry, CGE up to 80%. Gas content: 7.2-8.5% CH_4, 28-52.2% H_2, 15.9-19.3% CO, 20-32.4% CO_2, 3.8-8.9% N_2.
[87]	DEW	SS: LHV 14.26 MJ/kg dry, 18.75% MC, 33.4% VM, 11.6% ash, 36.3% fxc. UA: 45.55% C_4, 6.6% H_2, 1.1% N_2, 1.2% S_8, 33.9% O_2.	2-stage gasifier (FBR and tar-cracking reactors) in series. 800 °C temperature, air flow rate 13-17 L/min for 1h.	Products: 65.5-75.3% syngas, 15-22.4% char, 9% condensate liquid and tar. Syngas LHV: 5.4-6.1 MJ/m^3 dry, CGE of 67-92.4%. Gas content: 4.5-5.4% CH_4, 14.6-22.6% H_2, 9.7-12.4% CO, 10.6-10.9 CO_2, 51.6-54.5% N_2.
[87]	DEW and coal	Coal: 1% MC, 22.5% VM, 17.8% ash, 64.95% fxc. UA: 78.5% C_4, 0.6% H_2, 0.43% N_2, 0.4% S_8, and 2.32% O_2.	2-stage gasifier (FBR and tar-cracking reactors) in series. 800 °C temperature, air flow rate 13-17 L/min for 1h. Coal:DEW mix ratio of 70:30, 50:50, and 30:70.	Products: 74% syngas, 12.5-13.7% char, 11.8-13.3% condensate liquid and tar. Syngas LHV: 5.1-5.4 MJ/m^3 dry, CGE of 80.6-84.3%. Gas: 3.8-4% CH_4, 24-26.6% H_2, 9.5-10.4% CO, 11.1-12.5% CO_2, 46.2-50.8% N_2.
[88]	Dry SS	LHV 15.1 MJ/kg dry, 8.2% MC, 56.9% VM, 30.3% ash, 4.6% fxc. UA: 39.8% C_4, 6.4% H_2, 5.6% N_2, 1.2% S_8, 24.7% O_2.	2-stage gasifier in series with 0.2 equivalence ratio at 760-815 °C, 90-100 min reaction time, and use of AC as additive.	Products: 68.6-76.9% syngas, 12-19.5% char, 6.2-20% condensate liquid and tar. Syngas LHV of 5.4-7.5 MJ/m^3 dry. Gas content: 2.7-7% CH_4, 9.6-34.1% H_2, 9.2-17.2% CO, 6.5-14.6 CO_2, 38.4-64.4% N_2.
[89]	Dry SS	LHV 14.1 MJ/kg dry, 4.7% MC, 51.3% VM, 24.1% ash. UA: 39.46% C_4, 5.8% H_2, 5.35% N_2, 0.9% S_8, 24.4% O_2.	2-stage gasifier. EqR of 13 L/min at 785-810 °C. 10.4-16.6 g/min SS feeding rate for 75-220 min reaction, using additives.	Generated syngas LHV was 5.65-7.1 MJ/m^3 dry. Gas composition: 3.2-5.8% CH_4, 11.8-31.3% H_2, 9.1-18.4% CO, 7.6-14.7% CO_2, 39.5-54.4% N_2.

SS: Sewage sludge; DEW: Dewatered sludge; PMS: Paper-mill sludge; SD: Sawdust; Dlm: Dolomite; HHV: Higher heating value; LHV: Lower hearing value; CGE: cold gas efficiency; MC: Moisture; UA: Ultimate Analysis; fxc: Fixed carbon; sp: straw pellets; OM: Organic Matter; LTCFB: Low Temperature Circulating Fluidised Bed; FBR: fluidised-bed reactor; EqR: Equivalence ratio

c. Pyrolysis

Sludge pyrolysis (also known as liquefaction) operates at temperatures between 350 and 500 °C in a restricted oxygen environment. Some parameters, including temperature, heating rate, residence time, pressure, sludge characteristics, reactor type, and process design, can influence pyrolysis efficiency [71]. The main co-product generated from this process, which can be used as a renewable energy source, is bio-oil, which has a calorific value of 30–37 MJ/kg [90]. Syngas and biochar are also co-products generated that can be used for electricity generation and carbon sequestration or soil amendments, respectively [91]. Various types of pyrolysis have been reported in the literature, with the most prevalent methods outlined in Table 2.5.

Table 2.5: Types of pyrolysis and their characteristics

Type	**Residence time (min)**	**Temperature (°C)**	**Heating rate (°C/s)**	**Pressure (MPa)**
Slow	> 60	300–700	0.1–1	0.1
Intermediate	10	500–650	1–10	0.1
Fast	0.0083–0.33	550–1,250	10–300	0.1
Flash	< 0.0083	800–1,300	> 1,000	0.1
Microwave	30	500–1,000	< 5	–
Vacuum	30–120	300–600	0.1–1	0.01–0.02
Hydro	240	350–600	10–300	5–20

Table 2.6 presents an overview of pyrolysis research on sewage sludge, including municipal sludge from different locations and co-pyrolysis with other substrates. The sludge feedstocks exhibited a wide range of properties, including moisture content (2–79%), volatile matter (27–82%), fixed carbon (0.3–15.6%), ash content (17–63%), and higher heating values (6.56–24.42 MJ/kg). Pyrolysis was conducted using various reactor technologies and approaches, including fluidized bed reactors, bench-scale bubbling or conical spouted bed reactors, microwave-assisted systems, and fast or flash pyrolysis approaches, typically at temperatures ranging from 300–900 °C and atmospheric pressure. Reaction times and heating rates varied depending on the reactor type and study. The generated products included bio-oil, biochar, and syngas, with yields strongly dependent on temperature, feedstock composition, and pyrolysis method. Bio-oil yields ranged from ∼8% to 71%, biochar from ∼14% to 75%, and gas yields from ∼4% to 47%. Gas composition commonly contained 8–59% H_2, 8–18.9% CH_4, 6.5–24.1% CO_2, and 12–31.4% CO, with the gas LHV varying widely (e.g., 5.6–14 MJ/kg in co-pyrolysis studies). Co-pyrolysis with lignocellulosic biomass generally enhanced gas yield and hydrogen content, while catalytic pyrolysis (e.g., with HZSM-5 or ZSM-5) increased biochar and bio-oil quality. In general, these studies demonstrate that feedstock properties, pyrolysis temperature, reactor design, and the use of catalysts or co-feedstocks significantly influence the generated product composition and energy recovery from sewage sludge pyrolysis.

Table 2.6: Studies focused on sewage sludge pyrolysis

Ref	**Sludge**	**Sludge composition**	**Parameters**	**Generated products**
[92]	WWTP in Medellin, Colombia	HHV 6.6 MJ/kg dry, 6.1% MC, 27.24% VM, 3.3% fxc, 63.4% ash. UA: 12.8% C_4, 1.7% H_2, 1.2% N_2, 0.6% S_8, 16.2% O_2	Fluidised bed reactor at atm pressure, and temperature between 300 °C and 800 °C.	At 500-600 °C, bio-char, bio-oil and gas yield were 14-27%, 28-39%, 45-47%, respectively. Gas content at 600-800 °C: 43–50% H_2, 20–37% CO_2, 12–20% CO, and 8–10% CH_3 .
[93]	Municipal WWTP in Dalian, China	76.6% MC, 27.2% VM, 3.3% fxc, 63.4% ash. UA: 12.8% C_4, 1.7% H_2, 1.2% N_2, 0.5% S_8, 16.2% O_2. HHV 13.6 MJ/kg	Sludge pyrolised for 4h under 3 °C/min at 500-800°C.	Char, bio-oil and gas yields were 17.5-25%, 38-43.5%, and 37-42%, respectively.

Continued on next page

Table 2.6 – continued from previous page

Ref	Sludge	Sludge composition	Parameters	Generated products
[94]	Carter's Creek WWTP in Texas, USA	HHV 18.5 MJ/kg dry, 2% MC, 68% VM, 14% fxc, 18% ash. UA: 39.4% C_4, 5.6% H_2, 7.8% N_2, 0.8% S_8, and 28.6% O_2.	Fast pyrolysis using a bench-scale bubbling FBR at 425-550°C.	Bio-oil, biochar and biogas yields: 35.7%, 28.7% and 23.5%, respectively. Bio-oil HHV: 24.3 MJ/kg (at 425°C) and 37.6 MJ/kg (at 550°C). Biochar HHV: 7.4 MJ/kg.
[95]	WWTP in Barcelona, Spain.	HHV 11 MJ/kg, 5.6% MC, 54% VM, 9% fxc, 37% ash. UA: 25.5% C_4, 4.5% H_2, 5% N_2, 2% S_8, 25.8% O_2.	Flash pyrolysis using a CSBR at 450-600°C.	Char and bio-oil yields at 450°C, 500°C, 550°C, 600°C were around 51%, 46%, 44%, 43%, and 45%, 48.5%, 48.5%, 46%, respectively. Gas yield: 4%-11%.
[96]	WWTP in Barcelona, Spain.	same as Ref. [95]	SS fast co-pyrolysis with lignocellulosic biomass in a CSBR.	At 500 °C, yield for the gas, bio-oil and biochar were between 6-12%, 55-62%, and 32-33%, respectively.
[97]	WWTP in Minnesota, USA.	78% MC, 82.2% VM, 0.3% fxc, 17.5% ash. UA: 43.4% C_4, 7% H_2, 5.6% N_2, and 26.4% O_2. HHV 21.21 MJ/kg.	A cfMAP (1 kW, 2,450 MHz) at 450-600°C. Used ZSM-5 as catalyst	Bio-oil, bio-char and gas HHV: 2.2-7.7 MJ/kg, 2.14-5.4 MJ/kg, and 5.6-9.4 MJ/kg. Char, bio-oil and gas yields: 33-62.5%, 16-40%, and 21.5-40%.
[98]	WWTP in Minnesota, USA.	4.5% MC, 68.6% VM, 0.3% fxc, 16.4% ash. UA: 53.24% C_4, 7.4% H_2, 6.12% N_2, and 33.25% O_2. HHV 24.42 MJ/kg.	Microwave pyrolysis (750W, 2450 MHz) at 450-600°C, using HZSM-5 as catalyst.	Char, bio-oil and gas yields: 48-72%, 8-21%, and 20-33%. Oil, char and gas yields using catalyst: 18-21%, and 49-52.5%, and 26.5-31%.
[99]	WWTP in Xi'an, China	SS: 4.5% MC, 63% VM, 5.5% fxc, 27% ash. UA: 29% C_4, 6% H_2, 4% N_2, 1.6% S_8, 21% O_2.	Fast pyrolysis (fixed bed quartz tube reactor) at 500-900 °C.	Char, bio-oil and gas yields: 14-35%, 37.5-71%, and 15-27.5%, respectively. Gas content: 8-36% H_2 and below 7% CH_4
[100]	WWTP in Spain.	UA: 27.9% C_4, 4.7% H_2, 4.5% N_2, 1.4% S_8, 34.6% O_2. HHV 12.5 MJ/kg.	Bench-scale stirred batch reactor at 525 °C.	At 525 °C, the bio-char, bio-oil and gas yields were approx. 50%, 41%, and 9%, respectively. LHV of the pyrolised SS was 10 MJ/kg.
[101]	WWTP in Beijing, China.	SS: 2.25% MC, 61.5% VM, 6.7% fxc. 53.2% C_4, 7.5% H_2, 6.4% N_2, 2% S_8, 30.9% O_2. Cb: 4.6% MC, 78.1% VM, 15.64% fxc. 49.2% C_4, 6.3% H_2, 0.5% N_2, 0.3% S_8, 43.7% O_2.	Reactor at 400-800 °C, pyrolysis rate of 20 °C/min under N_2 (99.99 %, flow rate = 25 ml/min). 1:1 SS:Cb mixing ratio	The yield for char were 30.4-75.1%, and bio-oil around 10.2-51.8%. Gas yield varied between 14.7% and 20% with CH_4 and CO below 10%. H_2 ranged from 22% to 59%, and CO_2 from 35% to 59%.
[102]	Nanjing WWTP, Jiangsu province, China.	SS: 79% MC, 31.5% VM, 5.3% fxc. 21% C_4, 9% H_2, 3.5% N_2, 1% S_8, 3% O_2. SD: 6.2% MC, 73.6% VM, 14.4% fxc. UA: 49.5% C_4, 7.1% H_2, 0.3% N_2, 0.4% S_8, 43% O_2.	Co-pyrolysis of SD and SS in a bed reactor. Parameters: 900 °C at 20 °C/min for 0.5h with 16 g/min feeding rate.	Gas content: HHV vary between 13-14 MJ/kg. Dry gas yield varied from for 0.24-0.74 m^3/kg. The H_2, CH_4, CO_2 and CO varied between 29.13-42.35%, 10.5-18.9%, 14.6-24.1% and 26.8-31.4%, respectively.
[103]	WWTP in Australia.	SS: 20-80% MC, UA: 35.7% C_4, 5.2% H_2, 3.5% N_2, 25.4% O_2, 0.7% S_8 wt%.	Temperature of 450-850 °C, 1 atm and feed rate of 265 kg/h.	Biochar, bio-oil, gas yields: 43.2-53%, 37.7-40.4%, 9.3-17.2%. At 850 °C, gas yield increasd and HHV drop (23 to 20 MJ/kg).

HHV: Higher heating value; LHV: Lower hearing value; VM: Volatile matter; UA: Ultimate analysis; MC: Moisture; fxc: Fixed carbon; wt: wet basis; cfMAP: continuous fast microwave-assisted pyrolysis; SD: sawdust; Cb: Corncob; SS: sewage sludge; FBR: Fluidised bed reactor; CSBR: conical spouted bed reactor

d. Hydrothermal treatment

Hydrothermal treatment applies high pressure and high temperature the sewage sludge in the presence of water in order to generate useful products, including biogas, biofuels, and solid biochar. Hydrothermal treatment methods (see Table 2.7) can be classified in three groups: Hydrothermal Carbonisation (HTC), Hydrothermal Liquefaction (HTL), and Hydrothermal Gasification (HTG). HTC focuses on producing carbon-rich solids (hydrochar) and offers benefits in carbon sequestration and soil enhancement. However, it has lower energy recovery compared to other processes. HTL generates bio-crude oil with high energy density. It requires further upgrading and involves complex operating conditions. HTG efficiently converts organic materials into syngas, and it is highly effective for waste-to-energy conversion, but there are high operational costs and material challenges [71].

Some researchers have investigated the energy potential of the pyrolysis of sewage sludge, as shown in Table 2.7.

Table 2.7: Characteristics of HTC, HTL and HTG

	HTC	**HTL**	**HTG**
Temperature	150-280°C	280-375°C	> 375°C
Pressure	0.1-11MPa	8-22MPa	> 22.1MPa
Water state	Subcritical	Sub/near critical	Supercritical
Generated Products	Solid (char), biocrude (small amount) and gas	Small amount of solid (char), liquid (biocrude), water-soluble fractions	Char (small amount), gas fuel (Syngas), water-soluble fractions
Advantages	Sludge stabilisation, volume reduction, energy recovery, soil conditioner	Can use wet sludge without the need for drying	Can produce high concentrations of hydrogen

Table 2.8 presents an overview of studies applying HTC and HTL to sewage sludge from various WWTPs worldwide. HTC was typically performed at moderate temperatures (100–500 °C) and high pressures (up to 35 MPa) to convert wet sludge into hydrochar, whereas HTL was conducted at higher temperatures (200–400 °C) and pressures to produce biocrude. Feedstock characteristics, including moisture content, volatile matter, and elemental composition, strongly influenced the energy content and yields of products. Hydrochar from HTC achieved HHVs ranging from 12 to 25 MJ/kg, with yields typically above 70% depending on temperature and residence time. HTL generated bio-crude with HHVs up to 45 MJ/kg, with yields of 20–50% depending on operating conditions and catalysts used. Hydrogen and methane production were observed in both HTC and HTL processes, generally enhancing gas yields. Overall, these studies demonstrate that hydrothermal treatments can efficiently convert sewage sludge into solid or liquid fuels, with process parameters and feedstock composition being key factors in determining product quality and energy recovery.

Table 2.8: Studies that applied hydrothermal treatments using sewage sludge

Ref Type	**Location**	**Sewage sludge**	**Parameters**	**Generated products**
[104] HTC	Jiangxinzhou WWTP, in China.	82.5% wt MC, UA: 40% C_4, 6.2% H_2, 6% N_2, 20.5% O_2, 5.6% S_8. 18 MJ/kg HHV	1 L reactor under 35 MPa (max.) and 500 °C (max.)	Gas production: 1.59L (200°C, 2 MPa), and 2.86L (360°C, 19.4 MPa). H_2, CH_4 yields were 0.14 and 0.24 mol/kg (380°C).
[105] HTC	WWTP in Nanjing, China.	89 wt% MC. UA: 25.6% C_4, 4.4% H_2, 4.6% N_2, 22% O_2, 0.2% S_8, 11 MJ/kg HHV	5 reactors, operating at 200-250 °C, and 2-26 MPa.	H_2 yield reached 0.7 mol/kg at 450°C, accounting for 11.2 v/v% of the syngas. At 400 °C, H_2 yield was below 0.15 mol/kg.
[106] HTC	WWTP in Republic of Korea	66.9 wt% VM, UA: 38.55% C_4, 6.46% H_2, 8.05% N_2, 46.50% O_2, 0.44% S_8. 16.5 MJ/kg HHV.	1 L reactor under temperature ranging 180-280 °C for 0.5h.	Fuel HHV around 17.3-22.4 MJ/kg when the temperature was 180-280 °C. Energy recovery efficiency decreased (from 92.2% to 89.6%) with the temperature increase.
[107] HTC	WWTP in Japan.	86 wt% MC, UA: 51% C_4, 6.6% H_2, 8.8% N_2, 32% O_2, 1.4% S_8. 18.8 MJ/kg HHV	180-240 °C under 15-45 min reaction.	Product HHV values: 18.30-20.17 MJ/kg. For temperature higher than 200 °C, ER was 40%.
[108] HTC	WWTP in Changsha, China.	89.3 wt%, 47.5% VM. UA: 25% C_4, 4% H_2, 5% N_2, 15% O_2, 1% S_8. HHV: 11 MJ/kg	0.5 L reactor at 180–300 °C under 30–480 min	Maximum HVV: 12.06 MJ/kg at 260 °C under 1h reaction. Lowest HHV: 9.8 MJ/kg at 260 °C under 3h.
[109] HTC	Domestic WWTP in Sri Lanka.	81 wt% MC, UA: 34.4% C_4, 5.2% H_2, 5% N_2, 23% O_2, 2% S_8. HHV: 15.2 MJ/kg	Reactor operating at 100–200 °C up to 1h.	Maximum (89.01%) and minimum (73.73%) char yields achieved with 13.6-16.2 MJ/kg HHV.
[110] HTC	WWTP in Karmiel, Israel.	UA: 40.3% C_4, 5.8% H_2, 4.7% N_2, 19.4% O_2. HHV: 18 MJ/kg, 81 wt% MC	0.5 L stirred reactor at 200-300 °C up to 2h.	Hydrochar HHV: 18.2 MJ/kg (200 °C) and 21.5 MJ/kg (300 °C). BMP yield (in mL CH_4/gCOD): 26 (lowest) to 236 (highest).
[111] HTC	WWTP in Shimodate, Japan	79 wt% VM, UA: 49% C_4, 7% H_2, 2.5% N_2, 33.4% O_2, 0.6% S_8. HHV: 21 MJ/kg.	0.2 L reactor for 0.5h at 180 °C, and different mixing ratios	SS hydrochar HHV: 21.59 MJ/kg (180 °C, 0.5h), HTC input energy: 115.96-117.7 MJ, Hydrochar HHV: 23.4-25.3 MJ/kg.
[112] HTC	WWTP in Republic of Korea.	72.3 wt% VM, UA: 52% C_4, 8% H_2, 6.4% N_2, 32.6% O_2, 1% S_8 (db), 20.6 MJ/kg HHV	1 L reactor at 180-270 °C under 0.5h reaction.	Hydrochar HHV: 18.7-23.4 MJ/kg (180-270 °C). Char yields: 40.78% (minimum) to 93.13% (maximum).

Continued on next page

Table 2.8 – continued from previous page

Ref Type	Location	Sewage sludge	Parameters	Generated products
[113] HTL	Adelaide Control Plant, in Canada.	62.2 wt% VM, 96.1 wt% MC, UA: 38.0% C_4, 5.23% H_2, 7.2% N_2, 25.2% O_2, 0.75% S_8, HHV of 16.0 MJ/kg.	0.1 L reactor under 2 MPa at 200-350°C up to 1h reaction.	Oil, solid and water-soluble products (WSP) content: 11.3-33.6 wt%, 9.9-61.2 wt%, and 27.3-62.3 wt%. Up to 0.8L of biogas was produced in 31 days.
[114] HTL	WWTP at Viborg, Denmark.	4 wt% DM, UA: 46.5% C_4, 6.1% H_2, 3.3% N_2, 31.2% O_2, 0.4% S_8, HHV: 20 MJ/kg	20l reactor with 1.66L/min feeding rate at 350°C.	Bio-crude yield: 24.5 wt% with 33.6% chemical ER, 26.9 MJ/kg HHV.
[115] HTL	Marselisborg WWTP, in Denmark	Not informed	20 mL batch reactor at 340 °C under 20 min reaction	HHV: 36-37.7 MJ/kg with 55.5-66.8% ER. Bio-crude, gas, solid products yields: 30.7-35.4%, 9.7-16.2% and 19.5-19.6%.
[116] HTL	Daugavgriva municipal WTTP in Riga, Latvia.	80.5 wt.% MC, 56.8% VM, UA: 52.0% C_4, 7.6% H_2, 7.5% N_2, 30.4% O_2, 2.6% S_8, HHV: 15.3 MJ/kg	Batch autoclave reactor at 200-300 °C under 10-100 min reaction	Highest bio-oil yield: 47.8 wt.% with 70% ER, at 5.0 MPa, 300 °C and 40 min. Lowest: 34.5% with 52% ER and 36.2 MJ/kg HHV, at 200 °C.
[117] HTL	WTTP in Aalborg Forsyning, Denmark.	73.4 wt.% MC, 50.5%, VM UA: 51% C_4, 7.2% H_2, 7% N_2, 34.8% O_2, 1% S_8, HHV: 22 MJ/kg	0.1 L reactor at 350-400 °C, 10 MPa pressure, and 15 min reaction time	Bio-crude HHV at 350 °C was 35.3 MJ/kg (no catalyst) and 36.6 MJ/kg (with catalyst, and ER was 64% (no catalyst) and 74.6% (with catalyst)
[118] HTL	Beishiqiao WWTP in Xi'an, China	90 wt.% MC, UA: 33.9% C_4, 5.1% H_2, 5.8% N_2, 16.5% O_2, 3.2% S_8, HHV of 16.1 MJ/kg	4.4 mL batch reactors under 18 MPa and 260-350 °C	Highest biocrude: 35.4 MJ/kg HHV, 50.2% ER, at 340 °C. At 260 °C, ER was 32.6%.
[119] HTL	WWTP in State College, PA, USA.	97.8 wt.% MC, UA: 46.5% C_4, 7.0% H_2, 2.1% N_2, 33.3% O_2, 0.8% S_8, HHV of 19.9 MJ/kg	Isothermal (673 K, 1h), non-isothermal (773 K, 1 min).	Biocrude yield: with additives was 10.2-21.7 wt%, isothermal was 25-29 wt%, and non-isothermal was 10.9-27.5 wt%.
[120] HTL	Qinghe WWTP, in China.	53.5 wt.% OM, UA: 44.7% C_4, 7.6% H_2, 7.2% N_2, 39.6% O_2, 1% S_8, HHV: 21.3 MJ/kg	1 L stainless reactor, 400 °C (max.) and 20 MPa.	Bio-oil HHV was 29.05 MJ/kg (no treatment), and reached up to 45 MJ/kg (with treatment).
[121] HTL	Qinghe WWTP, in China	84.5 wt.% MC, UA: 46.7% C_4, 6.8% H_2, 8.1% N_2, 37.6% O_2, 0.8% S_8.	0.6 L reactor at 210-330 °C, 30 MPa under 0.5h.	Biocrude yield at 210 °C: 39.9% with LC was 86.3%, att 270 °C, it was 47.5% and 97.7%, and 330 °C, 40.8% and 90.1%.
[122] HTL	WWTP in China.	UA: 28.9% C_4, 4.5% H_2, 4.2% N_2, 13.9% O_2, 0.6% S_8.	0.5 L at 350-400 °C, for 0.5h, 35 MPa	Bio-crude HHV: 37.8-39 MJ/kg (HHV was 37.4 MJ/kg forr SS with no pyrolysis)
[123] HTL	WWTP in Doha, Qatar.	HHV: 17 MJ/kg, 83.6 wt.% MC, UA: 30.5% C_4, 6.2% H_2, 5.5% N_2,	0.1 L reactor under 30-120 min and 275-400 °C.	For 0.5h reaction at 350 °C, maximum and minimum biocrude yield were 44.8% and 20%.
[124] HTL	H.C. Morgan WPPT, in USA.	82 wt.% MC, 53% VM, UA: 33% C_4, 5% H_2, 5% N_2, 26% O_2, 1% S_8, HHV: 14 MJ/kg	1.8 L reactor at 350 °C, and 1h. Used red mud (RM) catalyst.	The biocrude yield varied between 27.1-38.3%, and HHV was 28.3-30.4
[125] HTL	WWTP in Shenyang City, China	84.9 wt.% MC, UA: 40.6% C_4, 4.7% H_2, 3.7% N_2, 49.6% O_2, 1.2% S_8, HHV: 14 MJ/kg	Batch-type 0.5 L reactor at 340 °C and 40 min reaction time.	Bio-oil HHV was 32.2 MJ/kg. With treatment, and increased to 33.5-35.3 MJ/kg with maximum value of 37.2 MJ/kg

BMP: Biomethane Potential; MC: Moisture; UA: Ultimate Analysis; db: dry weight basis; OM: Organic Matter; WSP: Water-soluble products; ER: Energy recovery; LC: Liquefaction conversion; HHV: Higher heating value

e. Supercritical water

There are two main methods to treat sewage sludge via supercritical water technologies: supercritical water gasification (SCWG) and supercritical water oxidation (SCWO). SCWO and SCWG (also known as HTG) are considered promising technologies for treating organic wastes, including sewage sludge, because they not only generate fuel gases (including hydrogen), but also have low environmental and social impacts. In supercritical water processes, the feedstock (i.e., sewage sludge) is subjected to a supercritical water environment (temperature and pressure higher than 374 °C and 22.1 MPa), and the organic compounds in the feedstock are dissolved. The by-products of SCWO are typically water vapour, carbon dioxide, and hydrogen (can be generated as a secondary product depending on the composition of the feedstock and reactor operation conditions), whereas the SCWG method generates syngas, which is primarily composed of hydrogen but also contains smaller amounts of carbon dioxide and methane. The composition of the gases generated from SCWO and SCWG may vary depending on different factors, including the feedstock composition, temperature, pressure, residence time, and the presence

of catalysts [18], [126], [127]. Some companies, such as General Atomics, EcoWaste Technologies, Chematur, and Supercritical Fluids International, have been developing both small and large-scale SCWO systems that can be applied to a range of areas, including wastewater treatment [126]. Ref. [127] studied different SCWO systems (small and large-scale systems), which were implemented in different locations across several years and based on different feedstocks, including sewage sludge. The authors summarised the main information of different systems, highlighting their location, year of construction, company name, system capacity, and feedstock type. They also highlighted the common operation challenges, which include (i) corrosion due to both a high temperature and pressure, (ii) corrosion due to acid formation, (iii) salt precipitation or plugging, and (iv) high energy consumption and operating costs. Some of the plants stopped operations due to technical and/or economic reasons. Ref. [128] reviewed supercritical technologies exploring their influence on hydrogen production based on different parameters (i.e., sludge properties, moisture, and temperature). They presented some real-world projects, including small and large-scale plants, including the pilot-scale systems developed by Duke University, University of Missouri, University of Valladolid, and Xi'an Jiaotong University). Commercial projects were also highlighted as follows:

- HydroProcessing: An SCWO system implemented in the Harlingen WWTP in Texas, USA, in 2001. Some operating parameters of this system included a 150 ton/day capacity, 592 °C temperature, 24.5 MPa pressure, 20–90 s reaction time, and 6–9% solid content. The consumption of heater, oxygen, and pumps were 4.1 MWh/dry ton of sludge, 1.5 ton/dry of ton sludge, and 0.55 MWh/dry ton of sludge, respectively. The capital and operating costs of the project were about US$3 M and US$100/dry ton of sludge, respectively.

- Chematur AB: Two SCWO systems were developed: (i) the first system had a 250 kg/h capacity for demonstration purposes, and (ii) the second had a capacity of 1.1 ton/h, built with a plan to treat the sewage sludge of Kobe, Japan. The operational parameters of the second system included a 25 MPa pressure, 30–90 s reaction time, 400–600 °C, and operation at 15% dry solids. The consumption of natural gas, oxygen, cooling water, and electricity was around 21.9 Nm^3/dry ton sludge, 1.05 ton/dry ton sludge, 100 m^3/dry ton sludge, and 228.6 kWh/dry ton sludge, respectively. The capital and operating costs of the project were about £5 million and £70/dry ton sludge, respectively.

- SuperWater solution: It was implemented at the Iron Bridge Regional Water Reclamation facility in Orlando, USA. Tested between 2009 and 2011, the SCWO system had a capacity of 5 t/d. The capital and operating costs were around US$268/dry ton sludge and US$33.7 million, respectively. The system's parameters included 35 dry ton sludge/d capacity, a 600 °C operating temperature, 26 MPa pressure, a 30–60 s reaction time, and 10% dry sludge.

Table 2.9 summarises research on SCWG of sewage sludge for hydrogen production. Feedstocks generally had high moisture content (35–88 wt%) and variable organic and elemental composition. SCWG was typically performed at high temperatures (380–750 °C) and pressures (20–30 MPa), using batch or continuous reactors. Reaction times varied from seconds to 1h. Hydrogen yields were strongly influenced by temperature, residence time, catalysts, and feedstock composition. Maximum hydrogen production ranged from ∼0.12 mol/kg (low temperature/no catalyst) up to ∼11.8 mol/kg (600 °C), with hydrogen content in gas streams reaching 38–60 vol% in some studies. Methane and carbon dioxide were also produced, but in smaller amounts. In summary, these studies show that SCWG can efficiently convert wet sewage sludge into hydrogen-rich gas, with higher temperatures, appropriate catalysts, and optimised residence times leading to improved hydrogen yield and gas composition.

Table 2.9: Studies related to supercritical water gasification on sewage sludge

Ref	Location	Sewage sludge	Parameters	Gas production
[129]	WWTP in Jiangsu, China.	74-88% wt MC, UA: 7.6-31% C_4, 2.3-6.2% H_2, 0.4-3.5% N_2, 20.2-34.1% O_2, 1-3.3% S_8, 14 MJ/kg HHV	316 L batch reactor at 400°C and 1h reaction .	Gas production: 10.7-43.3 mol/kg (average of 18.9 mol/kg).
[130]	Beishiqiao WWTP, in China.	84% wt MC, UA: 38.2% C_4, 2.4% H_2, 4.7% N_2, 23.7% O_2, 1% S_8, LHV: 14.6 MJ/kg	Batch reactor (70°C/min) at 550-750 °C and 30 MPa	H_2 production up 18.9 mol/kg under 750 °C and 20 min
[131]	WWTP in Zhengzhou, China .	79% wt MC, 65% wt OM, UA: 7.4% C_4, 15.5% H_2, 1.3% N_2, 55.7% O_2, 0.88 g/L TOC	0.6 L batch reactor at 380-460°C, 27 MPa, 6 min retention time.	H_2 production (in mol/kg): 2.5 (380°C), 19.9 (460°C). CH_4 was 1.8 (380 °C), 8.2 (460 °C).
[132]	WWTP in Jiangsu, China.	77-88% wt MC, UA: 7.6-27.5% C_4, 2-5.2% H_2, 0.4-3.8% N_2, 13-34% O_2,, 1-2.5% S_8, 12.6 MJ/kg HHV	316 L batch reactor at 400°C, 10 min reaction and 24 Mpa .	With no catalyst, H_2 yield was 1.06 mol/kg, With catalysts, H_2 was between 2.68 and and 4.8 mol/kg.
[133]	WWTP in Nanjing, China.	83.2 wt% MC, 45.1 wt% OM, UA: 19.5% C_4, 3.7% H_2, 3.2% N_2, 18.5% O_2, 0.2% S_8, 8.7 MJ/kg HHV	316 L batch reactor at 400°C, 1h reaction time and 22.1 MPa.	With 2-10 wt% Ni, H_2 yield was 0.6-1.05 mol/kg. With H_2O_2, H_2 yield decreased from 0.31 mol/kg (2 wt%) to near 0.01 mol/kg (10 wt%).
[134]	WWTP in Jiangsu, China.	74 wt% MC, 26.2 wt% OM, UA: 13% C_4, 2.1% H_2, 1.9% N_2, 4.2% O_2, 1% S_8, 4.8 MJ/kg HHV	316 L batch reactor at 400°C, 0.5 reaction time	H_2 yield: 0.16 mol/kg (no FA), 0.52 mol/kg (1 wt% FA), 1.2 mol/kg (2 wt% FA), 3.47 (4 wt% FA), and 10.07 mol/kg (6 wt% FA).
[135]	WWTP in Japan.	79.16 wt% MC, UA: 43.1% C_4, 6.6% H_2, 4.4% N_2, 25.9% O_2, 2.4% S_8	316 L continuous reactor at 500-600 °C, 5-60s, and 25 MPa.	H_2 content: 38.5-39.4 vol% (550-600 °C). CO_2 content: 49.5 vol% (500 °C)
[136]	Domestic WWTP in Japan.	78.8 wt% VM, UA: 38.3% C_4, 5.9% H_2, 7.9% N_2, 33% O_2, 1% S_8.	Bench-scale reactor under 600°C, 23 MPa and 1h reaction time.	Total gas yield of 9.8 mol/kg with a composition of 60% H_2.
[137]	WWTP in Nanjing, China.	75 wt% MC, 41 wt% OM, UA: 19.5% C_4, 3.7% H_2, 3.2% N_2, 14.3% O_2, 0.2% S_8, 9.5 MJ/kg HHV	Batch reactor under 23 MPa, 400 °C for 10 min.	H_2 yield: 0.12 mol/kg (no catalyst) and 0.47 mol/kg (1 cycle of Ni).
[138]	WWTP in Hangzhou, China.	35.1 wt% VM, 57.4 wt% OM, UA: 18.9% C_4, 2.2% H_2, 2.9% N_2, 12.8% O_2, 0.6% S_8, 5.9 MJ/kg LHV	0.5 L batch reactor under 26-28 MPa and 380-460 °C for 1h.	H_2 yield was 6.44 mol/kg with 38.4% of H_2 composition.
[139]	Paşaköy WWTP, in Turkey	57.4 wt% VM, UA: 29.4% C_4, 4.4% H_2, 18% O_2, 5.3% N_2, 0.5% S_8.	3.12 L reactor (20 L feeding tank), and 25 mL/min flow	H_2 production: increase from 3.4 L/h (500 °C) to 4.5 L/h (650 °C).
[140]	Xi'an WWTP, in China.	87% wt MC, 51 wt% VM, UA: 37.6% C_4, 4.4% H_2, 5.7% N_2, 24.4% O_2, 0.8% S_8, 9.64 MJ/kg HHV.	Batch reactor under 25 MPa pressure and 20 min reaction time.	H_2 yield (in mol/kg): 0.66 (400 °C), 1.93 (450 °C), 3.95 (500 °C), 7.44 (550 °C) and 11.81 (600 °C).

TCOD: Total Chemical Oxygen Demand; SCOD: Soluble Chemical Oxygen Demand; TSS: Total Suspended Solid; VSS: Volatile Suspended Solid; VFAs: Volatile Fatty Acids; TOC: Total organic carbon; UA: Ultimate Analysis; OM: Organic Matter; MC: Moisture;

2.2.1.3 Transesterification

The transesterification of sewage sludge is a chemical process in which the triglycerides/lipids (i.e., fats, oils, and greases) present in the feedstock are converted into biodiesel and glycerol by reacting them with an alcohol (usually methanol or ethanol) in the presence of a catalyst (typically an alkaline catalyst). This reaction produces methyl esters (biodiesel) and glycerol as by-products. The biodiesel produced is a fatty acid methyl ester (FAME) that can be used as a renewable fuel in diesel engines. It has properties similar to conventional diesel fuel but is derived from biological sources [141]. Two main techniques, lipid extraction and esterification/transesterification or direct in situ esterification/transesterification, are used to produce biodiesel from sewage sludge. Biodiesel production from sewage sludge can be divided into five main steps: (i) sludge pre-treatment (to improve lipid extraction), (ii) lipid extraction from sewage sludge, (iii) use of extracted lipids to generate biodiesel, (iv) use of catalysts (to optimise the process), and (v) extraction of valuable by-products. This process provides a great alternative to managing sewage sludge by reducing its volume and converting waste into a useful product [25]. Pyrolysis also generates biodiesel from sewage sludge, but not directly.

The byproducts of pyrolysis include gaseous products, solid char and bio-oil. The bio-oil can be further processed and refined to be converted into biodiesel. Pyrolysis can be adjusted to increase the desired bio-oil fraction and, consequently, biodiesel production [142].

Table 2.10 presents studies converting sewage sludge into biodiesel via transesterification and pyrolysis. Feedstocks included primary and secondary sludges from various WWTPs worldwide, often pretreated by drying or lipid extraction. Transesterification typically uses alcohols (methanol or ethanol), acid/base catalysts (e.g., H_2SO_4, KOH, KOH/AC) on its process, with reaction times of 0.5–24 h at 45–105 °C. Pyrolysis treatments used higher temperatures (150–650 °C) with short to moderate reaction times. Biodiesel yields varied widely, from ∼1–73% FAME depending on catalyst type, extraction method, temperature, and reaction duration. HHV of the produced biodiesel and bio-oil ranged from ∼36–44 MJ/kg. Enhancements using treatments, such as microwave, sonication, ultrasonication, or optimised catalysts, significantly increased lipid extraction and biodiesel yields. Generally, these studies show that sewage sludge can be a feasible feedstock for biodiesel production, with process optimisation strongly influencing yield and energy content of the final product.

Table 2.10: Studies on biodiesel production from sewage sludge

Ref	Type	Material	Operational parameters	Generated products
[143]	P	WWTP in Texas, USA.	Bench-scale FBR at 150-300 °C, 1-3 ratio of ethanol:bio-oil ratio. 2-4hs reaction time and Ni/HZSM5 as catalyst	Bio-oil HHV: 36.43 MJ/kg, Biodiesel HHV: 39.97 MJ/kg. Sludge-biodiesel max. yield of 89.33% at 150 °C and 3h reaction time.
[144]	T	WWTPs in Beijing, China	SS heated (45-75 °C), and added to methanol, H_2SO_4 and hexane for 8h.	Biodiesel yield: between 14.9% (average) and 16.6% (maximum) at 60 °C.
[145]	T	WWTP in Universidad Rey Juan Carlos, Spain	Extraction time of 2.5-4hs, Zr-SBA-15 catalyst used. Parameters: 209 °C; 2000 rpm, 50:1 methanol to saponifiable ratio and 12.5wt% catalyst, 3-6h reaction	Lipids extracted: 2.1wt% (SSS), and 7.4-13.6wt% (PSS). Lipid fraction for PSS using n-hexane was 17-46wt% for glycerides, FFA and unsaponifiable matter, 5.2-52 wt% using methanol. SSS using methanol: 17-62.3%. FAME yield: 6-15.5 wt%.
[146]	T	WWTP in Osong City, Korea.	1 L reactor using dewatered SS, methanol, n-hexane, and H_2SO_4. Reaction time of 1-8h at 55-105 °C	Maximum biodiesel yield: 8-9.7% (n-hexane), and 10 mL/g (methanol)
[141]	T	WWTP in Tamil Nadu, India.	Lipid extraction: 6 h using 50 mL of chloroform methanol (2:1 ratio), diethyl ether, n-hexane and ethanol	Lipids composition: 2-6.5g with 24.5-32.5% purity. Biodiesel properties: 40.6-43 MJ/kg HHV, 89.2-91.2% ester, cetane number: 65-72.6, saponification: 131-162 (mg of NaOH).
[147]	T	WWTP in Villapérez-Oviedo (Asturias, Spain).	Solvents: Hexane and methanol, extraction using 1:2 SS:hexane ratio. Samples stored after 1h drying at 105 °C. Solid-liquid extraction: 1:10 dry SS:hexane ratio for 4h, 9 extraction cycle/h. Mixture heated at 55 °C for 24 h.	Maximum production: 0.4g FAME/100 g dry SS (26.8% lipid extracted) for 24h reaction. Total lipids extraction: 9% (1.75g lipids/100g dry SS) using hexane. Using methanol (4% v/v), FAME concentration of 2.1% was. 0.4% obtained on solid-liquid procedure.
[148]	T	Municipal WWTP in Oviedo, Spain	Operation at 60 °C for 24 h using methanol at 4-70% fractions. 1:10 SS: methanol ratio. For the acid catalysis, H_2SO_4 in methanol (4% v/v) mixed with SS. Microwave, sonication and particle sieving used for lipid extraction.	Maximum biodiesel yield: 14.3% (FAME mass/ lipid content). Biodiesel yield for 5h reaction: 22.2% (0.4% H_2SO_4), and 7-14.5% (30-70% NaOH). FAMEs production and sonication increased by 110% (from 22.1 to 46.7%) and by 42% when used microwave.
[149]	T	Gangneung WWTP, in Korea.	0.08% (w/w) alkaline/acidic catalysts with 40 mL/g-lipid methanol and 20 mL/g-lipid n-hexane at 50°C for 24 h. Biodiesel extracted twice with n-hexane, centrifuged, separated and dried for 24h.	Carbohydrate, crude lipid, ash, crude protein were 9%, 14.5%, 18%, and 43%. Lipid content using ethanol and methanol was 3-5.7%. Lipid extraction was 10-14.5% under BDM, microwave, autoclave and ultrasonication treatments.
[150]	T	WWTP in Beijing, China	KOH, KOH/AC, and KOH/CaO used as catalysts. Optimised reaction for KOH/AC used SS:methanol ratio of 1:10 at 60°C, 300 rpm, for 8 h.	Biodiesel yield: 1.2%, 6% and 6.8% using KOH, KOH/CaO and KOH/AC as catalysts, respectively. H_2SO_4 considered better catalysts.

Continued on next page

Table 2.10 – continued from previous page

Ref	Type	Material	Operational parameters	Generated products
[151]	T	WWTP in Beijing, China.	SO_4^{2-}/Al_2O_3-SnO_2 catalysts prepared by 79 wt% of H_2SO_4. Mix: 10g SS, 0.2L n-hexane, 0.2L ethanol at 80 °C for 10h. 0.4-1.2g catalysts, 50 mL n-hexane, 128 mL methanol under 130-170°C for 0.5-6 h	Biodiesel yields: 50-57% at 130-170 °C, and increased from 33.7% to 73.3% under 0.5h-4h reaction, but for 6h, it was 72.1%. Highest FAME yield: 73.3% at 130 °C and 4h (10g dry SS with 0.8g catalyst).
[152]	T and P	Jungnang WWTP in Seongdong-Gu, Seoul city, Korea.	10g dried SS, 0.2L hexane solvent used to extract lipids at 80 °C for 24 h. Evaporator at 80 °C for 3 h used to extract solvent. SSRB was produced by pyrolysis. 20 g SSR used at 600 °C for 4h.	Highest biodiesel yield: 33.5 wt.% per SS extract at 305 °C via thermally induced transesterification for 1 min. Biodiesel yield from (trans)esterification was less than 1% with 5 wt.% H_2SO_4
[142]	P	WWTP in Pavia, Italy.	Microwave operating conditions: 180-650 °C and 1-28 min reaction	Highest value of oil to sludge: 25% at 280 °C, 8 min reaction. Lowest: 7% at 180 °C and 50 min

P: Pyrolysis; T: Transesterification; SSRB: Solid residue biochar; BDM: Bligh and Dyer method; PSS: Primary sludge; SSS: Secondary sludge; FAME: Fatty acid methyl esters.

2.2.1.4. Microbial Electrolysis Cell

A Microbial Electrolysis Cell (MEC) is an anaerobic process that converts organic matter contained in the wastewater into renewable fuel (mostly methane or hydrogen). MECs can utilise either wastewater or sludge as feedstocks, and this technology has the potential to reduce the costs associated with wastewater treatment and sewage sludge disposal, which are often the two main operating costs in a WWTP. In an MEC, the organic matter is oxidised through bacteria in the anode electrode, and hydrogen is produced as a by-product in the cathode by using a small electric voltage. An MEC's performance can be measured in terms of organic removal and hydrogen production, and is directly dependent on the magnitude of the electric voltage. Usually, when an MEC is fed with municipal wastewater, the electric current generated is low which is expected since municipal wastewater is known for its low organic matter content when compared to other feedstocks. This is one of the key challenges of applying this technology when used to treat municipal wastewater. The first commercial MEC reactor (Ecovolt) was developed by Cambrian Innovation to treat high-strength wastewater [153].

Small-scale experiments using MEC and domestic wastewater as feedstock have been reported in the literature, as shown in Table 2.11. Dual- and single-chamber MECs were employed, ranging from 0.42 L to 175 L, considering different anode-to-cathode area ratios. Operational parameters varied, including HRT from 4h to 8 days, temperatures between 21–40 °C, and stirring or semi-continuous feeding modes. Hydrogen production rates ranged from 5.2 to 145 L/m^2.d with purities up to 95%, while methane yields were 77–111 L/kgCOD depending on conditions. COD removal efficiencies ranged from 25% to 73.5%, and energy recovery reached 48.7% in some studies. These findings demonstrate that MECs can effectively produce biohydrogen or methane from municipal wastewater under controlled small-scale conditions.

Table 2.11: Studies on MEC technology applied to municipal wastewater

Ref	Feedstock	Operational parameters	Generated products
[154]	Wastewater from Howdon WWTP, in Newcastle, UK	100 L dual-chamber MEC with 6 cells cassettes (88 L). Surface area: 16.4 m^2/m^3 (anode), 3.4 m^2/m^3 (cathode) with 4:1 anode-cathode ratio	Constant H_2 generation for 1 year of 7L/m^3.d. Average energy recovery and coulombic efficient were 48.7% and 41.2%.
[155]	Wastewater from Rubi WWTP, in Barcelona, Spain	130 L dual-chamber MEC with 10 cells cassettes. Anode-to-cathode ratio volume of 3.5:1, and used an anionic exchange membrane (AEM) to separate the chambers.	H_2 production was 32 L/m^3.d with 95% of purity (5% was CH_4). The OM removal efficiency was around 25% for a 2 days retention time and OLR of 0.25 gCOD/L.d.
[156]	Domestic WWTP in England	175 L dual-chamber MEC (specific area: 13 m^2/m^3 (cathode), 34 m^2/m^3 (anode)), and 5h HRT.	Average H_2 production of 5.2 L/m^3.d with 93% purity, and 63.5% COD removal

Continued on next page

Table 2.11 – continued from previous page

Ref	Feedstock	Operational parameters	Generated products
[157]	Gold Bar WWTP in Alberta, Canada	Dual-chamber MEC (0.42L Anode, 0.17L cathode) with 40 cm^2 membrane. Semi-continuous fed mode (45 mL/d), 8 days residence time	H_2 production rate: 145 L/m^3.d and the COD removal efficiency was up to 73%.
[158]	Sludge from the J WWTP in Jinju, Republic of Korea	2.5 L reactor (16 mm spacing anode-cathode). Reactors operated at 30°C, 35°C and 40°C for 6 days, stirred at 100 rpm. 7:3 Raw:seed sludge mix ratio	CH_4 production: 111 L/m^3 (35°C), 85 L/m^3 (30 °C), and 98 L/m^3 (40°C). CH_4 yield (in L/kgCOD): 77.1 (40°C) to 82.1 (30 °C)
[159]	SS collected from a WWTP in Leon, Spain.	Single-chamber 3L membraneless MEC (batch and continuous operation) at 21 °C with different HRTs (4, 8, 12 and 24h)	CH_4 production rate of 1.4 L/m^3.d and 54% COD removal. Energy and net consumptions was 2.9 and 2.1 kWh/kgCOD.

2.2.1.5. Microbial Fuel Cell

Microbial fuel cells (MFCs) are similar to MEC, but it converts the organic matter contained in the municipal wastewater into electricity directly. In this process, the MFC converts chemical energy contained in the organic compounds into electrical energy under anaerobic conditions through the catalytic reactions of microorganisms. Bacteria oxidise the organic matter contained in the wastewater at the anode, and the reduction reaction occurs at the cathode. During the oxidation, electrons are released and transferred to the anode, generating the electrical current that drives the MFC. When the electrons reach the cathode, they are combined with electron acceptors (i.e., oxygen) and protons (i.e., hydrogen) to generate water and close the electrochemical circuit. The main parameters that influence the performance of MFCs include the pH, temperature, substrate characteristics, bacterial activity, electrode materials, and internal resistance. MFCs vary in design, size, and power density. For example, small-scale cells can have a high-power density (i.e., above 500 W/m^3), while large ones may have lower density (i.e., 30 W/m^3). The MFC scale-up usually occurs via enlarging the single reactor or combining multiple reactors in one system. MFC technology has been receiving much attention in research, but it is still in the early stages of development [160], [161]. The main drawbacks of MFCs include the process efficiency, power density, longer start-up times, performance variability, and sensitivity. However, the main advantages of MFCs include energy savings (i.e., aeration and sludge treatment processes) and reduced sludge production. MFCs can operate in either batch or continuous mode, which usually depends on the wastewater characteristics, cell design, microorganism groups, and electrode materials [161]. Table 2.12 summarises studies on MFC technology applied to municipal and domestic wastewater treatment. The reported performance varies widely due to differences in microbial activity, electrode materials and configurations, system design, substrate type and concentration, and operating conditions. COD removal ranged from 13% to 95%, energy recovery between 0.0034–0.060 kWh/m^3, and coulombic efficiency ranged from 4.7% to 75%. Operation times and HRT also differed substantially, from hours to over a year. These results highlight that MFC performance is highly system- and site-specific, and optimising multiple parameters is critical to achieving consistent wastewater treatment and energy recovery.

Table 2.12: Studies related to MFC technology using municipal or domestic wastewater

Ref	Feedstock	Wastewater COD	MFC System	COD rem.	Power density	ER	CE	OT and HRT
[162]	WW from 2 WWTPs (Xiao Jiahe and Yong Feng WWTPs), in China.	60-100 mg/L (Xiao Jiahe), 0.2-0.4 g/L (Yong Feng)	1,000 L system (50 stacked modules, 20 L each)	70-80%	60 W/m^3	0.033 kWh/m^3	41-75%	100 days to 1 year, and 2h HRT.

Continued on next page

Table 2.12 – continued from previous page

Ref	Feedstock	Wastewater COD	MFC System	COD rem.	Power density	ER	CE	OT and HRT
[160]	WW from Pepper's Ferry Regional WWTP, USA.	155 mg/L	96 tubular MFC modules (2L liquid each)	76.8%	NI	0.006 kWh/m^3	NI	1 year, 18h HRT
[163]	Primary WW from the Pennsylvania State University WWTP, USA.	376-428 mg/L.	3 cells size: 0.028 L, 0.22 L and 85 L. Cathode area: 7.3 to 15 m^2/m^3	75-80%	83 to 304 W/m^3	NI	13-27%	NI
[164]	Pennsylvania State University WWTP, in US.	480 mg/L (raw), 1.01 g/L (acetate)	2L reactor, 0.86 L anode volume; CaSA: 29 m^2/m^3.	57%	22 W/m^3	NI	4.4%-42%	8h HRT
[165]	WW from Haeundae WWTP, in Korea	144 mg/L	5 MFC in series. CaSA: 400 m^2/m^3	34%	16.7 W/m^3	NI	12%	8 months, 2.5h HRT
[166]	Primary WW from a municipal WWTP, in Switzerland	200-450 mg/L	1m^3 system (64 MFC units with 16.25 L each)	34.4-95.4%	NI	0.015-0.060 kWh/m^3	4.7-14.9%	18 months
[161]	Primary clarifier WW of a WWTP, in Switzerland	Up to 130 mg/L	45 L (4 units with 11.2L each) in a full-scale WWTP.	13.5-67%	73-82 mW/m^2	0.012 kWh/m^3	24.8%	9 months, 12-44h HRT
[167]	Mumbai municipal WWTP, in India	1,650 mg/L	0.7 L system	68%	621 mW/m^2	NI	47-48%	NI
[168]	Al Gabal Al Asfar WWTP, in Egypt.	92-350 mg/L	2x0.3L chamber (anode-cathode)	Up to 72.85%	117-209 mW/m^2	NI	NI	24h HRT
[169]	Taiping municipal WWTP, in China	200-350 mg/L	1.5m^3 system	63%-92%	406 mW/m^3	0.0034 kWh/m^3	NI	5h HRT

WW: Wastewater; CE: Coulombic efficiency; OT: Operation Time; ER: Energy Recovery; CaSA: Cathode surface area

2.2.1.6. Hydropower

Hydroelectric power is known as one of the most economical and popular energy resources. Hydropower is an affordable source of electricity, and compared to other sources, it has a relatively low cost during the project lifespan in terms of maintenance and operation costs. It is a flexible type of renewable energy resource that can be widely applied in WWTPs by using the water flow potential to generate renewable energy [170]. In a WWTP, the possible locations for installing a hydropower system typically include the upstream (raw/untreated wastewater) or downstream (treated effluent). Usually, it is classified based on size, including micro (1–100 kW), mini (0.1–1 MW), small (1–10 MW), and large (above 10 MW). The power output from a hydropower turbine is directly dependent on the water flow rate and available head. There are different types of hydropower turbines available in the industry, including the Archimedes screw, Crossflow, Francis, Kaplan, Pelton, and Propeller [171]. Ref. [171] listed 46 WWTPs that had installed hydropower systems (17 micro, 22 mini, and 7 small). Among them, 12 plants used Pelton turbines, 10 used Kaplan, 2 used the Propeller type, 2 used Francis, 2 used pumps working as turbines (PATs). The adoption of hydropower technology appears less attractive compared to other renewable energy technologies. Table 2.13 illustrates hydropower plants installed at different WWTPs [172].

Table 2.13: Hydropower plants installed in WWTPs

WWTP	Location	Turbine type	Capacity (kW)	Flow (m^3/s)	Head (m)
North Head, Sydney	Australia	Kaplan	4,500	3.5	60
Emmerich	Germany	Archimedes	13	0.4	3.8
As Samra	Jordan	Pelton	1,600	3.2	104

Continued on next page

Table 2.13 – continued from previous page

WWTP	Location	Turbine type	Capacity (kW)	Flow (m^3/s)	Head (m)
As Samra	Jordan	Francis	1,680	-	41
Aïre, Geneva	Switzerland	Kaplan	200	3.2	5
Engelberg	Switzerland	Pelton	50	0.16	54.4
Grächen	Switzerland	Pelton	262	0.09	365
La Douve I, Leysin	Switzerland	Pelton	430	0.08	545
La Douve II, Leysin	Switzerland	Pelton	75	0.108	83
Morgental, St. Gallen	Switzerland	Pelton	1,350	0.84	190
Profay, Le Chable	Switzerland	Pelton	350	0.1	449
La Asse, Nyon	Switzerland	Pump as turbine	220	0.293	94.3
Elsholt	UK	Archimedes	180	2.6	-
Deer Island, Boston	USA	Kaplan	2,000	13.1	8.8
Point Loma, San Diego	USA	Francis	1,350	7.6	27
Hsinchu	Taiwan	NI	11	-	-
Taichung	Taiwan	NI	68	-	-

Table 2.14 illustrates studies assessing the application of hydropower technologies in WWTPs worldwide. The investigations cover various turbine types, including siphon, archimedes screw, kaplan, and propeller systems, across plants located in different countries, such as South Africa, Ireland, Poland, the US, South Korea, Pakistan, Turkey, and Canada. Reported available heads ranged from 1.5 to 16.3 m, with flow rates up to 377,800 ML/d, resulting in installed capacities up to 271 kW. Energy generation potential varied from tens of MWh to several GWh per year, while economic evaluations indicated payback periods between 2.4 and 16.9 years, depending on CAPEX, OPEX, and annual savings. In general, the studies highlight that hydropower can be a feasible and cost-effective energy recovery option in WWTPs with sufficient head and flow, though site-specific conditions strongly influence the technology selection, energy output, and financial viability.

Table 2.14: Studies on hydropower technologies applied in WWTPs

Ref	Study objective	Main findings
[171]	Assess the hydro potential in WWTPs	• 49 real cases studies of hydro application in WWTPs, detailing hydro projects in terms of installed capacity, potential energy generation, available head and water flow.
[173]	Benefits of hydro in the Zeekoegat WWTP, in South Africa.	• 3 x 6.7 kW siphon turbines based on head net (3.6m) and flow discharge (0.37 m^3/s). • Economic results: 30 years project's operation with a 9 years payback period. CAPEX, OPEX, and maintenance costs of US$69,000, US$7,520, and US$691, respectively.
[174]	Feasibility study in Zeekoegat WWTP, in South Africa.	• Plant's load of 29-81.4 kW. 3 Siphon turbine selection: 6.9 kW output (each unit). • System could produce up to 181.3 GWh/y, and based on a 20-years project, there would be a potential cost savings of $437,500/y.
[175]	Evaluate the energy recovery potential and economic viability of WWTPs in Ireland and UK	• In the UK, 5 of 11 WWTPs were found economically viable for hydropower, with 3.1-8.8 years pb, 25.5–234 kW capacity, CAPEX of €0.22-0.82 M, €22,000-203,000 in annual savings , and 1.7-8.5m head and (Beckton, Knostrop, Crosness, Minworth, and Long Reach). In Ireland, of 14 plants (1.75 GWh/y), only 2 were economically viable, namely Ringsend (5.1y pb, 3.7m head, 4.4m^3/s flow, 103 kW, €0.44 M of CAPEX, and €87,000 in annual savings) and Carrageenan (7.7y pb, 4m head, 1.2m^3/s flow, 30 kW, €0.19 M of CAPEX, and €25,400 in annual savings).
[176]	Hydro potential for Torun WWTP (Poland)	• 2 systems: 24.8 kW (highest), based 0.56 m^3/s flow and 7.5m available net head (66.35% system efficiency), and 14.8 kW (lowest) for a 0.39 m^3/s flow (53.7% efficiency).
[170]	Hydro study in a WWTP in Wisconsin (US)	• WWTP: 190 MGD, 3m head, 6.5-9 m^3/s flow. Hydro system: 271 kW Kaplan turbine (150-207 kW output), 5,000-10,000 kg/s mass flow, and 1.56 GWh/y in potential savings.
[177]	Study the potential of hydro turbines in 4 different WWTPs, in Ireland.	• WWTPs: Ringsend, Carrigrennan, Navan, and Greystones (8,000-377,800 ML/d flow, and 3.7-16.3m head). Power output, annual savings, CAPEX and payback period: For Ringsend, it was 103 kW, €87,000/y, €442,000 under 5.1 years pb, for Carrigrennan: 30 kW, €25,400/y, €195,000 under 7.7 years pb. For Navan: 11.8 kW, €10,000/y, €77,200 and 7.8 years, and for Greystones: 3.5 kW, €3,000/y, €50,000 and 16.9 years.

Continued on next page

Table 2.14 – continued from previous page

Ref	Study objective	Main findings
[178]	Hydro potential in Kiheung Respia WWTP, in South Korea.	• WWTP parameters: 0.35 m^3/s flow rate, and 4.3 m available head. 96% of treated effluent could be generate up to 68 MWh/, based on a 12.3 kW system capacity and 83% overall system efficiency.
[179]	Hydro potential for a WWTP, in Pakistan	• WWTP parameters: 1.5m head and 0.24m^3/s flow rate. Archimedes screw turbine considered based on the plant's details, with a proposed system capacity of 1.96 kW.
[180]	Studied potential of propeller type in WWTPs	• Proposed systems could generate up to 3.8 GWh/y, electricity saving up to 15.7% and $260,500 in annual cost. CAPEX varied from $191,400 to $528,00 and 15 years pb.
[181]	Find the optimal hydro option for Tatlar WWTP (Turkey)	• Two options: a) Archimedean turbine: Energy generation, CAPEX, O&M, and energy revenue were 7.88 GWh/y, €709,000/y, €13,600/y and €2,172,000 under 2.4y, and b) Kaplan: 8.6 GWh/y, €773,500/y, €57,000/y and €2,279,000 for 3.2 years pb.
[182]	Hydro study in Clarkson WWTP (Canada)	• Based on the WWTP's treatment capacity of 350 ML/d, up to 1.1 GWh/year of electricity could be generated on-site.

pb: payback period; O&M: Operation and maintenance costs; MGD: Mega gallons per day

2.2.1.7. Water Electrolysis

Water electrolysis is a technology in which an electric current is passed through water, splitting it into hydrogen and oxygen. This method is valued for its potential to generate clean hydrogen fuel (also known as green hydrogen) when the electricity used comes from a renewable source. In WWTPs, hydrogen can be used to power CHP technologies (i.e., FCs, GTs, or even modified ICEs), or can be injected into the gas network following the standards regarding the hydrogen-blending constraints. The oxygen produced can be used in the aeration process, which is vital for the biological treatment of wastewater. In the activated sludge process, oxygen is supplied to the aeration tanks to support the growth of aerobic microorganisms that break down organic pollutants. Additionally, in advanced treatment stages such as membrane bioreactors (MBRs) or in systems focusing on nutrient removal, controlled oxygen levels can improve the performance of both nitrification and denitrification processes. Water electrolysis is a promising technology, and the possibility of using treated effluents from municipal WWTPs as the source of water for electrolysis could enhance sustainable hydrogen production in these facilities. However, to utilise the treated effluent from a WWTP as a water supply, it must meet specific requirements, including being purified and demineralised and exhibiting a conductivity lower than 5 μS/cm [183], [184].

Additionally, depending on the quality of the treated effluent, some further tertiary treatments may be required, including chemical treatments, accelerated filtration, ultrafiltration, nanofiltration, coagulation, reverse osmosis, ion exchange, and electrodeionisation. Water electrolysis can be a competitive technology in terms of costs. For example, hydrogen production via water electrolysis can range between US$2.05-10.5/kg H_2, whereas the costs for sewage sludge pyrolysis can be around US$1.2–2.2/kg H_2, and the steam methane reform method is about US$1.14/kg H_2 [184]. Following the stoichiometry balance, 9 kg of deionised water is required to generate 1 kg of hydrogen and 8 kg of oxygen. However, in real-world applications, electrolyser manufacturers recommend using a higher quantity of water (between 10 and 22.4 kg), considering water losses (i.e., 10%) and water used for equipment cleaning (around 25%) [183]. Few studies have investigated the utilisation of water electrolysis technology in WWTPs, as illustrated in Table 2.15.

Table 2.15: Studies exploring the electrolysis technology utilisation in WWTPs

Ref	WWTP	Study aim	Methods	Gas production
[185]	Mainz WWTP, in Germany. WW inflow up to 55 ML/d (6.3 ML/h peak)	Feasibility of 1.25 MW WE in a WWTP, powered by PV and biogas cogen systems. H_2 could be injected into the gas network or to fuel FC buses, and O_2 used for ozone production and, later, advanced WW treatment	WWTP power consumption of 8,200 MW/y, 227 MWh/y PV generation, 6,173 MWh/h cogen generation (biogas use), and 1,800 MWh/y imported from the grid.	H_2 and O_2 production were 2,975 MWh/y and 600 ton/year. For a 2% vol of H_2 feed-in limit, 1,240 MWh/y of H_2 could be injected into the network, and 1,735 MWh, could be used in FC buses
[186]	Effluents (PEf, RWW, ScE, TE) collected from a municipal WWTP in Gyeongsan, South Korea	Generate H_2 from low-grade and WW using alkaline water splitting technology. Based on this investigation, the potential applicability for achieving energy independence in municipal WWTP is planned	WW was filtered via UF membrane to produce ATW. After treatment, COD, TN, TDS (in mg/L) in the treated effluent were 2.8-37.9, 0.9-28.7 and 44-377.	H_2 production was lower with low-grade waters (19.2-22.8 mL/h.L), improved after UF treatment (20.4-23.4 mL/h.L), and highest with control waters (23.6-26.6 mL/h.L)

OMP: Organic micropollutant; WW: wastewater; RWW: raw wastewater; PEf: primary effluent; ScE: secondary effluent; TE: tertiary effluent; SW: Surface water; ATW: Advanced treated water; UF: ultrafiltration; TN: Total nitrogen; COD: Chemical oxygen demand; TDS: total dissolved solids; WE: Water electrolyser

2.2.2 Non-Site-Specific Sources

Non-site-specific sources do not rely on a specific geographical location or environment to be used. This group includes renewable energy technologies that are not tailored to the particular characteristics or location, such as solar energy and wind [10].

2.2.2.1. Solar Energy

Solar energy has the least environmental impact compared to other types of renewable energy resources. It can be used in multiple pathways in WWTPs, and some researchers have studied its application, including solar thermal and PV generation. Solar thermal energy can also be used in several applications, such as heating, heat pumps, and sludge drying. Sludge drying can be used to dewater digested sludge, which is a very important stage of sewage sludge management in a WWTP. It not only reduces the amount of waste to a minimum but also helps eliminate odours and pathogen problems. Traditional thermal drying systems are very complex and require high investment and operational costs [187]. Solar PV is the most widely used type, especially due to its scalability, flexibility, and lower costs, and is usually used combined with AD. For example, in [10], from 105 WWTPs investigated in the USA, 41 plants adopted a PV system.

2.2.2.2. Wind

Although wind generation is one of the most widely used technologies, it is not commonly used in water facilities, mainly due to its initial costs and the complexity of building a small-scale plant. Most studies consider hybrid configurations consisting of PVs, batteries, and biogas systems. Few researchers have investigated the use of wind turbines alone in WWTPs.

2.2.2.3. Hybrid

Due to the intermittency and uncertainty of renewable energy resources, a single technology may be unreliable and add challenges in terms of the dynamic load demand of a WWTP. A hybrid system combines two or more power generation resources to improve the generation potential, which can help overcome the issues of a single technology, providing a cost-effective system with flexible capacity [10].

Table 2.16 presents some studies on non-site-specific renewable energy technologies in WWTPs, including solar, wind, and hybrid systems. Solar thermal systems were widely applied for sludge drying, achieving moisture reductions from 79% to 5% and system efficiencies of 24–81%, with payback periods ranging from 2.9 to 3.5 years. Solar PV installations across WWTPs demonstrated potential to supply 8–100% of plant electricity demand, depending on plant's size, with a wider range of installed capacities reported. Wind energy was less commonly applied, with a 100 kW turbine providing limited contribution to the WWTP's electricity demand. Hybrid systems combining different technologies, including PV, batteries, anaerobic co-digestion, biomass, micro-hydropower, and fuel cells, demonstrated great capacity for significant energy generation and cost savings, with LCOE ranging from €0.01–0.25/kWh and payback periods from 3 to 19 years. Generally, the studies indicate that integrating renewable energy technologies can substantially reduce WWTP energy consumption, carbon emissions, and operational costs, with economic feasibility highly dependent on system type, scale, and site-specific conditions.

Table 2.16: Solar, wind and hybrid system generation in WWTPs

Ref	Type	Study aim	Main findings
[188]	Solar thermal	Studied the influence of a solar dryer in a WWTP in Morocco.	• Drying system operating at 50, 70 and 90°C with air flow rate of 0.083m^3/s. • Solar system: 2.5m^2 collector, drying chamber, fan, and thermo-regulator. • Solar dryer system could reduce up to 60% of the sludge volume
[189]	Solar thermal	Design a drying sludge system for a WWTP, in Turkey.	• Proposed system: average collector efficiency, LCOH and O&M costs were 50.17%, 0.017-0.02$/kWh, and 6.41-7.86 $/year with a 2.9-3.5 years pb. • SMER was 0.77-1.34 kg/kWh and SEC was 1.77-2.86 kWh/kg
[190]	Solar thermal	Proposed a thin layer sandwich-like chamber for drying sludge	• Best result: under a 5mm sludge thickness layer with 6.72g/h drying rate and 0.5 kW/m^2 solar radiation. • Sludge moisture decreased (79% to 5%). Heat utilisation efficiency was 24.3%.
[191]	Solar thermal	Studied the sludge thin-layer during hot air forced drying	• Experiments conducted in a bench-scale convective dryer. • Sewage sludge exposed to 100-200 °C and hot air speeds up to 2m/s. • Surface heat transfer coefficients: 21.4-40.9 W/m^2.K. Average mass transfer was 1,270 – 3,460 m/s and surface heat coefficients was 10.66-26.96 W m^2.K.
[192]	Solar thermal	Studied the V-groove solar air heater for drying sludge.	• Average system's efficiency was 70.1-81.7% and SEC was 2.4-5.4 kWh/kg • Minimum and maximum temperatures were 82.1 °C and 86.4 °C, respectively.
[193]	Solar PV	Assessed PV systems in 105 WWTPs in California, U.S., to identify the opportunities	• 39% of WWTPs had PV with average 0.86 MW size (sizes: 12kW-4.2 MW). • Total PV capacity installed in WWTPs: 35.5MW (34% had a 1MW system). • Solar PV supplied 8-30% of WWTPs with flow above 5 MGD (biogas supplied 25-65%), and below 5 MGD, solar PV supplied 30-100%. • Sacramento WWTP: a 4.2MW PV system supplied 8% of the plant's demand.
[10]	Solar PV	Analyse of PV system potential savings in a WWTP, in Romania.	• WWTP peak and off-peak flowrate was 745 L/s and 322 L/s, respectively. • Proposed PV system could reduce up to 40% of the total energy demand, and 12% of the carbon emission.
[194]	Solar PV	SBBGR in the treatment process by solar.	• Propose PV system: 5.1 kW to supply heating/cooling demand. • SBBGR thermal energy generation of 14.5 kWh with 4 months operation.
[195]	PV-battery	PV-battery system implemented in 2 x decentralised WWTP, in Netherlands	• Average consumption (in MWh/month): 1.1 (BEVER III) to 2.3 (MBR). • A 15 kWp PV and 20-kWh BESS suste, to supply 75% (winter) to 100% (summer) of BEVER III, and 30 kWp PV and 50-kWh BESS to meet 65% (winter) up to 100% (summer) for MBR plant.
[196]	Wind	Assessed the benefits of a 100-kW wind turbine in a WWTP located in Texas, US.	• Wind project to supply electricity to the WWTP cost about $610,900 in 2012. • WWTP load demand of 189.3 m^3/d which requires about 236,000 kWh/year. • In 3 years, plant produced 155.7 MWh and saved $16,000/y in electricity costs. • To be a positive NPV, the system would need to generate about 557 MWh/.
[197]	Hybrid	Evaluated AcoD and PV in a WWTP in Lourdes, Portugal.	• AcoD of 40% sludge and 60% food waste under 37 °C, 1.12 g TVS/L.d OLR, and 15 days HRT, with an implementation costs of €524,000. • Proposed a 730 kWp PV system 1,250 MWh/y generation with 12y pb.
[198]	Hybrid	Propose a 20 MW solar-biomass system for a WWTP in Spain.	• System generation: up to 148.9 GWh (0.85 cap. factor), and €211M CAPEX. • The system achieved an LCOE of €0.25/kWh, with 15% exergetic efficiency for solar system 34% for biomass.

Continued on next page

Ref	Type	Study aim	Main findings
[199]	Hybrid	Analyse the benefits of a PV-battery in a WWTP (23,000 PE), in Romania	• WWTP configuration: influent pumping, SBR biological reactor, blower station, water pumping, sludge thickening and dewatering. • 315 kW installed capacity, and 537.2 MWh/y electricity consumption • System: 310.5 kWp PV and 862 kWh BESS. LCOE: €0.01/kWh (PV) to €0.154/kWh (PV-BESS). CAPEX of BESS €396,540 and €634,675 for PV.
[200]	Hybrid	Investigate the benefits of a hybrid generation in a WWTP.	• WWTP: Thermal, electrical and O_2 demand were 8.7 MW, 4.1 MW, 40t/d. Biogas supply of 404,750 GJ/y. 5 system proposed: PV only (10 MW), PV+HP (15 MW+2.18 MW), PV+HP+TES (15 MW+5 MW+43.5 MW), and PV + electrolyser (15 MW+2.175 MW). IRR of 5-12.7%, 8,570–13,204 t/CO_2 avoided.
[201]	Hybrid	Combined MEC and MH to assess the benefits in a WWTP.	• MH system (water flow) - S1: 0.1-1.1 m^3/s, S2: 0.1-1.1 m^3/s (10 m head), S3: 0.1-0.55 m^3/s (10 m head), and S4: 0.035-0.55 m^3/s (20 m head)) • MH system: 13.1 to 91.6 kW which could power 0.47 to 2.8 GW MEC system. • MHP-MEC system CAPEX between US$45.4M-453.8 M with 2-19.7 years pb
[202]	Hybrid	LCOE analysis for a system in the Collegno WWTP, in Italy.	• LCOE of €0.123-0.141/kWh, for 3 different systems with a 9-19 years pb, and for SOFC only, LCOE was €0.144/kWh, 20y pb and 1 MW/y generation. • If SOFC production increase to 2, 5 or 10 MW/y, payback would be 3-7.5 years.
[203]	Hybrid	Evaluate the benefits of SOFC, solar thermal, and GT in a WWTP, in Italy.	• 4 scenarios adopted: SOFC only, SOFC + ST, GT + SOFC, and Trigen. • CAPEX and OPEX: €1.2-1.33 M, and €113,000-134,000 with 5 years pb, and €0.069-0.087/kWh LCOE. 28-39.4% electrical load could be supplied, and total energy savings of €220,000-€380,000 yearly.

LCOE: Levelised cost of electricity; LCOH: Levelised cost of heating; SMER: Specific moisture extraction rate; SEC: Specific energy consumption; pb: payback period; MGD: Mega gallons per day; OLR: Organic load rate; HRT: Hydraulic retention time; SBBGR: Sequencing Batch Biofilter Granular Reactor; GT: Gas turbine; SOFC: Solid Oxide fuel cell AcoD: Anaerobic co-digestion; MH: micro-hydropower; CST: Concentrating solar thermal

Tables 2.17 and 2.18 present large-scale renewable energy projects implemented in WWTPs globally, including some in Australia. Wind energy projects, such as 4.5–7.5 MW installations in the US, were able to supply 25–60% of plant electricity demand with substantial cost savings. Solar PV systems ranged from small-scale 309 kW units to multi-MW installations, covering 8–70% of facility demand depending on plant size. Combined systems integrating different energy sources, such as PV, wind, hydro, fuel cells, and biogas, were shown to significantly reduce electricity costs and achieve high on-site energy self-sufficiency; for example, Deer Island WWTP (US) combined 2 MW hydro, 736 kW PV, and 2 × 600 kW wind turbines to supply 8.85 GWh/y, reducing electricity costs by 25%. In Australia, projects similarly utilised PV, hydro, biogas, and hybrid systems, including Hunter Water's 6 MW solar PV across multiple sites, Icon Water's mini-hydro and PV installations (supplying up to 13% of demand), and SA Water's 154 MW PV with 34 MWh BESS (generating 242 GWh annually, meeting 70% of electricity needs). Overall, these studies demonstrate that large-scale renewable energy integration in WWTPs can substantially reduce reliance on grid electricity, lower operational costs, and enhance energy sustainability, with hybrid and multi-technology systems offering the greatest potential for maximizing on-site energy generation.

Table 2.17: Large-scale renewable energy projects in WWTPs

Ref	WWTP	Location	System	Main findings
[204]	ACUA	New Jersey, US	7.5 MW Wind	• A 7.5 MW wind farm (commissioned in 2006) can supply ∼60% of plant's demand, US$12.5 M CAPEX (recovered 20% in the first year of operation)
[205]	Field's Point	Providence, US.	4.5 MW Wind	• Project CAPEX: US$14 M, able to reduce in %40 the electricity costs (US$2.5M to US$1.5M/y), supplying up to 25% of plant's annual demand.
[206], [207]	JRDWRF	Pueblo city, US	309 kW-solar PV	• PV system can cover approx. 40% of the facility's electricity demand. • Project received fund support and tariff rebates from the energy utility.
[208]	EMWD	California, US.	PV, FC, and GT	• PV system: 21 MW capacity across 5 sites (45 GWh/y and supply 30% electrical demand), and US$2 M/y in revenue. FC system: Could supply 25-40% of the energy needs for 2 sites, using on-site biogas generation and save up to US$1 M/y, and 8 GTs (60 kW each) could provide up to US$300,000/y.

Continued on next page

Ref	WWTP	Location	System	Main findings
[209]	PL	San Diego, U.S.	Hydro,FC, biogas	• Project CAPEX: US$45 M. System generates 5.5 MW and consumes 2 MW (3.5 MW is sold). Upgraded biogas power 3 FC systems (2.6 MW-4.5 MW).
[210], [211]	Werdhölzli	Switzerland	Incineration	• Plant treats sludge from 70+ WWTPs (approximately 100,000 m^3 ton/y). • System capacity: 875 kW electrical and 4,450 kW thermal
[212], [213]	Deer Island	Boston, US	Wind,PV, hydro	• System: 2x600 kW wind, 736 kW PV, 2 MW hydro (8.85 GWh/y), reducing electricity costs by 25%. WWTP energy demand of 18 MW/y (US$16 M/y).

Table 2.18: Renewable energy projects in WWTPs in Australia

Ref	WWTP	System	System capacity / characteristics
[214]	Hunter Water	6 MW solar PV	• Total of 3 MW capacity at Dungog, Tanilba Bay and Karuah plants. • 3.1 MW Balickera park solar system as the biggest plant
[215]–[217]	Icon Water	720 kW PV, 1.23 MW Hydro	• 630 kW hydro capacity (3.4 GWh/y), and 600 kW on Googong mini-hydro, up to 4.2 GWh/y (13% Icon's Water demand in 2015-16). 2.3 MW to be installed.
[218], [219]	QLD Melbourne Water	Hydrothermal liquefaction	• System can produce up to 12-15 ML/d of biofuel yearly. • Project cost around $11.8 mi (partnership with Gladstone oil refinery).
[220]	Loganholme WWTP	Sludge gasification	• Convert 34,000 ton of sludge into syngas, and CAPEX of AU$17.3 M. Previously, biosolids disposal costs was AU$1.8 M/y (30% of plant's operating costs).
[215]	Melbourne Water	25 MW biogas, 25 MW hydro, 24 MW PV	• 86.2%, 0.02% and 93.6% of the energy produced from biogas, hydro and PV used on-site. New hydro projects in 3 WWTPs can generate up to 7.1 GWh/y. • In ETP, biogas and solar systems could supply up to 48% of plant's demand, whereas in WTP, solar system could generate up to 12.4 GWh/y.
[221]	SA Water	154 MW PV, 34 MWh BESS	• Generate 242 GWh supplying 70% of SA Water's electricity demand yearly. • Total CAPEX of AU$300 mi for the proposed system.
[222]	Sydney water	PV, biogas, hydro	• Produces 20% of its electricity needs through on-site generation
[223], [224]	Water Corporation	PV, wind, biogas, and hydro	• Plans to participates in pilot programs to provide grid services, invest AU$30 mil in a solar projects and generate 1.5 GWh from renewables.

2.2.3 Challenges and Opportunities

Most wastewater treatment facilities are not primarily designed to be cost-efficient systems. Almost 90% of the energy consumption in WWTPs is related to three stages: secondary treatment, pumping, and sludge treatment combined with dewatering [1]. The most common alternatives that these facilities adopt to reduce energy costs in WWTPs include (i) optimising energy consumption by improving efficiency, (ii) on-site power generation to reduce operating costs related to energy importation from the main grid, and (iii) energy demand management [2]. Planning and operation studies are essential to understand the potential risks and evaluate the opportunities for WWTPs. They can help design the best power generation configuration and find the optimal operation strategy for the generation system. Power system planning is a critical techno-economic assessment used to investigate and plan future system expansion, feasibility, and generation potential. The main objective of power generation planning is to determine the necessary generating capacity to satisfy the load demand in real time. In the system's planning, it is ideal to have a generation capacity that can supply 100% of the load at any time. Still, it is very challenging to match the generation and demand, especially if the system is composed of renewable energy sources [225]. The planning process can be considered an optimisation problem in which the optimal solution consists of finding the optimal system configuration, including the best technological generation mix, optimal size, capacity, location, and construction time with minimum investment cost [225]. Due to the uncertainty and intermittency, adopting a hybrid configuration system is usually a good alternative for WWTPs. Hybrid systems can maximise the energy generation potential from different resources, and lead to a better cost-effectiveness, energy efficiency, modularity, and flexibility [8]. Although there

are several technological solutions and strategies to increase economic benefits for a WWTP, their implementation in a full-scale plant is still very limited. The biggest challenge is commonly related to capital and operating costs. Because of the vast number of available technology resources, determining the optimal planning design and operation strategy of power generation in WWTPs is not an easy task and is no longer a simple technical problem, but rather a complex and difficult challenge that requires an integrated and comprehensive approach to provide a cost-effective solution [226].

2.3 Research Gaps

Wastewater treatment plants (WWTPs) are known to be high energy consumers. Therefore, it is important to explore alternatives that reduce both energy consumption and operational costs, while also minimising carbon emissions. The literature review has identified that there is no one-size-fits-all solution to this problem. Thus, further investigation in this research topic is needed. Several models have been proposed in the literature, each addressing specific challenges, including increasing biogas production, optimising operational processes, or improving on-site renewable energy generation. This review has highlighted that improving self-sufficiency in WWTPs can be a suitable alternative through the integration of biogas utilisation, renewable energy generation, and operational optimisation. While various energy optimisation models and commercial tools exist, there remains a gap which includes the lack of a comprehensive single model specifically tailored to WWTP applications. In the authors' view, a valuable contribution would be proposing and developing a tool that could:

(i) optimise biogas utilisation,
(ii) optimise the operation strategy of the on-site power generation system,
(iii) identify the optimal planning of the power generation system, and
(iv) minimise the operating costs for the WWTP.

Such a model could contribute to energy resilience and sustainability in WWTP operations.

2.4 Summary

This literature review highlighted different renewable energy technologies that can be adopted by WWTPs to improve energy efficiency, reduce operating costs, and move toward sustainability, with a focus on providing an overview of the current status of each technology by exploring their energy recovery potential, benefits, and drawbacks. AD is still the most widely used alternative to treat sludge and recover energy in a WWTP due to its mature technology, sewage sludge treatment efficiency, low operating costs and biogas production as a co-product. In the USA, almost 50% of all the wastewater is treated through AD. Co-digestion and pre-treatment methods are some alternatives to improve biogas production and process efficiency, although the latter is primarily used to enhance sludge biodegradability, sludge management, and reduce environmental impact. Thermochemical processes, including pyrolysis and gasification, can also offer several benefits for treating sewage sludge by converting organic matter into valuable products while addressing the challenges associated with sludge management. Both gasification and pyrolysis are mature technologies that generate high-value co-products, including syngas and bio-oil, and can be used to generate electricity and heating. Additionally, hydropower and wind technologies offer significant benefits as renewable energy sources, but their application in WWTPs is limited due to several practical, technical, and economic challenges. For

example, conventional hydropower systems require a significant and consistent flow of water to generate electricity, and typically, WWTPs do not have sufficient flow rates or water head heights to support hydropower turbines effectively, and wind turbines require substantial space to operate efficiently. Many municipal facilities are located in urban areas or constrained sites where physical space is limited. On the other hand, other technologies, including MFCs and MECs, hold significant potential for sustainable energy production and municipal wastewater treatment. Despite their promising laboratory-scale performance, large-scale implementation of MECs and MFCs can face some challenges related to scalability, energy efficiency, capital and operational costs, material durability, microbial stability, reactor design, and regulatory approval. Therefore, more academic research and technological development are needed to achieve both technical advancements and system integration. Many of these challenges can be addressed, opening up opportunities for bioelectrochemical technologies to contribute to sustainable energy production, waste treatment, and environmental management on larger-scale facilities. Overall, the successful adoption of renewable energy technologies involves overcoming several challenges that span technical, economic, regulatory, and operational domains. It is important to address these challenges and technology limitations to outline future prospects for achieving a more energy-efficient and sustainable wastewater treatment.

Chapter 3

Biogas Model

3.1 Introduction

In this chapter, the biogas model is presented. This proposed model estimates the biogas production from sewage sludge while considering the semi-continuous feeding operation. To validate the proposed model, the simulated results are calibrated and validated against real data from a full-scale municipal WWTP located in Sydney, Australia. The main contribution of this work is the combination of the advantages of both the steady-state model, including simplicity, reduced complexity, fewer parameters, and faster computation time, and the dynamic aspects, including capturing time-dependent behavioral changes, predictive control, and real-time adjustments, into a single model.

This chapter is organised as follows. Section 3.2 starts by providing a general background related the anaerobic digestion process in a WWTP. Section 3.3 presents previous works related to anaerobic digestion models. Section 3.4 discusses the model framework, including explaining the proposed biogas model, first-in, first-out (FIFO) methodology, and model formulation. Section 3.5 presents the model validation against historical data of a large-scale WWTP, and Section 3.6 summarises the main findings of this chapter.

3.2 Background

Wastewater treatment plants (WWTPs) play a crucial role in maintaining public health and environmental sustainability. These facilities are important agents for removing contaminants and pathogens from wastewater in compliance with water quality standards, and, then returning the treated water to the environment [13]. The WWTP treatment process is highly complex and costly, which can jeopardise the environment if not appropriately treated [1], [2]. Municipal wastewater can be treated using two main technologies, anaerobic and aerobic processes [227].

Anaerobic digestion is one of the most widely used alternatives for wastewater and sewage sludge treatments, and also for energy recovery in WWTPs due to its several benefits, including biogas production, reduced greenhouse gas emissions, efficient sludge reduction, pathogen and odour control, and cost-effectiveness [227]. This biological process consists of decomposing organic matter (i.e., sewage sludge) by microorganisms in the absence of oxygen, generating biogas as a by-product and digested sludge [66]. Biogas is a renewable fuel composed mainly of methane and carbon dioxide and can be used in different applications, including combined heat and

power (CHP) systems to generate both electricity and heating, boilers for heating processes, or it can be upgraded into biomethane and be injected into the gas network system [228].

The digestion of sewage sludge usually happens in four stages inside an anaerobic reactor [229]. These digesters are traditionally designed and engineered to operate under two main configurations: batch or semi-continuous feeding modes [230]. In the batch mode, the substrate (i.e., sewage sludge) is added to the reactor all at once at the beginning of the process. The feedstock remains for a certain period of time until it is digested (digested sludge). Then, it is removed and a new batch cycle is restarted. In a semi-continuous mode, the organic material is added to the anaerobic digester at regular intervals (i.e., hourly or daily) at a constant or variable flow rate, while an equivalent amount of digested material is removed, keeping this system in a continuous state of operation [230], [231]. Most large-scale WWTPs operate using a semi-continuous process [232].

Anaerobic digestion is a complex biochemical reaction that takes into consideration several parameters [233]. Modelling this process can be very complex due to several factors, including the complex microbial ecosystem interactions, feedstock composition and degradability, and dynamic parameters (i.e., temperature, pressure, pH levels, organic loading rate, complex kinetics, process stability, and control). One of the biggest challenges in modelling is to integrate multiple parameters, linear and non-linear equations, objective functions, and several constraints. Therefore, new optimisation tools, forecasting models, and control strategies that seek to address these challenges and opportunities are essential [234]. Accurate representation of the anaerobic digestion process is crucial for optimising reaction performance, ensuring system stability, and maximising benefits. Several methods have been used to model the digestion process, including mathematical and empirical models, each with its pros and cons. Additionally, there is simulation software that replicates the anaerobic reaction [235].

Among the available approaches used in academia and industry, mathematical models are widely regarded as an effective methodology not only for simulating the digestion operation but also for developing control strategies, evaluating the system's performance and design under different scenarios, optimising operational parameters, and replicating the complex reaction phenomena. By simulating different scenarios with operational strategies, these models can promote a deeper and more accurate understanding of the system's time-dependent characteristics and optimisation response, leading to potential improvements [232], [236]. Furthermore, they can serve as a valuable tool for WWTP operators, enabling them to improve and monitor process management. It is important that these models are calibrated and validated against experimental data [237], [238].

3.3 Related Works

Several studies have presented different methods to represent the anaerobic digestion process, including estimating the theoretical methane and/or biogas production. For example, Ref. [239] developed a model to estimate the biogas production in an Up Flow Anaerobic Sludge Blanket (UASB) reactor, and real data from two WWTPs (Laboreaux and Nova Contagem) under three scenarios (worst, typical and best). The model, based on Monte Carlo simulation, incorporated the inherent variability and uncertainty of sewage sludge characteristics by generating multiple random input scenarios to predict a range of possible outcomes for biogas and methane production, providing a more realistic and robust estimation compared to deterministic models. For the Laboreaux WWTP, the methane yield from the measured and simulated

data was 45.2 L/m^3 of treated sewage and 40–81.4 L/m^3 of treated sewage, respectively, while the sludge production values were 101.2 g/m^3 (measured) and 90.3–103.2 g/m^3 (simulated). Ref. [240] presented a data-driven approach that optimised controllable variables of the anaerobic digestion process, such as pH, retention time, organic load rate, temperature, sludge flow rate, total solids and volatile solids. If temperature was the only variable to be optimised (39 °C), an improvement of 5.3% in biogas production could be achieved, while optimising all variables led to a maximum improvement of 21%. Ref. [241] proposed a model to forecast biogas production from primary sewage sludge. The proposed model accounted for different stages of anaerobic digestion and incorporated formulations to represent the kinetic stage, chemical stoichiometry, and acid/base chemistry. Validation against data from a large-scale WWTP showed strong alignment between the model results and measured data. The model's predicted COD values closely matched the measurements, being 20.2, 22.4, and 23.6 gCOD/L for retention times of 10, 15, and 20 days, respectively. Methane production based on measured data was 14.3, 15.0, and 15.8 L/L of sludge, whereas the simulated data yielded 11.9, 13.4, and 13.9 L/L of sludge for the same retention times. Ref. [242] proposed a COD degradation-based model of anaerobic digestion to simulate methane and biogas production from sewage wastewater. The authors considered three main compound categories in wastewater: easily degradable, difficult to degrade, and non-degradable. COD removal could occur via both biological and nonbiological processes. For example, methane production was estimated from degraded COD under the following conditions: 26 °C, 500 m^3/d flow, and wastewater composed of sucrose, formic and acetic acids. This gave a theoretical methane production of 88.2 m^3/d.

Ref. [243] developed a model to replicate the dynamic behaviour of anaerobic digestion, considering six main conversion processes and five additional microbial processes. The model was calibrated with lab experiments using sewage sludge from the Zurich-Glatt WWTP under mesophilic conditions (35 °C) and 20 days retention time. The resulting biogas flow was between 4,000 and 5,500 m^3/d. Ref. [244] proposed a mathematical model to estimate the energy potential generated from anaerobic digestion in a UASB reactor. Input parameters included COD removal efficiency, reaction temperature, sludge production coefficient, average influent flow rate, and methane loss. Validation against two full-scale WWTPs showed average methane and biogas yields of 42.2 and 81.3 L/m^3 wastewater and 60.3-101.6 L/m^3 wastewater, respectively. Ref. [245] developed a model to estimate biogas production based on first-order kinetics as a modified version of the Gompertz function of the anaerobic digestion. Validation against a full-scale 3 MW biogas plant showed a biogas production of 1,008–1,152 m^3/h, equivalent to approximately 25,000 m^3/d, with a total of 381,000 m^3 over 15 days. Ref. [246] proposed the Anaerobic Digestion Model No 1 (ADM1), which later became one of the most widely used methodologies to simulate anaerobic digestion conditions. Developted by the International Water Association (IWA), ADM1 is designed to replicate the anaerobic digestion process with high accuracy, particularly focusing on maximising efficiency and biogas generation. It accounts for both biochemical and physicochemical stages. Ref. [247] applied ADM1 to sewage sludge. The simulated results were calibrated and validated against 360 days of real operational data from a full-scale anaerobic digestion system. Parameters included a 40-day retention time, influent flow of 380 m^3/d, and influent COD of 42.8 g/L. The simulation results closely matched measured methane flows, which were 1,500 and 4,000 m^3/d, with an average value of 2270 m^3/d. Although several models have been developed to estimate biogas production and methane yield from sewage sludge, most assume batch feeding modes. However, municipal WWTPs typically operate under semi-continuous feeding. Therefore, models that incorporate the dynamic behaviour of semi-continuous sludge feeding are essential for accurately replicating real-world plant operations.

3.4 Model Framework and Design

This section presents the model framework of the biogas model, including the general assumptions and mathematical formulation. To validate the effectiveness of the proposed model, a comparison against real data from a large-scale WWTP is conducted.

3.4.1 FIFO Methodology

FIFO methodology can be applied in various contexts to describe how items are selected, processed, consumed, or accounted for. It follows the principle that the first components to enter a system are the first ones to be used, sold, or processed, while newer items are considered last [248], [249]. The use of the FIFO approach is intended to represent the feeding process mode as a semi-continuous process of sewage sludge added into the anaerobic digesters. The semi-continuous feeding mode reflects the real-world process in which a large-scale WWTP operates. Therefore, this proposed model aims to replicate a realistic, semi-continuous operating process of sewage sludge treatment.

Based on the FIFO methodology and its application to the anaerobic digestion process, a semi-continuous and dynamic flow of sewage sludge is added into the anaerobic digester as an individual "parcel". In this model, we assume there is no mix between the different "parcels" inside the anaerobic digester, and the volume of sewage sludge in the anaerobic digester must be kept constant. To model the sewage sludge flow rate, discrete-time equations are formulated to track the quantities of sludge entering and exiting the digester at each time step. This proposed model allows us for understanding the dynamic process and time-domain behaviour of the sludge-feeding process at each time step, considering the FIFO principle that the first added sludge will be the first to exit the anaerobic digester when the maximum volume is reached, as illustrated in Figure 3.1.

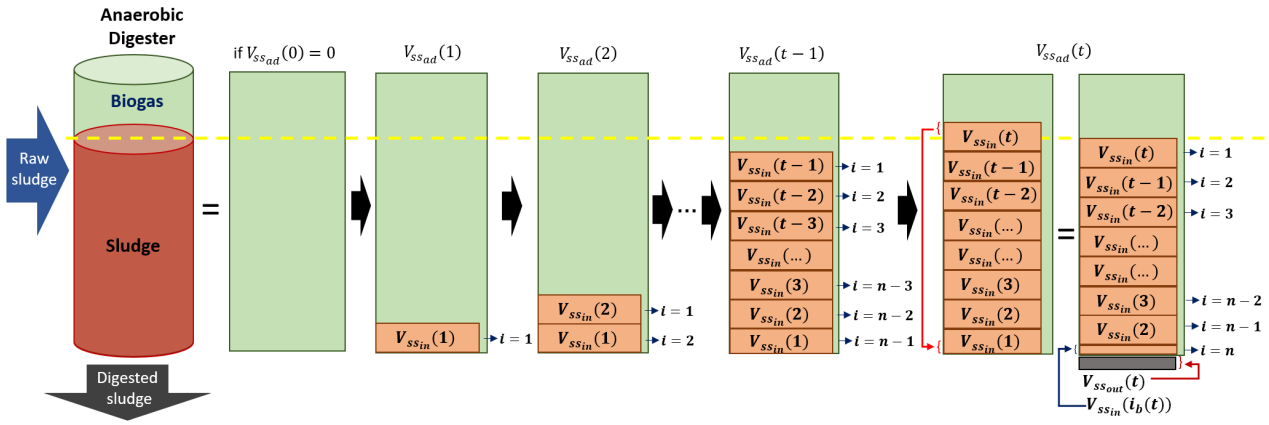

Figure 3.1: FIFO methodology representing a semi-continuous feeding mode of sewage sludge flow into an anaerobic digester

3.4.2 Semi-Continuous Operation

As shown in Figure 3.1, at the beginning of the process, when $t = 0$, the anaerobic digester is empty ($V_{ss_{ad}}(0) = 0$). For $t = 1$, the sludge volume inside the anaerobic digester is equal to the sum of the initial volume of sludge at t= 0 and the volume of sludge that enters at t = 1 ($V_{ss_{ad}}(1) = V_{ss_{in}}(0) + V_{ss_{ad}}(1)$). The retention time ($n$) for the sludge $V_{ss_{in}}(1)$, when t

= 1, is 1 day. There is a maximum operation volume of sewage sludge inside the anaerobic digester, expressed as $V_{ss_{ad}}^{\max}$. Because the maximum volume of sludge inside the digester is not reached at $t = 1$, there is no discharge of sludge ($V_{ss_{out}}(1) = 0$). Letting $i_b(t)$ be the index of the bottom parcel of sewage sludge at time t, then $i_b(1) = 1$. When $t = 2$, the total volume of sludge inside the anaerobic digester is equal to the sum of the sludge volume at $t = 1$ and the sludge volume that enters the digester at $t = 2$, minus the discharge of sludge at $t = 2$ ($V_{ss_{ad}}(2) = V_{ss_{ad}}(1) + V_{ss_{in}}(2)$ - $V_{ss_{out}}(2)$). The retention time (n) of the sludge that enters the digester at $t = 1$ ($V_{ss_{in}}(1)$) is 2 days, and the retention time (n) of the sludge that entered the digester at $t = 2$ ($V_{ss_{in}}(2)$) is 1 day. Since the maximum volume of sludge inside the digester is not reached at $t = 2$, there is no discharge of sludge yet $V_{ss_{out}}(2) = 0$, and $i_b(2) = 1$. At time t, when the maximum volume of sludge inside the digester is reached ($V_{ss_{ad}}(t) \geq V_{ss_{ad}}^{\max}$), a portion of the oldest parcel of sludge (the first parcel that enters, $V_{ss_{in}}(1)$) will be discharged from the anaerobic digester ($V_{ss_{out}}$(t)). The amount of sludge to be discharged ($V_{ss_{out}}(t)$) is equal to the sum of all the parcels of sludge that entered the digester up to the current time, from t=0 to t, ($V_{ss_{ad}}(t) = V_{ss_{in}}(0) + V_{ss_{in}}(1) + V_{ss_{in}}(2) + \ldots + V_{ss_{in}}(t1) + V_{ss_{in}}(t)$) minus the maximum volume of sludge that can maintained inside the anaerobic digester ($V_{ss_{ad}}^{\max}$). As illustrated in Figure 3.1, there is a remaining volume of sludge from the oldest parcel ($i_b(t) = 1$) that is retained in the digester ($V_{ss_{in}}(i_b(t))$, since it exceeds the discharged sludge volume ($V_{ss_{out}}(t)$). The retention time (n) of the oldest parcel of sludge remaining inside the digester ($V_{ss_{in}}(1)$ is equal to t, whereas the retention time (n) of the sludge entering the digester at t ($V_{ss_{in}}(t)$) is 1 day. The retention time (n) of each parcel corresponds to the number of days for which each parcel is stored before its disposal. The retention time (n) varies over time since it is a time-dependent variable directly associated with the sludge flow rate into the digester. For example, as illustrated in Figure 3.2, when $t = 8$, the retention time for the oldest sludge parcel (i.e., $i_b(8) = 1$) is 8 days.

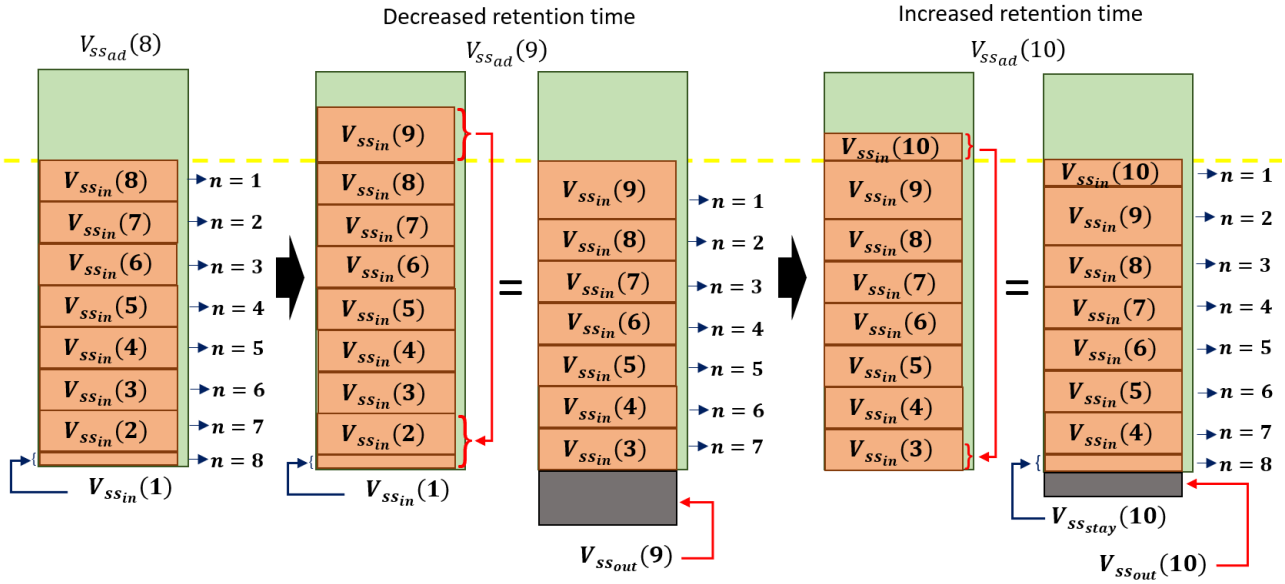

Figure 3.2: Retention time changing behaviour

When $t = 9$, a larger amount of sludge enters the digester ($V_{ss_{in}}(9)$). The amount of sludge that is discharged ($V_{ss_{out}}(9)$) includes the entire volume of the oldest sludge parcel in the digester ($V_{ss_{in}}(1)$) and a portion of the second oldest parcel ($V_{ss_{in}}(2)$). The retention time (n) for the new oldest parcel ($i_b(9) = 3$) is now 7 days, reduced by 1 day. Similarly, when $t = 10$, due

to the lower volume of sewage sludge entering the digester ($V_{ss_{in}}(10)$), the amount of sludge discharged ($V_{ss_{out}}(10)$) removes only a portion of the oldest parcel (i.e., $i_b(9) = 3$). Therefore, $i_b(10) = 3$. The retention time (n) for the oldest parcel is now 8 days, increased by 1 day.

3.4.3 Model Formulation

a. Anaerobic digestion model

Steady-state models aim to simplify the complexity of the system design and operating parameters for the anaerobic digestion process. They are useful for some reasons, including providing simple and quick estimation results, enabling sensitivity investigation, estimating product concentrations and benchmarking [250]. The anaerobic digestion model presented in [241] comprises three sequential parts: the kinetic stage, chemical stoichiometry, and acid/base chemistry, and was validated against a real WWTP. The same model is used as a reference to calculate the theoretical methane production based on a given retention time. The unbiodegradable fraction of sewage sludge is calculated as shown in (3.1). Eq. (3.1) is discretised using the concept of the raw and settled wastewater and the COD fractions in the sewage sludge. $f_{ss_{unb}}$, $f_{ss_{unb,raw}}$, and $f_{ss_{unb,set}}$ are the unbiodegradable fractions of sewage sludge, raw wastewater and settled wastewater, respectively. $f_{ss_{rem}}$ is the sludge fraction removed from the sedimentation tank [241].

$$f_{ss_{unb}} = f_{ss_{unb,set}} + \frac{(f_{ss_{unb,raw}} - f_{ss_{unb,set}})}{f_{ss_{rem}}} \tag{3.1}$$

In sequence, the residual biodegradable organic concentration (S_{bp}) and influent biodegradable particulate (S_{bpi}) are defined in (3.2) and (3.3), respectively.

$$S_{bp} = \frac{S_{ti} + [f_{ss_{unb}} + E_s \cdot (1 - f_{ss_{rem}})] - S_{te}}{E_s - 1} \tag{3.2}$$

$$S_{bpi} = S_{ti} \cdot (1 - f_{ss_{unb}}) - S_{bsai} \tag{3.3}$$

where S_{ti}, S_{te}, and S_{bsai} are the total influent, total effluent, and influent volatile fatty acid (VFA) concentrations, respectively. E_s is the biodegradable COD fraction removed and converted to sludge, defined in (3.4). Eq. (3.5) illustrates the fraction of biodegradable COD removed and converted to methane (E_{ch4}).

$$E_s = \frac{Z_{ad}}{(S_{bpi} - S_{bp})} \tag{3.4}$$

$$E_{ch4} = 1 - E_s \tag{3.5}$$

Equations (3.6) and (3.7) define the acidogen biomass concentration (Z_{ad}) and volumetric hydrolysis/acidogenesis rate (r_h). Y_{ad}, b_{ad}, and n are the pseudo acidogen yield coefficient, acidogen endogenous respiration rate, and retention time, respectively. K_m and K_s are the Michaelis and substrate dissociation constants, respectively.

$$Z_{ad} = \frac{Y_{ad} \cdot [S_{bpi} - S_{bp}]}{1 + b_{ad} \cdot n \cdot (1 - Y_{ad})} \tag{3.6}$$

$$r_h = \frac{K_m \cdot S_{bp} \cdot Z_{ad}}{K_s + S_{bp}} \tag{3.7}$$

Equations (3.8) and (3.9) calculate the methane production concentration (S_m) and the final methane production volume (Q_m), respectively. T_{ad} and P_{ad} are the temperature and pressure inside the digester. The final methane production volume (Q_m) is given in liter of methane divided by liter of influent (L_{ch4}/L_{inf}) and will be used to calculate the biogas production.

$$S_m = (1 - Y_{ad}) \cdot n \cdot r_h \tag{3.8}$$

$$Q_m = \frac{(S_m + S_{bsai})}{64} \cdot 8.314 \cdot \frac{T_{ad}}{P_{ad}} \tag{3.9}$$

b. Proposed Biogas Model

The proposed model aims to extend the steady-state anaerobic digestion model presented in [241] by incorporating the time-dependent domain and dynamic behaviour (semi-continuous feeding mode) to represent the sewage sludge treatment process. FIFO methodology is used to describe the anaerobic digestion operation process in a large-scale municipal WWTP, and it has been used in different fields to represent dynamic behaviour characteristics [248], [249], [251]. The objective of the proposed model is to forecast biogas and methane production based on a dynamic and semi-continuous feeding mode of sewage sludge into the anaerobic digester. The reactor temperature is a controllable variable, but in this study, it is a fixed parameter. Constraint (3.10) states that the sum of the volume of biogas ($V_{biogas_{ad}}(t)$) and sewage sludge inside the anaerobic digester ($V_{ss_{ad}}(t)$) should be lower than the total volume of the anaerobic digester ($V_{ad}^{\max}$) at time t.

$$V_{biogas_{ad}}(t) + V_{ss_{ad}} \leq V_{ad}^{\max} \tag{3.10}$$

Equation (3.11) represents the total sludge volume inside the digester, where ($V_{ss_{in}}(t)$) is the volume of sewage sludge that enters the digester at time t. Equation (3.12) defines the total sludge volume that stays inside the digester, as explained in Section 3.4.3. $V_{ss_{out}}(t)$ is the volume of sludge that leaves the digester at time t. $n(t,i)$ is the retention time associated with the sewage sludge parcel i ($i = i_b(t), i_b(t)+1, ..., t$) at time t, t is the time step, and $i_b(t)$ is the index of the bottom parcel of sewage sludge at time t. Note that $n(t,i) = t - i + 1$, and $i_b(t)$ $= i_{b_{new}}$, where $i_{b_{new}}$ is the least index such that $\sum_{i=i_b(t-1)}^{i_{b_{new}}} V_{ss_{in}}(i) - V_{ss_{out}}(t) \geq 0$. The methane production from the anaerobic digestion process of sewage sludge is calculated in (3.13), where $V_{m_{ad}}(t)$ is the total volume of methane generated. Q_m is the methane production volume, as calculated in (3.9).

$$V_{ss_{ad}}(t) = \sum_{i=i_b(t)}^{t} V_{ss_{in}}(i) \tag{3.11}$$

$$V_{ss_{in}}(i_b(t)) = \sum_{i=i_b(t-1)}^{i_b(t)} V_{ss_{in}}(i) - V_{ss_{out}}(t) \tag{3.12}$$

$$V_{m_{ad}} = \sum_{i=i_b(t)}^{t} V_{ss_{in}}(i) \cdot Q_m(n(t,i)) \tag{3.13}$$

Based on the methane generation in (3.13), the biogas quantity can be calculated in (3.14), where $c_{m_{ad}}(t)$ is the average methane concentration in the biogas. Constraint (3.15) states the

biogas inside the digester should be greater than the minimum volume of biogas ($V^{\min}_{biogas_{ad}}$) and lower than the maximum volume of biogas ($V^{\max}_{biogas_{ad}}$).

$$V_{biogas_{ad}}(t) = \frac{V_{m_{ad}}(t)}{c_{m_{ad}}(t)} \tag{3.14}$$

$$V^{\min}_{biogas_{ad}} < V_{biogas_{ad}}(t) \leq V^{\max}_{biogas_{ad}} \tag{3.15}$$

This model assumes that the biogas obeys the ideal gas law. Therefore, the relationship between the biogas volume at ambient temperature and biogas volume inside the anaerobic digester is described in (3.16). $V_{biogas_{ad}}(t)$ is biogas volume inside the digester, whereas $T_{amb}(t)$, $P_{amb}(t)$ and $V_{biogas_{amb}}(t)$ are the ambient temperature, pressure and biogas volume, respectively. Constraints (3.17) and (3.18) limit the temperature and pressure inside the digester. $P^{\max}_{ad}$, $T^{\max}_{ad}$, $P^{\min}_{ad}$, and $T^{\min}_{ad}$ are the maximum and minimum limits for pressure and temperature inside the digester.

$$\frac{P_{ad}(t) \cdot V_{biogas_{ad}}(t)}{T_{ad}(t)} = \frac{P_{amb}(t) \cdot V_{biogas_{amb}}(t)}{T_{amb}(t)} \tag{3.16}$$

$$P^{\min}_{ad} < P_{ad}(t) \leq P^{\max}_{ad} \tag{3.17}$$

$$T^{\min}_{ad} < T_{ad}(t) \leq T^{\max}_{ad} \tag{3.18}$$

3.5 Model Validation

Model validation aims to determine whether the model is able to accurately replicate the system's behaviour, which can be evaluated in two ways: operationally (i.e., by comparing the output of the model with observed data) and conceptually (i.e., by checking if the theory and assumptions of the proposed model are followed and justifiable) [252], [253]. The main objective of the proposed model is to forecast the biogas production from sewage sludge. To test the effectiveness of the methodology, we compare the real data (historical) of a large-scale WWTP located in Sydney, Australia, over a period of 3 years (2020 to 2022) against the results of the model's simulation. The WWTP considered in this study has a capacity to treat an average flow of around 500 million liters of raw sewage daily through primary treatment and anaerobic digestion. The sludge captured in the primary sedimentation tanks is treated at mesophilic temperature, and the digested sludge is dewatered before its disposal. The biogas generated from the anaerobic digestion of sewage sludge is collected and used to produce electricity via cogeneration (CHP) engines or in hot water boilers to generate heat, and the excess is flared (there is no gas storage on-site). The total biogas production in the WWTP was calculated as the sum of the amount of biogas used in the CHP, boiler, and the amount flared.

3.5.1 Data Inputs

Some key inputs used in the model were collected from the large-scale WWTP mentioned in Section 5, which including the following:

• Total volume of the anaerobic digester system: 35,000 m^3;
• Maximum sludge volume inside the digester: 31,500 m^3 (about 90% of the total anaerobic digester volume);
• Maximum volume of biogas stored inside the digester: 3,500 m^3 (about 10% of the total

anaerobic digester volume);
• Digester pressure of 105 kPa and temperature of 37 °C.

Other parameters were adopted from Ref. [241], including the following:

• Settled and raw wastewater unbiodegradable particulates COD fractions are 0.040 and 0.150, respectively;
• The fraction of COD removed from the sedimentation tank is 0.35;
• Acidogen endogenous respiration rate and pseudo acidogenic yield coefficient are 0.041 d^{-1}, 0.013 gCOD biomass/gCOD organics hydrolysed, respectively;
• Substrate dissociation constant, Michaelis constant, and influent VFA concentration are 6.76 gCOD/L, 3.34 gCOD organics/(gCOD biomass·d), and 2.25 gCOD/L, respectively.

The sewage sludge flow rate fed into the digester daily from 2020 to 2022 is illustrated in Figure 3.3. Based on the WWTP historical data, the COD concentration in the raw sewage sludge ranged between 42 and 68.7 gCOD/L.

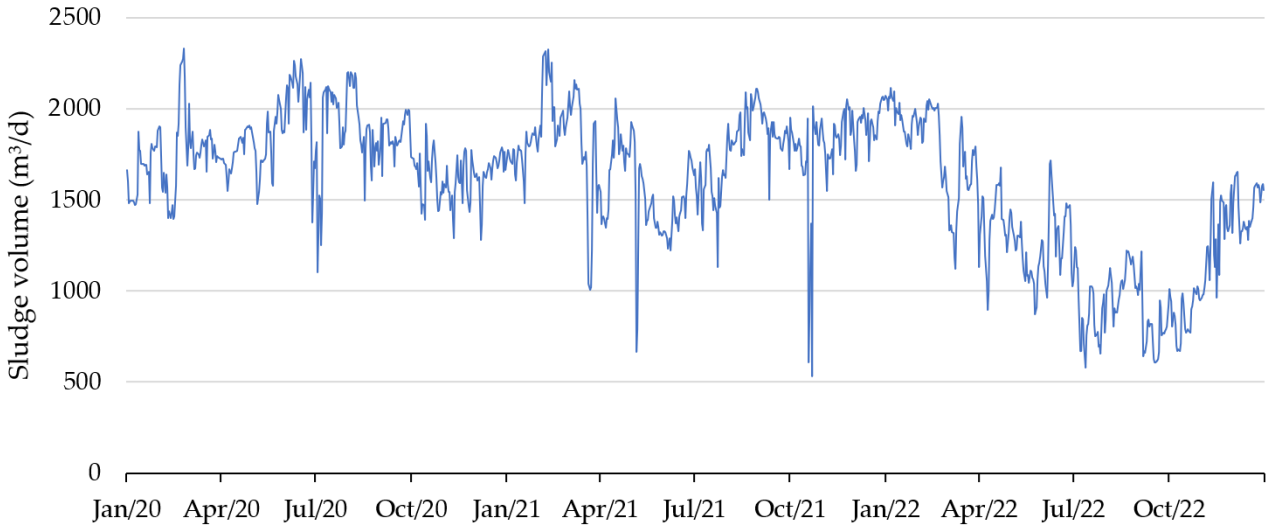

Figure 3.3: Sewage sludge flow fed into the anaerobic digester

3.5.2 Simulation Results

a. Biogas production

The biogas production from the proposed model and historical data are illustrated in Figures 3.4–3.6 for each year, including 2020, 2021 and 2022. It can be seen that the biogas production from the historical data is more non-linear compared to the proposed model. The historical data reveal significant declines in biogas production in some specific periods, such as Feb-20, Jul-20, Aug-20, Mar-21, May-21, Mar-22, Jul-22 and Sep-22. Even though the biogas production from the WWTP shows some abrupt changes, the proposed method accurately follows the overall generation trend of the historical data. Although biogas production is theoretically considered a continuous process with a steady gas generation flow rate [254], [255], particularly in batch mode, in large-scale plants can exhibit some fluctuations on the biogas production. These deviations are influenced by the semi-continuous feeding operations and other operational characteristics that can affect the continuous and steady generation of biogas. These variations may arise due to numerous factors, including feedstock quality, inconsistent or variable feeding rates, microbial community stability, equipment malfunctions, and routine system maintenance.

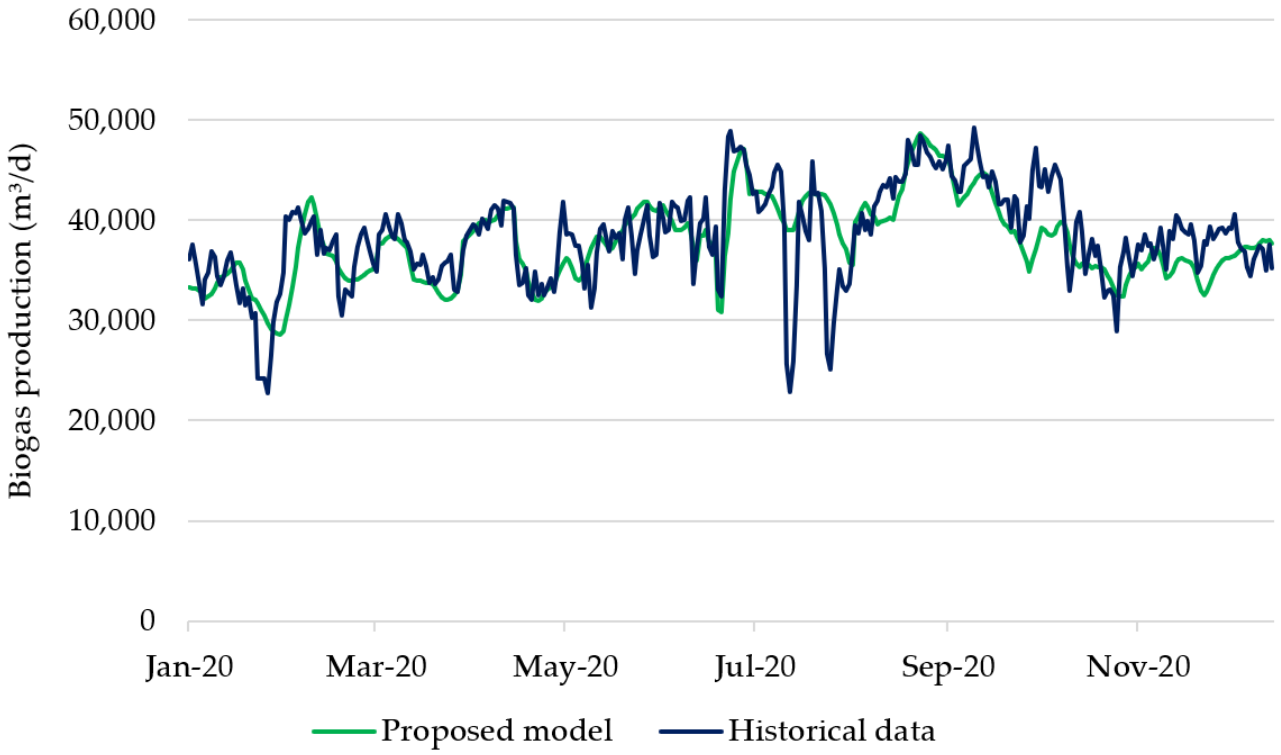

Figure 3.4: Biogas production in 2020 (historical data vs. proposed model)

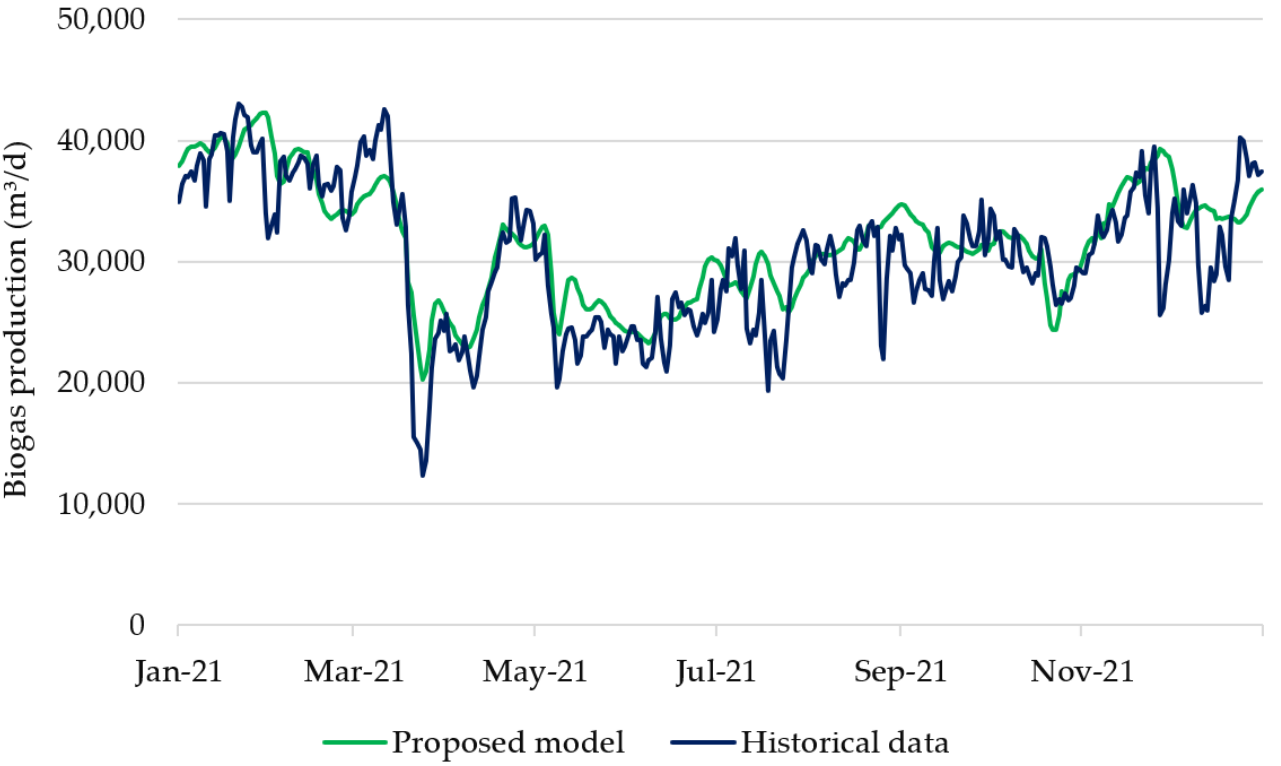

Figure 3.5: Biogas production in 2021 (historical data vs. proposed model)

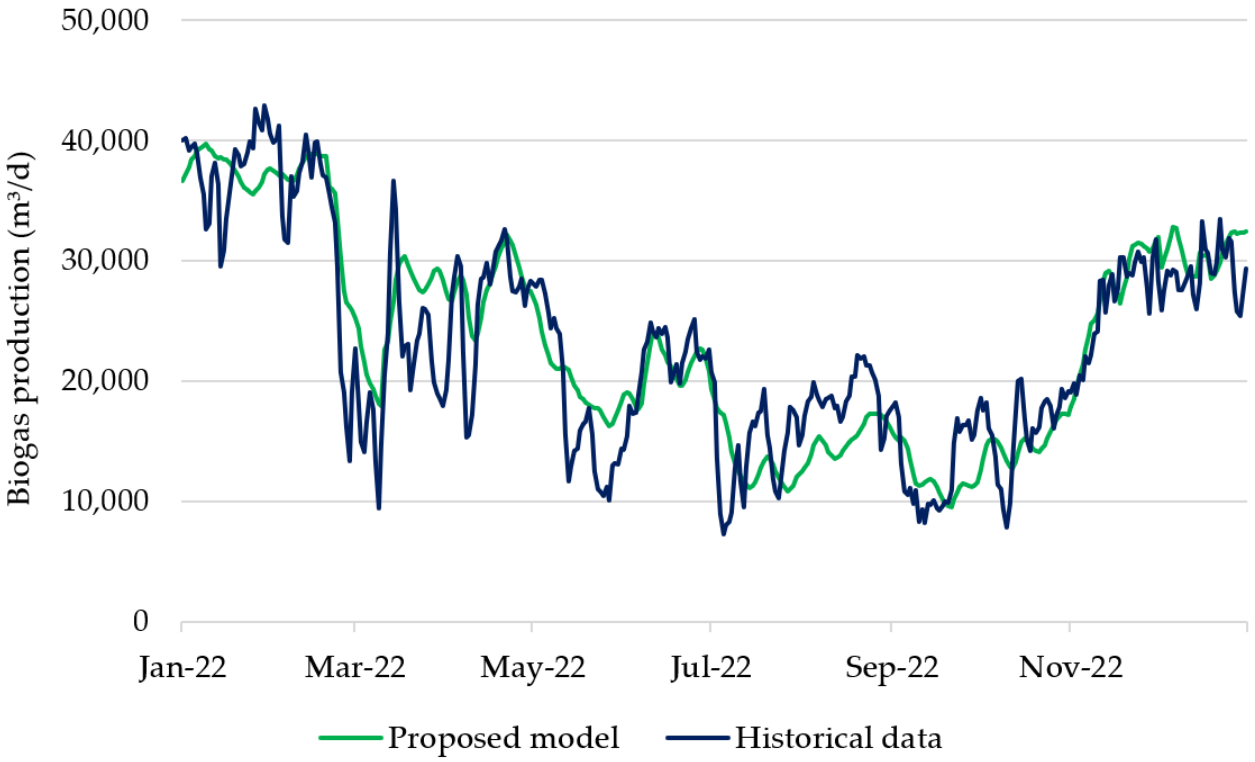

Figure 3.6: Biogas production in 2022 (historical data vs. proposed model)

For instance, as shown in Table 3.1, significant drops in sewage sludge-feeding quantity into the anaerobic digesters, including on Jul-20, Mar-21, May-21, Mar-22 and Sep-22, which likely contributed to the observed decreases in biogas production during the same periods, as shown in Figures 3.4–3.6. Based on these results, the proposed model demonstrates strong potential to forecast biogas production from sewage sludge in a large-scale WWTP. One explanation for this alignment is the adoption of dynamic retention time used in the semi-continuous feeding mode of sewage sludge, whereas in steady-state models, the retention time is considered constant. Table 3.1 compares the average biogas production from the proposed model and historical data from 2020 to 2022, month by month. It can see that the minimum and maximum error values are between 0.07% (Oct-21) and 18.74% (Aug-22), respectively. Eq. (3.19) calculates the error (ϵ_{biogas}) between the average historical biogas production ($V_{biogas_{hist,ave}}$) and the average biogas production forecasted by the proposed model ($V_{biogas_{model,ave}}$) for each month (Jan-20 to Dec-22). The error is expressed as a percentage (%), and the average biogas values is given in m^3/d.

$$\epsilon_{biogas} = \frac{|V_{biogas_{hist,ave}} - V_{biogas_{model,ave}}|}{V_{biogas_{hist,ave}}} \tag{3.19}$$

The comparison of historical biogas production with the proposed model indicates that the model generally reproduces the observed trends with moderate deviations. The average biogas production based on the WWTP historical data is 37,337 m^3/d, 31,695 m^3/d and 23,350 m^3/d for 2020, 2021 and 2022, respectively, while, the estimated average biogas production based on the proposed model is 37,960 m^3/d, 30,465 m^3/d and 23,080 m^3/d for the same period. Considering the entire 3-year period, the average biogas production is 30,794 m^3/d for the historical data and 30,503 m^3/d for proposed model, resulting in an average error of less than 5%. As shown in Table 3.1, the months with higher errors were Mar-22 and Aug-22. Monthly

biogas production varied significantly across the three years, with peaks typically occurring in mid-year months (e.g., June–September 2020) and troughs in early and late months (e.g., May–July 2022). The model tended to slightly overestimate production in some months (e.g., Jan–Apr 2020) and underestimate in others (e.g., Mar–Aug 2022), with individual monthly errors ranging from 0.07% to 18.74% and an average error of 4.64 %.

Table 3.1: Average biogas production (historical data vs. proposed model)

Month	**Hist (m^3)**	**Model (m^3)**	**Error (%)**
Jan-20	30,367	32,181	5.64
Feb-20	34,190	34,023	0.49
Mar-20	36,000	36,862	2.34
Apr-20	36,696	37,585	2.37
May-20	35,320	35,704	1.07
Jun-20	39,706	39,027	1.74
Jul-20	40,667	40,561	0.26
Aug-20	40,487	38,365	5.53
Sep-20	45,099	45,693	1.30
Oct-20	38,498	41,641	7.55
Nov-20	34,969	36,195	3.39
Dec-20	36,039	37,714	4.44
Jan-21	40,029	38,650	3.57
Feb-21	36,532	36,392	0.38
Mar-21	30,842	30,450	1.29
Apr-21	28,073	27,673	1.45
May-21	27,284	24,619	10.83
Jun-21	25,918	24,493	5.82
Jul-21	28,272	26,848	5.30
Aug-21	31,828	30,184	5.45
Sep-21	31,928	29,913	6.74
Oct-21	29,768	29,746	0.07
Nov-21	35,591	33,011	7.82
Dec-21	34,252	33,604	1.93
Jan-22	37,695	37,973	0.73
Feb-22	35,238	33,362	5.63
Mar-22	25,286	22,121	14.31
Apr-22	28,085	27,654	1.56
May-22	19,933	17,904	11.33
Jun-22	20,913	21,522	2.83
Jul-22	13,350	13,937	4.21
Aug-22	15,193	18,697	18.74
Sep-22	11,952	12,620	5.30
Oct-22	14,844	15,934	6.84
Nov-22	26,978	26,288	2.62
Dec-22	30,762	28,946	6.27
Average	**-**	**-**	**4.64**

In addition, to assess the performance of the proposed model, common metrics including Mean Absolute Error (MAE), Mean Squared Error (MSE), Root Mean Squared Error (RMSE), and the coefficient of determination (R^2) were considered, as shown in Table 3.2. Over the entire 2020–2022 period, the model achieved an average MAE of 2,703 m^3, RMSE of 3,569 m^3, and R^2 of 0.85, suggesting that it reliably captures both seasonal and inter-annual trends in biogas production, and also the proposed model has captured a significant amount of the variance in the data, and the predictions are fairly accurate.

Table 3.2: Performance metrics to assess the proposed biogas model

Period	MAE (m^3)	MSE $(m^3)^2$	RMSE (m^3)	R^2
2020	2,480	12,106,013	3,479	0.85
2021	2,663	12,008,002	3,465	0.65
2022	2,966	14,101,002	3,755	0.89
2020-2022	2,703	12,737,762	3,569	0.85

b. Retention time

Figures 3.7–3.9 illustrate the results of the calculated dynamic retention time in relation to the volume of sewage sludge fed into the anaerobic digester for each year 2020, 2021 and 2022. Figure 3.10 presents the results for the entire period (2020 to 2022). The retention times shown in these figures correspond to the oldest sludge parcel that remained inside the digester (see explanation in Section 3.4.2). It can be observed that the retention time changes dynamically across the entire period. The relationship between retention time and sewage sludge volume is inversely proportional: as the sewage sludge volume increases, the retention time decreases, and vice versa. This behavior is expected because the volume of sludge inside the digester remains constant across the entire period (2020 to 2022). In 2020, the retention time fluctuated between a minimum of 14 days and a maximum of 19 days, whereas, in 2021, it reached a maximum of 22 days and a minimum remained 14 days. However, in 2022, a larger variation in retention times was observed due to significant changes in the volume of sewage sludge fed into the digester. In Oct-22, the retention time had its peak of 38 days, and the minimum remained at 14 days.

3.5.3 Batch and Semi-Continuous Operation Modes

Digestion feeding modes can have a direct impact on the reactor operation, and two patterns are more common: batch and semi-continuous. The main difference between them relies on two operational parameters: retention time and flow rate, which are fixed and defined in the batch process but variable in the semi-continuous operation [256], [257]. These two parameters are major influencers of anaerobic digestion performance and efficiency [15].

In a commercial-scale batch process, biogas production tends to be more predictable and stable than in continuous or semi-continuous feeding systems. This is because all the substrate is loaded at once, allowing microbial activity to follow a defined progression and reducing the impact of operational fluctuations [258]. Batch processes offer advantages such as operational simplicity, economic benefits, and a lower risk of pipeline blockage. Biogas generation typically peaks at the beginning of the digestion cycle and gradually decreases as the available organic matter is consumed. These systems also require a larger inoculum and overall system size. In contrast, continuous or semi-continuous feeding can produce more variable biogas flows due to fluctuations in influent characteristics and overlapping microbial stages. However, microbial populations in batch systems are less susceptible to sudden shocks, resulting in more consistent operation [257]. The semi-continuous regime is usually more commonly used when the feedstock production is variable, as is often the case in WWTPs [232], [259]. This operational mode allows for more regular feeding and removal of sludge, which can help maintain a relatively constant methane generation [257]. In practice, different volumes and compositions of sewage sludge are added, and digestate is withdrawn at each interval [7], [36]. While this approach supports continuous operation, it introduces additional complexity due to fluctuating substrate characteristics, overlapping microbial activity stages, and potential sensitivity to operational disturbances. As a result, short-term biogas production can be less predictable compared to

batch processes, although the system provides a more steady long-term output and can adapt to variable influent conditions.

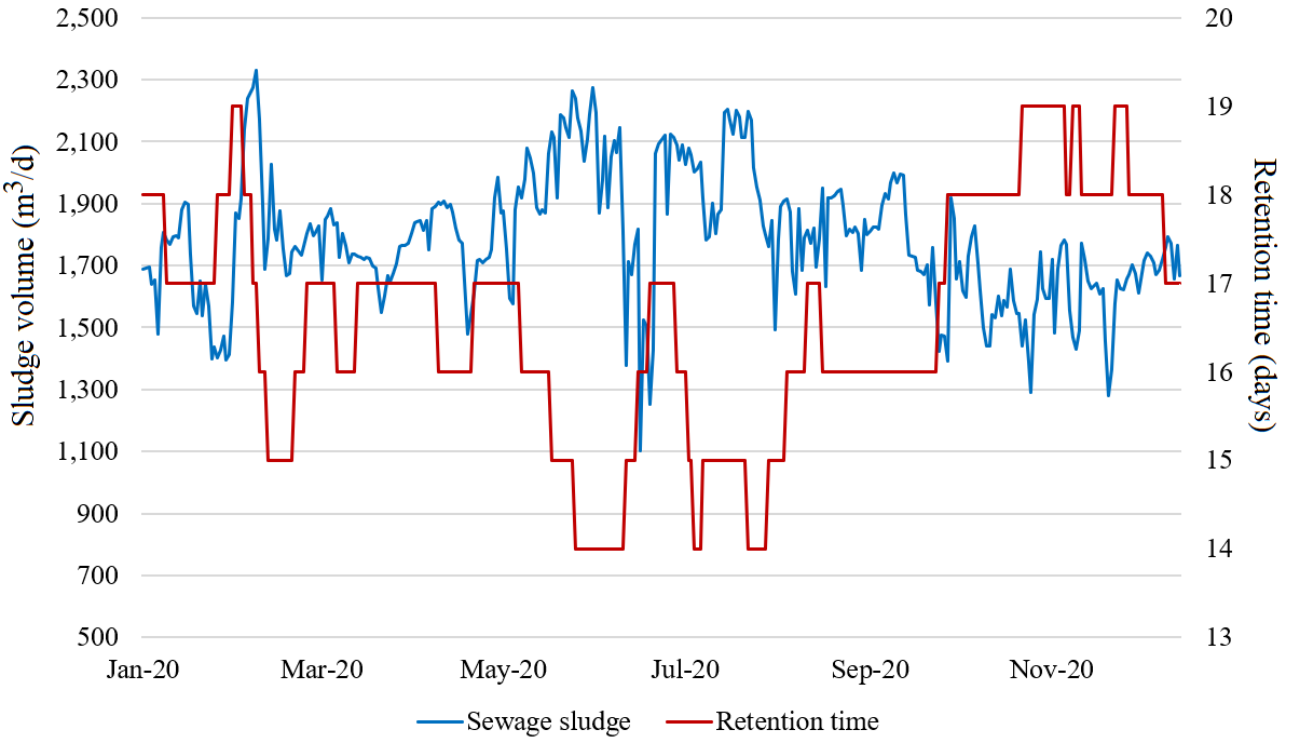

Figure 3.7: Retention time and sewage sludge flow in 2020

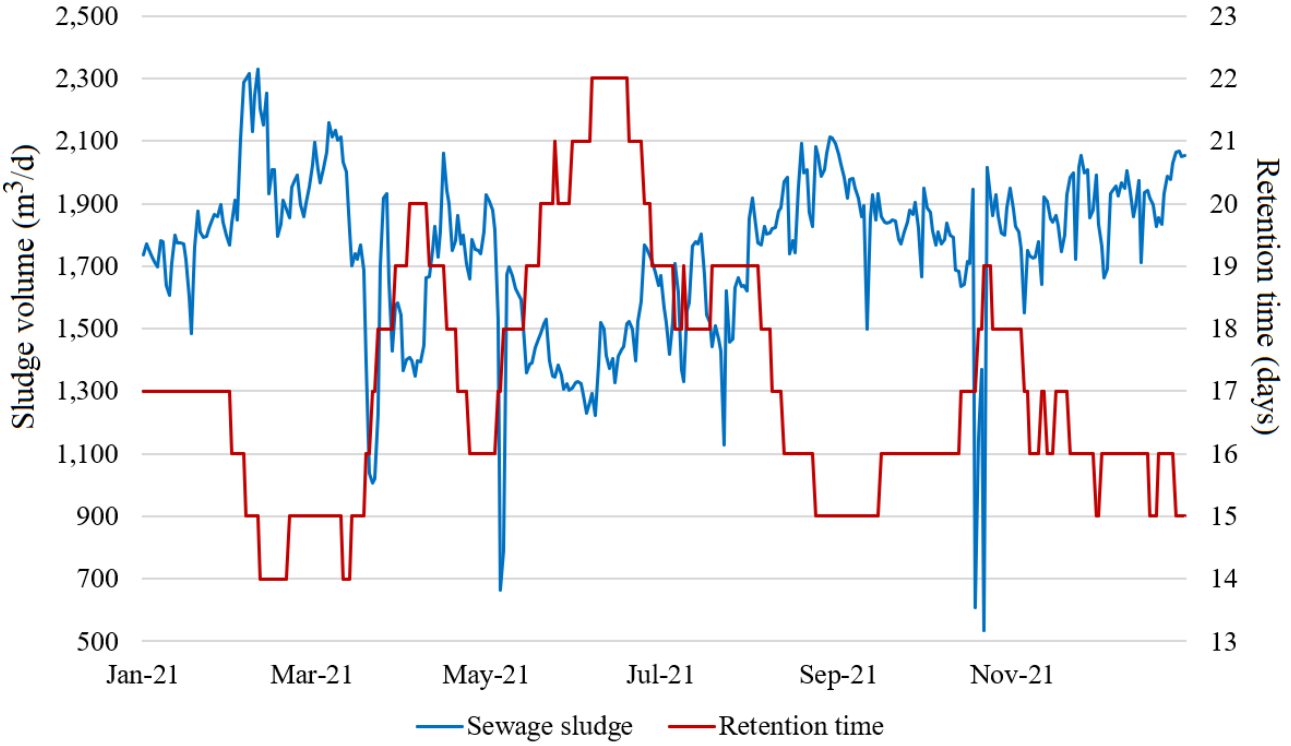

Figure 3.8: Retention time and sewage sludge flow in 2021

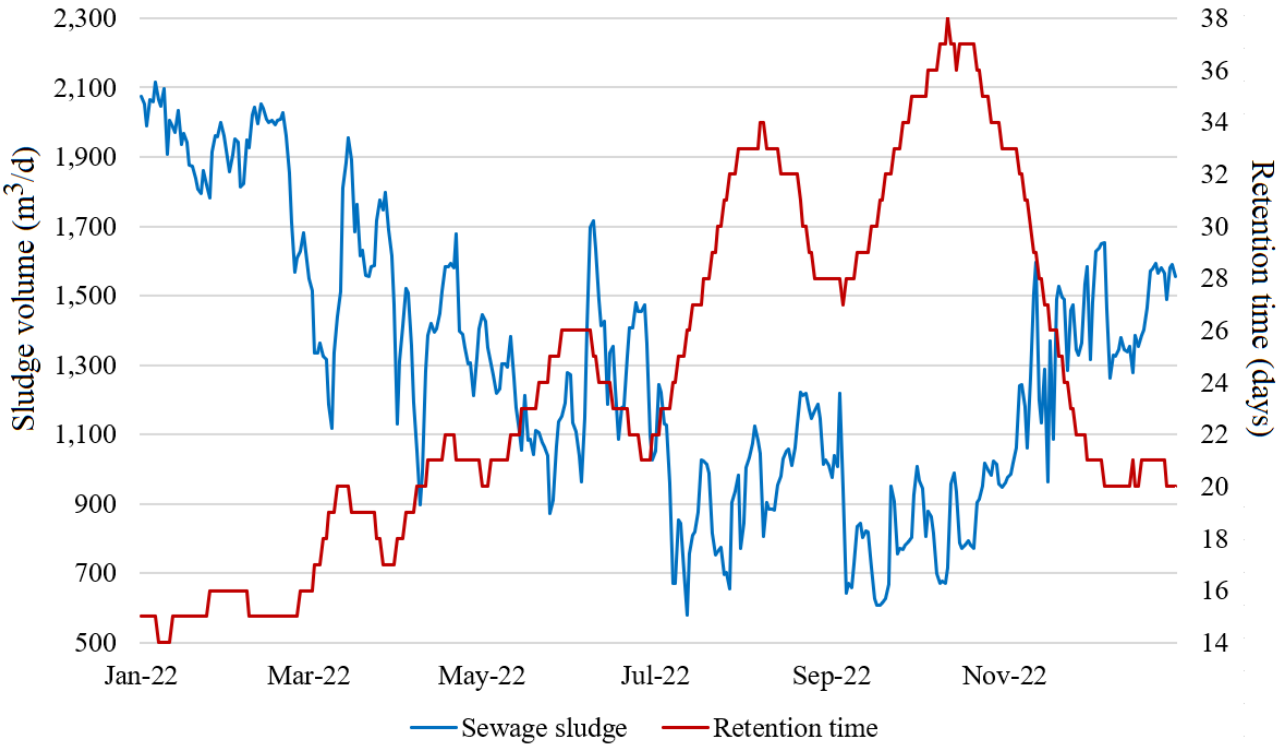

Figure 3.9: Retention time and sewage sludge flow in 2022

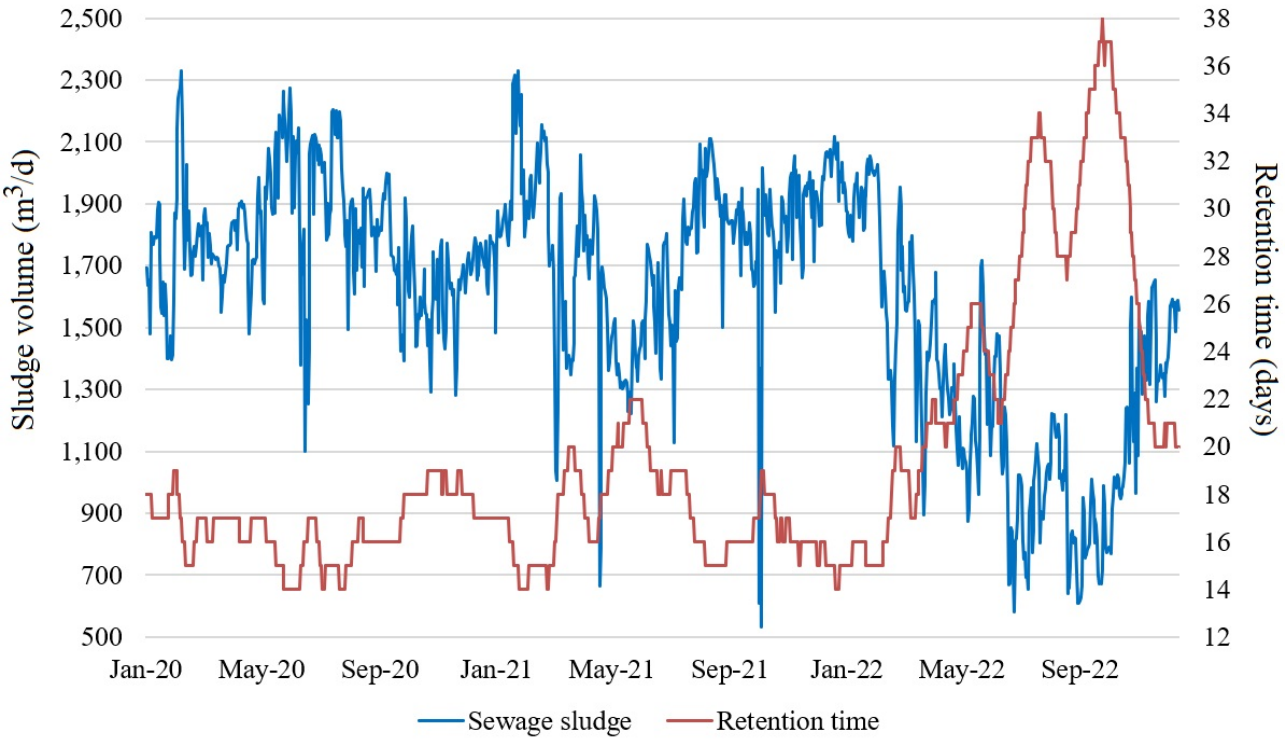

Figure 3.10: Retention time and sewage sludge flow from 2020 to 2022

The variability in the composition and quantity of incoming material can create challenges

in maintaining optimal temperature, pH, hydraulic retention time, as well as in ensuring sufficient availability of organic material. Such fluctuations may disrupt microbial activity and community balance, leading to inconsistencies and uncertainties in biogas production rates and incomplete sludge degradation. Continuous feeding can also introduce toxic or inhibitory compounds (e.g., heavy metals, salts, ammonia, fatty acids) present in the raw sludge, which may reduce digestion performance and efficiency. Additionally, in continuous processes, microorganisms can be washed out with the removed digestate material, reducing the microbial population inside the reactor [232], [257], [260].

Most existing methods found in the literature focus on batch process [239], [241], [243], [244], rather than the semi-continuous operations [261]. As a result, comparing biogas production and anaerobic digestion performance between batch and semi-continuous processes is challenging, due to their distinct characteristics and operational conditions. In this study, we propose a semi-continuous model based on first-in, first-out (FIFO) methodology to replicate the continuous feeding operation characteristics. To the best of the authors' knowledge, this is the first model introducing the concept of dynamic retention time for a semi-continuous anaerobic digestion process.

In this proposed semi-continuous model, retention time is calculated based on the flow rate of sewage sludge entering the digester, while the digester volume is kept constant throughout the operation. As explained in Section 3.4.2, when a new sewage sludge volume enters the digester from the top, the same sludge volume in the digester is removed from the bottom. Retention time adjusts accordingly, depending on the inflow rate.

3.5.4 Biogas Model Limitations

A key limitation of the proposed method relates to the assumption of no mixing between sludge parcels. Each parcel of incoming sewage sludge ($V_{ss_{in}}(t)$) is treated as an independent element, with no interaction with other parcels. This assumption allows the FIFO methodology to replicate the anaerobic digestion process with dynamic retention time. If mixing were considered, the independence of sludge parcels would be lost, and the FIFO approach would no longer be valid. Nonetheless, this simplification permits each parcel to have a distinct retention time inside the digester [248], [249].

3.6 Summary

In large-scale WWTPs, sewage sludge treatment is inherently dynamic, making it essential to employ models that replicate semi-continuous processes. This chapter introduced a novel biogas production model that combines the simplicity of steady-state approaches with the dynamic behavior of semi-continuous feeding, using a FIFO methodology. The model captures time-dependent retention times based on daily sludge inflows while maintaining a constant digester volume, enabling a more realistic simulation of large-scale anaerobic digestion.

Validation was performed using three years of historical data from a full-scale municipal WWTP in Sydney, Australia. The comparison between modeled and historical biogas output showed a low average error of less than 5% over the three years, with monthly errors ranging from 0.07% to 18.74%. This demonstrates the model's strong capability for accurately forecasting biogas production. Despite significant fluctuations in historical biogas production, the model consistently captured the general non-linear trends. Model performance was also evaluated

using common metrics such as MAE, MSE, and R^2, indicating that the model explained a significant portion of data variance.

The model further addresses key challenges associated with continuous processes, including variations in feedstock composition and dynamic sewage sludge flow, both of which can affect digestion efficiency biogas yield. The assumption of no mixing between sludge parcels, while necessary to enable dynamic retention time tracking, remains a limitation, as it simplifies the microbial interactions and homogenisation processes within the anaerobic digester. Overall, the proposed model represents a meaningful advancement in semi-continuous anaerobic digestion modeling, providing a practical and computationally efficient tool for optimising and managing biogas production in WWTPs.

Chapter 4

Operation Model: Current Assets

4.1 Introduction

In this chapter, an optimal operation model for the power generation system of a WWTP is proposed, focusing on the existing infrastructure (current generation assets), which is the CHP units, and also the reliance on the main power grid. The model aims to minimise the operational costs of the plant while optimising the utilisation of the biogas generated on-site. By integrating real operational constraints and asset performance data, the model supports informed decision-making to enhance energy efficiency and cost-effectiveness. Some case scenarios are investigated and discussed in the end of the chapter.

This chapter is organised as follows. Section 4.2 provides a background regarding the proposed operation model considering the current assets of the power generation system in the WWTP. Section 4.3 presents the model framework and formulation. Section 4.4 presents the simulation results of four different case studies in order to test the effectiveness of the proposed model, and provides some discussion regarding the case studies' results. Finally, Section 4.5 summarises the main findings of the chapter.

4.2 Background

The wastewater treatment process generates a by-product known as sewage sludge. Sewage sludge contains high levels of pollutants, organic content and water, and it must be properly treated before it is disposed of. Although only accounting for approximately 1% to 2% of the total volume of the wastewater treated in a WWTP, the cost of sewage sludge treatment and management can be significant [15]. Anaerobic digestion is one of the most widely used technologies for treating sewage sludge and recovering energy in WWTPs. This biological process involves the breakdown of organic matter by microorganisms in the absence of oxygen, making it an effective method for both sludge treatment and energy recovery. A valuable by-product of this process is biogas, which can be captured and used as a renewable energy source. In the United States, approximately 48% of wastewater is treated using anaerobic digestion in WWTPs [262]. In Australia, around 55% of the WWTPs utilise biogas generated from anaerobic digestion to produce bioenergy, with further opportunities for enhancing biogas production and utilisation in both existing and new facilities [1]. WWTPs, which have anaerobic digestion technology for wastewater and sewage sludge treatment, usually consume 40% less energy than

plants that do not have this operation process [9]. In some cases, when the plant combines different strategies and technologies, including co-digestion, renewable energy generation, energy management strategies, etc., energy self-sufficiency can reach up to 100% [66]. Therefore, taking advantage of anaerobic digestion technology by utilising biogas for power generation can be a great option to increase energy efficiency and reduce energy costs in WWTPs [2]. Most WWTPs follow traditional operation guidelines established based on historical processes [263], [264]. At the same time, due to more stringent effluent standards and the increase in the volume of wastewater generated globally, energy demand for WWTPs has been increasing, adding more challenges to the daily operation of these facilities. There are some models presented in the literature that explore the opportunities for minimising operating costs for a WWTP; however, there is still a need to further investigate this topic. Exploring operating models can be an important methodology to address the current challenges and limitations. Therefore, an operation model which aims to minimise the energy operating costs for a municipal WWTP is proposed in this chapter. Although there are different models in the literature exploring the opportunities for utilising renewable energy resources to minimise operating costs, there are not many models focused on the optimisation of biogas power generation in WWTPs. Additionally, this proposed method incorporates the biogas production model proposed in [265] which considers the semi-continuous process while optimising the biogas utilisation to reduce the operating costs of a large-scale WWTP.

Current assets - Power generation system

Historical and technical data for a large-scale WWTP, which treats around 500 million liters of sewage wastewater daily, was used in this study. The plant is located in Sydney, Australia, and it is composed only of primary treatment. The power generation of the considered WWTP is composed of a cogeneration system (also known as CHP). The CHP engines generate electricity and heat that is primarily used on-site, and if there is any excess of electricity, it is exported to the grid. The heat recovered from the CHP system is used in the anaerobic digester, and if the heat is not enough to maintain the temperature at the desired level, boilers are used to supply the remaining heat load required. If there is not sufficient biogas on-site to meet the heating demand from the anaerobic digester system, natural gas can be imported from the gas network and used to supply the heating demand. Additionally, the anaerobic digester operates in a mesophilic temperature range.

Figure 4.1 shows a diagram of the WWTP used in the current assets scenario. The WWTP receives the influent (raw sewage) and a preliminary treatment removes large debris. Subsequently, there is a primary treatment which consists of grit removal and primary sedimentation. The raw sewage sludge produced in the sedimentation tank enters the anaerobic digester (AD) where it is treated, generating biogas as a co-product. The generated biogas can be used in the CHP system, which generates power and heat, and/or boilers to generate extra heat, if needed. If the on-site biogas is not enough to supply the thermal energy required for the anaerobic digesters, the WWTP can import natural gas from the gas grid to be used in the boilers. After digestion, the digested sludge is disposed of.

Most WWTPs are primarily operated based on standard and traditional guidelines that were established from operational experience and historical processes. Therefore, these facilities usually do not explore their maximum operation capacity and/or efficiency. In order to take advantage of this potential, an operation model is proposed and the results are compared with the historical and operational data from a large-scale WWTP. As mentioned previously,

the proposed operation model aims to minimise the operating costs for the WWTP, and the formulation is presented in the following.

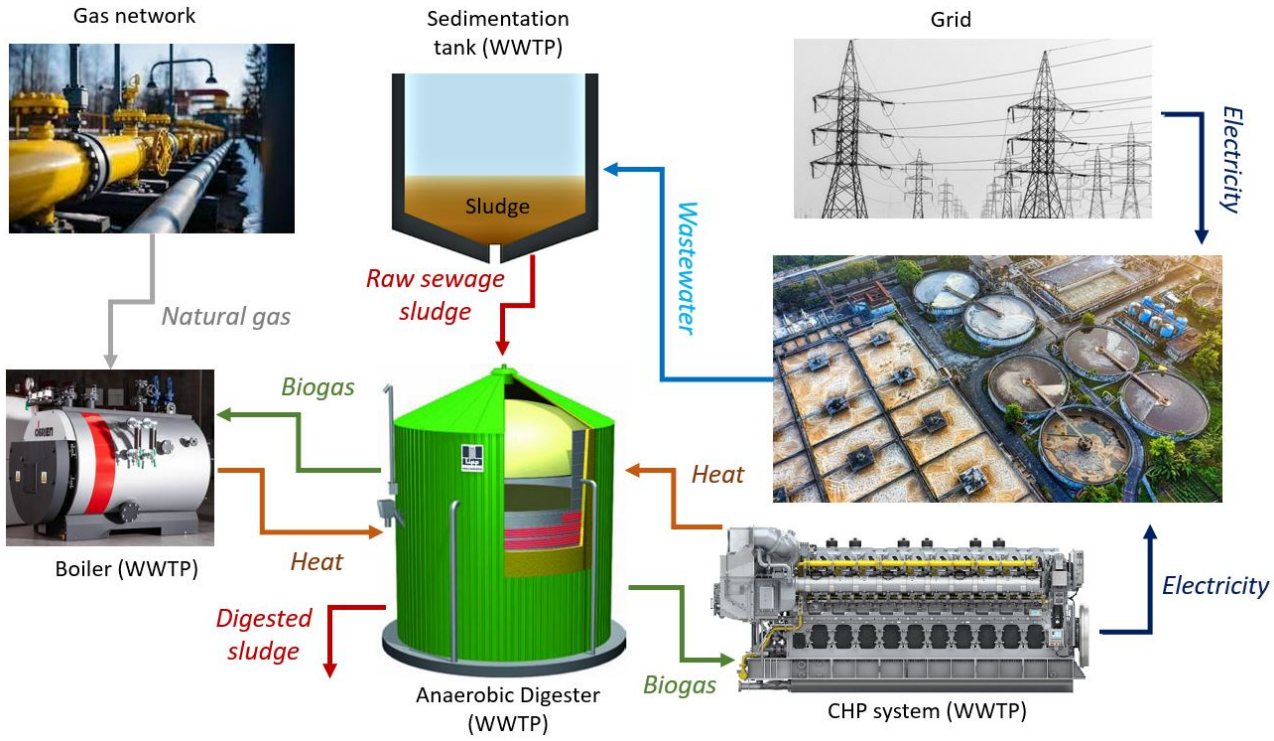

Figure 4.1: System configuration (Current Power Generation Assets)

4.3 Model Framework and Design

In this section, the model framework for the operation model of the current power generation assets is presented, including the general assumptions and mathematical formulation.

In this study, an operation model is proposed and it aims to minimise the operating costs of a large-scale WWTP using only the current power generation assets. The outputs of the operation model include an optimal temperature for the anaerobic digestion and the minimal operating costs for the WWTP. The operation model uses the biogas model proposed in [265] to calculate and forecast the biogas production based on a range of mesophilic temperatures, which is omitted here. The optimisation problem is formulated as a mixed integer linear problem (MILP), and the model formulation is provided below.

As presented in Section 3.4.3b, the equations related to biogas volume inside the digester are defined in (3.10 - 3.15).

Eq. (4.1) describes the time constraint for the volume of the biogas inside the anaerobic digester, where $V_{biogas_{ch}}(t)$ and $V_{biogas_{dis}}(t)$ are the biogas volumes stored and discharged, respectively.

$$V_{biogas_{ad}}(t) = V_{biogas_{ad}}(t-1) + [V_{biogas_{ch}}(t) - V_{biogas_{dis}}(t)] \tag{4.1}$$

In this study, the optimisation model considers three optimisation horizons: 1 month, 1 year and 3 years, covering the period from 2020 to 2022. To describe the initial conditions of the

biogas level, constraint (4.2) is presented. Constraint (4.2) ensures that the biogas volume inside the anaerobic digester at the end of each day ($V_{biogas_{ad}}(24*d)$) is equal to the initial state of biogas volume, denoted as $V_{biogas_{ad_{ini}}}$. Note that n_d is the number of days of the optimisation horizon.

$$V_{biogas_{ad}}(24*d) = V_{biogas_{ad_{ini}}}, d = 1, 2, 3, \ldots, n_d \tag{4.2}$$

Figure 4.2 illustrates the biogas and natural gas utilisation in the WWTP, which summarises the formulation defined in (4.3)-(4.14). As shown in Figure 4.2, the biogas generated can be directly used in the CHP and boilers, flared or stored (*"charging"*) in the storage. The stored biogas can be further *"discharged"* to supply the CHP, boilers, or flared. Natural gas can also be imported from the grid to supply the boilers.

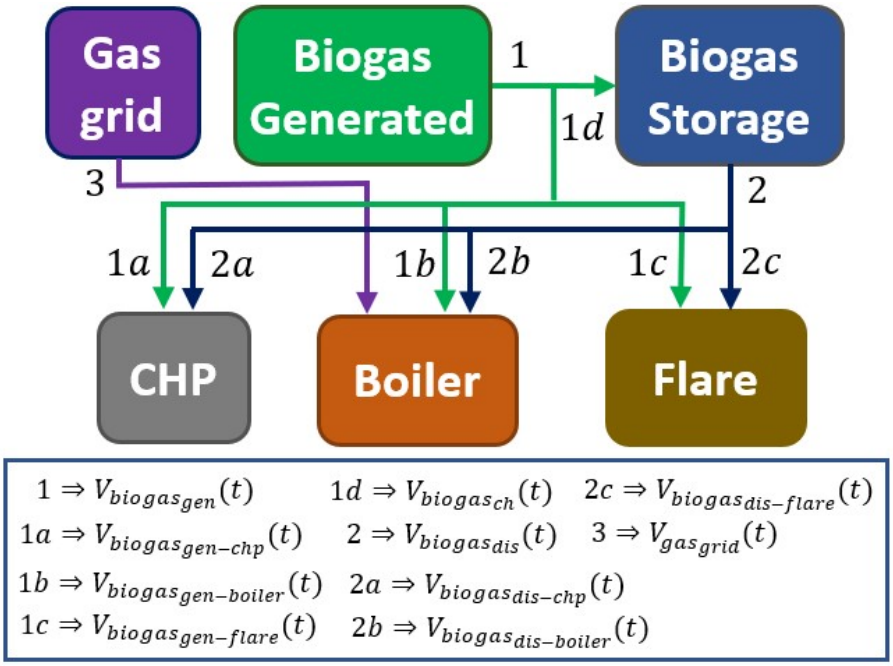

Figure 4.2: Biogas and natural gas components (Current WWTP configuration)

Eqs. (4.3) and (4.4) define the boundaries for the two operations - biogas charging and discharging, respectively. The binary variable $u_{ad}(t)$ is used to control whether biogas charging or discharging occurs at a specific time t, ensuring that both states do not happen simultaneously. $r_{biogas_{ch}}$ and $r_{biogas_{dis}}$ are the maximum charging and discharging rates for the biogas operation in the anaerobic digestion system, respectively, and Δt is the time interval.

$$0 \leq \frac{V_{biogas_{ch}}(t)}{\Delta t} \leq r_{biogas_{ch}} \cdot u_{ad}(t) \tag{4.3}$$

$$0 \leq \frac{V_{biogas_{dis}}(t)}{\Delta t} \leq r_{biogas_{dis}} \cdot [1 - u_{ad}(t)] \tag{4.4}$$

The total volume of biogas generated in the WWTP ($V_{biogas_{gen}}(t)$) can be divided into different components, including CHP system ($V_{biogas_{gen-chp}}(t)$), boiler ($V_{biogas_{gen-boiler}}(t)$), flare ($V_{biogas_{gen-flare}}(t)$) and/or stored ($V_{biogas_{gen-stored}}(t)$), the latter of which is referred to as *"charging"*, as shown in (4.5) . Similarly, Eq. (4.6) represents the breakdown for the stored component

($V_{biogas_{dis}}(t)$) (t)), which includes (*"discharging"*) biogas to supply the CHP ($V_{biogas_{dis-chp}}(t)$), boiler ($V_{biogas_{dis-boiler}}(t)$), and flare ($V_{biogas_{dis-flare}}(t)$). Constraint 4.7 limits the upper and lower boundaries of the generated biogas, where $V^{\max}_{biogas_{gen}}$ is the maximum biogas volume that can be generated in the WWTP.

$$V_{biogas_{gen}}(t) = V_{biogas_{gen-chp}}(t) + V_{biogas_{gen-boiler}}(t) + V_{biogas_{gen-flare}}(t) + V_{biogas_{ch}}(t) \tag{4.5}$$

$$V_{biogas_{dis}}(t) = V_{biogas_{dis-chp}}(t) + V_{biogas_{dis-boiler}}(t) + V_{biogas_{dis-flare}}(t) \tag{4.6}$$

$$0 \leq V_{biogas_{gen}}(t) \leq V^{\max}_{biogas_{gen}} \tag{4.7}$$

4.3.1 Biogas Components

a. CHP system

Eq. (4.8) states the total volume of gas consumed by the CHP system, $V_{biogas_{chp}}(t)$, which is equal to the sum of two components: $V_{biogas_{gen-chp}}(t)$ and $V_{biogas_{dis-chp}}(t)$. Constraint (4.9) states the upper and lower boundaries of the total biogas volume used in the CHP units, where $V^{\max}_{biogas_{chp}}$ is the maximum value.

$$V_{biogas_{chp}}(t) = V_{biogas_{gen-chp}}(t) + V_{biogas_{dis-chp}}(t) \tag{4.8}$$

$$0 \leq V_{biogas_{chp}}(t) \leq V^{\max}_{biogas_{chp}} \tag{4.9}$$

b. Boiler

Similarly, Eq. (4.10) states the total volume of gas consumed in the boilers, $V_{biogas_{boiler}}(t)$. Constraints (4.11) and (4.12) state the upper and lower boundaries of the total volume of biogas and natural gas can that can be used in the boilers, and express the maximum volume of natural gas that can be imported from the gas network, respectively. $V^{\max}_{biogas_{boiler}}$ is the maximum volume of gas (including both biogas and natural gas) that can be used by the boilers, and $V^{\max}_{gas_{grid}}$ is the maximum volume of natural gas that can be imported from the gas network. $V_{gas_{grid}}(t)$ and $u_{gas}(t)$ are the volume of natural gas imported, and the binary variable which controls whether natural gas is imported or not from the network, respectively.

$$V_{biogas_{boiler}}(t) = V_{biogas_{gen-boiler}}(t) + V_{biogas_{dis-boiler}}(t) \tag{4.10}$$

$$0 \leq V_{biogas_{boiler}}(t) + V_{gas_{grid}}(t) \leq V^{\max}_{biogas_{boiler}} \tag{4.11}$$

$$0 \leq V_{gas_{grid}} \leq V^{\max}_{gas_{grid}} \cdot u_{gas}(t) \tag{4.12}$$

c. Flare

Eqs. (4.13) and (4.14). state the total biogas flared ($V_{biogas_{flare}}(t)$) and the upper and lower boundaries, respectively. $V^{\max}_{biogas_{flare}}$ is the maximum value of biogas that can be flared in the WWTP.

$$V_{biogas_{flare}}(t) = V_{biogas_{gen-flare}}(t) + V_{biogas_{dis-flare}}(t) \tag{4.13}$$

$$0 \leq V_{biogas_{flare}}(t) \leq V^{\max}_{biogas_{flare}} \tag{4.14}$$

4.3.2 Current Power Generation Assets

a. CHP system

The electrical power ($P_{chp}(t)$) and heating power ($Q_{chp}(t)$) from the CHP system are defined in (4.15) and (4.16), respectively, and Eq. (4.17) expresses the quantity of heating power generated from the boilers ($Q_{boiler}(t)$). As stated in (4.17), the boilers can be supplied by two sources, on-site biogas or natural gas imported from the gas grid. $\eta_{e_{chp}}$, $\eta_{th_{chp}}$ and $\eta_{th_{boiler}}$ are the electrical and thermal efficiencies for the CHP system, and thermal efficiency for the boilers. $c_{p_{biogas}}$, $c_{p_{gas}}$,and k_{jw} are the calorific power of biogas and natural gas, and the conversion factor from MJ to kWh, respectively.

$$P_{chp}(t) = \frac{V_{biogas_{chp}}(t) \cdot c_{p_{biogas}} \cdot \eta_{e_{chp}} \cdot k_{jw}}{\Delta t} \tag{4.15}$$

$$Q_{chp}(t) = \frac{V_{biogas_{chp}}(t) \cdot c_{p_{biogas}} \cdot \eta_{th_{chp}} \cdot k_{jw}}{\Delta t} \tag{4.16}$$

$$Q_{boiler}(t) = \frac{[V_{biogas_{boiler}}(t) \cdot c_{p_{biogas}} + V_{gas_{grid}}(t) \cdot c_{p_{gas}}] \cdot \eta_{th_{boiler}} \cdot k_{jw}}{\Delta t} \tag{4.17}$$

Constraints (4.18) and (4.19) define the upper and lower boundaries of the electrical power and heating power from the CHP units, and constraint (4.20) limits the maximum heating power in the boilers. $P^{\max}_{chp}$ and $Q^{\max}_{chp}$ are the maximum limits of the electrical power and heating power generation from the CHP system, and $Q^{\max}_{boiler}$ is the maximum limit for the boilers.

$$0 \leq P_{chp}(t) \leq P^{\max}_{chp} \tag{4.18}$$

$$0 \leq Q_{chp}(t) \leq Q^{\max}_{chp} \tag{4.19}$$

$$0 \leq Q_{boiler}(t) \leq Q^{\max}_{boiler} \tag{4.20}$$

b. Grid

Eqs. (4.21) and (4.22) impose the boundaries for the power imported from the grid ($P_{grid}(t)$) and exported to the grid ($P_{sold}(t)$), respectively. $P^{\max}_{grid}$ and $P^{\max}_{sold}$ are the maximum imported

and exported limits, and $u_{grid}(t)$ is the binary variable that is 1 if the grid is supplying power during period t, and 0 otherwise.

$$0 \leq P_{grid}(t) \leq P_{grid}^{\max} \cdot u_{grid} \tag{4.21}$$

$$0 \leq P_{sold}(t) \leq P_{sold}^{\max} \cdot [1 - u_{grid}] \tag{4.22}$$

c. Balance equation (Electrical component)

Eq. (4.23) defines the power balance equation in the WWTP. $P_{wwtp}(t)$ is the power consumption from the WWTP.

$$P_{grid}(t) + P_{chp}(t) = P_{wwtp}(t) + P_{sold}(t) \tag{4.23}$$

d. Thermal (Sewage Sludge)

Eq. (4.24) states that the combined heating power generated by the CHP and boilers should be equal to or higher than the total thermal power required from the anaerobic digester system ($Q_{ad}(t)$). In this model, it is assumed that the total heating power used in the anaerobic digestion is equal to the total thermal power required for heating the sludge ($Q_{ss}(t)$), as shown in (4.25). Eq. (4.26) represents the heating balance equation for the anaerobic digestion system, where $Q_{ad_{loss}}(t)$, $m_{ss}(t)$, h_{ss} and d_{ss} are the heating loss power in the anaerobic digesters, sludge mass flow into the digester, specific heat capacity of sludge, and sludge density, respectively. $T_{1_{ss}}(t)$ and $T_{ad}(t)$ are the sludge temperatures in the sedimentation tank and in the anaerobic digester, respectively. Note that $T_{ad}(t)$ is the decision variable to be determined.

$$Q_{ad}(t) \leq Q_{chp}(t) + Q_{boiler}(t) \tag{4.24}$$

$$Q_{ad}(t) = Q_{ss}(t) \tag{4.25}$$

$$Q_{ss}(t) = m_{ss}(t) \cdot h_{ss} \cdot [T_{ad_{ss}}(t) - T_1(t)] \cdot d_{ss} \cdot k_{jw} + Q_{ad_{loss}}(t) \tag{4.26}$$

Constraint (4.27) limits the temperature inside the anaerobic digester. Operational temperatures for the acidogenesis and methanogenesis stages typically range from 25 °C to 35 °C and 32 °C to 42 °C, respectively [15]. Mesophilic temperature regimes, which operate between 30 °C and 40 °C, have long been adopted for anaerobic digestion due to their good operational performance, low energy demand, and good process stability. In this study, a mesophilic temperature regime was considered, with the operational temperature for the anaerobic digestion ranging between 34 °C and 40 °C [266], [267].

$$T_{ad}^{\min} \leq T_{ad}(t) \leq T_{ad}^{\max} \tag{4.27}$$

Eq. (4.28) expresses the equation calculating the specific heat of the sludge (h_{ss}). h_w, h_{ds}, and $c_{ts_{ss}}$ are the specific heat capacity of water, the specific heat capacity of digested sludge, and the total solids concentration in the sludge, respectively.

$$h_{ss} = h_w \cdot (1 - c_{ts_{ss}}) + h_{ds} \cdot c_{ts_{ss}} \tag{4.28}$$

e. Objective Function

The objective function defined in (4.29) aims to minimise the operating costs of the WWTP, and it includes two parts: electricity costs and gas costs. $c_{ele_{imp}}(t)$ and $c_{ele_{exp}}(t)$ are the electricity prices for importing and exporting from the grid, and $c_{gas_{imp}}(t)$ is the gas price for importing natural gas if there is not enough biogas on-site. $c_{ele_{use}}(t)$ and $c_{gas_{use}}(t)$ represent the electricity and gas network usage prices, respectively, while $c_{ele_{cap}}(t)$ and $c_{ele_{other}}(t)$ correspond to electricity prices associated with network capacity and other charges (including environmental and system operator costs), respectively. λ_{dlf} is the distribution loss factor for the load for a specific location in the network grid, and $P_{wwtp_{cap}}(t)$ is the demand capacity of the WWTP.

$$
\begin{aligned}
Min \sum_{t} \Bigg\{ \Bigg[& P_{grid}(t) \cdot \lambda_{dlf} \cdot \big(c_{ele_{imp}}(t) + c_{ele_{use}}(t) + c_{ele_{other}}(t) \big) \\
& + P_{wwtp_{cap}}(t) \cdot c_{ele_{cap}}(t) - P_{sold}(t) \cdot c_{ele_{exp}}(t) \Bigg] \cdot \Delta t \\
& + \Bigg[V_{gas_{grid}}(t) \cdot \big(c_{gas_{imp}}(t) + c_{gas_{use}}(t) \big) \Bigg] \Bigg\}
\end{aligned}
\tag{4.29}
$$

As mentioned previously, the primary heating source for the anaerobic digester comes from the CHP units, which operate solely on on-site generated biogas. Boilers serve as a supplementary heating source and can operate on either this biogas or natural gas supplied from the external gas network. The proposed optimisation provides an optimal temperature for the anaerobic digestion process to achieve the minimum operating cost for the WWTP.

4.4 Simulation Results

This section presents the outcomes of the proposed operation model using the current power generation assets. Firstly, the key assumptions that underpin the analysis and simulation framework are highlighted. In sequence, the simulation results from the selected case studies are presented. The findings are analysed and discussed to highlight their implications, uncover patterns, and assess their alignment with the research objectives.

4.4.1 Inputs and Assumptions

This section presents the main inputs and key assumptions that underpin the analysis and simulation framework. Subsequently, the simulation results from the selected case studies are presented. The findings are analysed and discussed to highlight their implications, uncover patterns, and assess their alignment with the research objectives.

As previously mentioned, a large-scale WWTP located in Sydney, Australia, was used as a reference to perform the analysis in this study. The considered WWTP treats an average of 500 million liters of sewage wastewater daily and operates the anaerobic digestion at a temperature of 38°C. Figure 4.3 illustrates the daily biogas production and sewage sludge volume from the primary settlement tank, which feeds the anaerobic digester. Figure 4.4 shows the electricity consumption of the WWTP.

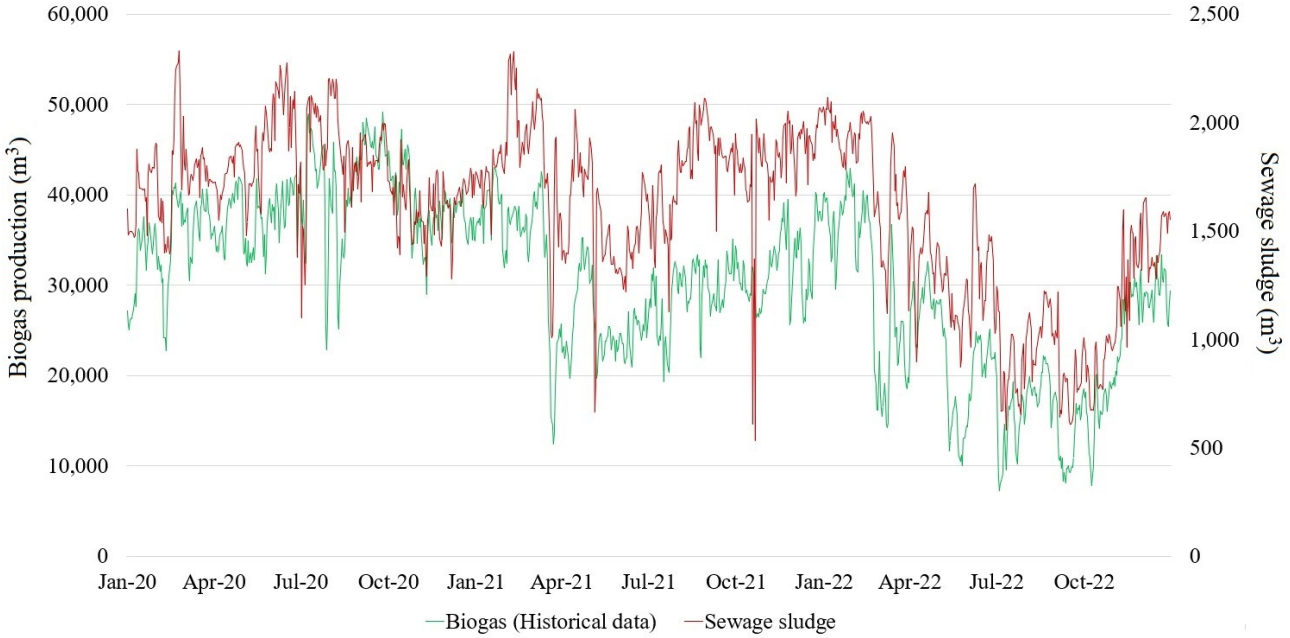

Figure 4.3: Biogas generation per day (in m^3) and sewage sludge volume that feeds the anaerobic digester per day (in m^3)

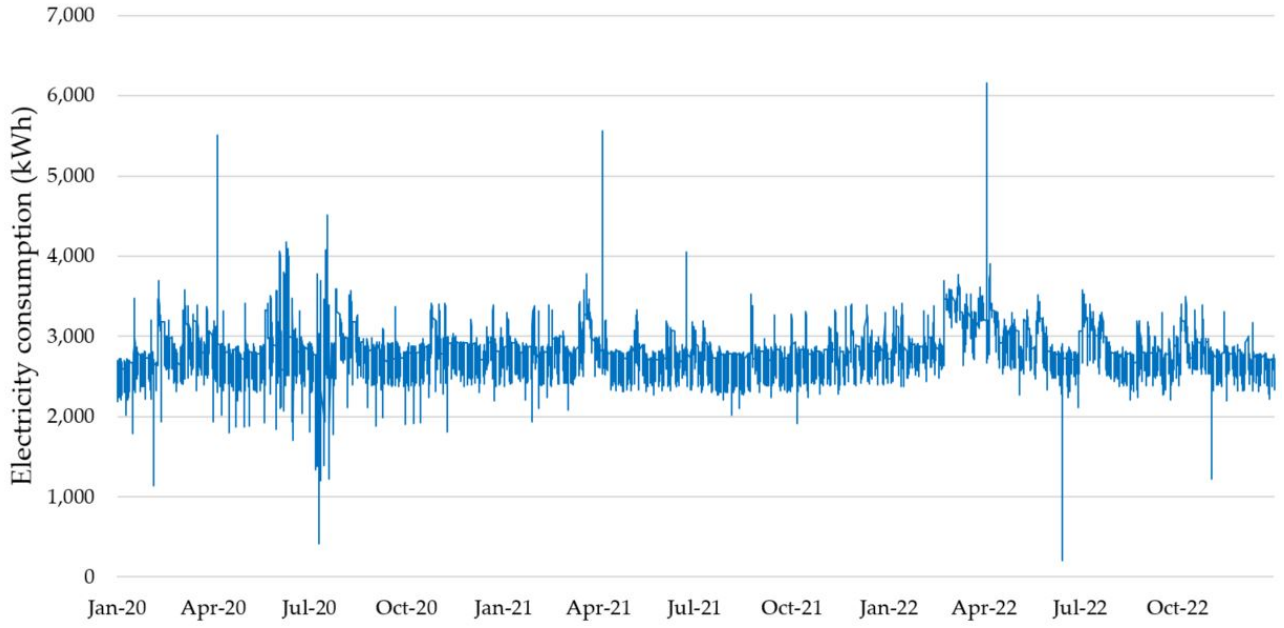

Figure 4.4: Electricity consumption of the WWTP

Table 4.1 shows the historical data for the WWTP, including gas production and utilisation, power generated from the CHP system, and power imported from the grid, from 2020 to 2022. As mentioned above, the operating temperature of the anaerobic digestion is fixed as 38°C. The power generation system in the WWTP used in this study consists only of a CHP system. The biogas generated is used first on the CHP, which provides both electricity (used on-site) and heating power (used to heat the digester). If the thermal power generated by the CHP is not enough to maintain the temperature of the digester at the determined operating level, the boiler is used to provide the required difference. If there is not sufficient biogas on-site, natural gas is imported from the gas network and used in the boiler.

Table 4.1: Historical data components of the WWTP

Year	Biogas generated (m^3)	Biogas CHP (m^3)	Biogas boiler (m^3)	Biogas flared (m^3)	WWTP (kWh)	CHP (kWh)	Grid (kWh)
2020	13,905,311	6,143,317	1,924,351	5,837,644	28,372,386	17,641,459	10,730,927
2021	11,123,326	5,411,314	1,508,443	4,203,568	25,640,542	13,896,518	11,744,024
2022	8,357,947	4,848,034	1,483,518	2,026,395	26,244,362	12,054,349	14,190,013

Some input data, parameters, and assumptions used in the case studies are listed below:

• Methane concentration is 65% (average concentration based on historical data);
• The thermal and electrical efficiencies of the CHP system are 38% and 32%, respectively;
• The thermal efficiency of the boiler system is considered to be 80%;
• The total thermal losses on the anaerobic digestion system are 381 kW;
• CHP has a generating capacity of 2,400 kW electrical power and 2,850 kW thermal power;
• The total volume of the anaerobic digestion system is 31,800 m^3, 90% of which is used for sewage sludge digestion and 10% is used as storage.

The electricity prices (given in c/kWh) for buying from the retailer, exporting back to the grid, and network charges under the Ausgrid EA370 tariff are presented in Table 4.2 .

Table 4.2: Electricity and network prices

Year	Electricity Importing		Network Usage			Electricity Exporting
	Peak	Off-peak	Peak	Shoulder	Off-peak	
2020	13.99	7.85	2.74	1.78	1.15	6.55
2021	11.28	6.13	2.80	1.81	1.17	5.11
2022	10.68	5.29	2.85	1.81	1.193	4.41

A fixed gas price of \$0.0387/MJ and a network charge of \$0.52/day were assumed. In this study, the WWTP is considered to sell biomethane directly to the gas market. Unlike several European countries with well-established feed-in tarriff schemes for biomethane injection, Australia currently lacks a nationwide framework. As a result, the exported gas energy price is assumed to be 30% of the imported gas price.

4.4.2 Case Studies

The optimisation of the operation model aims to minimise the operating costs of the power generation system for a specific WWTP.

An academic solver, Gurobi, was used to solve the optimisation problem. By minimising the operating costs, the proposed operation model finds the optimal operating temperature of the anaerobic digestion. Since the temperature is a decision variable, the optimal digestion temperature can vary depending on the time period under consideration.

Different case studies were examined, including:
• Base case: Optimised case considering the CHP system only. If the biogas surplus cannot be stored on top of the digesters, it is flared to maintain the system's secure and safe operation.
• Case 1: In addition to the base case, it considers a biogas upgrading system which converts raw biogas into biomethane for injection into the gas network.
• Case 2: In addition to Case 1, it considers co-digestion of sewage sludge and fat, oil, and grease (FOG) to increase biogas production.

• Case 3: In addition to Case 2, it considers a 50% increase in the capacity of the CHP system.

a. Base Case

Tables 4.3 and 4.4 show the simulation results based on three different optimisation horizons for the base case. Table 4.3 illustrates the results for the 1-year and 3-year optimisation horizons from 2020 to 2022, including the operating digestion temperature, total operating cost, total biogas consumed by both the CHP system and boiler, the biogas flared, and the total gas imported from the grid for the WWTP. Over the 3-year optimisation horizon (2020–2022), the digester operating at $T_{ad} = 34$°C produced a total of 34.5 million m^3 of biogas. The majority of this gas was directed to the CHP, with 26.8 million m^3 utilised (approximately 78% of production), while the boiler consumed only 0.8 million m^3 (about 2%). Despite this high CHP share, a considerable amount, 6.8 million m^3 (20%), was flared due to the lack of storage, limited boiler operation and/or limited CHP capacity. The CHP system generated approx. 55.8 GWh across the three years, which significantly reduced grid reliance. Nevertheless, grid imports still reached 24.5 GWh, particularly in 2022 when biogas production declined to 8.6 million m^3, the lowest in the period. Although the highest volume of biogas was generated in 2020, operating costs was about $1.4 million and decreased in 2021 despite lower biogas production. In 2020, operating costs reached the highest value ($1.48 million), largely due to higher grid electricity purchases and reduced biogas availability compared to previous years. Across the 3-year horizon, total operating costs amounted to $3.87 million, confirming the strong link between biogas availability, CHP utilisation, and cost performance

Table 4.3: Result summary for 1-year and 3-year optimisation horizons - Base case (Current generation assets)

Year	T_{ad} **(°C)**	**Biogas gen** (m^3)	**Biogas CHP** (m^3)	**Biogas boiler** (m^3)	**Biogas flared** (m^3)	**Gas grid** (m^3)	**Grid imp. (kWh)**	**CHP gen (kWh)**	**Energy sold (kWh)**	**Elec. costs ($)**	**Gas costs ($)**	**Op. costs ($)**
2020	34	14,139,666	9,964,719	211,815	3,963,132	3,842	7,675,034	20,728,273	30,921	1,386,626	5,545	1,392,171
2021	34	11,720,727	9,428,533	266,941	2,025,253	0	6,034,120	19,612,917	6,496	1,003,878	190	1,004,068
2022	34	8,594,513	7,444,189	322,226	828,098	5	10,760,159	15,485,151	949	1,475,500	197	1,475,697
20-22	34	34,454,906	26,836,671	800,983	6,817,252	3,847	24,470,262	55,824,741	37,714	3,866,176	5,932	3,872,109

In this Base Case, Table 4.3 presents the results for the 1-month optimisation horizon from 2020 to 2022, while Figure 4.5 provides a breakdown of electricity consumption at the WWTP, generation from the CHP, and imports from the grid. Additionally, Figure 4.6 shows the monthly biogas production alongside its utilisation in the CHP and boiler systems, as well as the amount flared.

As shown in Table 4.3 and Figure 4.5, the CHP system ensured a reliable supply of electricity across all months, generating between 1.6–1.8 GWh per month, far exceeding grid imports or exports. Electricity imported from the main grid, however, showed significant variability, ranging from under 200 MWh, in low-demand months, to more than 1.5 GWh when biogas production was low and, consequently, CHP output was insufficient, as observed in mid-2022. Electricity exports were minimal, indicating that nearly all generated electricity was consumed on-site. Operating costs closely followed the level of grid reliance: when imports were low, costs fell in the range of $47,000–$70,000, whereas months of heavy grid dependence saw costs escalate above $175,000. On average, monthly operating costs remained between $90,000 and $150,000, highlighting the sensitivity of operating expenses to external electricity purchases.

Table 4.4: Result summary for 1-month optimisation horizon - Base case (Current generation assets)

Period	T_{ad} **(°C)**	**Biogas gen** (m^3)	**Biogas CHP** (m^3)	**Biogas boiler** (m^3)	**Biogas flared** (m^3)	**Grid imp. (kWh)**	**CHP gen (kWh)**	**Energy sold (kWh)**	**Elec. costs ($)**	**Gas costs ($)**	**Op. costs ($)**
Jan-20	34	890,754	744,991	19,077	126,686	790,501	1,549,706	0	137,298	5,371	142,669
Feb-20	40	1,071,685	783,295	5,564	282,825	579,032	1,629,383	2,379	105,673	15	105,688
Mar-20	40	1,170,679	857,429	82	313,167	882,364	1,783,596	0	151,399	16	151,415
Apr-20	34	1,082,287	830,643	0	251,644	824,158	1,727,875	453	143,186	16	143,201
May-20	34	1,168,472	858,393	0	310,080	467,429	1,785,600	1,868	91,857	16	91,874
Jun-20	34	1,438,646	830,703	985	606,958	580,933	1,728,000	9,310	106,372	16	106,388
Jul-20	38	1,376,051	841,374	75,553	459,124	736,056	1,750,199	16,793	127,512	16	127,528
Aug-20	39	1,386,501	858,288	146,235	381,978	725,206	1,785,382	0	128,283	16	128,299
Sep-20	34	1,393,769	830,700	74,188	488,881	462,598	1,727,994	14	90,952	16	90,967
Oct-20	34	1,160,026	855,610	33,894	270,522	507,716	1,779,811	33	95,937	16	95,953
Nov-20	35	993,105	822,032	18,737	152,336	511,525	1,709,963	688	97,309	16	97,324
Dec-20	39	1,111,633	855,425	30,133	226,075	599,468	1,779,426	0	109,761	16	109,777
Jan-21	40	1,267,015	855,459	20,525	391,032	595,598	1,779,497	0	94,877	16	94,893
Feb-21	38	1,195,497	775,310	3,773	416,415	404,525	1,612,773	35	71,473	15	71,488
Mar-21	40	1,035,389	796,245	1,791	237,353	641,637	1,656,321	0	101,712	16	101,728
Apr-21	40	873,108	770,951	32	102,126	695,035	1,603,706	712	106,370	16	106,385
May-21	38	721,299	690,311	0	30,988	1,100,783	1,435,961	0	155,506	16	155,522
Jun-21	34	650,376	642,917	0	7,460	587,460	1,337,374	256	91,793	16	91,808
Jul-21	34	779,937	766,005	2,261	11,672	368,255	1,593,417	3	67,289	16	67,305
Aug-21	34	1,077,673	857,654	58,471	161,548	189,555	1,784,062	3,637	47,239	16	47,255
Sep-21	34	1,018,515	824,678	77,365	116,472	209,192	1,715,468	1,079	48,666	16	48,682
Oct-21	34	916,331	775,933	73,209	7,188	385,543	1,614,071	594	70,204	16	70,220
Nov-21	34	1,118,288	830,703	44,941	242,645	286,561	1,728,000	139	57,995	16	58,011
Dec-21	38	1,167,844	858,390	71,719	237,734	536,621	1,785,594	15	88,835	16	88,852
Jan-22	0	1,176,049	858,386	52,814	264,849	400,320	1,785,587	85	69,710	16	69,726
Feb-22	40	1,048,344	775,199	7,988	265,156	466,234	1,612,543	0	74,537	15	74,552
Mar-22	40	854,718	819,288	0	35,430	955,212	1,704,255	0	131,277	16	131,293
Apr-22	40	847,798	802,718	0	45,079	515,030	1,669,788	0	81,258	16	81,274
May-22	38	617,813	617,813	0	0	896,809	1,285,155	0	122,664	16	122,680
Jun-22	35	621,075	620,796	279	0	675,879	1,291,359	0	96,685	16	96,700
Jul-22	34	408,373	369,288	39,085	0	1,502,020	768,180	0	191,343	16	191,359
Aug-22	34	465,108	368,390	96,718	0	1,379,156	766,313	0	175,028	16	175,044
Sep-22	34	353,877	239,892	113,985	5	1,489,637	499,015	0	187,273	23	187,296
Oct-22	34	454,127	385,083	69,044	0	1,391,985	801,036	0	178,078	16	178,094
Nov-22	34	798,920	752,815	2,069	44,036	776,034	1,565,981	225	110,306	16	110,322
Dec-22	40	1,053,751	858,287	22,778	172,686	262,911	1,785,380	1,146	54,153	16	54,169

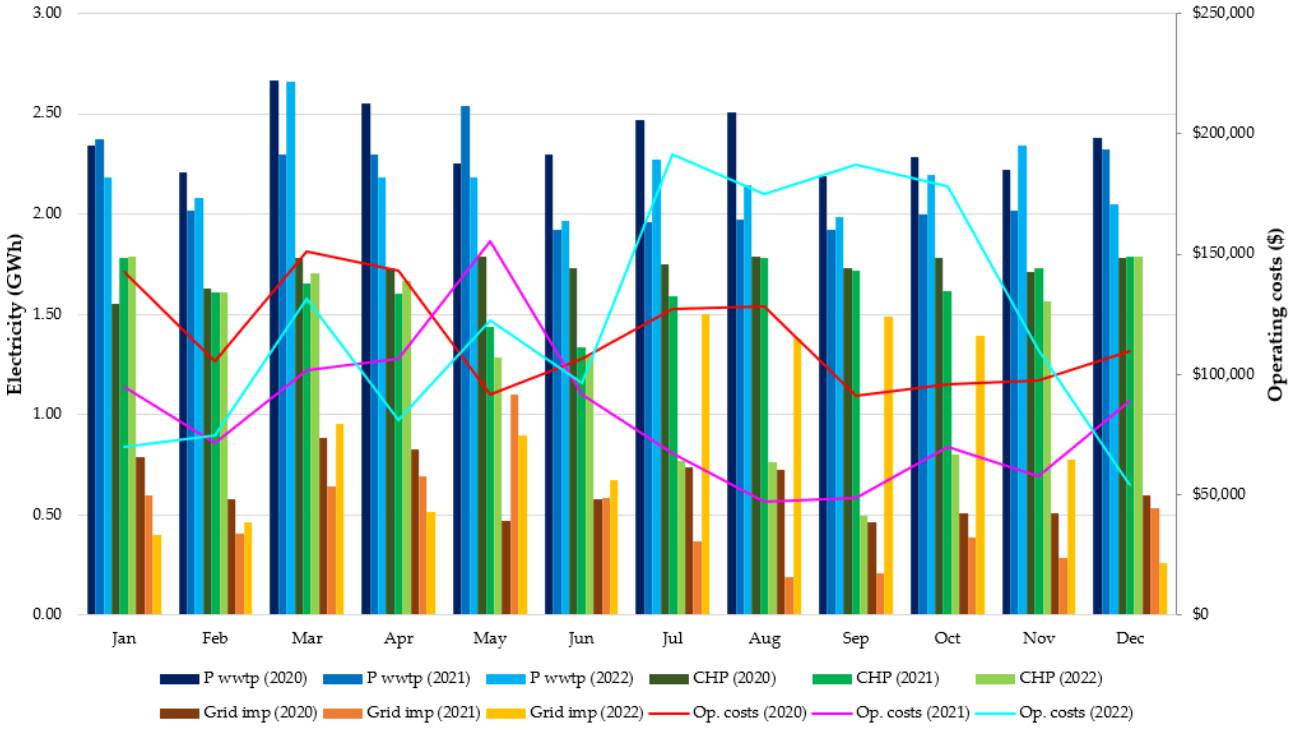

Figure 4.5: Breakdown of electricity components - Base Case (Current generation assets)

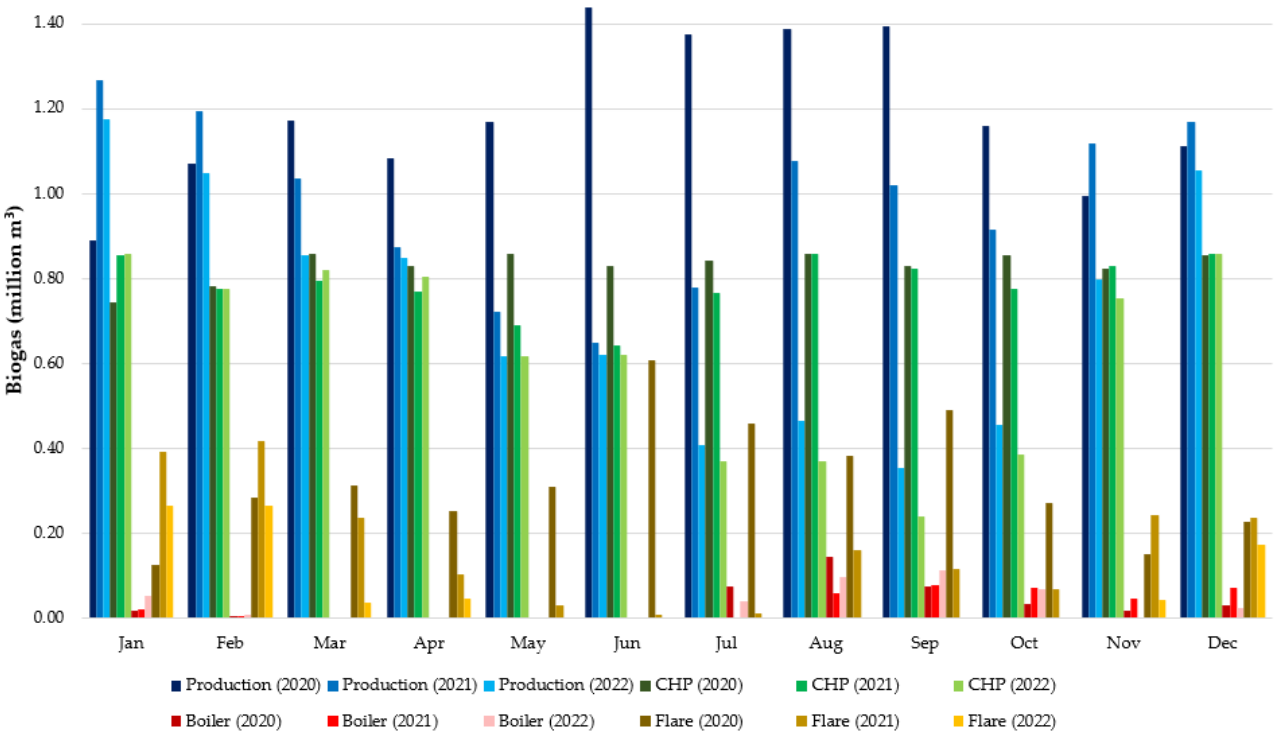

Figure 4.6: Biogas production and utilisation - Base Case (Current generation assets)

As illustrated in Figure 4.6 and Table 4.3, biogas generation was generally high, with most months exceeding 1 million m^3, peaking at around 1.4 million m^3 in mid-2020. The lowest production occurred in Sep-22, with only about 353,800 m^3 generated. The majority of biogas was consistently directed to the CHP system, which consumed approximately 800,000–860,000

m^3 per month. In contrast, the boiler played only a minor and intermittent role, with consumption remaining minimal in most months but rising to around 100,000 m^3 in Aug-20, Aug-22, and Sep-22, when the CHP utilisation was reduced. When the digester operated at 38–40 °C, monthly biogas generation commonly exceeded 1.1 million m^3, as seen in early 2020 and 2021. In comparison, at 34–35 °C, generation typically dropped to around 850,000–1,000,000 m^3. Surplus gas was often flared, particularly during months of high production combined with low boiler use, exceeding 600,000 m^3 in some cases due to the absence of biogas storage facilities on-site. In contrast, periods of efficient utilisation, such as mid-2022, saw flaring fall close to zero. Overall, the results indicate that while the CHP provided a stable and efficient pathway for biogas conversion, significant surpluses were frequently lost through flaring, representing a missed opportunity for additional energy recovery and cost optimisation.

b. Case 1

For Case 1, biogas storage and biogas upgrading system were considered. As shown in Figure 4.7, the biogas generated can be directly used in the CHP and boiler, stored (*"charging"*) or upgraded into biomethane and sold to the gas grid. The stored biogas can be further *"discharged"* to supply the CHP and boiler, or be upgraded and sold. Natural gas can also be imported from the grid to supply the boiler.

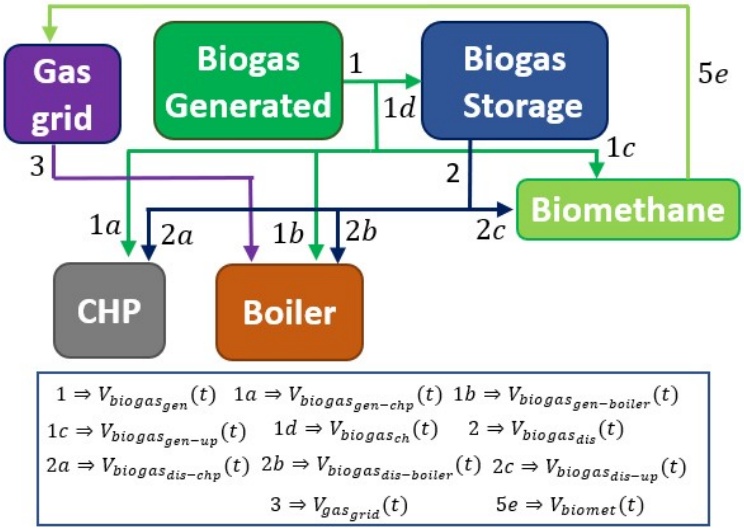

Figure 4.7: Biogas, biomethane and natural gas components (Case 1 - Operation model)

The biogas upgrading system is required to convert the raw biogas into biomethane to meet the gas network requirements for grid injection. In Australia, the system operator, AEMO, defines the lower and upper limits for gas heating values to be 36 MJ/m^3 and 42.3 MJ/m^3, respectively, which translates to a minimum concentration of 93% of methane in the biomethane. Additionally, the maximum levels of hydrogen sulphide, sulphur and moisture in the biomethane are 5.2 mg/m^3, 50 mg/m^3 and 73 mg/m^3, respectively [15], [67]. For Case 1, the following assumptions were considered:

- The power consumption of the biogas upgrading system is 0.25 kW/m^3 biogas.
- All converted biomethane is injected into the gas network.

Eqs. (4.30) and (4.31) are updated (based on Eqs. (4.5) and (4.6)) to consider the biogas component that will be further stored and upgraded into biomethane.

$$V_{biogas_{gen}}(t) = V_{biogas_{gen-chp}}(t) + V_{biogas_{gen-boiler}}(t) + V_{biogas_{gen-up}}(t) + V_{biogas_{ch}}(t) \tag{4.30}$$

$$V_{biogas_{dis}}(t) = V_{biogas_{dis-chp}}(t) + V_{biogas_{dis-boiler}}(t) + V_{biogas_{dis-up}}(t) \tag{4.31}$$

Eq. (4.32) describes the biogas to be upgraded ($V_{biogas_{up}}(t)$) to biomethane, and contraint (4.33) states its upper and lower boundaries, $V^{\max}_{biogas_{up}}$ is the maximum value of biogas that can be upgraded. $V_{biogas_{gen-up}}(t)$ and $V_{biogas_{dis-up}}(t)$ are the portions of the biogas generated and discharged which will be upgraded to biomethane, respectively.

$$V_{biogas_{up}}(t) = V_{biogas_{gen-up}}(t) + V_{biogas_{dis-up}}(t) \tag{4.32}$$

$$0 \leq V_{biogas_{up}}(t) \leq V^{\max}_{biogas_{up}} \tag{4.33}$$

Eq. (4.34) describes the total volume of biomethane converted ($V_{biomet}(t)$), and constraint (4.35) states the upper and lower boundaries, where $V^{\max}_{gas_{inj}}$ is the upper limit for gas injection into the gas network. Eq. (4.36) defines the conversion factor from upgrading raw biogas into biomethane, where k_{up} is the conversion factor from raw biogas to biomethane, and $c_{ch4_{biomet}}$ is the methane concentration into the biomethane.

$$V_{biomet}(t) = V_{biogas_{up}}(t) \cdot k_{up} \tag{4.34}$$

$$0 \leq V_{biomet}(t) \leq V^{\max}_{gas_{inj}} \cdot [1 - u_{gas}(t)] \tag{4.35}$$

$$k_{up}(t) = \frac{c_{ch4_{biogas}}}{c_{ch4_{biomet}}} \tag{4.36}$$

Eq. (4.37) defines the power used in the biogas upgrading system, and constraint (4.38) states the power used in the upgrading system, where $P^{\max}_{up}$, and r_{up} represent the maximum allowable power for the upgrading system and the power consumption rate per unit of biogas upgraded, respectively.

$$P_{up}(t) = \frac{[V_{biogas_{gen-up}}(t) + V_{biogas_{dis-up}}(t)]}{\Delta t} \cdot r_{up}(t) \tag{4.37}$$

$$0 \leq P_{up}(t) \leq P^{\max}_{up} \tag{4.38}$$

The balance equation in (4.39) is also reformulated (based on Eq. (4.23) to include the power required from the biogas upgrading system ($P_{up}(t)$).

$$P_{grid}(t) + P_{chp}(t) = P_{sold}(t) + P_{wwtp}(t) + P_{up}(t) \tag{4.39}$$

The objective function for Case 1 is updated as shown in (4.40) to incorporate the revenue from biomethane injection.In this context, $c_{gas_{exp}}(t)$ denotes the price of biomethane injected into the gas network.

$$\begin{aligned} Min \sum_t \Bigg\{ \Bigg[& P_{grid}(t) \cdot \lambda_{dlf} \cdot \big(c_{ele_{imp}}(t) + c_{ele_{use}}(t) + c_{ele_{other}}(t)\big) \\ & + P_{wwtp_{cap}}(t) \cdot c_{ele_{cap}}(t) - P_{sold}(t) \cdot c_{ele_{exp}}(t) \Bigg] \cdot \Delta t \\ & + \Bigg[V_{gas_{grid}}(t) \cdot \big(c_{gas_{imp}}(t) + c_{gas_{use}}(t)\big) - V_{biomet}(t) \cdot c_{gas_{exp}}(t) \Bigg] \Bigg\} \end{aligned} \tag{4.40}$$

Table 4.5 presents the simulation results based on 1-year and 3-year optimisation horizons from 2020 to 2022. Over the 3-year optimisation horizon (2020–2022) at $T_{ad} = 34$°C, total

biogas production remained 34.45 million m^3, consistent with the base case. In this scenario, 24.34 million m^3 (approx. 71%) of biogas was utilised by the CHP system, while the boiler consumed 0.8 million m^3 (around 2%). A significant portion, 9.31 million m^3, was upgraded into biomethane, resulting in approximately 6.37 million m^3 of biomethane which was injected into the gas grid. The CHP system produced 50.63 GWh of electricity, slightly lower than the base case, due to a share of the biogas being diverted for upgrading. Grid electricity imports accounted for 31.95 GWh, representing the portion of electricity demand not covered by CHP system. Total operating costs over the three-year period amounted to $2.01 million, a substantial reduction compared to the base case. This cost saving was primarily attributed to the added revenue from biomethane injection, which led to negative gas costs (i.e., financial credits or offsets of up to $2.66 million over 3-years). In summary, the results show that integrating biogas upgrading enables the WWTP to maintain on-site electricity generation via CHP while producing an additional revenue through biomethane injection. This dual benefit enhances operational flexibility, improves energy efficiency, and significantly reduces overall operating costs.

Table 4.5: Result summary for 1-year and 3-year optimisation horizons - Case 1 (Current generation assets)

Year	T_{ad} **(°C)**	**Biogas gen** (m^3)	**Biogas CHP** (m^3)	**Biogas boiler** (m^3)	**Biogas upgrade** (m^3)	**Biomethane** (m^3)	**Grid imp. (kWh)**	**CHP gen (kWh)**	**Elec. costs ($)**	**Gas costs ($)**	**Op. costs ($)**
2020	34	14,139,666	8,984,902	212,616	4,942,149	3,381,470	10,917,832	18,690,091	1,779,502	-1,408,504	370,998
2021	34	11,720,727	8,701,151	266,949	2,752,626	1,883,376	8,228,856	18,099,842	1,225,879	-787,393	438,486
2022	34	8,594,513	6,655,228	322,182	1,617,103	1,106,439	12,804,655	13,843,982	1,663,235	-462,489	1,200,746
20-22	34	34,454,906	24,341,300	801,747	9,311,859	6,371,272	31,951,298	50,633,955	4,668,645	-2,658,381	2,010,264

For Case 1, Table 4.6 presents the results for the 1-month optimisation horizon from 2020 to 2022, providing a detailed overview of the system's operational performance. Figure 4.8 complements this by showing the breakdown of electricity consumption at the WWTP, generation from the CHP system, and imports from the grid, while Figure 4.9 illustrates the monthly biogas production along with its utilisation across the CHP, boiler and upgrading systems.

Table 4.6: Result summary for 1-month optimisation horizon - Case 1 (Current generation assets)

Period	T_{ad} **(°C)**	**Biogas gen** (m^3)	**Biogas CHP** (m^3)	**Biogas Boiler** (m^3)	**Biogas upgrade** (m^3)	**Biomethane** (m^3)	**Grid imp. (kWh)**	**CHP gen (kWh)**	**Elec. costs ($)**	**Gas costs ($)**	**Op. Costs ($)**
Jan-20	34	890,754	661,649	19,077	210,029	143,704	1,016,374	1,376,340	163,772	-54,722	109,050
Feb-20	39	1,068,261	725,567	2,395	340,298	232,836	781,810	1,509,301	130,636	-97,351	33,285
Mar-20	40	1,170,679	776,473	82	394,124	269,664	1,149,299	1,615,192	183,150	-112,751	70,400
Apr-20	40	1,103,439	751,066	20	352,353	241,084	1,077,326	1,562,343	173,242	-100,800	72,443
May-20	39	1,187,503	793,076	2,580	391,847	268,106	699,393	1,649,730	119,893	-112,099	7,794
Jun-20	35	1,443,332	774,381	3,557	665,394	455,270	855,129	1,610,842	141,665	-190,367	-48,702
Jul-20	34	1,358,353	807,231	18,657	532,464	364,318	923,404	1,679,174	152,666	-152,333	333
Aug-20	34	1,364,281	843,399	55,161	465,722	318,652	872,609	1,754,409	147,294	-133,236	14,058
Sep-20	34	1,393,769	821,657	74,188	497,924	340,685	605,875	1,709,184	109,772	-142,451	-32,679
Oct-20	34	1,160,026	835,958	33,894	290,174	198,540	621,107	1,738,931	109,852	-83,009	26,844
Nov-20	34	989,880	790,972	10,555	188,353	128,873	622,535	1,645,354	110,527	-53,876	56,651

Continued on next page

Table 4.6 – continued from previous page

Period	T_{ad} (°C)	Biogas gen (m^3)	Biogas CHP (m^3)	Biogas Boiler (m^3)	Biogas upgrade (m^3)	Biomethane (m^3)	Grid imp. (kWh)	CHP gen (kWh)	Elec. costs ($)	Gas costs ($)	Op. Costs ($)
Dec-20	36	1,100,944	824,648	3,107	273,190	186,919	731,788	1,715,404	125,587	-78,149	47,438
Jan-21	36	1,250,824	792,407	179	458,238	313,531	841,317	1,648,338	120,012	-131,095	-11,083
Feb-21	34	1,180,121	660,575	0	519,546	355,479	773,044	1,374,106	109,082	-148,638	-39,556
Mar-21	34	1,015,541	649,181	0	366,360	250,668	1,039,144	1,350,404	141,165	-104,807	36,358
Apr-21	34	856,371	616,875	0	239,496	163,866	1,074,699	1,283,203	144,273	-68,509	75,764
May-21	34	712,022	603,879	0	108,143	73,993	1,307,611	1,256,169	175,549	-30,926	144,624
Jun-21	34	650,376	619,745	0	30,632	20,959	643,064	1,289,172	97,344	-8,749	88,595
Jul-21	34	779,937	740,094	2,247	37,596	25,724	431,550	1,539,519	73,584	-10,741	62,843
Aug-21	34	1,077,673	840,375	58,471	178,826	122,355	266,566	1,748,120	55,119	-51,150	3,970
Sep-21	34	1,018,515	811,876	77,365	129,274	88,451	267,064	1,688,836	54,524	-36,972	17,551
Oct-21	34	916,331	767,766	73,232	75,333	51,544	420,773	1,597,080	73,750	-21,538	52,211
Nov-21	34	1,118,288	807,287	44,941	266,060	182,041	401,645	1,679,292	69,852	-76,110	-6,257
Dec-21	34	1,152,823	826,741	10,686	315,397	215,798	681,291	1,719,759	103,622	-90,225	13,396
Jan-22	34	1,153,505	774,960	421	378,124	258,717	668,308	1,612,045	94,537	-108,173	-13,636
Feb-22	34	1,028,247	644,508	0	383,740	262,559	834,027	1,340,684	108,319	-109,781	-1,462
Mar-22	34	838,334	639,162	0	199,171	136,275	1,379,696	1,329,564	170,082	-56,971	113,111
Apr-22	34	831,546	601,807	0	229,739	157,190	990,394	1,251,858	124,714	-65,717	58,996
May-22	34	609,867	554,020	0	55,847	38,211	1,043,471	1,152,454	135,267	-15,963	119,305
Jun-22	34	619,058	596,642	124	22,292	15,252	731,696	1,241,115	101,620	-6,363	95,258
Jul-22	34	408,373	368,608	39,172	592	405	1,503,583	766,766	191,522	-153	191,368
Aug-22	34	465,108	368,390	96,718	0	0	1,379,156	766,313	175,028	16	175,044
Sep-22	34	353,877	239,924	113,953	0	0	1,489,570	499,083	187,267	39	187,306
Oct-22	34	454,127	385,083	69,044	0	0	1,391,985	801,036	178,078	16	178,094
Nov-22	34	798,920	712,909	2,069	83,942	57,434	879,807	1,482,969	119,829	-24,002	95,827
Dec-22	34	1,033,551	768,299	736	264,516	180,984	515,083	1,598,190	77,246	-75,667	1,579

As presented in Table 4.6, the operating costs varied significantly across months, largely influenced by seasonal changes in biogas production and energy demand. In months of high-production, including June–August 2020, the biogas generation exceeded 1.35 million m^3, allowing significant biomethane injection (approx. 455,000 m^3 in June 2020) which resulted in revenues generation for the WWTP ($190,367 in June 2020) and reduced overall operational costs. The CHP system generated about 1.61–1.75 GWh, keeping electricity costs moderate despite relatively high grid imports (approx. 0.85 GWh in June 2020). In medium-production months (i.e, Jan–May 2020), biogas production ranged between 0.89–1.19 million m^3. The biomethane injection contributed positively but did not fully offset energy needs, resulting in modest operating costs (i.e., $33,285 in Feb-20 and $70,400 in Mar-20). CHP generation remained high (approx. 1.38–1.61 GWh), while grid imports varied from 0.7 to 1.15 GWh to balance electricity demand. During low biogas production months in 2021–2022, including Jun 2021 (around 650,000 m^3), Jul 2022 (about 408,000 m^3), and Sep 2022 (354,000 m^3), operating costs fluctuated widely. Lower biogas availability reduced CHP output (down to 0.5 GWh in Sep 2022) and increased reliance on grid imports (1.49 GWh in Sep 2022), which raised electricity costs. However, biomethane injection still contributed in several months, except Aug 2022 to Oct 2022, offsetting gas costs and reducing total operating costs.

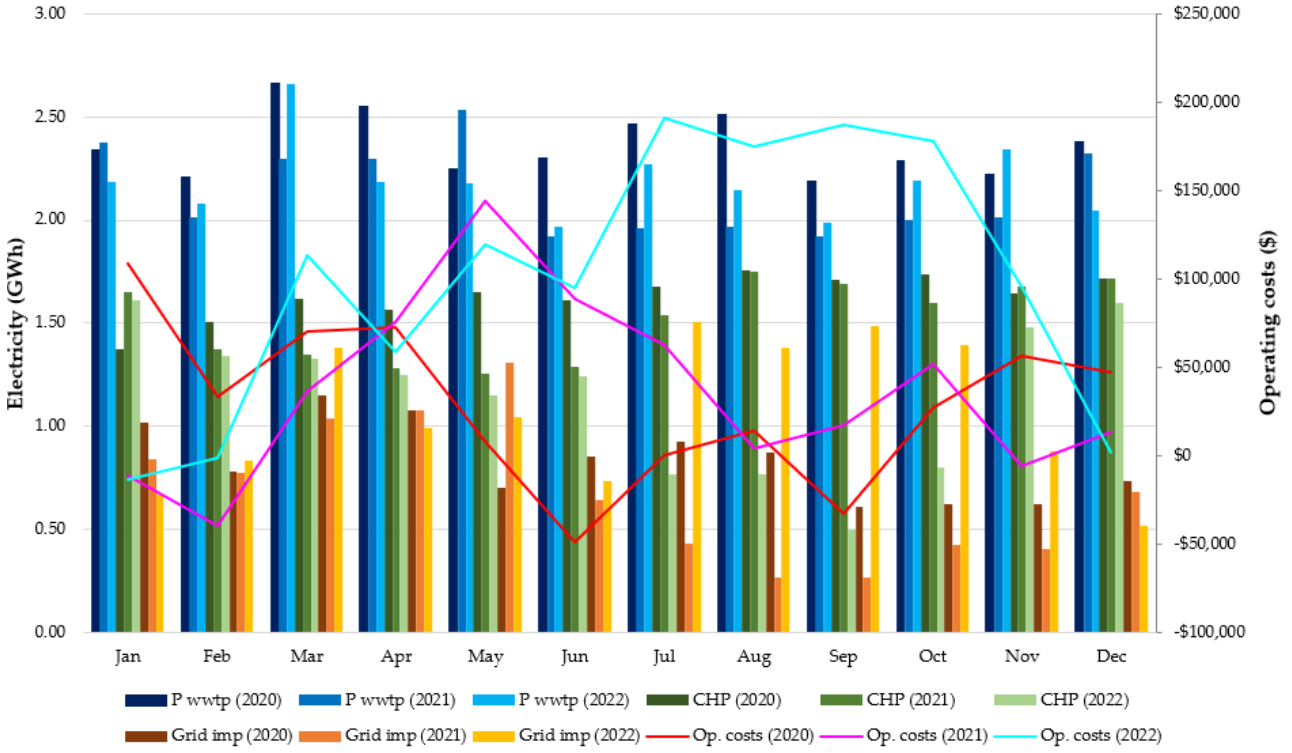

Figure 4.8: Breakdown of electricity components - Case 1 (Current generation assets)

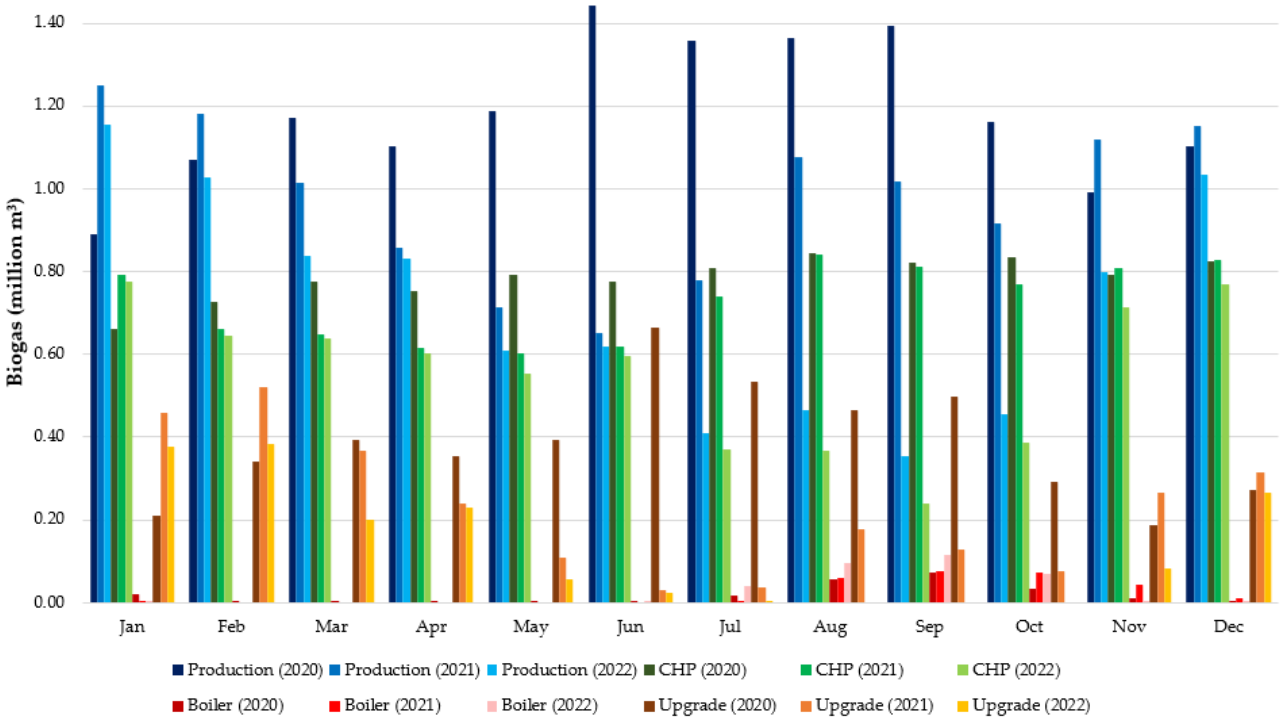

Figure 4.9: Biogas production and utilisation - Case 1 (Current generation assets)

In summary, across the three-year period, total operating costs amounted to approx. $2.01 million, with monthly variations ranging from revenue-generating months (i.e., Jun 2020, Sep 2020) to peaks above $175,000 (i.e., Jul 2022 to Oct 2022). These results highlight the critical role of biomethane upgrading and CHP utilisation in reducing net costs, smoothing seasonal fluctuations, and maintaining economic efficiency despite variations in biogas production and electricity demand.

c. Case 2

Case 2 incorporates biogas storage, biomethane injection, and the co-digestion of sewage sludge and FOG. Co-digestion is a widely adopted strategy to enhance biogas production and increase methane yield by mixing two or more feedstocks prior to the anaerobic digestion process [15].

For Case 2, the following additional assumptions were considered (in addition to the assumption for Case 1):

• The operational cost of co-digestion (including delivery of FOG to the WWTP and its mixing with sewage sludge) is assumed to be \$80/tonne of substrate, covering both transportation and mixing costs.
• A mixing ratio of 1:0.05 (sewage sludge to FOG) is used for the co-digestion process.

The objective function is updated accordingly, as shown in (4.41), to include the co-digestion cost component. $V_{fog}(t)$ and c_{fog} represent the volume of FOG collected and transported to the WWTP, and its associated cost, respectively.

$$\begin{aligned} Min \sum_{t} \Bigg\{ \Bigg[& P_{grid}(t) \cdot \lambda_{dlf} \cdot \left(c_{ele_{imp}}(t) + c_{ele_{use}}(t) + c_{ele_{other}}(t) \right) \\ & + P_{wwtp_{cap}}(t) \cdot c_{ele_{cap}}(t) - P_{sold}(t) \cdot c_{ele_{exp}}(t) \Bigg] \cdot \Delta t \\ & + \Bigg[V_{gas_{grid}}(t) \cdot \left(c_{gas_{imp}}(t) + c_{gas_{use}}(t) \right) - V_{biomet}(t) \cdot c_{gas_{exp}}(t) + V_{fog}(t) \cdot c_{fog} \Bigg] \Bigg\} \end{aligned} \tag{4.41}$$

Table 4.7 presents the results for both the 1-year and 3-year optimisation horizons, highlighting the impact of increased biogas production through co-digestion and its utilisation in the WWTP.

Table 4.7: Result summary for 1-year and 3-year optimisation horizons - Case 2 (Current generation assets)

Year	T_{ad} (°C)	Biogas gen (m^3)	Biogas CHP (m^3)	Biogas boiler (m^3)	Biogas upgrade (m^3)	Biomethane (m^3)	Grid imp. (kWh)	CHP gen (kWh)	Elec. costs (\$)	Gas costs (\$)	AcoD costs (\$)	Op. costs (\$)
2020	34	20,356,832	9,048,879	205,550	11,102,403	7,596,381	12,324,814	18,823,173	1,977,202	-3,174,217	2,083,572	886,558
2021	34	18,649,060	8,932,845	254,677	9,461,537	6,473,683	9,424,121	18,581,804	1,356,982	-2,706,949	2,038,276	688,309
2022	34	14,036,244	8,116,856	2,999	5,916,389	4,048,056	10,839,048	16,884,411	1,416,910	-1,692,610	1,515,670	1,239,971
20-22	34	53,042,136	26,098,572	463,704	26,479,860	18,117,799	32,587,881	54,289,372	4,751,073	-7,573,642	5,637,519	2,814,950

Over the three-year horizon, total biogas production reached approximately 53.04 million m^3, significantly higher than in the Base case and Case 1 scenarios. Around 26.10 million m^3 (approximately 49%) was used in the CHP system, producing 54.29 GWh of electricity, while the boiler had a minimal consumption of only 0.46 million m^3. The remaining amount was used by the biogas upgrading system, which converted approx. 26.48 million m^3 of biogas into 18.12 million m^3 of biomethane which was used for grid injection, generating considerable revenues and offsetting costs (\$3.17 million in 2020, \$2.71 million in 2021), reflecting benefits obtained from biomethane sales. Electricity costs remained moderate due to the CHP's contribution, although grid imports were still required, ranging from 9.42 GWh/y to 12.32 GWh/y, to meet the WWTP's demand. The overall operational costs, including AcoD expenses, amounted to

$2.81 million over three years. Notably, AcoD costs had a significant impact on total operating expenses compared to cases without AcoD operation, underscoring the need to carefully evaluate its implementation; while co-digestion enhances biogas production, it also entails high operating costs. Over the three-years period, approximately $7.57 million could be generated by exporting biomethane to the gas grid, but AcoD operating costs accounted for more than $5.64 million. Therefore, performing a thorough economic analysis is always necessary to assess the profitability of integrating AcoD and biomethane injection into plant operations.

Table 4.8 summarises the results for a 1-month time horizon for Case 2, highlighting the effect of co-digestion on biogas production, biomethane generation, and plant operational costs. Anaerobic digester temperatures ranged from 34°C to 40°C, peaking during the warmer months of February to May, which coincided with higher biogas production. The biogas consumed by the CHP system ranged between approximately 601,000 m^3 and 1,055,000 m^3 per month, generating between 1.25 GWh and 1.75 GWh of electricity. The maximum electricity generation by the CHP system was observed during August 2020, August 2021, and December 2022. Biogas upgrading reached up to 1.08 million m^3 per month in Jun-20, which translated into substantial revenues for the WWTP, helping to offset operational expenses. Grid electricity imports varied from around 403,000 kWh to over 1.3 GWh, particularly during months with lower CHP output or low biogas production. Total operational costs ranged from about $6,360, in Jan 2022, to nearly $170,000 in Oct 2022, while biomethane injection generated revenues in several months (between $12,800 and $309,000), helping to reduce the total WWTP's operating costs. This monthly analysis demonstrates the combined influence of temperature, biogas production, and biomethane injection on electricity generation, grid dependence, and the plant's financial performance, underlining the importance of monitoring seasonal variations and performing a careful economic assessment when implementing co-digestion strategies.

Table 4.8: Result summary for 1-month optimisation horizon - Case 2 (Current generation assets)

Period	T_{ad} **(°C)**	**Biogas gen** (m^3)	**Biogas CHP** (m^3)	**Biogas boiler** (m^3)	**Biogas upgrade** (m^3)	**Biomethane** (m^3)	**Grid imp. (kWh)**	**CHP gen (kWh)**	**Elec. costs ($)**	**Gas costs ($)**	**AcoD costs ($)**	**Op. costs ($)**
Jan-20	37	1,418,189	745,739	15,702	656,748	449,354	953,132	1,551,262	155,964	-184,145	164,586	136,405
Feb-20	40	1,579,480	747,606	5,564	826,310	565,370	857,469	1,555,145	141,353	-236,409	163,212	68,156
Mar-20	40	1,728,006	777,134	82	950,790	650,540	1,287,090	1,616,567	202,914	-272,024	176,873	107,763
Apr-20	40	1,638,703	751,136	20	887,547	607,269	1,210,980	1,562,488	192,301	-253,930	169,947	108,318
May-20	40	1,734,273	806,884	6,422	920,967	630,135	802,950	1,678,453	135,492	-263,491	178,996	50,997
Jun-20	35	1,858,963	775,065	3,290	1,080,608	739,364	957,511	1,612,264	156,449	-309,169	195,627	42,908
Jul-20	34	1,831,469	812,648	18,368	1,000,453	684,520	1,029,132	1,690,443	167,622	-286,234	187,042	68,430
Aug-20	34	1,845,683	843,532	55,161	946,990	647,941	992,649	1,754,687	164,510	-270,937	189,471	83,044
Sep-20	34	1,860,772	821,657	74,188	964,926	660,213	722,626	1,709,184	126,603	-276,070	179,503	30,036
Oct-20	34	1,761,235	837,220	33,894	890,122	609,031	768,470	1,741,556	130,785	-254,666	162,266	38,385
Nov-20	34	1,572,173	795,628	10,555	765,990	524,098	757,260	1,655,038	129,218	-219,150	152,581	62,649
Dec-20	36	1,688,696	825,531	3,107	860,058	588,461	876,668	1,717,241	146,186	-246,064	163,470	63,591
Jan-21	38	1,858,458	820,926	4,520	1,033,011	706,797	925,684	1,707,664	131,656	-295,549	174,619	10,726
Feb-21	37	1,650,314	713,827	1,336	935,150	639,840	766,172	1,484,879	110,970	-267,551	181,309	24,727
Mar-21	40	1,633,111	777,533	1,676	853,902	584,249	894,035	1,617,398	127,347	-244,303	175,143	58,187
Apr-21	40	1,470,301	739,607	32	730,662	499,927	942,189	1,538,505	131,347	-209,042	160,705	83,010
May-21	40	1,393,627	744,063	0	649,563	444,438	1,151,360	1,547,775	157,801	-185,837	145,748	117,712

Continued on next page

Table 4.8 – continued from previous page

Period	T_{ad} (°C)	Biogas gen (m^3)	Biogas CHP (m^3)	Biogas boiler (m^3)	Biogas upgrade (m^3)	Biome-thane (m^3)	Grid imp. (kWh)	CHP gen (kWh)	Elec. costs ($)	Gas costs ($)	AcoD costs ($)	Op. costs ($)
Jun-21	39	1,278,110	756,902	3,282	517,927	354,371	479,579	1,574,481	76,683	-148,174	140,186	68,695
Jul-21	34	1,416,980	771,168	860	644,951	441,282	518,750	1,604,158	82,193	-184,518	154,974	52,649
Aug-21	34	1,624,657	840,558	58,471	725,628	496,482	402,886	1,748,501	71,419	-207,601	190,224	54,042
Sep-21	34	1,579,482	812,203	77,365	689,914	472,047	406,543	1,689,516	71,061	-197,383	179,302	52,980
Oct-21	34	1,518,170	796,975	62,346	658,849	450,792	505,892	1,657,841	84,019	-188,494	168,887	64,411
Nov-21	34	1,667,234	807,287	44,941	815,005	557,635	538,881	1,679,292	86,421	-233,174	177,193	30,441
Dec-21	34	1,703,785	826,819	10,686	866,280	592,718	818,849	1,719,922	120,282	-247,844	189,987	62,424
Jan-22	34	1,830,147	774,960	421	1,054,766	721,682	837,468	1,612,045	113,930	-301,774	194,205	6,361
Feb-22	38	1,648,246	711,372	578	936,296	640,624	833,079	1,479,772	111,799	-267,879	169,629	13,549
Mar-22	39	1,414,363	729,456	0	684,907	468,620	1,313,303	1,517,390	165,109	-195,950	155,701	124,860
Apr-22	40	1,334,768	692,266	0	642,502	439,607	905,416	1,440,028	117,799	-183,817	130,930	64,911
May-22	38	1,052,957	684,366	0	368,590	252,193	850,515	1,423,596	110,837	-105,445	117,031	122,423
Jun-22	34	1,072,289	669,017	0	403,272	275,923	676,390	1,391,666	90,839	-115,369	126,371	101,841
Jul-22	35	744,017	627,186	0	116,831	79,937	994,757	1,304,651	128,970	-33,412	86,778	182,336
Aug-22	34	835,936	711,262	75	124,599	85,252	697,075	1,479,544	96,766	-35,634	103,521	164,653
Sep-22	34	646,579	601,461	277	44,841	30,680	748,724	1,251,138	102,832	-12,814	76,556	166,573
Oct-22	34	768,243	680,361	0	87,882	60,130	799,728	1,415,264	108,412	-25,129	86,367	169,650
Nov-22	34	1,226,172	744,920	1,489	479,763	328,259	912,174	1,549,557	121,463	-137,254	123,186	107,395
Dec-22	36	1,559,187	795,036	3,163	760,988	520,676	583,584	1,653,807	86,078	-217,718	145,396	13,757

Figure 4.10 illustrates the breakdown of the total electricity in the WWTP from 2020 to 2022 for Case 2, and the total operating costs. Figure 4.11 shows the biogas production considering co-digestion of sewage sludge and FOG, and its utilisation in the CHP, boiler and upgrading systems in the WWTP. As shown in the figures, in 2020, total biogas production increased from 1.42 million m^3 in January to a peak of 1.86 million m^3 in September, with the CHP system consistently utilising roughly 45–50% of the produced biogas, generating between 1.55 and 1.75 GWh per month. The boilers had minimal consumption, while biogas upgrading contributed significantly to biomethane production, which ranged from around 0.66 to 1.08 million m^3 per month, providing substantial revenues that partially offset electricity and gas costs. Overall operational costs in 2020 fluctuated, with the highest total operating costs observed in January ($136,405), and the lowest in September ($30,036), largely reflecting the relationship of biomethane revenue, AcoD costs, and electricity costs. In 2021, monthly biogas production remained high but showed a slight decrease during mid-year, with the CHP continuing to utilise a major portion and biomethane production reaching up to 0.94 million m^3 in January. Operational costs exhibited greater variation, with very low total operating costs in January ($10,726) and February ($24,727) due to high biomethane revenues, while May reached the highest net cost ($117,712), reflecting higher AcoD expenses relative to biomethane benefits. Grid electricity imports remained similar consumption throughout the year. In 2022, biogas production declined compared to previous years, particularly from May to September, reaching a minimum of 0.65 million m^3 in September. CHP utilisation remained consistent, but biomethane production dropped, reducing the revenue offset for operational costs. Notably, operational costs had its peak in July and August, while January and December benefited from strong biomethane sales that nearly or completely offset the operating expenses. In summary, the results suggests that while co-digestion enhances biogas generation and biomethane injection can substantially

offset costs, operational expenses, especially from AcoD, can be significant and highly variable month to month. Careful economic assessment is therefore essential to ensure profitability across different seasons and years.

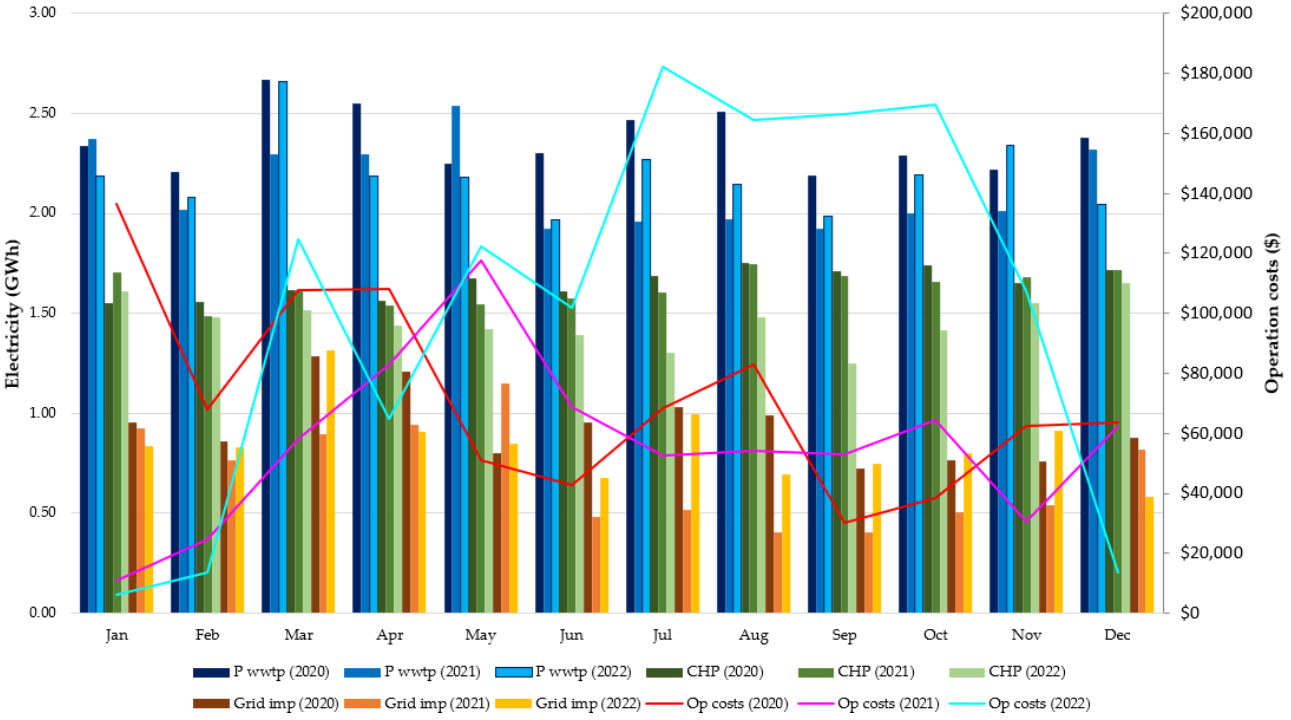

Figure 4.10: Breakdown of electricity components - Case 2 (Current generation assets)

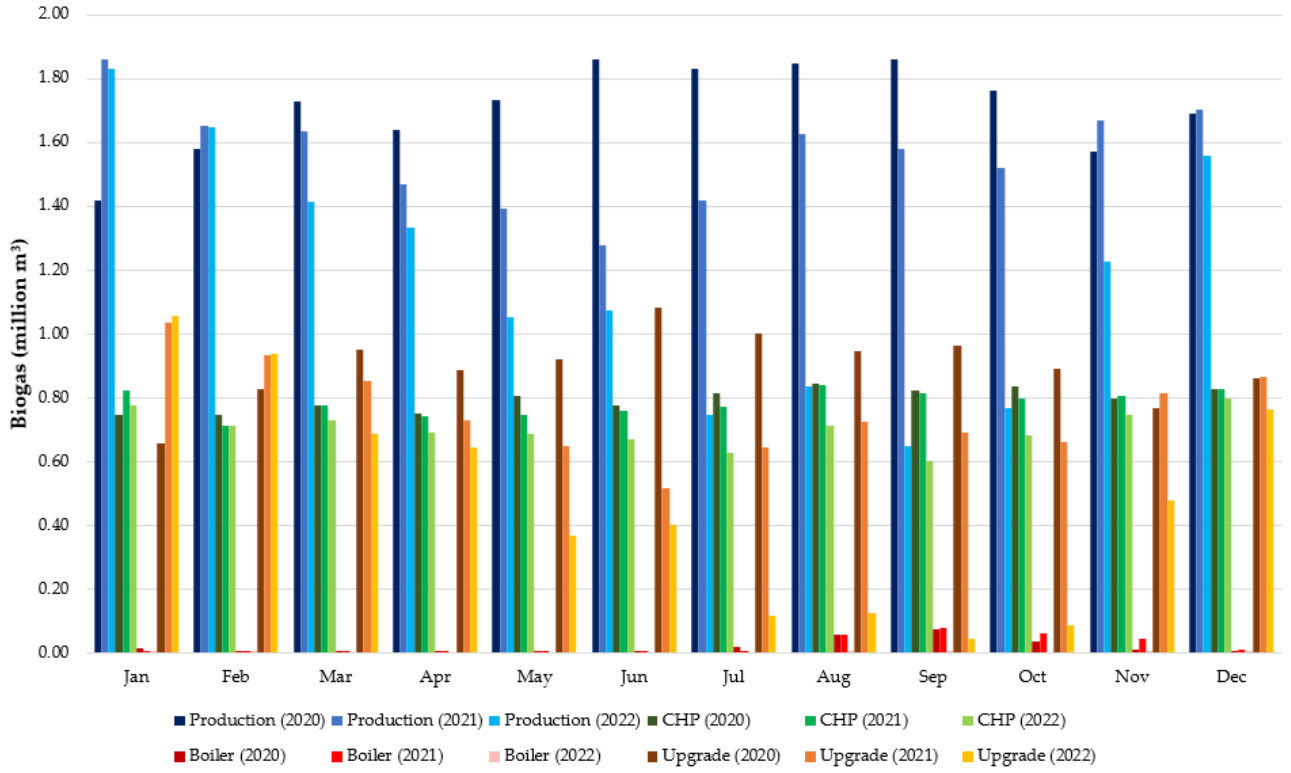

Figure 4.11: Biogas production and utilisation - Case 2 (Current generation assets

d. Case 3

Case 3 considers the biogas storage, biomethane injection, co-digestion of sewage sludge and FOG and also a 50% capacity increase of the CHP system. Tables 4.9 and 4.10 show the simulation results based on both 1-year and 3-year, and 1-month optimisation horizons, respectively. Similarly to Case 2, over the three-year period, total biogas production reached approximately 53.56 million m^3, with an average digester temperature of 37 °C. About 32.8 million m^3 (approx. 61%) was used by the CHP system, generating 68.20 GWh of electricity, while the boiler consumed a minimal 0.20 million m^3. The upgrading system converted 20.58 million m^3 of biogas into biomethane (yielding 14.08 million m^3 of biomethane) for grid injection, which contributed to revenues and offset operational costs. Overall, total operational costs over three years accounted for $2.40 million, with biomethane sales reducing the total operating costs, despite significant AcoD expenses ($5.64 million), highlighting the need to evaluate economic viability when implementing co-digestion and biogas upgrading strategies.

Table 4.9: Result summary for 1-year and 3-year optimisation horizons - Case 3 (Current generation assets)

Year	T_{ad} (°C)	Biogas gen (m^3)	Biogas CHP (m^3)	Biogas boiler (m^3)	Biogas upgrade (m^3)	Biomethane (m^3)	Grid imp. (kWh)	CHP gen (kWh)	Elec. costs ($)	Gas costs ($)	AcoD costs ($)	Op. costs ($)
2020	40	20,756,472	12,501,045	115,902	8,139,525	5,569,149	4,403,013	26,004,255	811,971	-2,323,411	2,083,572	572,132
2021	34	18,649,060	10,615,196	19,604	8,014,259	5,483,441	5,562,732	22,081,374	839,420	-2,292,853	2,038,276	584,843
2022	40	14,310,429	10,171,330	7,969	4,131,130	2,826,562	6,119,084	21,158,060	877,002	-1,181,811	1,515,670	1,210,862
20-22	37	53,562,164	32,785,964	196,100	20,580,101	14,081,121	17,202,054	68,200,260	2,650,517	-5,884,069	5,637,519	2,403,967

The one-month optimisation results for Case 3 show that biogas production generally ranged between 1.0–1.9 million m^3 per month, except from July to October 2022 when the biogas production was lower (i.e., between 0.65-0.84 million m^3). Most of the biogas was used by the CHP system, while a smaller share upgraded to biomethane. Grid electricity imports varied widely, from about 54,000 kWh to over 820,000 kWh, depending on biogas availability and CHP utilisation. Operating costs fluctuated significantly, from a revenue of $5,370, in Sep 2020, to over $180,000, in Jul 2022, largely influenced by AcoD costs, grid purchases, and the extent of biomethane revenue, which ranged between $6,800 and $238,000. Overall, the results highlight the strong interdependence between biogas generation, energy self-sufficiency, and operational costs at the WWTP.

Table 4.10: Result summary for 1-month optimisation horizon - Case 3 (Current generation assets)

Period	T_{ad} (°C)	Biogas gen (m^3)	Biogas CHP (m^3)	Biogas boiler (m^3)	Biogas upgrade (m^3)	Biomethane (m^3)	Grid imp. (kWh)	CHP gen (kWh)	Elec. costs ($)	Gas costs ($)	AcoD costs ($)	Op. costs ($)
Jan-20	38	1,422,914	907,747	16,377	498,790	341,277	576,639	1,888,265	95,062	-138,440	164,586	121,209
Feb-20	40	1,579,480	919,017	0	660,463	451,896	459,443	1,911,709	75,633	-188,957	163,212	49,888
Mar-20	40	1,728,006	977,565	0	750,440	513,459	820,071	2,033,499	124,965	-214,700	176,873	87,138
Apr-20	40	1,638,703	948,727	0	689,976	472,089	750,565	1,973,510	115,437	-197,400	169,947	87,983
May-20	40	1,734,273	970,460	0	763,813	522,609	423,395	2,018,719	72,910	-218,526	178,996	33,380
Jun-20	40	1,889,248	1,053,177	2,084	833,987	570,623	317,337	2,190,783	61,036	-238,605	195,627	18,058
Jul-20	40	1,867,532	1,122,434	11,131	733,967	502,188	318,105	2,334,849	62,993	-209,987	187,042	40,048
Aug-20	38	1,870,083	1,179,666	4,488	685,930	469,320	228,170	2,453,901	51,597	-196,242	189,471	44,825

Continued on next page

Table 4.10 – continued from previous page

Period	T_{ad} (°C)	Biogas gen (m^3)	Biogas CHP (m^3)	Biogas boiler (m^3)	Biogas upgrade (m^3)	Biome-thane (m^3)	Grid imp. (kWh)	CHP gen (kWh)	Elec. costs ($)	Gas costs ($)	AcoD costs ($)	Op. costs ($)
Sep-20	36	1,872,868	1,091,842	8,236	772,791	528,752	112,563	2,271,213	36,223	-221,096	179,503	-5,370
Oct-20	39	1,789,433	1,108,550	7,908	672,976	460,457	149,771	2,305,967	40,676	-192,536	162,266	10,406
Nov-20	40	1,603,100	1,055,738	1,454	545,908	373,516	161,167	2,196,110	41,684	-156,180	152,581	38,086
Dec-20	40	1,710,471	1,074,864	0	635,607	434,889	301,901	2,235,895	58,421	-181,844	163,470	40,047
Jan-21	40	1,870,326	1,039,504	0	830,823	568,458	420,460	2,162,341	65,112	-237,699	174,619	2,032
Feb-21	40	1,666,134	916,601	0	749,533	512,838	297,964	1,906,683	50,921	-214,442	181,309	17,787
Mar-21	40	1,633,111	936,555	0	696,556	476,591	523,907	1,948,190	75,990	-199,283	175,143	51,850
Apr-21	40	1,470,301	873,337	0	596,964	408,449	630,584	1,816,685	87,968	-170,788	160,705	77,885
May-21	40	1,393,627	904,876	0	488,751	334,408	776,640	1,882,293	105,769	-139,825	145,748	111,691
Jun-21	40	1,281,941	844,889	0	437,051	299,035	276,331	1,757,510	49,965	-125,034	140,186	65,118
Jul-21	39	1,439,996	925,777	1,804	512,416	350,600	164,004	1,925,770	39,549	-146,597	154,974	47,927
Aug-21	34	1,624,657	980,985	6,593	637,079	435,896	88,637	2,040,613	32,099	-182,265	190,224	40,058
Sep-21	34	1,579,482	970,816	7,289	601,377	411,469	54,468	2,019,458	27,957	-172,051	179,302	35,208
Oct-21	34	1,518,170	943,392	5,746	569,032	389,338	178,866	1,962,412	43,407	-162,796	168,887	49,498
Nov-21	35	1,672,792	984,181	1,043	687,568	470,441	139,053	2,047,261	36,245	-196,712	177,193	16,727
Dec-21	38	1,725,542	1,068,297	1,220	656,025	448,859	263,971	2,222,235	50,869	-187,686	189,987	53,169
Jan-22	40	1,866,150	1,037,977	180	827,993	566,521	233,655	2,159,165	44,467	-236,890	194,205	1,782
Feb-22	40	1,658,411	896,357	0	762,054	521,406	404,719	1,864,571	57,909	-218,025	169,629	9,513
Mar-22	40	1,418,772	948,070	0	470,702	322,059	805,000	1,972,142	99,040	-134,661	155,701	120,080
Apr-22	40	1,334,768	820,410	0	514,358	351,929	606,818	1,706,589	78,082	-147,153	130,930	61,859
May-22	38	1,052,957	772,883	0	280,073	191,629	644,256	1,607,726	83,794	-80,119	117,031	120,707
Jun-22	34	1,072,289	736,190	0	336,098	229,962	519,864	1,531,398	70,213	-96,149	126,371	100,435
Jul-22	35	744,017	685,742	0	58,275	39,872	858,312	1,426,458	111,303	-16,657	86,778	181,423
Aug-22	34	835,936	760,443	0	75,493	51,653	582,493	1,581,849	81,895	-21,584	103,521	163,832
Sep-22	34	646,579	622,318	277	23,983	16,410	700,123	1,294,525	96,547	-6,847	76,556	166,257
Oct-22	34	768,243	724,943	0	43,300	29,626	695,844	1,508,003	94,967	-12,373	86,367	168,960
Nov-22	39	1,246,447	929,756	26	316,664	216,665	486,909	1,934,047	71,245	-90,588	123,186	103,842
Dec-22	40	1,579,296	956,751	70	622,475	425,904	212,561	1,990,202	42,597	-178,087	145,396	9,907

Figures 4.12 illustrates the breakdown of the total electricity into that consumed (P wwtp), generated (CHP) and imported (Grid imp), while Figure 4.13 shows the biogas components, including production and its utilisation, from 2020 to 2022. The total biogas production varied from around 0.65 million m^3 in September 2022 to nearly 1.89 million m^3 in June 2020, mainly consumed by the CHP system, generating monthly electricity between 1.29 GWh and 2.45 GWh. Biogas upgrading contributed notably to biomethane supply, particularly in the early months of 2020 and 2021. In terms of costs, electricity expenses ranged from $28,000 to $125,000 per month, while gas costs were often generated a revenue, reflecting net savings from internal generation and biogas utilisation, reaching up to $238,605 in June 2020. AcoD operation costs remained a significant contributor, ranging from $76,556 to $195,627 monthly. Total operational costs showed substantial variability; for instance, in September 2020, the total operating resulted in a net revenue of $5,370, whereas in other months, particularly in mid-2022, costs were considerably higher, exceeding $181,000 in July 2022. These fluctuations highlight the sensitivity of monthly operational costs to both biogas allocation and seasonal variations in electricity and gas interactions.

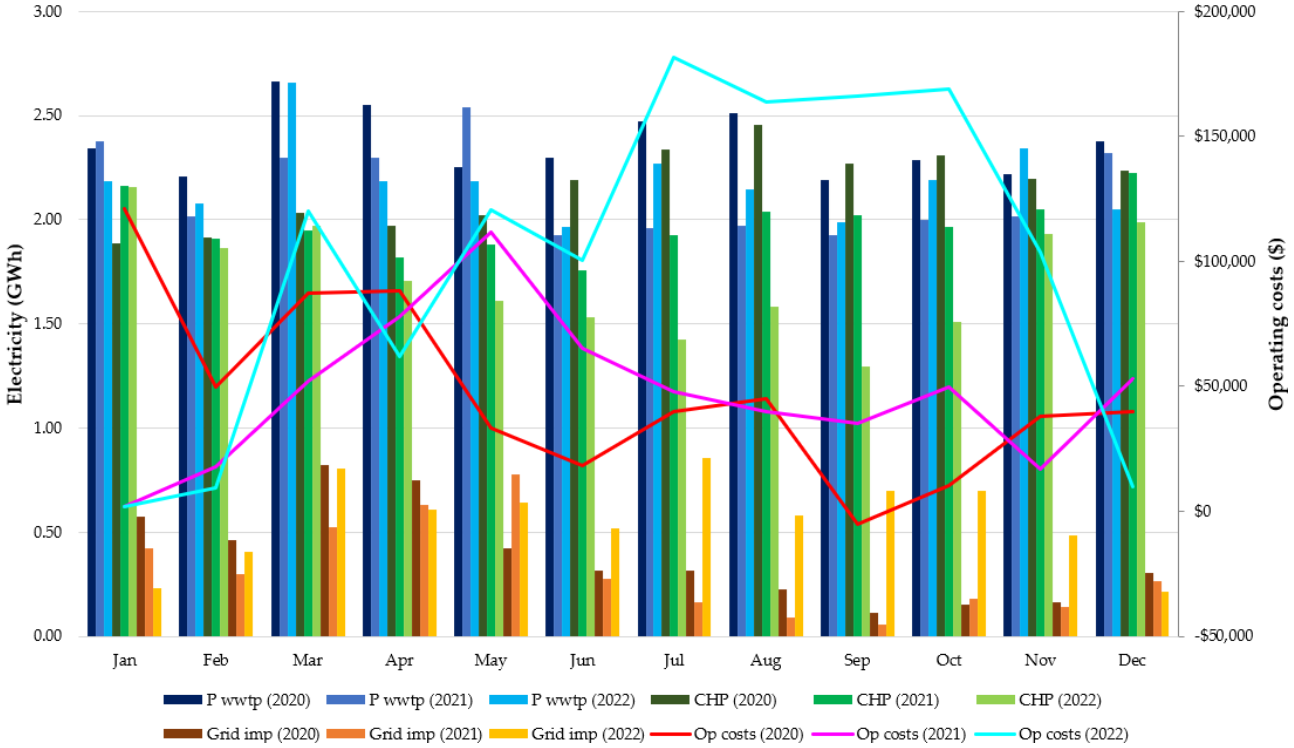

Figure 4.12: Breakdown of electricity components - Case 3 (Current generation assets)

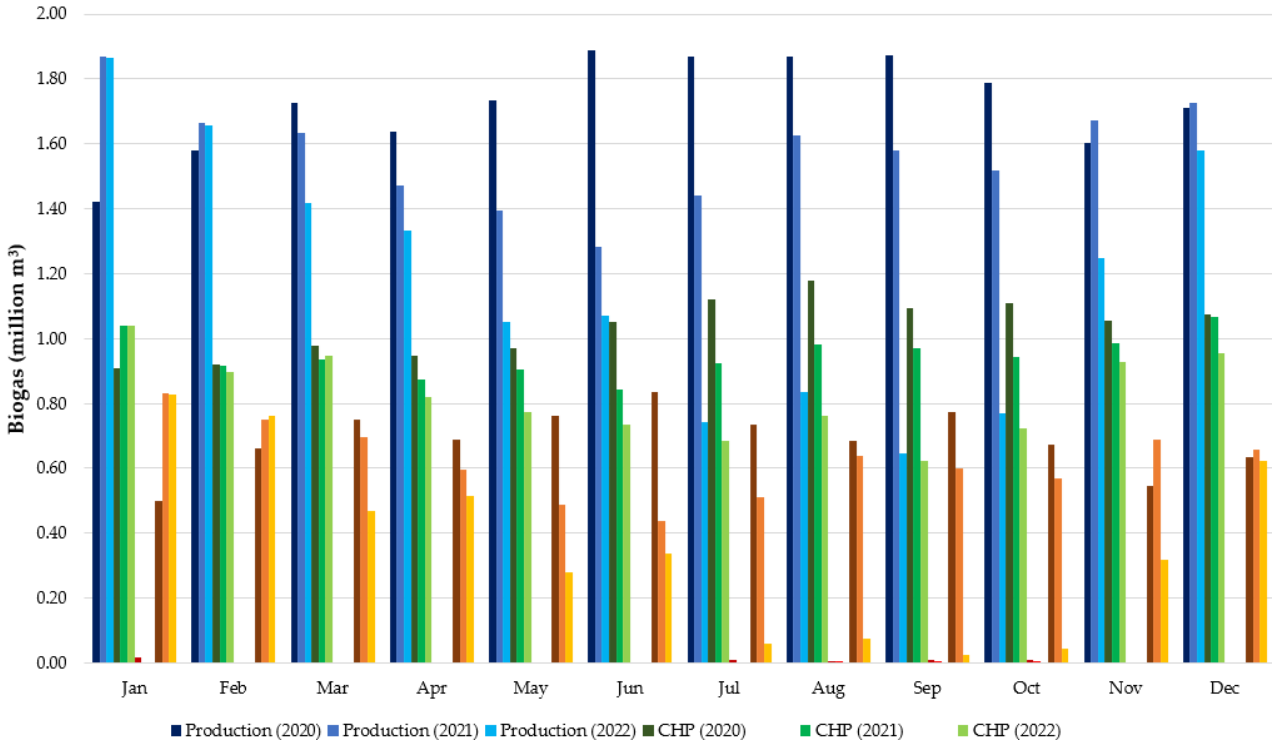

Figure 4.13: Biogas production and utilisation - Case 3 (Current generation assets

4.5 Summary

This chapter introduced an optimal operation model for the power generation system of a large-scale WWTP, with the primary objective of minimising operational costs through the efficient utilisation of existing generating assets, CHP units and boiler, and reliance on the main grid. The model was developed based on real-world operational constraints, historical performance data, and technical specifications from a full-scale plant located in Sydney, Australia. By formulating the problem as a mixed-integer linear program (MILP), the model identifies the optimal anaerobic digestion temperature, biogas utilisation strategy and minimal operating costs to meet the facility's energy demands. Different case studies were assessed to evaluate the model's performance and to explore alternative operational scenarios and strategies. Three optimisation horizons were considered for the period from 2020 to 2022.

Based on historical WWTP data, total biogas production over the three-year period (2020–2022) was approximately 33.4 million m^3, but decreased over the years from 13.9 million to 8.4 million m^3. CHP system was the primary user, consuming about 50% of the biogas produced, and nearly 15% was used in the boiler. Electricity generation from CHP decreased from 17.6 million kWh in 2020 to 12 million kWh in 2022, while grid electricity consumption increased from 10.7 million to over 14.1 million kWh, likely compensating for the reduced CHP output. The remaining part of the biogas was flared to meet the technical and safety standards. The anaerobic digester operated at a temperature of 38 °C. In the Base Case, the optimal temperature was found to be 34°C when the operating cost is minimised over the 3-year optimisation horizon, resulting in a total cost of approximately $3.87 million. The biogas utilisation in the CHP system increased significantly (from around 49% to 77.89%) compared to the historical data. In contrast, the boiler consumption accounted for only 2.3% of the total biogas generated at the WWTP and about 19.78% was flared. When analysing the 1-year optimisation horizon, the optimal anaerobic digestion temperatures were found to be 34°C for all three years. Additionally, the annual operating cost in 2020 and 2022 were around $1.4 million, and in 2021, it was $1 million.

In Case 1, the total operating cost over the 3-year optimisation horizon decreased to $2 million due to the adoption of biomethane injection. Although the electricity costs increased to $4.67 million (compared to the base case), the benefits of selling biomethane to the grid could offset around $2.66 million in the total operating costs. The average biogas utilization in the CHP system was slightly reduced to 70.6%, while around 27% of the biogas was upgraded into biomethane and injected into the gas grid. The ability to inject biomethane was likely the main factor contributing to the reduction in the plant's operating costs. For the 1-year optimisation horizon analysis, the optimal anaerobic digestion temperatures were found to be 34°C for all three years, while the annual operating costs in 2020 and 2021 were $371,000 and $438,500, but increased to $1.2 million in 2022. One possible reason for this increase could be the lower biogas production compared to 2020 and 2021. In Case 2, over the 3-year optimisation horizon, the adoption of co-digestion increased the biogas production by nearly 56% compared to Case 1. However, this also led to an increase of around 40% in the total operation costs, which was estimated at approximately $2.81 million, with the anaerobic digestion temperature set at 34°C. The primary driver of the cost increase may be related to the extra costs for transporting the co-digestion substrate (FOG), which was assumed to be $80/ton in this study. The biogas utilisation in the CHP system accounted for almost half of the total consumption, 0.8% used in the boiler, and the remaining amount was upgraded into biomethane and sold to the gas grid. When analysing the 1-year optimisation horizon, the annual operating cost for 2020

was $886,500, 2021 was $688,000 and 2022 increased to about $1.24 million, respectively, , compared with Case 1. Despite the increased biogas production and higher biomethane exports, these benefits were insufficient to offset the additional operating costs associated with co-digestion. Another potential limitation in Case 2 is the constrained capacity of the CHP system, which is further investigated in Case 3. In Case 3, a 50% increase in CHP system capacity was considered. As a result, the total operating costs were reduced by almost 17% (from $2.81 million to $2.4 million), compared to Case 2, while the anaerobic digestion temperature increased from 34°C to 37°C. By expanding the CHP system size, the biogas utilisation increased to approximately 61.7%, compensating for the decrease in the biomethane injection into the gas network. This suggests that the alternative of adopting co-digestion may be more viable and cost-effective option if the current CHP capacity is increased. When analysing the 1-year optimisation horizon, similar reductions in annual operating cost were observed for 2020, 2021 and 2022, decreasing to approximately $572,000, $584,000, and $1.21 million, respectively, compared to Case 2. Additionaly, the optimal anaerobic digestion temperatures were found to be 40°C in 2020 and 2022, and 34°C in 2021.

Chapter 5

Operation Model: Microgrid

5.1 Introduction

This chapter presents the second part of the operation model, where the power generation system of the WWTP is integrated within a microgrid framework. The proposed microgrid-based model aims to minimise operating costs, enhance energy resilience, reduce dependence on the main grid, and optimise the utilisation of on-site biogas. Simulation results based on different case scenarios were conducted to assess the economic opportunities available to the WWTP. Various renewable energy technologies are considered in the analysis, including photovoltaic (PV), battery energy storage systems (BESS), micro-hydro and combined and heat power (CHP) units. Additionally, the model explores participation in the electricity spot market and the adoption of co-digestion strategies to evaluate their economic suitability and viability.

This chapter is organised as follows: Section 5.2 provides background information on anaerobic digestion, sewage sludge treatment, and biogas utilisation in WWTPs. Section 5.3 presents the model framework and its mathematical formulation. Section 5.4 discusses the outcomes of four different case studies used to evaluate the proposed model's effectiveness. Finally, Section 5.5 summarises the the key findings from this chapter.

5.2 Background

Municipal wastewater treatment plants (WWTPs) are among the most significant energy consumers within urban water supply systems. They play a crucial role in processing and purifying wastewater from residential and commercial sources, ensuring that harmful contaminants are removed before the treated water is safely returned to natural water bodies. The average energy consumption for wastewater treatment is estimated to range between 0.62 and 0.87 kWh/m^3, excluding pumping energy, with electricity costs accounting for 25-50% of the total operational expenses of a WWTP. As population growth and stricter effluent discharge standards continue to drive demand, energy requirements in WWTPs are expected to rise further [1], [2].

The high energy demand of WWTPs translate into significant operating costs. With increasing energy prices and growing environmental sustainability concerns, there is an urgent need to explore innovative strategies to reduce energy consumption and associated costs in these facilities. One promising solution is the integration of microgrid systems into wastewater treat-

ment facilities. Microgrid is a localised energy system capable of generating, distributing, and operating independently or integrated with the main power grid. Typically, microgrids consist of a hybrid generation system, comprising distributed energy resources (DERs), both generation and storage technologies, alongside control systems to manage energy production and consumption. These systems offer operational flexibility, functioning in both grid-connected and islanded modes. It has become an important component in modern power systems due to its ability to effectively deliver reliable, flexible, clean and local controlled power, while meeting the power supply requirements [268]. The adoption of microgrids is widely recognised as an effective strategy to address high operational costs and reduce dependence on electricity supplied by the main grid. However, their successful integration requires addressing challenges such as technological maturity, economic feasibility, and regulatory frameworks. By leveraging local energy generation and advanced control strategies, microgrids can enhance energy efficiency, reliability, and cost-effectiveness. Their dynamic supply-and-demand management capabilities make them particularly suitable for large-scale facilities with substantial energy consumption [268]. The deployment of microgrids in wastewater treatment applications offers multiple benefits. From a technical perspective, a microgrid can provide stable power supply, support load balancing, and reduce reliance on the main grid during peak demand periods. Economically, the use of renewable energy and energy storage within a microgrid can significantly lower electricity bills by reducing demand charges and enabling participation in demand response programs. Moreover, environmental benefits arise from reduced greenhouse gas emissions, aligning with sustainability goals and regulatory pressures. However, realising these benefits requires careful planning, including system sizing, economic analysis, and optimisation of operational strategies tailored to the specific energy profiles of WWTPs [269], [270].

This chapter explores the economic and technical feasibility of integrating a microgrid system into a large-scale WWTP to reduce operating costs and enhance energy sustainability. The proposed approach evaluates microgrid architectures that integrate renewable energy sources, such as hydropower, PV, combined heat and power (CHP), and battery storage systems while also considering opportunities in the energy market. A mixed-integer linear programming (MILP) model is developed to optimise the operation of the WWTP by minimising energy costs while satisfying load demands. The model includes a detailed mathematical formulation of energy generation, consumption patterns, and operational constraints under real-world conditions. Case studies are conducted to assess the cost savings, performance, and technical viability of different microgrid configurations. While previous studies have explored strategies for microgrid operation, the key objective of this study is to evaluate the microgrid performance and operation strategies for a large-scale WWTP under real-world operating conditions.

Microgrid Configuration

Figure 5.1 illustrates the main components of the WWTP used in this study. The plant receives influent (raw sewage), which undergoes preliminary treatment to remove large debris. This is followed by primary treatment, consisting of grit removal and primary sedimentation. The raw sewage sludge produced in the sedimentation tank is then sent to anaerobic digesters for treatment, generating biogas as a co-product. The generated biogas can be utilised in the CHP system to produce both power and heat, and/or boilers to supply additional heat if required. If the on-site biogas is insufficient to meet the thermal energy demand of the anaerobic digesters, natural gas can be imported from the gas grid for boiler use. Conversely, any surplus biogas can be upgraded and injected into the gas network. Following digestion, the digested sludge is dewatered and disposed of. The plant also incorporates a microgrid system, which includes

PV system, BESS, micro-hydro, and a CHP system, to supply on-site electricity. Finally, after treatment, the effluent is discharged through hydro turbines that generate hydroelectric power from the outflow.

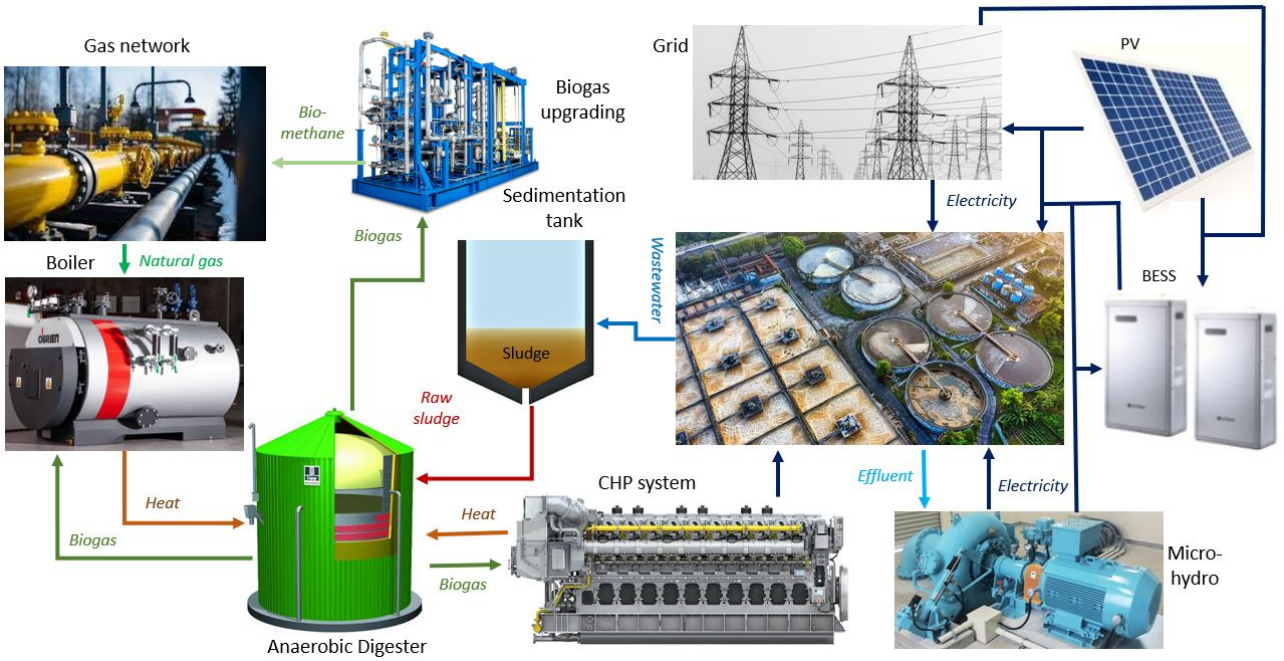

Figure 5.1: WWTP system configuration (Microgrid - Operation model)

The injection of biomethane into the gas grid can generate extra revenue for a WWTP, especially in cases of surplus biogas production, and this approach has been widely adopted in several European countries. Technical requirements and standards for biomethane vary between countries [268]. In Australia, the system operator AEMO defines the acceptable natural gas quality limits with higher heating values ranging from 37 MJ/m^3 to 42.3 MJ/m^3, which corresponds to a methane concentration of approximately 93% in the biomethane. Additionally, the maximum allowable concentrations of hydrogen sulphide, total sulphur and moisture within biomethane are 5.2 mg/m^3, 50 mg/m^3 and 73 mg/m^3, respectively [203], [271].

5.3 Model Framework and Design

This section presents the model framework for the operation of the microgrid system, including key assumptions and the mathematical formulation.

Chapter 5 builds upon the previous chapter 4. As a result, some equations are not repeated here, particularly Eqs. (4.1)-(4.28) from Section 4.3, with the exception of Eq. (4.23), which is updated and reintroduced as Eq. 5.8). Additional equations specific to the microgrid-based operation model are presented in the following subsections.

5.3.1 Microgrid Configuration

a. Battery Energy Storage System (BESS)

Eqs. (5.1)-(5.5) describe the energy of the battery storage system. Eq. (5.1) defines the battery's energy state over time, where $E_b(t)$ is the energy stored in the battery at time t.

To prevent deep discharge and overcharge, constraint (5.2) ensures that state-of-charge of the battery remains within predefined minimum and maximum energy levels, denoted by $E_b^{\min}$ and $E_b^{\max}$, respectively. $P_{b_{dis}}(t)$ and $P_{b_{ch}}(t)$ represent the battery discharging and charging power, and η_{dis} and η_{ch} are the discharging and charging efficiencies, respectively.

$$E_b(t) = E_b(t-1) + \left[\eta_{ch}.P_{b_{ch}}(t) - \frac{P_{b_{dis}}(t)}{\eta_{dis}}\right] \tag{5.1}$$

$$E_b^{\min} \leq E_b(t) \leq E_b^{\max} \tag{5.2}$$

Similarly to the biogas model formulation presented in (4.2), constraint (5.3) ensures that the final energy level of the battery system at the end of each day is equal to the initial energy level ($E_{b_{ini}}$). This condition maintains daily energy balance in the battery system and supports a consistent operation pattern across the optimisation horizon. n_d represents the number of days in the optimisation horizon..

$$E_b(24 * d) = E_{b_{ini}}, d = 1, 2, 3, \ldots, n_d \tag{5.3}$$

Eqs. (5.4) and (5.5) impose the upper boundaries for the battery system's charging and discharging power, respectively. $r_{b_{ch}}$ and $r_{b_{dis}}$ are the maximum charging and discharging rates for the battery system, and $u_b(t)$ is a binary decision variable equal to 1 when the battery is charging at time t, and 0 otherwise.

$$0 \leq P_{b_{ch}}(t) \leq r_{b_{ch}} \cdot u_b(t) \tag{5.4}$$

$$0 \leq P_{b_{dis}}(t) \leq r_{b_{dis}} \cdot [1 - u_b(t)] \tag{5.5}$$

b. Micro-hydro

Eq. (5.6) describes the power generated for the hydro turbine system, denoted as ($P_{hyd}(t)$), where η_{turb}, p_w and g are the turbine efficiency, water density and gravitational acceleration, respectively. $V_{ef}(t)$ is the effluent volumetric flow rate, and H is the available net head (effective vertical drop). Constraint (5.7) sets the upper limit on power generation from the micro-hydro system, where $P_{hyd}^{\max}$ is the maximum allowable hydro power output.

$$P_{hyd}(t) = p_w \cdot g \cdot V_{ef}(t) \cdot H \cdot \eta_{turb} \tag{5.6}$$

$$0 \leq P_{hyd}(t) \leq P_{hyd}^{\max} \tag{5.7}$$

c. Balance equation (Electrical component)

Eq. (5.8) defines the power balance equation for the WWTP, incorporating contributions from the microgrid components. $P_{pv}(t)$ represents the power generated by the PV system.

$$P_{grid}(t) + P_{chp}(t) + P_{pv}(t) + P_{b_{dis}}(t) + P_{hyd}(t) = P_{wwtp}(t) + P_{sold}(t) + P_{b_{ch}}(t) \tag{5.8}$$

d. Objective Function

The objective function, defined in (5.9), aims to minimise the total operating costs of the WWTP. It consists of two main components: electricity and gas costs.

$$
\begin{aligned}
Min \sum_{t} \Bigg\{ \Bigg[& P_{grid}(t) \cdot \lambda_{dlf} \cdot \left(c_{ele_{imp}}(t) + c_{ele_{use}}(t) + c_{ele_{other}}(t) \right) \\
& + P_{wwtp_{cap}}(t) \cdot c_{ele_{cap}}(t) - P_{sold}(t) \cdot c_{ele_{exp}}(t) \Bigg] \cdot \Delta t \\
& + \Bigg[V_{gas_{grid}}(t) \cdot \left(c_{gas_{imp}}(t) + c_{gas_{use}}(t) \right) \Bigg] \Bigg\}
\end{aligned}
\tag{5.9}
$$

5.4 Simulation Results

This section presents the outcomes of the proposed operation model of the microgrid system. Firstly, the key assumptions that underpin the analysis and simulation framework are highlighted. In sequence, the simulation results from the selected case studies are presented. The findings are analysed and discussed to highlight their implications, uncover patterns, and assess their alignment with the research objectives.

5.4.1 Inputs and Assumptions

The characteristics and inputs of the WWTP used in this study were detailed in Section 4.4.1 Additionally, other assumptions and inputs are presented in the following. As previously mentioned, a large-scale WWTP located in Sydney, Australia, was used as a reference to perform the analysis in this study. In addition to the CHP system, the generating system consists of:

- 3 MW solar PV,
- 1 MWh battery, and
- 250 kW micro-hydro.

The gas import price was considered at a fixed rate of \$0.0387/MJ, with a network charge of \$0.52/day. Currently, there is no legislated feed-in tariff for renewable gases injected into the gas network in Australia. Therefore, in this study, we assumed that the WWTP would sell biomethane directly to the gas market. Thus, the gas export price used the gas market reference price published by AEMO. Figure 5.2 illustrates the gas energy price for the Gas Supply Hub (GSH) which includes forecasted and actual gas prices traded in NSW, Australia, from 2020 to 2022 [272]. Figure 5.3 shows the effluent flow from the WWTP in 2021.

In all cases, the biogas production and utilisation are based on the output of the biogas model proposed in Chapter 3.

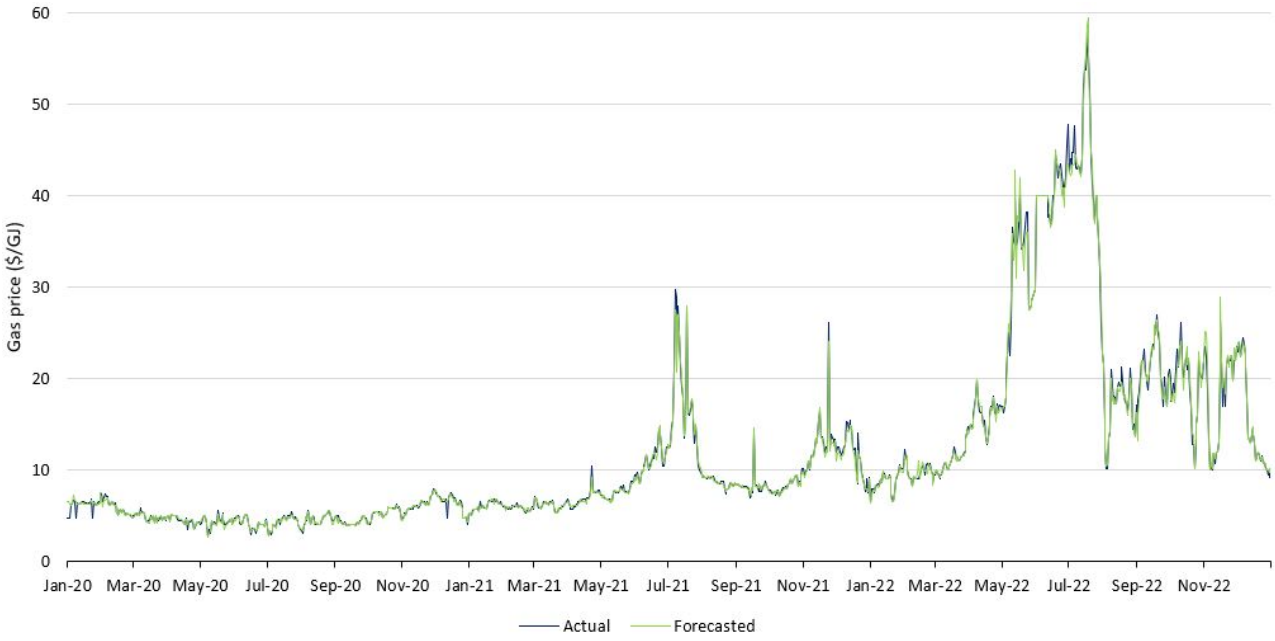

Figure 5.2: Forecasted and actual gas prices in NSW, Australia, from 2020 to 2022

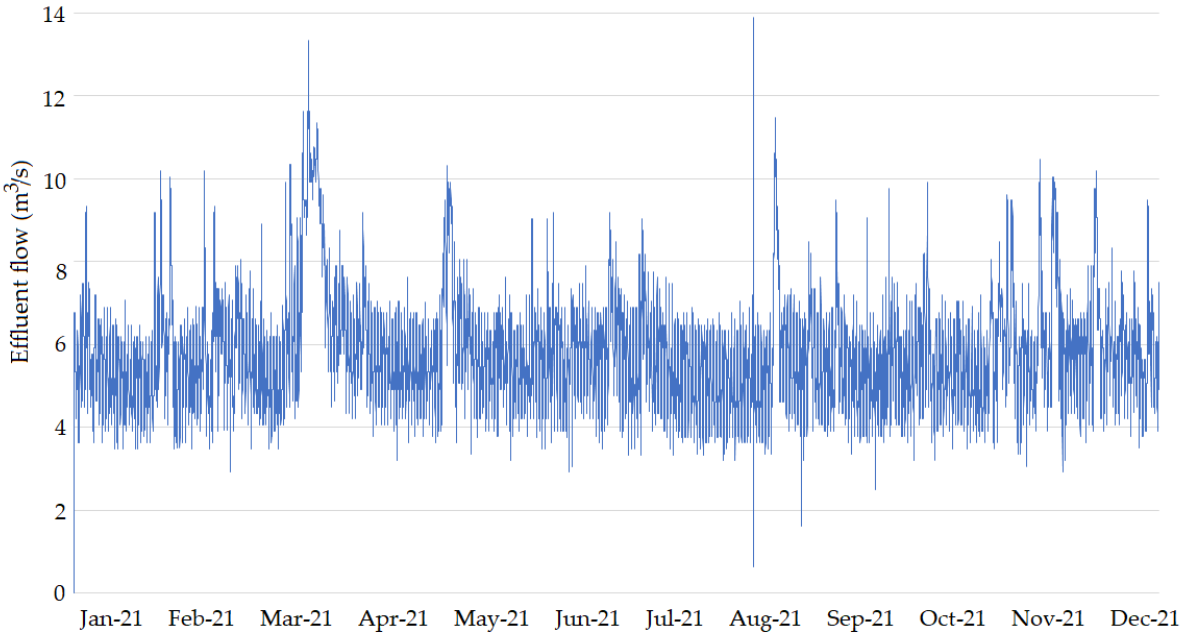

Figure 5.3: Effluent flow from a large-scale WWTP in 2021

5.4.2 Case Studies

To evaluate the effectiveness and robustness of the proposed operational model, it is important to examine different scenarios. In this section, some case studies are analysed to provide a comprehensive overview by exploring various contexts, including the adoption of only a traditional microgrid (i.e., PV, battery, CHP system, micro-hydro), biomethane injection into the

grid, co-digestion of sewage sludge, participation in market services. By engaging with multiple real-world scenarios, it becomes possible to assess the model's adaptability, identify potential limitations, and refine its components based on empirical evidence. The following case studies were considered:

• Case 1: This case considers a microgrid that includes PV, battery, hydro, and CHP systems. Biogas is flared when surplus production exceeds storage capacity.
• Case 1a: Building on Case 1, this case includes a biogas upgrading system and biomethane injection into the gas network.
• Case 2: In addition to Case 1a, this case adopts a co-digestion system and additional biogas storage.
• Case 3: In addition to Case 1a, it assumes that the WWTP is 100% exposed to the electricity spot market (both import and export electricity prices are based on the NSW, Australia spot market from 2020 to 2022).
• Case 4: In addition to Case 3, it assumes that the WWTP also purchases electricity through bilateral contracts to avoid high spot market prices. Additionally, the WWTP purchases gas directly from the gas market.

An academic solver, Gurobi, was used to solve the optimisation problem, and the results are summarised below. Some additional formulations were necessary to account for co-digestion, gasification, sludge drying, participation in electricity market, and these are presented in the following.

a. Case 1

Table 5.1 summarises the optimisation results for 1-year and 3-year optimisation horizons from 2020 to 2022, including the digestion temperature, biogas components, electricity and thermal energy generated and consumed and operating costs.

Over the 2020–2022 period, the total production was approximately 34.5 million m^3 of biogas. The majority (around 77.8%) of this biogas was used in CHP units, contributing significantly to electricity and heat generation, while a smaller portion (2.6%) was directed to boilers, and nearly 20% was flared, indicating potential for better utilisation. Biogas production steadily declined year by year, dropping from 14.1 million m^3 in 2020 to 8.6 million m^3 in 2022, which directly impacted CHP performance. As a result, CHP electricity output also decreased from 20.7 GWh in 2020 to 15.5 GWh in 2022, though over the three years, it remained the dominant electricity source, generating over 55.7 GWh in total. Complementary sources such as PV and micro-hydro systems, produced approximately 5.08 GWh/y and 0.89 GWh/y, respectively. The system's dependence on grid electricity varied: import volumes dropped in to 2.96 GWh in 2021 but reached a peak of 6.27 GWh in 2022. In contrast, electricity exports to the grid peaked in 2021 (2.95 GWh) before reducing in 2022 (1.43 GWh). These trends influenced operating costs, which were lowest in 2021 (approx. \$523,000) and highest in 2022 (approx. \$969,000), driven primarily by reduced self-generation and increased reliance on external electricity. Overall, while the system was largely self-sufficient in earlier years, the declining biogas availability in 2022 led to higher imports and costs, highlighting the need for improved biogas utilisation strategies and diversification of energy sources.

Table 5.1: Result summary for 1-year and 3-year optimisation horizons - Case 1 (Microgrid system)

Period	2020	2021	2022	2020-2022
Temperature in the digester (°C)	34	34	34	34
Biogas production (m^3)	14,139,666	11,720,727	8,594,513	34,454,906
Biogas used in the CHP (m^3)	9,962,668	9,411,214	7,435,338	26,809,190
Biogas used in the boiler (m^3)	271,582	294,319	331,328	897,134
Biogas flared (m^3)	3,905,049	2,015,200	827,847	6,748,551
Natural gas imported (m^3)	3,842	1,994	0	5,836
Boiler thermal generation (kWh)	1,443,446	1,545,707	1,723,042	4,709,829
CHP thermal generation (kWh)	24,609,760	23,247,557	18,366,755	66,224,072
Thermal energy required for the AD (kWh)	20,432,800	20,272,234	15,087,058	55,792,091
WWTP electricity consumption (kWh)	28,372,386	25,640,541	26,244,362	80,257,289
CHP electricity generation (kWh)	20,724,008	19,576,890	15,466,741	55,767,575
PV generation (kWh)	5,088,570	5,073,374	5,073,685	15,235,630
Micro-hydro generation (kWh)	894,416	892,129	892,129	2,678,673
Electricity bought from the grid (kWh)	4,105,824	2,951,582	6,270,525	13,327,846
Electricity sold back to the grid (kWh)	2,409,303	2,822,359	1,427,574	6,659,236
BESS energy charged (kWh)	319,284	318,714	319,430	956,555
BESS energy discharged (kWh)	288,154	287,640	288,286	863,291
Electricity costs ($)	772,082	519,727	969,289	2,261,282
Gas costs ($)	5,546	2,970	190	8,705
Total operating costs ($)	777,627	522,696	969,479	2,269,987

Similarly, Table 5.2 illustrates the summary results for 1-month optimisation horizon from 2020 to 2022. The biogas generation varied between 350,000 m^3 and 1.45 million m^3 during this, achieving its peak in June 2020. The CHP system consistently consumed the largest portion of biogas each month, with usage ranging from 239,000 m^3 (September 2022) to 858,000 m^3 (i.e., May 2020, January 2021 and December 2022). However, as biogas production declined in 2022, the CHP's share also dropped notably in the second half of the year. Biogas flaring remained a significant pathway in 2020 and 2021, sometimes exceeding 400,000 m^3/month (e.g., June and July 2020), but was largely avoided in 2022, indicating improved utilisation. Boiler usage of biogas varied significantly, spiking above 500,000 kWh/month in late 2022 as CHP generation fell. The thermal energy generation from CHP units was the main source to supply the heating demand in the WWTP, consistently exceeding 2 GWh/month in 2020–2021, but declined gradually to around 1.5 GWh or less by mid-2022. The combined electricity generation from CHP, PV, and micro-hydro sources remained high and stable in early years (2.2–2.3 GWh/month), before decreasing in 2022 due to reduced CHP output. The system was generally capable of exporting electricity in 2020 and 2021, with peaks over 300,000 kWh/month, but exports fell to zero in many months of 2022 as grid imports rose sharply (notably exceeding 1 GWh/month in July–October 2022), reflecting increased dependency on external supply. Monthly operating costs were highly sensitive to biogas availability and energy imports. Total operating costs were relatively low and stable in 2020 and 2021 (mostly under $90,000/month, with some as low as $13,000), but surged in mid-2022, peaking at $149,000 in July and $139,000 in September, aligning with the lowest levels of self-generation and highest grid imports. However, by December 2022, operating costs had dropped again, showing recovery in system performance.

Table 5.2: Result summary for 1-month optimisation horizon - Case 1 (Microgrid system)

Period	T_{ad} **(°C)**	**Biogas gen** (m^3)	**Biogas CHP** (m^3)	**Biogas Boiler** (m^3)	**Biogas Flare** (m^3)	**Gas grid** (m^3)	**Heat Boiler (kWh)**	**Heat CHP (kWh)**	**CHP, PV & Hyd (kWh)**	**Energy imp. (kWh)**	**Energy exp. (kWh)**	**Op. Costs ($)**
Jan-20	34	890,754	742,941	21,127	126,686	3,842	139,070	1,835,212	2,089,792	413,368	160,325	84,224
Feb-20	40	1,071,685	783,330	12,086	276,268	0	62,853	1,934,980	2,171,279	272,159	234,932	51,231
Mar-20	40	1,170,679	857,429	1,915	311,334	0	9,961	2,118,020	2,302,524	516,794	150,717	95,005
Apr-20	38	1,096,389	830,703	0	265,686	0	0	2,052,000	2,228,765	494,076	168,696	90,436
May-20	38	1,183,697	858,393	3,589	321,715	0	18,662	2,120,400	2,231,384	246,889	224,470	48,046
Jun-20	37	1,452,704	830,703	35,465	586,537	0	184,431	2,052,000	2,059,648	355,934	113,438	70,173
Jul-20	38	1,376,051	841,374	86,629	448,048	0	450,506	2,078,361	2,180,242	436,470	144,605	81,165
Aug-20	39	1,386,501	858,288	154,272	373,941	0	802,279	2,120,141	2,272,242	402,574	161,587	76,928
Sep-20	39	1,416,469	830,703	176,362	409,404	0	917,156	2,052,000	2,229,469	242,400	278,735	43,592
Oct-20	35	1,163,804	855,587	47,864	260,354	0	248,911	2,113,469	2,348,899	217,272	276,013	40,441
Nov-20	35	993,105	822,032	18,741	152,331	0	97,463	2,030,581	2,277,551	235,126	289,321	42,166
Dec-20	39	1,111,633	855,425	30,139	226,069	0	156,737	2,113,068	2,324,018	269,102	211,572	53,297
Jan-21	39	1,262,968	855,446	11,983	395,539	95	63,034	2,113,121	2,323,821	240,819	186,904	47,117
Feb-21	38	1,195,497	775,323	12,084	408,091	0	62,841	1,915,200	2,135,709	187,431	303,492	31,547
Mar-21	39	1,032,081	795,725	1,814	234,542	0	9,431	1,965,598	2,176,966	346,444	222,811	57,797
Apr-21	40	873,108	769,698	1,284	102,126	0	6,679	1,901,306	2,109,936	369,001	178,352	62,351
May-21	37	718,980	681,163	7,373	30,444	627	43,111	1,682,607	1,860,351	691,235	12,200	111,884
Jun-21	34	650,376	639,686	3,231	7,460	0	16,803	1,580,150	1,657,319	327,290	57,508	60,313
Jul-21	34	779,937	759,334	8,938	11,666	0	46,479	1,875,705	2,009,736	136,270	181,703	32,081
Jul-21	34	779,937	759,334	8,938	11,666	0	46,479	1,875,705	2,009,736	136,270	181,703	32,081
Aug-21	34	1,077,673	857,653	58,479	161,541	0	304,114	2,118,573	2,267,671	65,553	360,603	14,026
Sep-21	34	1,018,515	824,678	77,644	116,193	0	403,781	2,037,118	2,215,153	68,909	357,921	13,883
Oct-21	34	916,331	771,804	77,346	67,181	1,275	411,919	1,906,507	2,175,163	168,105	341,607	30,278
Nov-21	37	1,129,216	830,703	96,628	201,885	0	502,508	2,052,000	2,298,433	95,923	377,379	16,703
Dec-21	38	1,167,844	858,390	71,873	237,580	0	373,770	2,120,393	2,329,585	238,589	243,314	43,521
Jan-22	38	1,168,534	858,393	24,154	285,987	0	125,611	2,120,400	2,327,909	154,003	293,450	30,894
Feb-22	40	1,048,344	775,199	8,719	264,426	0	45,343	1,914,894	2,136,987	198,446	254,271	35,995
Mar-22	40	854,718	819,288	142	35,288	0	736	2,023,803	2,223,402	522,837	84,126	85,054
Apr-22	40	847,798	802,718	0	45,079	0	0	1,982,873	2,184,343	231,319	228,289	42,692
May-22	36	613,840	611,416	2,424	0	0	12,606	1,510,319	1,714,564	491,294	21,246	81,358
Jun-22	34	619,058	615,567	3,491	0	0	18,157	1,520,571	1,607,165	370,974	8,345	65,506
Jul-22	34	408,373	368,364	40,009	0	0	208,063	909,932	1,203,721	1,069,133	0	149,248
Aug-22	34	465,108	367,767	97,342	0	0	506,217	908,456	1,247,169	900,984	0	128,972
Sep-22	34	353,877	238,932	114,945	0	0	597,761	590,210	993,704	997,506	0	139,761
Oct-22	34	454,127	384,109	70,018	0	0	364,121	948,825	1,361,577	834,143	0	124,581
Nov-22	34	798,920	751,661	3,224	44,035	0	16,766	1,856,751	2,137,885	397,203	190,745	64,348
Dec-22	40	1,053,751	858,287	22,783	172,681	0	118,479	2,120,138	2,328,165	83,837	362,286	18,684

The main aspects of the Base Case included:

• CHP remained the primary energy generation source, maximising biogas utilisation whenever available;
• Flaring was substantially reduced in 2022, indicating better control and system efficiency;

• Energy imports increased in late 2022 due to lower biogas production, which heavily influenced operating costs;
• 1-monthl analysis reveals seasonal impacts and biogas limitations that were less apparent in annual summaries, offering valuable insights for operational planning and system optimisation.

b. Case 1a

In this case, biomethane injection into the gas grid is considered, similar to Case 1 in Chapter 4. The biogas generated can be directly used in the CHP and boiler, stored (*"charged"*), or upgraded into biomethane and sold to the gas grid. The stored biogas can later be *"discharged"* to supply the CHP and boiler, or be upgraded and sold. Additionally, natural gas can also be imported from the grid to supply the boilers.

The balance equation in (5.10) is updated to include the microgrid components and the power required from the biogas upgrading system to convert raw biogas into biomethane.

$$P_{grid}(t) + P_{chp}(t) + P_{pv}(t) + P_{b_{dis}}(t) + P_{hyd}(t) = P_{wwtp}(t) + P_{sold}(t) + P_{b_{ch}}(t) + P_{up}(t) \quad (5.10)$$

The objective function for Case 1a is defined in (5.11), where $c_{gas_{market}}(t)$ represents the gas market price of the biomethane injected into the gas network.

$$\begin{aligned} Min \sum_t \Bigg\{ \Bigg[& P_{grid}(t) \cdot \lambda_{dlf} \cdot \big(c_{ele_{imp}}(t) + c_{ele_{use}}(t) + c_{ele_{other}}(t)\big) \\ & + P_{wwtp_{cap}}(t) \cdot c_{ele_{cap}}(t) - P_{sold}(t) \cdot c_{ele_{exp}}(t) \Bigg] \cdot \Delta t \\ & + \Bigg[V_{gas_{grid}}(t) \cdot \big(c_{gas_{imp}}(t) + c_{gas_{use}}(t)\big) - V_{biomet}(t) \cdot c_{gas_{market}}(t) \Bigg] \Bigg\} \end{aligned} \quad (5.11)$$

Table 5.3 summarises the optimisation results for the 1-year and 3-year optimisation horizons from 2020 to 2022, including digestion temperature, biogas components, electricity and thermal energy generated and consumed, and operating costs. Negative values in the operating gas costs indicate revenue generated for the WWTP. As shown in the table, the annual biogas production remains consistent with Case 1, totalling 34.45 million m^3 over the three years. However, its utilisation pattern shifts significantly due to the introduction of biogas upgrading to biomethane. A total of 10.26 million m^3 of biogas was upgraded, resulting in 7.02 million m^3 of biomethane. Consequently, less biogas was directed to the CHP unit (22.1 million m^3, down from 26.8 million m^3 in Case 1) and boilers (2.07 million m^3, up slightly from 0.9 million m^3). This change led to a reduction in CHP generation, but an increase in boiler usage to compensate for thermal demands. Importantly, flaring is entirely eliminated, showing improved overall gas utilisation.

The CHP system's electricity output dropped to 46.01 GWh from 55.77 GWh in the base case, reflecting the reduced biogas utilisation by the CHP. Boiler thermal generation, on the other hand, more than doubled to 10.82 GWh, while CHP thermal output experienced a marginal decreased to 54.64 GWh. Despite this shift, the system was still able to meet the thermal demands of the anaerobic digester, which remained constant at 55.79 GWh. On the electricity

side, grid imports surged, particularly in 2022, reaching 13.15 GWh, contributing to a three-year total of 21.5 GWh. Simultaneously, electricity exports dropped dramatically to just 2.51 GWh, a sharp contrast to the 6.66 GWh exported in the base case. The system maintained stable PV and micro-hydro generation (15.24 GWh and 2.68 GWh respectively), and BESS operations remained nearly unchanged. The biogas upgrading system itself consumed 2.57 GWh, which slightly impacted electricity balance but was offset by the additional revenue potential from biomethane. Additionally, the economic performance significantly improved under this scenario. Gas costs generate significant revenue with the exportation of biomethane to the gas grid, reaching $2.89 million over three years, a substantial improvement compared to the gas costs in the Base Case. While electricity costs increased (from $2.26 million to $3.42 million) due to higher grid reliance, the total operating costs dropped dramatically to $524,864, a 77% reduction compared to $2.27 million in the Base Case.

Table 5.3: Result summary for 1-year and 3-year optimisation horizons - Case 1a (Microgrid system)

Period	**2020**	**2021**	**2022**	**2020-2022**
Temperature in the digester (°C)	34	34	34	34
Biogas production (m^3)	14,139,666	1,720,727	8,594,513	34,454,906
Biogas used in the CHP (m^3)	9,853,133	8,406,355	3,859,574	22,119,062
Biogas used in the boiler (m^3)	213,894	536,567	1,322,036	2,072,497
Biogas upgraded to biomethane (m^3)	4,072,639	2,777,804	3,412,904	10,263,347
Biomethane volume (m^3)	2,786,542	1,900,603	2,335,145	7,022,290
Natural gas imported (m^3)	3,842	1,994	0	5,836
Boiler thermal generation (kWh)	1,141,540	2,805,529	6,875,135	10,822,205
CHP thermal generation (kWh)	24,339,186	20,765,359	9,533,910	54,638,454
Thermal energy required for the AD (kWh)	20,432,800	20,272,234	15,087,058	55,792,091
WWTP electricity consumption (kWh)	28,372,386	25,640,541	26,244,362	80,257,289
CHP electricity generation (kWh)	20,496,156	17,486,618	8,028,556	46,011,330
PV generation (kWh)	5,088,570	5,073,374	5,073,685	15,235,630
Micro-hydro generation (kWh)	894,416	892,129	892,129	2,678,673
Electricity bought from the grid (kWh)	4,619,884	3,735,917	13,149,672	21,505,473
Electricity sold back to the grid (kWh)	1,677,442	821,205	15,193	2,513,840
Biogas upgrading consumption (kWh)	1,018,160	694,451	853,226	2,565,837
BESS energy charged (kWh)	318,355	326,568	320,624	965,547
BESS energy discharged (kWh)	287,315	294,728	289,363	871,406
Electricity costs ($)	896,567	717,486	1,802,678	3,416,731
Gas costs ($)	-481,174	-635,203	-1,775,489	-2,891,867
Total operating costs ($)	415,392	82,283	27,189	524,864

Table 5.4 illustrates the summary results for 1-month optimisation horizon from 2020 to 2022 for Case 1a. As highlighed, the biogas production had its peak in June 2020 at 1.44 million m^3, consistently with a minimum generation of 1 million m^3 in 2020 and 2021, except in some months from Apr-21 to Jun-21. This high production was primarily used in the CHP units, with monthly usage often above 800,000 m^3 for both electricity and heat generation. However, starting in mid-2021, a shift in utilisation patterns is evident: biogas to CHP declined, and more gas was diverted to biogas upgrading (for biomethane) and boilers. Notably, in 2022, biogas-to-CHP use dropped significantly (falling to zero in June 2022) and staying extremely low or sporadic through the year, indicating operational constraints or shifting priorities. Instead,

biogas boiler usage surged, peaking at 226,776 m^3 in June 2022, alongside a dramatic increase in biogas upgrading, particularly in April–June 2022, when over 500,000 m^3/month was upgraded. This shift heavily impacted heat and power generation. The heat generated by the CHP system consistently exceeded 2 million kWh/month, maintaining a strong base load. Combined with PV and hydro, total renewable electricity generation exceeded 2.3 million kWh in several months (i,e, 2.34 million kWh in Oct 2020). However, as CHP utilisation dropped in 2022, CHP heat output plummeted to as low as 4,560 kWh in July 2022, and overall renewable electricity generation dropped to a low of 326,684 kWh in June 2022. To meet heat demands, heat from boilers surged, reaching a peak of 1.18 million kWh in June 2022.

These operational shifts directly influenced energy imports and exports. Initially, in 2020 and early 2021, electricity imported from the main grid was moderate. In contrast, 2022 saw a dramatic rise in imports, with peak monthly imports of over 1.88 million kWh in July, and consistently high values throughout the year. Energy exports, on the other hand, declined steadily, with zero exports recorded in many months of 2022. This translated into significant changes in operational costs. Based on the high price of gas market rates, as shown in Figure 5.2, the system operated focused on maximising the biomethane exporting in 2022, which generated a profit in several months, which a peak of around $170,000 in June 2022. In the same month, the biogas utilisation in the CHP dropped to zero, boiler usage increased to meet the heat demand in the WWTP, and the biogas was prioritised towards upgrading and biomethane exportation. However, despite these profits, the system also experienced notable fluctuations in operational costs later in the year, particularly from August to October 2022, with costs exceeding $115,000 per month. This pattern underscores the financial impact of increased reliance on energy imports and the reduced efficiency in biogas resource utilisation.

Table 5.4: Result summary for 1-month optimisation horizon - Case 1a (Microgrid system)

Period	T_{ad} **(°C)**	**Biogas gen** (m^3)	**Biogas CHP** (m^3)	**Biogas Boiler** (m^3)	**Biogas upgrade** (m^3)	**Biome-thane** (m^3)	**Gas grid** (m^3)	**Heat Boiler (kWh)**	**Heat CHP (kWh)**	**CHP, PV & Hyd (kWh)**	**Energy imp. (kWh)**	**Energy exp. (kWh)**	**Op. Costs ($)**
Jan-20	34	890,754	708,172	21,127	161,456	110,470	3,842	139,070	1,749,324	2,017,466	422,686	56,940	66,699
Feb-20	40	1,071,685	769,692	5,566	296,427	202,818	0	28,944	1,901,292	2,142,910	302,394	162,676	19,557
Mar-20	40	1,170,679	857,429	83	313,167	214,272	0	429	2,118,020	2,302,524	558,862	114,493	65,743
Apr-20	40	1,103,439	830,703	20	272,717	186,596	0	102	2,052,000	2,228,765	527,024	133,473	68,061
May-20	40	1,191,309	858,393	6,424	326,492	223,389	0	33,408	2,120,400	2,231,384	284,556	180,514	21,585
Jun-20	35	1,443,332	830,703	3,291	609,338	416,916	0	17,114	2,052,000	2,059,648	464,151	69,358	26,308
Jul-20	34	1,358,353	840,900	17,908	499,545	341,794	0	93,128	2,077,189	2,179,255	514,057	96,408	39,945
Aug-20	34	1,364,281	858,259	55,168	450,854	308,479	0	286,896	2,120,070	2,272,182	466,674	112,914	40,193
Sep-20	34	1,393,769	830,703	74,196	488,870	334,490	0	385,852	2,052,000	2,229,469	301,005	215,123	4,344
Oct-20	34	1,160,026	853,250	33,900	272,876	186,705	0	176,292	2,107,697	2,344,038	246,477	232,160	12,156
Nov-20	34	989,880	810,062	10,558	169,260	115,810	0	54,906	2,001,013	2,252,652	249,115	236,095	21,435
Dec-20	36	1,100,944	838,020	3,109	259,815	177,768	0	16,166	2,070,076	2,287,814	291,599	132,902	21,947
Jan-21	37	1,254,872	831,031	1,131	422,710	289,223	94	6,597	2,052,811	2,273,034	282,613	72,180	-5,463
Feb-21	37	1,191,653	726,489	1,337	463,827	317,355	0	6,953	1,794,572	2,034,128	227,594	126,117	-21,420
Mar-21	39	1,032,081	761,106	168	270,807	185,289	0	871	1,880,083	2,104,953	368,062	104,704	24,457
Apr-21	39	870,319	729,083	1,383	139,853	95,689	0	7,194	1,800,979	2,025,449	383,508	73,410	43,777
May-21	38	721,299	681,213	8,827	31,259	21,388	628	50,675	1,682,731	1,860,455	697,775	11,027	107,237
Jun-21	34	650,376	593,217	8,300	48,860	33,431	0	43,162	1,465,362	1,560,656	378,693	0	54,414
Jul-21	34	779,937	479,750	105,369	194,818	133,297	0	547,961	1,185,078	1,428,156	584,862	0	-4,711
Aug-21	34	1,077,673	767,329	93,242	217,102	148,543	0	484,898	1,895,454	2,079,781	75,651	128,514	-19,135

Continued on next page

Table 5.4 – continued from previous page

Period	T_{ad} (°C)	Biogas gen (m^3)	Biogas CHP (m^3)	Biogas Boiler (m^3)	Biogas upgrade (m^3)	Biomethane (m^3)	Gas grid (m^3)	Heat Boiler (kWh)	Heat CHP (kWh)	CHP, PV & Hyd (kWh)	Energy imp. (kWh)	Energy exp. (kWh)	Op. Costs ($)
Sep-21	34	1,018,515	806,680	79,937	131,898	90,246	0	415,706	1,992,658	2,177,714	76,788	295,100	-8,885
Oct-21	34	916,331	728,470	94,060	93,801	64,179	1,275	498,840	1,799,466	2,085,023	172,006	231,818	16,991
Nov-21	34	1,118,288	647,925	119,332	351,031	240,179	0	620,574	1,600,503	1,918,225	186,588	0	-71,353
Dec-21	34	1,152,823	774,809	33,023	344,991	236,047	0	171,734	1,913,931	2,155,722	288,687	33,067	-36,731
Jan-22	34	1,153,505	744,111	19,287	390,108	266,916	0	100,299	1,838,100	2,090,183	211,086	15,193	-35,782
Feb-22	34	1,028,247	632,712	7,947	387,589	265,193	0	41,325	1,562,923	1,840,589	337,476	0	-33,775
Mar-22	34	838,334	610,175	1,155	227,004	155,318	0	6,008	1,507,252	1,788,412	930,446	0	63,983
Apr-22	34	831,546	254,244	46,629	530,673	363,092	0	242,491	628,034	1,043,426	1,276,616	0	-40,195
May-22	34	609,867	49,023	153,918	406,926	278,423	0	800,438	121,096	544,693	1,741,643	0	-70,344
Jun-22	34	619,058	0	226,776	392,282	268,403	0	1,179,330	0	326,684	1,741,180	0	-170,103
Jul-22	34	408,373	1,846	205,226	201,301	137,732	0	1,067,263	4,560	441,302	1,881,864	0	27,273
Aug-22	34	465,108	283,519	136,973	44,616	30,527	0	712,318	700,348	1,071,920	1,087,344	0	125,697
Sep-22	34	353,877	138,193	161,999	53,685	36,732	0	842,461	341,365	784,151	1,220,478	0	134,696
Oct-22	34	454,127	241,066	137,456	75,604	51,729	0	714,828	595,481	1,064,024	1,150,540	0	116,166
Nov-22	34	798,920	423,619	117,206	258,095	176,592	0	609,519	1,046,422	1,455,503	953,427	0	-1,429
Dec-22	34	1,033,551	480,894	107,545	445,111	304,550	0	559,281	1,187,904	1,543,125	617,956	0	-89,187

The main highlights of Case 1 included:

• Biogas upgrading enabled monetisation, turning gas costs into a net revenue stream;
• CHP usage and electricity generation decreased, leading to higher grid dependence;
• Boiler usage and thermal output increased to maintain digester heating;
• Despite increased electricity costs, total operating costs were significantly reduced, driven by biomethane income;
• Flaring was entirely eliminated, indicating efficient and environmentally responsible system operation.

c. Case 2

Co-digestion is integrated with the microgrid system. The operating costs for Case 2 are defined in (5.12), including the costs associated with the co-digestion component.

$$\begin{aligned} Min \sum_{t} \Bigg\{ \Bigg[& P_{grid}(t) \cdot \lambda_{dlf} \cdot \left(c_{ele_{imp}}(t) + c_{ele_{use}}(t) + c_{ele_{other}}(t) \right) \\ & + P_{wwtp_{cap}}(t) \cdot c_{ele_{cap}}(t) - P_{sold}(t) \cdot c_{ele_{exp}}(t) \Bigg] \cdot \Delta t \\ + \Bigg[& V_{gas_{grid}}(t) \cdot \left(c_{gas_{imp}}(t) + c_{gas_{use}}(t) \right) \\ & - V_{biomet}(t) \cdot c_{gas_{market}}(t) + V_{fog}(t) \cdot c_{fog} \Bigg] \Bigg\} \end{aligned} \tag{5.12}$$

The same assumptions for the co-digestion characteristics adopted in Case 2 of Chapter 4 (Section 5.4.2) are applied here, including substrate (FOG), operational costs, and mixing

ratio. Additionally, the biogas storage of 60,000 m^3 is considered. Part of the formulation defined in Case 2 of Chapter 4 (Section 5.4.2) is reused for this Case 2 (Eqs. (4.30) to (4.38).

Optimisation results for Case 2 over 1-year, and 3-year horizons (2020–2022) is presented in Table 5.5, and results for 1-month horizon are shown in Table 5.6. The results cover biogas production and utilisation, biomethane export, natural gas usage, thermal and electricity generation and consumption, as well as gas, electricity, and total operating costs. As illustrated in Table 5.5, in Case 2, the integration of co-digestion using sewage sludge and FOG resulted in a significant boost in biogas production, reaching over 53 million m^3 from 2020 to 2022, approximately 54% higher than Case 1a. This increase enabled a slightly higher biogas utilisation in the CHP units, totalling 23.1 million m^3, and lower utilisation in the boilers, reaching 1.87 million m^3. However, the substantial portion of biogas, approximately 28 million m^3, was directed to the upgrading system, resulting in 19.2 million m^3 of biomethane exported to the grid. Compared to Case 1a, the volume of biogas upgraded was nearly three times higher, highlighting the system's prioritisation of revenue-generating biomethane and potential constrains on CHP generation capacity. Over a 3-years horizon, CHP thermal generation exceeded 57 GWh, which was sufficient to fully cover the AD thermal demand (55.8 GWh). However, some additional support was still provided by the boiler's thermal output (9.75 GWh), as thermal energy could not be stored or traded based on the WWTP's configuration. CHP also generated approximately 48 GWh of electricity complemented by PV and micro-hydro production of 15.24 GWh and 2.68 GWh, respectively. Compared to Case 1a, grid importation increased slightly, while electricity consumption for biogas upgrading rose significantly, from 2.56 GWh to 7 GWh. Conversely, electricity exports decreased by almost 55%, dropping to 1.38 GWh from 2.5 GWh in Case 1a, likely due to the shift toward self-consumption and biomethane upgrading. Natural gas imports were negligible in both cases, with Case 2 recording only 3,301 m^3 over three years. Over 3-years horizon, electricity costs amounted $3.6 million, while gas revenues reached $7.7 million, primarily driven by large-scale biogas production from co-digestion and subsequent biomethane export. However, this gain was offset by co-digestion costs, which added $5.6M to the operational expenses, resulting in total operating costs for approximately $1.54 million. Despite these additional costs, the system achieved net revenue of almost $950,000 in 2022, indicating that co-digestion became economically favourable when combined with high gas market prices.

Table 5.5: Result summary for 1-year and 3-year optimisation horizons - Case 2 (Microgrid system)

Period	**2020**	**2021**	**2022**	**2020-2022**
Temperature in the digester (°C)	34	34	34	34
Biogas generation (m^3)	20,356,832	18,649,060	14,036,244	53,042,136
Biogas used in the CHP (m^3)	9,991,350	8,986,576	4,134,058	23,111,454
Biogas used in the boiler (m^3)	205,114	456,498	1,207,450	1,869,314
Biogas upgraded to biomethane (m^3)	10,160,367	9,205,986	8,694,736	28,061,367
Biomethane volume (m^3)	6,951,830	6,298,832	5,949,030	19,199,883
Natural gas imported (m^3)	1,591	1,711	0	3,301
Boiler thermal generation (kWh)	1,078,769	2,386,983	6,279,240	9,746,303
CHP thermal generation (kWh)	24,680,610	22,198,618	10,211,941	57,089,858
Thermal energy required for the AD (kWh)	20,432,800	20,272,234	15,087,058	55,792,091
WWTP electricity consumption (kWh)	28,372,386	25,640,541	26,244,362	80,257,289
CHP electricity generation (kWh)	20,783,671	18,693,573	8,599,529	48,075,670

Continued on next page

Table 5.5 – continued from previous page

Period	2020	2021	2022	2020-2022
PV generation (kWh)	5,088,570	5,073,374	5,073,685	15,235,630
Micro-hydro generation (kWh)	894,416	892,129	892,129	2,678,673
BESS energy charged (kWh)	318,564	322,241	319,064	959,869
BESS energy discharged (kWh)	287,504	290,822	287,955	866,281
Electricity bought from the grid (kWh)	5,064,152	3,804,016	13,888,718	22,758,059
Electricity sold back to the grid (kWh)	887,272	489,635	4,907	1,381,814
Biogas upgrading consumption (kWh)	2,540,092	2,301,496	2,173,684	7,015,342
Electricity costs ($)	1,004,729	737,144	1,863,663	3,605,699
Gas costs ($)	-1,254,987	-2,121,238	-4,327,071	-7,703,452
Co-digestion costs ($)	2,083,572	2,038,276	1,515,670	5,637,519
Total operating costs ($)	1,833,314	654,183	-947,737	1,539,766

Table 5.6: Result summary for 1-month optimisation horizon - Case 2 (Microgrid system)

Period	T_{ad} (°C)	Biogas gen (m^3)	Biogas CHP (m^3)	Biogas Boiler (m^3)	Biogas upgrade (m^3)	Biomethane (m^3)	CHP, PV & Hyd (kWh)	Energy imp. (kWh)	Energy exp. (kWh)	Elec. costs ($)	Gas costs ($)	AcoD costs ($)	Op. costs ($)
Jan-20	34	1,404,014	771,751	12,347	619,916	424,153	2,149,721	405,071	56,965	84,739	-95,392	164,586	153,933
Feb-20	40	1,579,480	788,231	5,566	785,683	537,573	2,181,474	352,416	128,962	70,802	-113,955	163,212	120,059
Mar-20	43	1,744,300	858,099	5,019	881,183	602,915	2,303,916	670,647	85,666	122,071	-106,019	176,873	192,924
Apr-20	40	1,638,703	830,703	20	807,980	552,829	2,228,765	628,258	100,891	114,974	-89,064	169,947	195,857
May-20	40	1,734,273	858,393	6,424	869,456	594,891	2,231,384	378,067	138,285	73,797	-92,509	178,996	160,284
Jun-20	36	1,865,198	830,703	8,398	1,026,097	702,067	2,059,648	549,479	50,510	102,784	-104,863	195,627	193,548
Jul-20	34	1,831,469	852,441	17,908	961,120	657,609	2,203,263	586,814	77,779	108,135	-104,006	187,042	191,170
Aug-20	34	1,845,683	858,393	55,168	932,122	637,768	2,272,460	555,945	82,146	105,315	-103,530	189,471	191,256
Sep-20	34	1,860,772	830,703	74,196	955,872	654,018	2,229,469	380,307	177,675	71,817	-102,203	179,503	149,117
Oct-20	34	1,761,235	856,250	33,900	871,085	596,006	2,350,279	344,283	186,655	65,807	-114,629	162,266	113,444
Nov-20	34	1,572,173	818,926	10,558	742,689	508,155	2,271,091	319,499	181,561	62,530	-113,245	152,581	101,866
Dec-20	36	1,688,696	841,033	3,109	844,555	577,853	2,294,081	383,663	85,068	79,383	-131,629	163,470	111,224
Jan-21	38	1,858,458	841,535	4,542	1,012,381	692,682	2,294,883	387,078	51,117	72,827	-151,463	174,619	95,984
Feb-21	38	1,655,367	741,220	3,774	910,373	622,887	2,064,770	297,555	115,083	55,993	-131,725	181,309	105,577
Mar-21	40	1,633,111	828,394	1,677	803,041	549,449	2,244,922	350,416	93,979	65,732	-123,668	175,143	117,207
Apr-21	40	1,470,301	783,289	671	686,340	469,601	2,138,207	392,630	58,668	71,465	-119,005	160,705	113,165
May-21	40	1,393,627	798,694	1,740	593,193	405,869	2,104,835	610,620	27,771	100,346	-108,831	145,748	137,263
Jun-21	34	1,257,681	685,308	2,591	569,782	389,851	1,752,220	317,359	0	59,248	-160,147	140,186	39,287
Jul-21	34	1,416,980	504,036	97,854	815,089	557,693	1,478,675	689,411	0	107,769	-364,775	154,974	-102,032
Aug-21	34	1,624,657	782,050	86,521	756,086	517,322	2,110,403	152,959	101,700	38,950	-161,677	190,224	67,497
Sep-21	34	1,579,482	809,893	79,366	690,222	472,257	2,184,399	148,111	233,649	30,959	-140,635	179,302	69,626
Oct-21	34	1,518,170	760,439	80,445	677,286	463,406	2,151,524	213,876	194,364	42,461	-135,654	168,887	75,694
Nov-21	34	1,667,234	673,438	107,700	886,096	606,276	1,971,295	267,230	0	57,895	-286,314	177,193	-51,226
Dec-21	34	1,703,785	790,577	26,023	887,186	607,022	2,188,522	383,685	25,420	73,118	-253,384	189,987	9,720
Jan-22	34	1,830,147	763,316	11,873	1,054,957	721,813	2,130,133	332,193	10,123	64,344	-228,412	194,205	30,137
Feb-22	37	1,642,773	671,394	12,605	958,774	656,004	1,921,054	399,823	0	69,630	-232,550	169,629	6,709
Mar-22	39	1,414,363	708,307	2,591	703,465	481,318	1,992,543	845,430	0	120,833	-194,552	155,701	81,983
Apr-22	34	1,309,008	255,173	46,188	1,007,648	689,443	1,045,357	1,393,928	0	185,104	-400,920	130,930	-84,886
May-22	34	1,039,252	49,197	153,835	836,219	572,150	545,055	1,848,604	0	239,295	-610,308	117,031	-253,982
Jun-22	34	1,072,289	0	226,776	845,512	578,509	326,684	1,854,488	0	238,428	-852,840	126,371	-488,042

Continued on next page

Table 5.6 – continued from previous page

Period	T_{ad} (°C)	Biogas gen (m^3)	Biogas CHP (m^3)	Biogas Boiler (m^3)	Biogas upgrade (m^3)	Biome-thane (m^3)	CHP, PV & Hyd (kWh)	Energy imp. (kWh)	Energy exp. (kWh)	Elec. costs ($)	Gas costs ($)	AcoD costs ($)	Op. ccosts ($)
Jul-22	34	741,414	7,463	202,558	531,393	363,584	452,988	1,952,701	0	252,059	-573,181	86,778	-234,344
Aug-22	34	835,936	377,751	96,782	361,404	247,276	1,267,938	970,522	0	131,032	-159,131	103,521	75,422
Sep-22	34	646,579	199,866	132,704	314,008	214,848	912,440	1,157,273	0	154,899	-164,647	76,556	66,808
Oct-22	34	768,243	290,437	116,085	361,721	247,493	1,166,723	1,119,369	0	150,706	-179,554	86,367	57,519
Nov-22	34	1,226,172	440,408	113,269	672,495	460,128	1,490,427	1,022,044	0	138,645	-321,480	123,186	-59,649
Dec-22	34	1,549,097	495,856	101,333	951,908	651,305	1,574,248	713,526	0	107,697	-377,192	145,396	-124,098

The monthly optimisation results for Case 2 highlight significant operational shifts over the three-year period, particularly in response to the higher biogas produciton with co-digestion, as illustrated in Table 5.6. Biogas production was consistently high reaching over 1.8 million m^3, especially from January to June 2020, but reached its minimal generation in Sep-22 (below 0.65 million m^3). Biogas utilisation also shifted notably, while CHP usage dominated in the first two years, it was significantly reduced in 2022, with no usage recorded in June 2022, to prioritise biomethane upgrading. Boiler usage increased during this period to meet the heat demand, peaking at 226,776 m^3 in June 2022. Biomethane upgrading became a primary strategy in 2022, particularly during months with high gas market prices, supporting financial performance. Microgrid generation was high in 2020 and 2021 (typically exceeding 2 million kWh per month) but dropped considerably in 2022, particularly between April and July when CHP output and biogas production declined. As a result, energy imports increased in 2022, peaking at 1.95 million kWh in July, indicating reduced energy self-sufficiency. Electricity exports, which were frequent in previous years, dropped to zero in most months of 2022. In terms of operating costs, electricity costs increased significantly in 2022, reaching over $250,000 per month in July and August due to high grid dependence. However, gas costs were consistently negative, reflecting revenue from biomethane sales, with a peak income of $852,000 in June 2022. Co-digestion (AcoD) costs remained steady, ranging from $160,000 to $195,000 per month, and contributed to the overall cost profile. Total operational costs were generally above $100,000 per month in 2020 and early 2021, peaking at nearly $194,000 in June 2020. In contrast, several months in 2022 achieved strong profitability, such as May, June and July, as high gas prices made biomethane exports highly lucrative, outweighing rising electricity import costs.

The key highlights of Case 2 included:

• Biogas production increased by approx. 54% in Case 2 due to co-digestion;
• More biogas was directed to biomethane upgrading, prioritising higher revenue despite increased boiler usage;
• CHP and boiler thermal output were significantly higher, fully meeting AD heat demands and allowing greater system flexibility;
• Electricity imports increased in 2022 as a trade-off for reduced CHP use in favour of biomethane export;
• Operating costs initially was high in 2020 and 2021, but in 2022, the system demonstrated strong profitability potential, achieving $947,000 in operational costs by taking advantage on high gas market prices;
• Co-digestion costs had a significant impact on operating expenses but were largely offset by gas revenues, particularly under favourable market conditions;

c. Case 3

In this Case 3, the WWTP is assumed to purchase electricity directly from the spot market. Eq. (5.13) defines the power balance equation, which has been modified to incorporate the electricity component bought from the spot market ($P_{spot}(t)$).

$$\begin{aligned} P_{spot}(t) + P_{hyd}(t) + P_{pv}(t) + P_{chp}(t) + P_{b_{dis}}(t) = \\ P_{wwtp}(t) + P_{sold}(t) + P_{b_{ch}}(t) + P_{up}(t) \end{aligned} \tag{5.13}$$

Constraint (5.14) defines the upper and lower bounds of the power purchased from the spot market.

$$0 \leq P_{spot}(t) \leq P_{grid}^{\max} \cdot u_{grid}(t) \tag{5.14}$$

The operating cost equation for is reformulated as defined in (5.15), where $c_{spot}(t)$ represents the electricity spot market price. The spot market price considered in this study corresponds to the state of New South Wales (NSW), Australia.

$$\begin{aligned} Min \sum_t \Bigg\{ \Bigg[& P_{spot}(t) \cdot \lambda_{dlf} \cdot (c_{spot}(t) + c_{net_{use}}(t) + c_{ele_{other}}(t)) \\ & + P_{wwtp_{cap}}(t) \cdot c_{ele_{cap}}(t) - P_{sold}(t) \cdot c_{ele_{exp}}(t) \Bigg] \cdot \Delta t \\ & + \Bigg[V_{gas_{grid}}(t) \cdot \big(c_{gas_{imp}}(t) + c_{gas_{use}}(t)\big) - V_{biomet}(t) \cdot c_{gas_{market}}(t) \Bigg] \Bigg\} \end{aligned} \tag{5.15}$$

Table 5.7 presents a summary of the operational results for Case 3 (Microgrid system) across different optimisation horizons, including the 1—year horizons for 2020, 2021, 2022, as well as the aggregated three-year period (2020–2022). The digester temperature was maintained at a constant 34°C throughout the period. Biogas generation declined year-on-year, similar to previous cases, dropping from approximately 14.1 million m^3 in 2020 to 8.6 million m^3 in 2022, with a cumulative total of 34.45 million m^3 over the three years. Most of this biogas was used in the CHP system (22.17 million m^3), followed by upgrading to biomethane (10.64 million m^3), and smaller amounts diverted to boilers (1.64 million m^3). The corresponding biomethane output over the three years was around 7.28 million m^3. Thermal generation from the CHP and boilers was 54.76 GWh and 8.85 GWh, respectively, while CHP also produced 46.11 GWh of electricity. Energy consumption for biogas upgrading declined steadily, from 1.15 GWh in 2020 to just 0.55 GWh in 2022. Over the 3-year horizon, electricity purchased from the spot market amounted to more than 21.16 GWh, while electricity exports to the grid declined to just over 2.07 GWh during the same period. As a result, electricity costs increased sharply, from \$544,000 in 2020 to over \$2.15 million in 2022. However, this was partially offset by revenue from biomethane sales, reflected in negative gas costs totalling \$2.22 million over the three years. Total operating costs in 2020 and 2021 reached a small revenue of \$1,500 and \$56,000, respectively, but increased to over \$1.31 million in 2022, resulting in a cumulative operating cost of approximately \$1.26 million across the entire period.

Table 5.7: Result summary for 1-year and 3-year optimisation horizons - Case 3 (Microgrid system)

Period	2020	2021	2022	2020-2022
Temperature in the digester (°C)	34	34	34	34
Biogas generation (m^3)	14,139,666	11,720,727	8,594,513	34,454,906
Biogas used in the CHP (m^3)	9,275,294	7,039,098	5,853,449	22,167,841
Biogas used in the boiler (m^3)	267,523	826,321	548,480	1,642,324
Biogas upgraded to biomethane (m^3)	4,596,849	3,855,308	2,192,583	10,644,740
Biomethane volume (m^3)	3,145,213	2,637,842	1,500,189	7,283,243
Natural gas imported (m^3)	5,068	4,877	30,476	40,421
Boiler thermal generation (kWh)	1,429,747	4,334,283	3,083,963	8,847,992
CHP thermal generation (kWh)	22,911,809	17,387,963	14,459,177	54,758,948
CHP electricity generation (kWh)	19,294,155	14,642,495	12,176,149	46,112,798
PV generation (kWh)	5,088,570	5,073,374	5,073,685	15,235,630
Micro-hydro generation (kWh)	894,416	892,129	892,129	2,678,673
BESS energy charged (kWh)	619,091	664,667	686,426	1,970,184
BESS energy discharged (kWh)	558,730	599,862	619,499	1,778,091
Biogas upgrading consumption (kWh)	1,149,212	963,827	548,146	2,661,185
Electricity bought from the spot market (kWh)	5,392,290	6,672,301	9,096,352	21,160,943
Electricity sold back to the grid (kWh)	1,087,472	611,125	378,880	2,077,477
Electricity costs ($)	544,372	774,906	2,159,138	3,478,416
Gas costs ($)	-545,937	-830,917	-844,902	-2,221,756
Total operating costs ($)	-1,564	-56,011	1,314,235	1,256,660

Table 5.8 presents a detailed monthly summary of the microgrid system's performance under a 1-month optimisation horizon from January 2020 through December 2022. Electricity generation from the microgrid (CHP, PV, and micro-hydro) remained fairly stable over the years, generally ranging from 1.4 to 2.3 GWh per month. However, reliance on electricity imports increased markedly over time. Early months such as May 2020 saw low spot market purchases (313 MWh), while by July 2022, imports had surged to over 1.08 GWh, a dramatic shift pointing to declining internal generation and growing dependency on external supply. This transition had significant cost implications. The operating costs ranged from strongly net revenue (such as in Jan-20, from Nov-21 to Feb-22, Dec-22) to significantly positive numbers (i.e., May-22 to Oct-22), reflecting the interplay between energy generation, market prices, and resource utilisation. In 2020, the system consistently achieved low or negative operating costs, indicating profitability or cost neutrality. This was largely driven by high biogas production (over 1.3 million m^3 per month), substantial biomethane upgrading volumes, and low reliance on electricity imports due to adequate generation from CHP, PV, and hydro sources. For instance, the operating costs in most of the months in 2020 and 2021 generated a net revenue for the WWTP, whereas in 2022, the lower biogas production, the total operation cost increased. The most severe case occurred in July 2022, where the operating cost peaked at $434,222, driven by low biogas generation (408,373 m^3), minimal biomethane output (9,876 m^3), and exceptionally high electricity imports exceeding 1.08 GWh, which alone cost $425,603. Similar high operating cost, including August and September, where limited gas upgrading further reduced revenue.

Table 5.8: Result summary for 1-month optimisation horizon - Case 3 (Microgrid system)

Period	T_{ad} (°C)	Biogas gen (m^3)	Biogas CHP (m^3)	Biogas Boiler (m^3)	Biogas upgrade (m^3)	Biome-thane (m^3)	Gas grid (m^3)	CHP, PV & Hyd (kWh)	Energy spot (kWh)	Energy exp. (kWh)	Elec. costs ($)	Gas costs ($)	Op. costs ($)
Jan-20	34	890,754	695,574	20,897	174,284	119,247	3,842	1,991,260	486,024	89,037	-16,836	-22,273	-39,109
Feb-20	38	1,064,837	711,848	1,735	351,253	240,331	0	2,022,585	381,869	105,444	40,607	-49,611	-9,004
Mar-20	40	1,170,679	823,766	1,177	345,737	236,557	0	2,232,497	577,130	52,399	62,318	-41,664	20,653
Apr-20	40	1,103,439	775,443	5,529	322,468	220,636	0	2,113,815	567,675	44,569	59,466	-34,854	24,612
May-20	38	1,183,697	808,242	2,767	372,687	254,997	0	2,127,062	312,953	91,332	38,783	-39,829	-1,046
Jun-20	35	1,443,332	811,857	3,291	628,184	429,810	0	2,020,446	481,170	40,552	53,368	-64,396	-11,027
Jul-20	34	1,358,353	832,648	18,680	507,024	346,911	0	2,162,090	521,078	82,083	58,188	-56,610	1,579
Aug-20	34	1,364,281	846,573	56,195	461,513	315,772	0	2,247,873	473,069	89,886	54,274	-50,642	3,632
Sep-20	34	1,393,769	808,528	81,321	503,920	344,787	0	2,183,342	302,814	165,678	36,847	-54,168	-17,320
Oct-20	34	1,160,026	828,106	39,578	292,341	200,023	0	2,291,735	262,896	188,400	29,029	-37,947	-8,918
Nov-20	34	989,880	771,065	16,493	202,323	138,431	0	2,171,531	283,587	178,931	24,718	-31,497	-6,779
Dec-20	34	1,093,819	757,149	11,492	325,177	222,490	0	2,119,589	402,445	56,612	35,855	-50,457	-14,603
Jan-21	34	1,242,728	693,003	1,584	548,140	375,043	94	1,985,913	551,672	21,638	55,324	-82,961	-27,637
Feb-21	34	1,180,121	583,587	6,362	590,173	403,802	0	1,736,867	455,425	24,120	47,475	-85,928	-38,453
Mar-21	34	1,015,541	548,478	5,292	461,771	315,948	0	1,662,651	760,774	5,340	70,892	-72,189	-1,297
Apr-21	34	856,371	549,357	7,842	299,172	204,696	0	1,651,590	746,686	20,588	70,402	-53,012	17,390
May-21	34	712,022	579,036	5,029	127,958	87,550	625	1,647,909	949,251	21,760	99,850	-22,133	77,717
Jun-21	34	650,376	556,425	20,495	73,456	50,260	0	1,484,122	524,800	59,481	48,615	-22,248	26,367
Jul-21	34	779,937	449,403	125,086	205,448	140,570	0	1,365,028	727,829	73,236	65,797	-90,176	-24,380
Aug-21	34	1,077,673	688,310	128,376	260,987	178,570	0	1,915,408	207,633	83,109	29,555	-55,419	-25,864
Sep-21	34	1,018,515	645,622	156,133	216,760	148,310	0	1,842,687	227,805	88,006	28,384	-44,779	-16,394
Oct-21	34	916,331	634,943	137,775	143,613	98,261	1,275	1,890,471	292,847	143,928	33,962	-27,068	6,894
Nov-21	34	1,118,288	560,255	159,191	398,842	272,892	0	1,735,857	468,758	85,107	45,762	-135,699	-89,937
Dec-21	34	1,152,823	674,972	73,940	403,911	276,360	0	1,948,045	533,568	52,575	63,114	-114,685	-51,571
Jan-22	34	1,153,505	748,901	7,714	396,891	271,557	0	2,100,147	293,410	104,046	42,364	-86,246	-43,882
Feb-22	34	1,028,247	611,210	9,673	407,365	278,723	0	1,795,862	434,282	45,131	58,386	-99,116	-40,731
Mar-22	40	854,718	748,314	1,917	104,487	71,491	0	2,075,764	643,185	28,144	101,270	-29,763	71,508
Apr-22	40	847,798	666,286	10,777	170,735	116,818	0	1,900,541	428,866	96,236	82,298	-67,434	14,864
May-22	34	609,867	488,321	8,500	113,047	77,348	0	1,458,505	782,476	25,959	244,633	-93,301	151,332
Jun-22	34	619,058	526,607	11,045	81,406	55,699	241	1,422,114	603,894	33,063	219,578	-82,781	136,797
Jul-22	34	408,373	367,669	26,269	14,434	9,876	15,145	1,202,276	1,085,912	8,881	425,603	8,619	434,222
Aug-22	34	465,108	358,296	106,065	747	511	776	1,227,469	940,156	15,594	170,367	748	171,116
Sep-22	34	353,877	237,868	114,413	1,597	1,092	2,194	991,490	1,013,434	9,871	198,412	2,076	200,488
Oct-22	34	454,127	357,710	86,568	9,849	6,739	106	1,306,662	915,087	19,768	179,961	-5,011	174,950
Nov-22	34	798,920	509,751	83,996	205,173	140,381	0	1,634,672	784,346	20,139	113,562	-103,206	10,356
Dec-22	34	1,033,551	496,753	101,639	435,160	297,741	0	1,576,113	619,084	34,062	70,891	-170,871	-99,980

d. Case 4

For this Case 4, it is assumed that the WWTP can buy electricity from both the electricity spot market and bilateral contrats. It is also considered that the WWTP purchases natural gas directly from the gas market.

Consumers can participate in and be exposed to the spot market to take advantage of low electricity prices during specific time periods. However, to avoid being totally exposed to the high prices of the spot market (also known as the *pool*), they can sign bilateral contracts with energy suppliers (i.e., retailers, generators) to reduce these risks and uncertainties. Typically,

the prices in bilateral contracts are higher than the average spot price, but they are fixed for the entire duration of the contract. Additionally, the consumer's self-production capability is an important resource for self-protection when spot prices are comparatively high. During this period, consumers can either take advantage of high prices to generate additional revenue by selling electricity to the market, or use the generated electricity on-site [11], [273].

Constraints (5.16) and (5.17) define the upper and lower limits of the power purchased through bilateral contracts and from the spot market, respectively. $P_{bil}^{\max}$ and $P_{spot}^{\max}$ are the maximum power limits specified in the bilateral contracts and for purchases from the spot market. $P_{bil}(t)$ represents the power bought under the bilateral contract.

$$0 \leq P_{bil}(t) \leq P_{bil}^{\max} \tag{5.16}$$

$$0 \leq P_{spot}(t) \leq P_{spot}^{\max} \tag{5.17}$$

Eq. (5.18) is rewritten to account for purchases from both the spot market and bilateral contracts ($P_{bil}(t)$), while Eq. (5.19) defines the power balance equation, reformulated to include electricity bought from both sources.

$$0 \leq P_{spot}(t) + P_{bil}(t) \leq P_{grid}^{\max} \cdot u_{grid}(t) \tag{5.18}$$

$$\begin{aligned} P_{spot}(t) + P_{bil}(t) + P_{hyd}(t) + P_{pv}(t) + P_{chp}(t) \\ + P_{b_{dis}}(t) = P_{wwtp}(t) + P_{sold}(t) + P_{b_{ch}}(t) + P_{up}(t) \end{aligned} \tag{5.19}$$

The operating cost in Case 4 is reformulated as defined in (5.20), where $c_{bil}(t)$ is is the electricity price from bilateral contracts.

$$\begin{aligned} Min \sum_t \Bigg\{ \Bigg[& [P_{spot}(t) \cdot \lambda_{dlf} \cdot (c_{spot}(t) + c_{ele_{use}}(t) + c_{ele_{other}}(t)) + \\ & P_{bil}(t) \cdot \lambda_{dlf} \cdot (c_{bil}(t) + c_{ele_{use}}(t) + c_{ele_{other}}(t)) + \\ & + P_{wwtp_{cap}}(t) \cdot c_{net_{cap}}(t) - P_{sold}(t) \cdot c_{ele_{exp}}(t) \Bigg] \cdot \Delta t \\ & + \Bigg[V_{gas_{grid}}(t) \cdot (c_{gas_{market}}(t) + c_{gas_{use}}(t)) \\ & - V_{biomet}(t) \cdot c_{gas_{market}}(t) \Bigg] \Bigg\} \end{aligned} \tag{5.20}$$

Table 5.9 shows the simulation results for the 1-year and 3-year optimisation horizons, while Table 5.10 presents the results for the 1-month optimisation horizon. The results include the electricity, gas, and total operating costs, as well as total biogas production, including biogas consumed by the CHP system and boilers and exported to the gas network. Additionally, electricity purchased from spot and bilateral contracts, and total electricity sold back to the grid, are highlighted.

Table 5.9: Result summary for 1-year and 3-year optimisation horizons - Case 4 (Microgrid system)

Period	**2020**	**2021**	**2022**	**2020-2022**
Temperature in the digester (°C)	34	34	34	34
Biogas generation (m^3)	14,139,666	11,720,727	8,594,513	34,454,906
Biogas used in the CHP (m^3)	9,294,878	7,057,580	5,775,102	22,127,561
Biogas used in the boiler (m^3)	246,831	805,165	447,412	1,499,408
Biogas upgraded to biomethane (m^3)	4,597,957	3,857,981	2,371,999	10,827,938
Biomethane volume (m^3)	3,145,971	2,639,671	1,622,947	7,408,589
Natural gas imported (m^3)	12,102	12,507	92,909	117,519
Boiler thermal generation (kWh)	1,375,607	4,282,258	3,032,891	8,690,756
CHP thermal generation (kWh)	22,960,186	17,433,617	14,265,644	54,659,447
CHP electricity generation (kWh)	19,334,893	14,680,941	12,013,174	46,029,008
PV generation (kWh)	5,088,570	5,073,374	5,073,685	15,235,630
Micro-hydro generation (kWh)	894,416	892,129	892,129	2,678,673
BESS energy charged (kWh)	620,425	661,248	661,146	1,942,819
BESS energy discharged	559,933	596,776	596,685	1,753,394
Biogas upgrading consumption (kWh)	1,149,489	964,495	593,000	2,706,984
Electricity bought from the spot market (kWh)	5,314,560	6,424,689	4,276,902	16,016,150
Electricity bought from bilateral contracts (kWh)	41,356	224,956	5,107,247	5,373,559
Electricity sold back to the grid (kWh)	1,091,428	626,581	461,313	2,179,323
Electricity costs ($)	536,704	741,076	1,917,504	3,195,284
Gas costs ($)	-551,094	-835,274	-988,060	-2,374,428
Total operating costs ($)	-14,390	-94,198	929,445	820,856

Table 5.10: Result summary for 1-month optimisation horizon - Case 4 (Microgrid system)

Period	T_{ad} **(°C)**	**Biogas gen** (m^3)	**Biogas CHP** (m^3)	**Biogas Boiler** (m^3)	**Biogas upgrade** (m^3)	**Biome-thane** (m^3)	**CHP, PV & Hyd (kWh)**	**Energy spot (kWh)**	**Energy con-tract (kWh)**	**Energy exp. (kWh)**	**Elec. costs ($)**	**Gas costs ($)**	**Op. costs ($)**
Jan-20	34	890,754	716,333	138	174,284	119,247	2,034,442	444,829	922	91,850	-20,689	-25,629	-46,318
Feb-20	38	1,064,837	711,848	1,735	351,253	240,331	2,022,585	381,007	1,128	105,683	40,584	-49,611	-9,027
Mar-20	40	1,170,679	823,766	1,177	345,737	236,557	2,232,497	577,130	0	52,399	62,318	-41,664	20,653
Apr-20	40	1,103,439	775,443	5,529	322,468	220,636	2,113,815	561,312	6,363	44,569	59,336	-34,854	24,482
May-20	38	1,183,697	808,242	2,767	372,687	254,997	2,127,062	312,667	286	91,332	38,778	-39,829	-1,051
Jun-20	35	1,443,332	811,857	3,291	628,184	429,810	2,020,446	478,102	3,067	40,552	53,201	-64,396	-11,195
Jul-20	34	1,358,353	832,648	18,680	507,024	346,911	2,162,090	514,599	6,480	82,083	57,970	-56,610	1,361
Aug-20	34	1,364,281	846,573	56,195	461,513	315,772	2,247,873	468,170	4,918	89,905	53,929	-50,642	3,287
Sep-20	34	1,393,769	808,528	81,321	503,920	344,787	2,183,342	301,778	1,036	165,678	36,828	-54,168	-17,340
Oct-20	34	1,160,026	828,124	39,560	292,341	200,023	2,291,772	260,229	2,985	188,758	28,949	-37,945	-8,996
Nov-20	34	989,880	771,065	16,493	202,323	138,431	2,171,531	282,224	1,364	178,931	24,680	-31,497	-6,817
Dec-20	34	1,093,819	757,149	11,492	325,177	222,490	2,119,589	401,418	1,316	56,901	34,962	-50,457	-15,496
Jan-21	34	1,242,728	693,014	1,573	548,140	375,043	1,985,936	551,649	0	21,638	55,323	-83,070	-27,747
Feb-21	34	1,180,121	583,587	6,362	590,173	403,802	1,736,867	455,425	0	24,120	47,475	-85,928	-38,453
Mar-21	34	1,015,541	548,562	5,208	461,771	315,948	1,662,826	759,648	953	5,340	70,743	-72,097	-1,355
Apr-21	34	856,371	549,357	7,842	299,172	204,696	1,651,590	739,246	7,581	20,729	70,209	-53,012	17,196
May-21	34	712,022	580,684	3,380	127,958	87,550	1,651,338	917,641	29,508	23,127	92,791	-22,568	70,223
Jun-21	34	650,376	562,991	13,929	73,456	50,260	1,497,782	495,363	19,464	63,024	44,861	-20,846	24,015

Continued on next page

Table 5.10 – continued from previous page

Period	T_{ad} (°C)	Biogas gen (m^3)	Biogas CHP (m^3)	Biogas Boiler (m^3)	Biogas upgrade (m^3)	Biomethane (m^3)	CHP, PV & Hyd (kWh)	Energy spot (kWh)	Energy contract (kWh)	Energy exp. (kWh)	Elec. costs ($)	Gas costs ($)	Op. costs ($)
Jul-21	34	779,937	447,272	122,387	210,278	143,875	1,360,596	680,685	58,958	79,312	65,977	-92,624	-26,647
Aug-21	34	1,077,673	688,310	128,376	260,987	178,570	1,915,408	207,311	322	83,109	29,545	-55,419	-25,874
Sep-21	34	1,018,515	645,622	154,014	218,879	149,759	1,842,687	228,334	0	88,006	28,382	-44,779	-16,397
Oct-21	34	916,331	649,526	121,933	144,871	99,122	1,920,806	269,960	545	151,557	30,768	-26,757	4,010
Nov-21	34	1,118,288	560,255	157,513	400,520	274,040	1,735,857	469,202	0	85,107	45,760	-135,699	-89,939
Dec-21	34	1,152,823	674,972	73,940	403,911	276,360	1,948,045	529,235	4,650	52,893	63,040	-114,685	-51,645
Jan-22	34	1,153,505	748,901	7,714	396,891	271,557	2,100,147	289,307	4,411	104,453	42,298	-86,246	-43,947
Feb-22	34	1,028,247	611,208	9,673	407,367	278,725	1,795,858	431,715	2,571	45,131	58,340	-99,117	-40,777
Mar-22	40	854,718	748,314	1,917	104,487	71,491	2,075,764	623,502	19,682	28,144	100,737	-29,763	70,975
Apr-22	40	847,798	662,994	10,777	174,026	119,071	1,893,694	240,837	206,969	107,770	75,763	-68,897	6,865
May-22	34	609,867	424,831	14,583	170,454	116,626	1,326,435	76,378	887,358	59,821	228,262	-135,130	93,132
Jun-22	34	619,058	369,078	48,003	201,978	138,195	1,094,427	25,894	951,271	48,060	258,779	-210,138	48,641
Jul-22	34	408,373	234,739	46,863	126,771	86,738	925,758	102,477	1,294,610	15,351	400,162	-113,001	287,160
Aug-22	34	465,108	429,274	4,031	31,803	21,760	1,375,115	538,263	290,418	44,095	133,814	11,778	145,592
Sep-22	34	353,877	288,216	5,620	60,042	41,081	1,096,222	364,240	574,059	25,047	165,604	2,275	167,879
Oct-22	34	454,127	331,152	11,217	111,758	76,466	1,251,417	453,132	544,361	22,257	180,979	-29,233	151,746
Nov-22	34	798,920	446,730	35,698	316,492	216,547	1,503,578	821,355	119,255	17,465	129,558	-151,895	-22,337
Dec-22	34	1,033,551	458,024	59,741	515,786	352,906	1,495,552	705,018	16,919	35,771	77,141	-185,952	-108,812

Comparing the electricity consumption and associated costs between Case 4 and Case 3, both cases purchased a similar total amount of electricity (approx. 21.39 GWh in Case 4 and 21.16 GWh in Case 3), but the total electricity cost in Case 4 was lower due to the use of bilateral contracts, which helped avoid higher spot market prices. This cost difference of approximately $283,000 illustrates the benefit of combining the contract-based electricity strategy to avoid the volatile prices in the spot market. The contrast is most pronounced in 2022: Case 3 purchased over 9.1 GWh entirely from the spot market, incurring $2.16 million in electricity costs, while Case 4 limited its spot market exposure to 4.28 GWh and sourced an additional 5.1 GWh from bilateral contracts, resulting in a lower electricity cost of $1.92 million. In earlier years (2020 and 2021), where both scenarios relied mainly on spot purchases, the cost differences were relatively minor—only around $7,600 in 2020 and $33,800 in 2021. However, the strategic use of bilateral contracts in Case 4 during 2022 clearly mitigated the financial impact of high spot market prices, underscoring the advantage of a diversified procurement approach. This comparison highlights that while energy consumption levels remained comparable, the inclusion of contract electricity in Case 4 provided critical cost resilience under adverse market conditions, particularly during periods of heightened price volatility.

5.5 Summary

This chapter presents the second component of the WWTP operation model, extending the framework presented in Chapter 4 by integrating a microgrid system to enhance energy resilience and reduce dependence on the main grid. The proposed optimisation model aims to minimise the plant's total operating costs by optimally coordinating multiple on-site energy systems, including CHP units, PV, BESS, and micro-hydro turbines, but also accounting for the biogas production and utilisation, and potential biomethane injeciton into the gas network. A large-scale WWTP located in Sydney, Australia, was used as the reference case, and case studies were conducted to evaluate the system's performance under various configurations and market

scenarios. The analysis was conducted through five case scenarios, including co-digestion, biogas upgrading for biomethane injection into the gas grid, and participation in energy spot markets, each assessed across three optimisation horizons of 1 month, 1 year, and 3 years.

In the baseline scenario (referred to as Case 1), the optimal AD temperature was identified as 34 °C, resulting in a total operating cost of approximately $ 2.27 million over a 3-year horizon when the objective was to minimise operational expenses in the WWTP. The amount of biogas used in the CHP, boiler and flared was around 77.8%, 2.6% and 19.6%, respectively. When 1-year horizon was analysed, the optimal AD temperature was found to be 34°C for all three years, 2020, 2021 and 2022, with corresponding annual operating costs of around $777,600, $522,700, and $969,500, respectively, as shown in Table 5.1. An alternative approach in Case 1a explored the use of biomethane injection in place of biogas flaring. This option significantly reduced the total operating costs, resulting in a $1.5 million reduction over three years. In this scenario, for a 3-years operation, biogas used in the CHP was reduced to 64.2%, while 29.8% was upgraded to biomethane, and the remaing portion was used in the boilers. As shown in Table 5.3, the revenue from biomethane sales was notably high in 2022 due to the high prices in gas market. As a result, total biomethane revenue reached approximately $1.78 million in 2022 and $2.9 million over three years from 2020 to 2022. When 1-year horizon was analysed, the cost of purchasing electricity from the grid was about $896,000 in 2020, $717,000 in 2021 and jumped to $1.8 million in 2022, whereas over a 3-year horizon it was $3.4 million. Case 2 introduced co-digestion as a strategy to boost biogas production, which increased by nearly 54% for the scenario with 3-year optimisation horizon, compared to Case 1. However, the added benefits were offset by the high costs associated with co-digestion operations. Biogas utilisation in the CHP and boiler accounted for 43.3% and 3.6% for a 3-years horizon, respectively, and more than 53% was converted into biomethane and exported to the gas network. As illustrated in Table 5.5, for 1-year horizon, the WWTP could generate $4.3 million in 2022 from gas trading due to the high prices on gas market. For 3-years horizon, biomethane injection generated a total benefit of approximately $7.7 million. Despite these earnings, the high co-digestion operating costs, around $5.64 million over 3-years optimisation horizon, along with $3.6 million in electricity costs, result in total operating expenses of about $1.54 million over the same period. In Case 3, the WWTP operated entirely on the electricity spot market, resulting in total operating costs of approximately $1.25 million over three years. In contrast, Case 4 applied a more diversified strategy by combining spot market participation, bilateral contracts, and direct gas market purchases. This approach provided a more economical benefit, enabling the WWTP to reduce the operating costs by around $400,000 and reduce overall operating costs to $821,000, primarily due to lower gas procurement expenses and also by purchasing electricity from the bilateral contracts.

When comparing all scenarios, Case 1a emerges as the most economically advantageous option, primarily due to the profits gained through biomethane export. Case 2 presents a scenario with increased biogas output, although its overall profitability is limited by high co-digestion costs. Case 3 highlights the risks of relying exclusively on volatile spot market pricing for electricity, whereas Case 4 demonstrates that a well-balanced energy procurement strategy can lead to cost reductions or even generate some profits. Overall, the findings suggest that integrating a microgrid system with biomethane in-jection can offer a valuable pathway to reducing WWTP operating costs. Additionally, co-digestion can enhance biogas production and revenue potential, but its economic viability is more challenging due to the high associated costs. Exposure to the electricity spot market combined with energy contracts can be another viable strategy that WWTP can explore to avoid high energy prices and reduce operating costs.

Chapter 6

Optimal Planning and Operation

6.1 Introduction

In this chapter, an optimal planning configuration for the power generation system is presented by integrating a microgrid system into a large-scale WWTP to reduce operating costs and enhance energy self-sufficiency. The proposed approach evaluates microgrid architectures incorporating distributed energy resources (DERs), such as hydropower, PV, CHP units, BESS, gasification, sludge drying system, water electrolysis and fuel cells. A multi-objective model is proposed to optimise both investment and operational costs of the microgrid while meeting electrical and thermal load demands. The model includes a detailed mathematical representation of energy generation, consumption patterns, and operational constraints under real-world conditions. Case studies based on different scenarios are conducted to assess cost savings, performance, and the technical viability of various microgrid configurations. The primary aim of this chapter is to evaluate microgrid performance and planning strategies for a large-scale WWTP under real-world operating conditions.

This chapter is organised as follows. Section 6.2 provides a background information on microgrid planning. Section 6.3 gives a brief overview of microgrid planning, highlighting the opportunities and generation technologies that can be implemented in WWTPs. Section 6.4 presents the proposed model, introducing the optimisation framework for microgrid planning, including the mathematical formulation, decision variables, constraints, and objective function. Section 6.5 presents the results of three case studies to evaluate the effectiveness of the proposed model, including a discussion of the findings. A sensitivity analysis is also conducted at the end of this section. Finally, Section 6.6 provides the conclusions.

6.2 Background

Municipal WWTPs are among the most significant energy users in the urban water sector. At the same time, the energy contained in municipal wastewater can be about five to ten times greater than the energy required for treatment processes [3], [4], [24]. For example, the total energy content in raw municipal wastewater at the North Toronto WWTP was found the be approximately nine times greater than the electrical required to operate the entire treatment plant [274], [275]. Despite this theoretical energy recovery potential, the number of self-sufficient facilities worldwide remains very limited. More and more WWTPs are actively

looking for new solutions and potential alternatives to reduce energy costs and maximise on-site generation [9]. WWTPs continue to face challenges in reducing their carbon footprint and meeting sustainability targets. To address these issues, a combination of energy efficiency measures and renewable energy generation through resource recovery technologies can offer an effective solution [3]. Renewable energy resources provide a viable alternative to meet growing energy demand, minimise operating costs from the main grid, and reduce greenhouse gas emissions. By adopting renewable energy sources, WWTPs can significantly reduce the overall energy demand, achieve energy self-sufficient, and in some cases, become energy-positive [10]. Two main groups of renewable energy resources can be used in WWTP: sector-specific and non-sector-specific. Sector-specific assets (also called site-specific) are energy technologies that recover energy embedded in the WWTP resources, such as chemical, hydraulic/kinetic, and thermal energy from influent/effluent wastewater and sewage sludge. Non-sector-specific types (also known as non-site specific) are independent of the plant's capabilities and do not rely on a specific site or location characteristics. Examples of sector-specific renewable resources include hydropower, gasification, pyrolysis, anaerobic digestion, microbial fuel cell (MFC), microbial electrolysis cell (MEC), whereas non-site specific technologies include wind and solar. Some site-specific resources, such as MEC and MFC, are still in the research and development stages and have not been widely implemented in large-scale facilities [11].

6.3 Microgrid Planning

High investment costs remain the main barrier to widespread adoption of microgrid systems. While microgrids offer substantial economic and reliability benefits to energy consumers, these advantages should be carefully evaluated against the associated investment to ensure a viable return on investment and to support the generation planning deployment. Accurately assessing the benefits of a microgrid can be challenging due to the intermittency and uncertain nature of renewable energy resources. Additional factors, such as load demand variability, volatile electricity market prices, and long-term maintenance and operational costs, can add further complexity [276]. Both planning and operation studies are essential to understanding potential risks and evaluating opportunities for WWTPs. Microgrid planning focuses on investment decisions for energy production and typically considers different technical aspects, including sizing, costs, technology selection, and uncertainties to provide confidence for end users [277]. Planning a microgrid system should include a critical assessment of generation potential, techno-economic feasibility, and the potential for future system expansion, with the main objective of determining the necessary generating capacity to meet the load demand in real time. Matching generation and demand is particularly challenging when the system relies on renewable energy sources. The planning process can be considered and formulated as an optimisation problem, with the objective of determining the more suitable technology, optimal generation mix, size, and capacity to achieve defined performance goals. Due to its challenges and complexity, each component can be treated and analysed independently or combined. As the power sector evolves according to technical, economic, and environmental trends, generation planning methods continue to develop to meet emerging needs [225]. Adopting a hybrid configuration of distributed energy resources (DERs) is an effective strategy for WWTPs to mitigate uncertainty and intermittency. By combining multiple technologies, hybrid systems can maximise energy generation potential while providing cost-effectiveness, improved energy efficiency, modularity, and operational flexibility [8]. Although several technological solutions exist to enhance economic benefits for WWTPs, implementation in full-scale plants remains

limited, primarily due to high capital and operating costs. The large number of available technology options makes determining the optimal planning and operation strategy for WWTP power generation a complex challenge requiring an integrated and comprehensive approach [226].

Figure 6.1 illustrates the main components of the microgrid used in this study, including CHP system, PV, battery and micro-hydro.

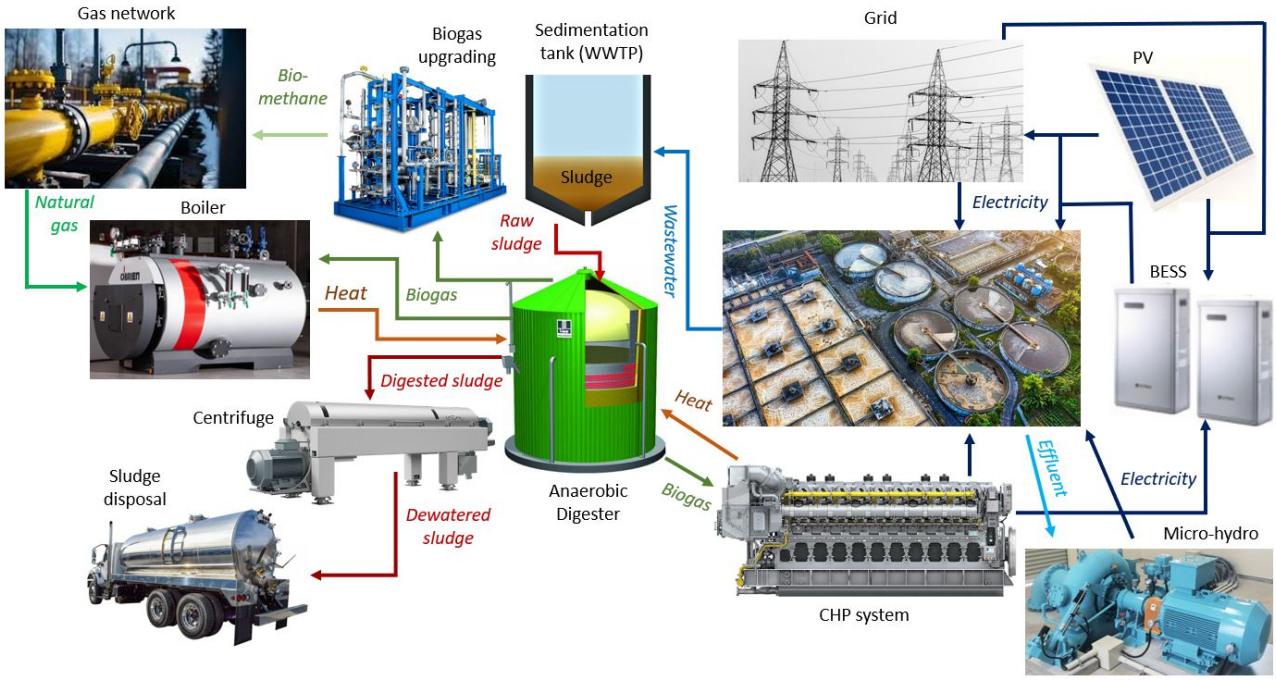

Figure 6.1: WWTP system configuration (Planning model)

As shown in Figure 6.1, the WWTP receives the influent (raw sewage) and a preliminary treatment removes large debris. This is followed by primary treatment, which includes grit removal and primary sedimentation. The raw sewage sludge produced in the sedimentation tank enters the anaerobic digesters, where the sludge is digested, generating biogas as a co-product. The biogas can be used in the CHP system to produce power and heat, and/or in boilers to generate additional heat if needed. If on-site biogas is not enough to meet the thermal energy demand of the anaerobic digesters, natural gas can be imported from the gas grid to be used for use in the boilers. On the other hand, any surplus biogas can be upgraded and injected into the gas network. After digestion, the sludge is commonly dewatered before disposal, primarily to reduce its water content, which ranges from approximately 95% to 99% in digested sludge, making it easier, safer, and more cost-effective to handle, transport, and dispose of. Dewatering technologies can reduce the sludge's volume and weight by up to 70%–80%.

6.4 Model Framework and Design

In this section, the model framework is presented, including the general assumptions and mathematical formulation. To validate the effectiveness of the proposed planning model, a comparison between simulation results and real data from a large-scale WWTP is conducted.

The proposed planning model aims to determine the optimal configuration for the WWTP's power generation system while minimising both investiment and operating costs. The model formulation incorporates some of the equations presented in the biogas modelling (Chapter 3) and the operation models (Chapters 4 and 5). Therefore, some of the formulations from Chapters 3, 4 and 5 are omitted in this section. The additional formulations and the multi-objective problem for this planning model are provided below.

6.4.1 Biogas Components

Constraint (6.1) ensures that the biogas volume inside the digester remains within the defined limits. $V_{ad_{unit}}^{\max}$ represents the maximum limit for a single biogas storage unit, and $n_{storage}$ is the number of biogas storage units. $s_{ad_{min}}$ is a scaling factor that determines the minimum biogas storage level relative to the maximum storage capacity.

$$V_{ad_{unit}}^{\max} \cdot s_{ad_{min}} \cdot n_{storage} \leq V_{biogas_{ad}}(t) \leq V_{ad_{unit}}^{\max} \cdot n_{storage} \tag{6.1}$$

Eqs. (6.2) and (6.3) define the boundaries for biogas charging and discharging, respectively, where $r_{biogas_{ch,unit}}$ and $r_{biogas_{dis,unit}}$ represent the maximum charging and discharging rates, respectively, for a single biogas unit in the anaerobic digestion system.

$$0 \leq \frac{V_{biogas_{ch}}(t)}{\Delta t} \leq r_{biogas_{ch,unit}} \cdot n_{storage} \cdot u_{ad}(t) \tag{6.2}$$

$$0 \leq \frac{V_{biogas_{dis}}(t)}{\Delta t} \leq r_{biogas_{dis,unit}} \cdot n_{storage} \cdot [1 - u_{ad}(t)] \tag{6.3}$$

Constraints (6.4), (6.5) and (6.6) limit the upper and lower boundaries of the total volume of gas used in the CHP units, boilers and upgrading system, respectively. $V_{chp_{unit}}^{\max}$, $V_{boiler_{unit}}^{\max}$, and $V_{up_{unit}}^{\max}$ are the maximum gas volumes that can be used in a single unit of CHP, boiler, and biogas upgrading systems, whereas n_{chp}, n_{boiler} and n_{up} are the total number of units for the CHP, boilers and biogas upgrading systems, respectively.

$$0 \leq V_{biogas_{chp}}(t) \leq V_{chp_{unit}}^{\max} \cdot n_{chp} \tag{6.4}$$

$$0 \leq V_{biogas_{boiler}}(t) + V_{gas_{grid}}(t) \leq V_{boiler_{unit}}^{\max} \cdot n_{boiler} \tag{6.5}$$

$$0 \leq V_{biogas_{up}}(t) \leq V_{up_{unit}}^{\max} \cdot n_{up} \tag{6.6}$$

Constraint (6.7) defines the lower and upper boundaries for power used in the upgrading system, where $P_{up_{unit}}^{\max}$ is the maximum power for a single biogas upgrading unit.

$$0 \leq P_{up}(t) \leq P_{up_{unit}}^{\max} \cdot n_{up} \tag{6.7}$$

6.4.2 Microgrid Components

a. CHP system and Boilers

Constraints (6.8) and (6.9) define the upper and lower boundaries of the electrical and thermal power from the CHP units, while constraint (6.10) limits the maximum thermal power in the

boilers. $P^{\max}_{chp_{unit}}$ and $Q^{\max}_{chp_{unit}}$ represent the maximum electrical and thermal power generation from a single CHP unit, and $Q^{\max}_{boiler_{unit}}$ is the maximum thermal power for a boiler unit.

$$0 \leq P_{chp}(t) \leq P^{\max}_{chp_{unit}} \cdot n_{chp} \tag{6.8}$$

$$0 \leq Q_{chp}(t) \leq Q^{\max}_{chp_{unit}} \cdot n_{chp} \tag{6.9}$$

$$0 \leq Q_{boiler}(t) \leq Q^{\max}_{boiler_{unit}} \cdot n_{boiler} \tag{6.10}$$

b. BESS

Constraint (6.11) snures that the battery energy remains within the maximum and minimum boundaries, where $E^{\min}_{b_{unit}}$ and $E^{\max}_{b_{unit}}$ are the minimum and maximum energy levels of a single battery unit, and n_b is the number of battery units.

$$E^{\min}_{b_{unit}} \cdot n_b \leq E_b(t) \leq E^{\max}_{b_{unit}} \cdot n_b \tag{6.11}$$

Eqs. (6.12) and (6.13) impose the boundary limits for maximum charging and discharging power for the battery storage system, respectively. $r_{b_{ch,unit}}$ and $r_{b_{dis,unit}}$ are the charging and discharging rates of a single battery unit, respectively.

$$0 \leq P_{b_{ch}}(t) \leq r_{b_{ch,unit}} \cdot n_b \cdot u_b(t) \tag{6.12}$$

$$0 \leq P_{b_{dis}}(t) \leq r_{b_{dis,unit}} \cdot n_b \cdot [1 - u_b(t)] \tag{6.13}$$

c. PV system

Eq. (6.14) describes the power generated by the PV system, $P_{pv}(t)$, where $P^{\max}_{pv_{unit}}$ is the maximum power output of a single PV unit, and n_{pv} is the total number of PV units.

$$0 \leq P_{pv}(t) \leq P^{\max}_{pv_{unit}} \cdot n_{pv} \tag{6.14}$$

d. Micro-hydro

Constraint (6.15) limits the maximum power of micro-hydro system, where $P^{\max}_{hyd}$ is the maximum power output of a single micro-hydro system unit, and n_{hyd} is the total number of micro-hydro units.

$$0 \leq P_{hyd}(t) \leq P^{\max}_{hyd_{unit}} \cdot n_{hyd} \tag{6.15}$$

e. Balance equation

Eq. (6.16) defines the power balance equation, where $P_{dew}(t)$ is the power consumed for dewatering the digested sludge.

$$\begin{aligned} P_{grid}(t) + P_{chp}(t) + P_{pv}(t) + P_{b_{dis}}(t) + P_{hyd}(t) = \\ P_{wwtp}(t) + P_{sold}(t) + P_{b_{ch}}(t) + P_{up}(t) + P_{dew}(t) \end{aligned} \tag{6.16}$$

f. Thermal (Sewage Sludge)

The dewatering process of digested sludge is primarily used to reduce its overall water content (approximately 95%-99%), thereby reducing the sludge volume and preparing it to meet environmental standards for disposal in landfills. Most WWTPs dewater sewage sludge because it is more economically feasible prior to final disposal, which may include landfilling, incineration, land application, or further drying/gasification. The main dewatering methods include centrifuge and belt filter press, which typically reduce the sludge water content to 75%-85%, and thermal drying, which can further lower the water content to 10%-20% after mechanical dewatering. In this study, it is assumed that the digested sewage sludge is dewatered using a centrifuge system, a common technology used in Australia [278].

Thermal equations for sewage sludge is defined in Section 4.3.2. Consequently, some of the formulation is omitted here. Additional formulations are provided in the following, including those related to the dewatering process for sewage sludge. Eqs. (6.17) and (6.18) define the total volume of dewatered sludge ($V_{dss_{dew}}(t)$) and the power used in the dewatering process ($P_{dew}(t)$), respectively. $r_{dss_{dew}}$ and $k_{dss_{dew}}$ represent the power consumption rate for sludge dewatering and the conversion factor from digested sludge to dewatered sludge, respectively.

$$V_{dss_{dew}}(t) = V_{ss_{out}}(t) \cdot k_{dss_{dew}} \tag{6.17}$$

$$P_{dew}(t) = V_{ss_{out}}(t) \cdot r_{dss_{dew}} \tag{6.18}$$

g. Objective Function

The total investment can be calculated as shown in (6.19). $c_{pv_{unit}}$, $c_{chp_{unit}}$, $c_{b_{unit}}$,$c_{hyd_{unit}}$, $c_{boiler_{unit}}$, $c_{up_{unit}}$ and $c_{storage_{unit}}$ are the costs (in \$/kW) of the solar PV, CHP, BESS, micro-hydro, boiler, biogas upgrading and storage systems units, respectively. In this study, operating and maintenance (O&M) costs for all technologies are already incorporated into the capital expenditure (CAPEX) of each unit system, as they can be accounted for as an incremental percentage of CAPEX, typically ranging from 2% to 5% [279], [280].

$$\begin{aligned} f_{inv} = {} & c_{pv_{unit}} \cdot n_{pv} + c_{chp_{unit}} \cdot n_{chp} + c_{b_{unit}} \cdot n_b + c_{hyd_{unit}} \cdot n_{hyd} \\ & + c_{boiler_{unit}} \cdot n_{boiler} + c_{up_{unit}} \cdot n_{up} + c_{storage_{unit}} \cdot n_{storage} \end{aligned} \tag{6.19}$$

Eq. (6.20) calculates the 1-year operating expenditure (OPEX), $f_{op_{1y}}$, of the WWTP, which includes three components: electricity costs, gas costs and sewage sludge disposal costs. $c_{ss_{disp}}$ represents the price associated with sewage sludge disposal.

$$\begin{aligned} f_{op_{1y}} = \sum_t \Bigg\{ & \Bigg[P_{grid}(t) \cdot \lambda_{dlf} \cdot \big(c_{ele_{imp}}(t) + c_{ele_{use}}(t) + c_{ele_{other}}(t) \big) \\ & + P_{wwtp_{cap}}(t) \cdot c_{ele_{cap}}(t) - P_{sold}(t) \cdot c_{ele_{exp}}(t) \Bigg] \cdot \Delta t \\ & + \Bigg[V_{gas_{grid}}(t) \cdot \big(c_{gas_{imp}}(t) + c_{gas_{use}}(t) \big) \\ & - V_{biomet}(t) \cdot c_{gas_{exp}}(t) + V_{dss_{dew}}(t) \cdot c_{ss_{disp}} \Bigg] \Bigg\} \end{aligned} \tag{6.20}$$

The operation model is designed with a 1-year operational horizon to reduce computational complexity and maintain tractability. However, to accurately assess the long-term economic performance of proposed objective function, the total OPEX is assessed over the full lifetime of the microgrid system using a Net Present Value (NPV) approach. This is achieved by projecting the annual OPEX from the one-year simulation over assumed microgrid operation lifetime, which is considered to be 12 years in this study. These projected annual OPEX values are then discounted to their present value using a fixed discount rate, as defined in (6.21), where N represents the number of years in the microgrid's operational lifetime (N=12). This approach allows the incorporation of both the initial CAPEX and the discounted cumulative OPEX into the proposed objective function, providing a realistic representation of the overall economic impact over the system's expected lifespan. The discount rate, denoted as r, reflects the effect of currency inflation.

$$f_{op} = \sum_{t=1}^{N} \frac{f_{op_{1y}}}{(1+r)^t} \tag{6.21}$$

A payback period (f_{pb}) can be calculated as shown in (6.22), where $C_{op_{hd}}$ is the 1-year OPEX based on current historical data when no microgrid system is yet implemented.

$$f_{pb} = \frac{f_{inv}}{C_{op_{hd}} - f_{op_{1y}}} \tag{6.22}$$

The objective functions presented in (6.19), (6.21), and (6.22) can be combined into a single objective function, defined in (6.23), which includes three main components of the proposed microgrid: CAPEX (f_{inv}), total OPEX (f_{op}), and payback period (f_{pb}).

$$f_{mo} = a_1 \cdot f_{inv} + a_2 \cdot f_{op} + a_3 \cdot f_{pb} \tag{6.23}$$

a_1, a_2 and a_3 are weighting factors applied to investment, operation, and payback period, respectively, and they must satisfy constraint (6.24). The weighting factors are determined by the decision-maker.

$$a_1 + a_2 + a_3 = 1 \tag{6.24}$$

6.5 Simulation Results

This section presents the outcomes of the proposed planning model. First, the key assumptions that underpin the analysis and simulation framework are outlined. In sequence, the simulation results from the selected case studies are presented. The findings are analysed and discussed to highlight their implications, reveal patterns, and assess their alignment with the research objectives.

6.5.1 Inputs and Assumptions

The WWTP characteristics, input data, parameters, and assumptions used in Sections 4.4.1 and 5.4.1 were also considered in the planning model. Outputs from the biogas model proposed in Chapter 3 were used as inputs to the planning model, assuming an anaerobic digestion operating temperature of 38 °C.

6.5.2 Case Studies

This section presents the case studies and main assumptions considered in the model to evaluate the proposed planning framework. Different case studies were considered to systematically explore the impact of incorporating different renewable energy technologies and resource recovery strategies in a WWTP. Apart from Case 1, the other cases require additional formulations to accurately represent the technical and economic aspects of the new components. The use of multiple case studies is essential to provide a comprehensive overview of the model's flexibility, assess the performance of different technological pathways, and identify the most effective strategies for enhancing energy efficiency and sustainability in WWTP operations.

The investment costs per unit of capacity for different technologies used in this study are presented in Table 6.1. The weighting factors a_1, a_2 and a_3 in (6.24) are assumed to be 0.6, 0.2 and 0.2, respectively. The cost of sludge disposal ranges from \$45 to \$105 per ton of waste, based on the Australian Government - DCCEEW (Department of Climate Change, Energy, the Environment and Water) [281]. The same costs were also applied to the co-digestion operating expenses.

Table 6.1: Unit costs for different technologies

Technology	**CAPEX Cost**
Boiler	\$1,800/kW
CHP	\$2,800/kW
PV	\$1,000/kW
BESS	\$500/kW
Micro-hydro	\$3,800/kW
Biogas upgrade	$\$3{,}500/\mathrm{m^3\,h^{-1}}$
Biogas storage	$\$200/\mathrm{m^3}$
Dryer	\$1,750/kW
Gasifier	\$5,800/kW
Electrolyser	\$3,000/kW
Fuel cell	\$5,500/kW

The case studies considered in this study are the following:

• Case 1: The microgrid includes a PV, battery, micro-hydro, boiler and CHP systems. Biogas storage and biogas upgrading system are also included.
• Case 2: In addition to Case 1, gasification of sewage sludge and sludge drying are considered.
• Case 3: In addition to Case 2, water electrolysis and fuel cell systems are included, alongside with co-digestion of sewage sludge.

In all cases, biogas production and utilisation are based on the model proposed in Chapter 3. For Case 2 and Case 3, additional formulations are required to account for the adoption of other technologies, including co-digestion, gasification, sludge drying, water electrolysis, and fuel cell systems, as detailed in the following sections.

a. Case 1

Table 6.2 provides a summary of the planning model results, including microgrid capacity, payback period, CAPEX and 1-year OPEX. The microgrid comprises a CHP unit, boiler, BESS, biogas upgrading and biogas storage systems, whereas PV and micro-hydro were not selected for this Case 1. Key observations from Table 6.2 indicate that the CHP unit represents the largest capacity in the microgrid (2,950 kWe), highlighting its central role in meeting both electrical and thermal demand. The boiler contributes an additional 230 kW of thermal energy, while the BESS provides 40 kW of electrical storage to improve operational flexibility. The biogas storage capacity is 800 m^3, and the biogas upgrading system can process up to 190 $m^3\,h^{-1}$, ensuring efficient utilisation of the biogas produced on-site. Additionally, the total CAPEX for this configuration is estimated at $9.52 million, with a payback period of 5.4 years, suggesting that, based on the assumptions considered, the investment may offer a reasonable return over the estimated payback period.

Note that the unit kWe (kilowatts electrical) is used to represent the size of the CHP system, as it specifically refers to the system's electrical power output. Since CHP units produce both electricity and heat, distinguishing between electrical (kWe) and thermal (kWth) outputs is essential for clarity. In this study, only the electrical generation capacity of the CHP was considered in the system sizing and optimisation, hence the use of kWe.

Table 6.2: Proposed microgrid configuration - Case 1 (Planning model)

Boiler (kW)	**CHP (kWe)**	**BESS (kW)**	**Biogas storage** (m^3)	**Biogas upgrade** ($m^3\,h^{-1}$)	**CAPEX ($ M)**	**Payback period (y)**
230	2,950	40	800	190	9.52	5.4

Table 6.3 illustrates the results for the WWTP 1-year operation, including the biogas generation and utilisation, natural gas importation, microgrid generation, power imported and exported to the grid, and annual OPEX. As highlighted, the total biogas production for 1-year operation was 11,746,008 m^3, mainly used in the CHP unit to generate electricity and heat (approximately 91.8%), while a portion was upgraded to biomethane and sold, generating $292,808 in revenue. The total electricity demand from the WWTP, which included the consumption of the WWTP, biogas upgrading system, battery charging, and sludge dewatering, was approximately 28.05 GWh, met by CHP generation, BESS and main grid. No electricity is exported, and BESS has limited storage flexibility. Economically, total OPEX is $4.68 million, with electricity costs reaching around $961,000, gas costs offsetting $292,808 (revenue from biomethane), and sludge disposal representing the largest expense ($4 million). Key findings from this Case 1 operational scenario indicate that the CHP unit plays a central role in meeting the WWTP's electrical and thermal demands, while biogas upgrading offers additional flexibility and revenue potential.

Table 6.3: Result summary for 1-year operation - Case 1 (Planning model)

Biogas production (m^3)	11,746,008
Biogas used in the CHP (m^3)	10,787,292
Biogas used in the boiler (m^3)	57,982
Biogas upgraded to biomethane (m^3)	900,735
Biomethane sold (m^3)	616,292
Biogas stored (m^3)	329,613
Biogas discharged (m^3)	329,613

Natural gas imported (m^3)	10,259
CHP thermal generation (kWh)	26,646,742
Boiler thermal generation (kWh)	417,452
Thermal energy required in the AD (kWh)	22,750,097
CHP electricity generation (kWh)	22,439,361
Electricity imported from the grid (kWh)	5,569,815
Electricity exported back to the grid (kWh)	0
WWTP consumption (kWh)	26,801,045
Energy charged by the battery (kWh)	53,810
Energy discharged from the battery (kWh)	43,586
Sludge dewatering consumption (kWh)	882,650
Biogas upgrading system consumption (kWh)	315,257
Electricity costs ($)	961,695
Gas costs ($)	-292,808
Sludge disposal costs ($)	4,012,044
1-year OPEX ($)	4,680,930

b. Case 2

In Case 2, sludge gasification and sludge drying systems are incorporated. Figure 6.2 illustrates the microgrid schematic for this scenario.

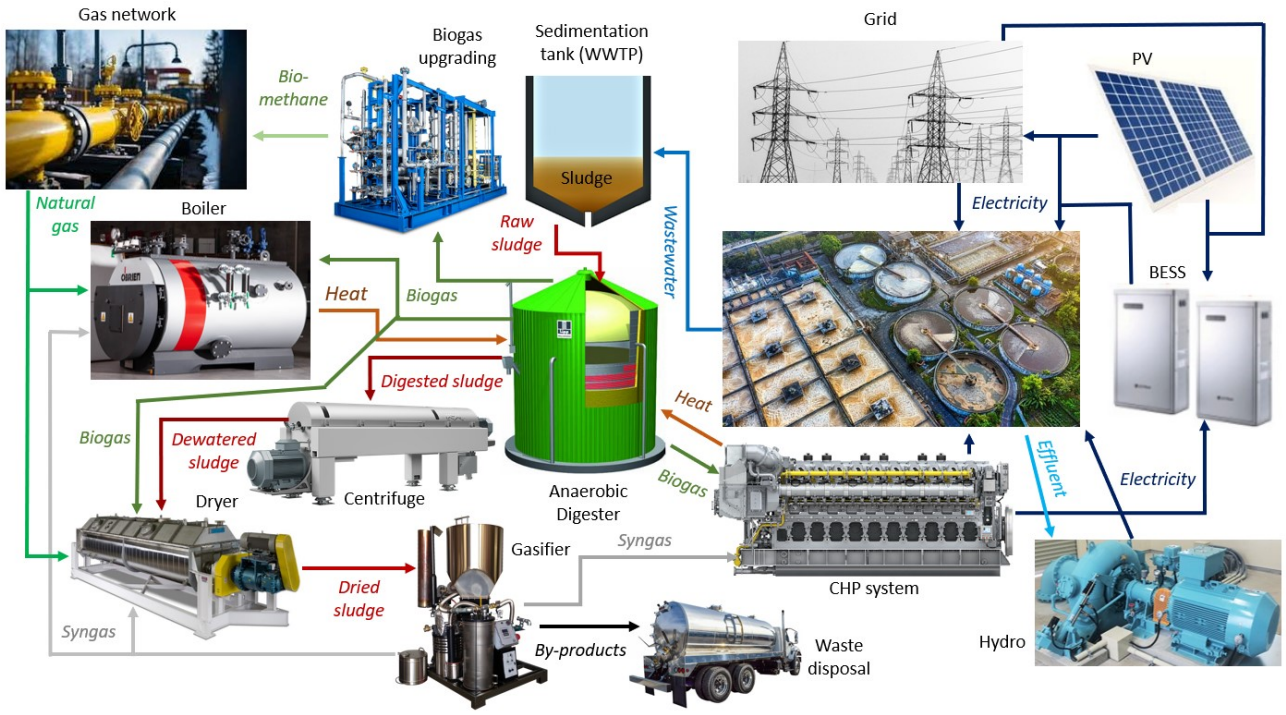

Figure 6.2: Microgrid configuration (Case 2 - Planning model)

Sludge gasification reduces disposal costs while converting sewage sludge into a renewable fuel gas (syngas) [11]. Syngas can be used in the CHP system or boiler. Its calorific value typically ranges from 5 to 10.8 MJ/kg [282]–[284], depending on different factors, including sludge moisture content, sludge composition, reactor type, residence time, oxygen equivalence ratio, and

process temperature [83], [285]. To be used as a feedstock in the gasification process, sewage sludge should achieve appropriate moisture level (around 10% to 20%). Therefore, dewatered sludge is further dried before gasification.

Eq. (6.25) is updated to account for total natural gas imports supplying both the boilers and sludge drying system.

$$V_{gas_{grid}}(t) = V_{gas_{boiler}} + V_{gas_{dryer}} \tag{6.25}$$

Eq. (6.26) expresses the total volume of dry sludge ($V_{ss_{dry}}(t)$) obtained from dewatered sludge for use in the gasification process, where $k_{dew_{dry}}$ is the conversion factor from dewatered sludge to dry sludge. Eqs. (6.27) and (6.28) define the power used in the gasification process ($P_{gasi}(t)$) and total syngas production ($V_{syn}(t)$, respectively. r_{gasi} and $k_{ss_{syn}}$ represent the gasifier electrical consumption rate and conversion factor from sludge to syngas, respectively. The gasifier consumption rate, r_{gasi}, is assumed to be 94 kWh/ton biosolid feed, based on [286], while the conversion factor, $k_{ss_{syn}}$, is considered 0.72 kg syngas/kg dried sludge [281]. Constraint (6.29) limits the maximum power consumption of the gasification system, where $P^{\max}_{gasi_{unit}}$ is the upper limit for a single gasification unit, and n_{gasi} is the number of gasification units.

$$V_{ss_{dry}} = V_{dss_{dew}} \cdot k_{dew_{dry}} \tag{6.26}$$

$$P_{gasi}(t) = V_{ss_{dry}}(t) \cdot r_{gasi} \tag{6.27}$$

$$V_{syn}(t) = V_{ss_{dry}}(t) \cdot k_{ss_{syn}} \tag{6.28}$$

$$0 \leq P_{gasi}(t) \leq P^{\max}_{gasi_{unit}} \cdot n_{gasi} \tag{6.29}$$

Figure 6.3 illustrates the utilisation of biogas, syngas and natural gas for Case 2.

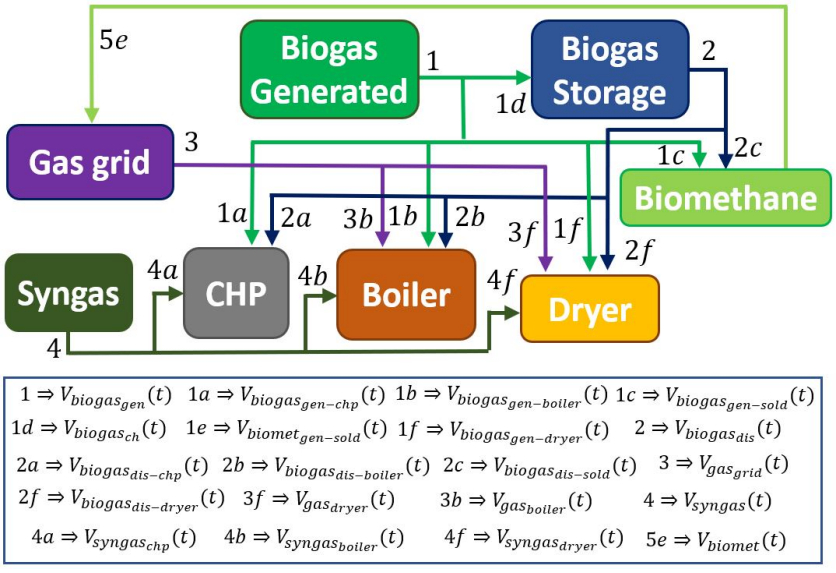

Figure 6.3: Biogas, biomethane and natural gas components (Case 2 - Planning model)

Eqs. (6.30) and (6.31) describe the thermal power generated by the dryer ($Q_{dryer}(t)$) and the thermal energy required to dry the dewatered sludge ($Q_{ss_{dry}}(t)$), respectively. Eq. (6.32) defines

the energy consumed by the sludge drying system ($Q_{dryer}(t)$) as equal to the total thermal power required for drying the sludge. $T_{ev}(t)$, h_{vap} and $\eta_{th_{dryer}}$ represent the water evaporation temperature (100 °C), the latent heat of vaporisation of water, and the thermal efficiency of the dryer, respectively. Constraint (6.33) limits the maximum thermal power consumption of the drying system, where $Q^{\max}_{dryer_{unit}}$ is the upper limit for a single dryer unit, and n_{dryer} is the total number of dryer units.

$$Q_{dryer}(t) = \frac{[V_{gas_{dryer}}(t) \cdot c_{p_{gas}} + V_{biogas_{dryer}}(t) \cdot c_{p_{biogas}} + V_{syn_{dryer}}(t) \cdot c_{p_{syn}}] \cdot \eta_{th_{dryer}} \cdot k_{jw}}{\Delta t} \tag{6.30}$$

$$Q_{ss_{dry}}(t) = \left[V_{ss_{dew}}(t) - V_{ss_{dry}}(t) \right] \cdot \left\{ h_w \cdot [T_{ev}(t) - T_{ad}(t)] + h_{vap} \right\} \cdot k_{jw} \tag{6.31}$$

$$Q_{dryer}(t) = Q_{ss_{dry}}(t) \tag{6.32}$$

$$0 \leq Q_{dryer}(t) \leq Q^{\max}_{dryer_{unit}} \cdot n_{dryer} \tag{6.33}$$

Eq. (6.34) indicates that the syngas volume ($V_{syn}(t)$) can be used in the CHP ($V_{syn_{chp}}(t)$), boiler ($V_{syn_{chp}}(t)$) and dryer ($V_{syn_{dryer}}(t)$).

$$V_{syn}(t) = V_{syn_{chp}}(t) + V_{syn_{boiler}}(t) + V_{syn_{dryer}}(t) \tag{6.34}$$

Eqs. (6.35) and (6.36) are rewritten to account for the portion of biogas used in the drying system, while Eqs. (6.37) and (6.38) are reformulated to consider the syngas allocated to the CHP units and boilers. $V_{biogas_{gen-dryer}}(t)$, $V_{biogas_{dis-dryer}}(t)$ represent the portions of biogas generated and discharged for drying the sewage sludge before it enters the gasifier, respectively, and $V_{biogas_{dryer}}(t)$ is the total biogas consumed in the drying system.

$$\begin{aligned} V_{biogas_{gen}}(t) &= V_{biogas_{gen-chp}}(t) + V_{biogas_{gen-boiler}}(t) \\ &+ V_{biogas_{gen-up}}(t) + V_{biogas_{gen-dryer}}(t) + V_{biogas_{ch}}(t) \end{aligned} \tag{6.35}$$

$$V_{biogas_{dis}}(t) = V_{biogas_{dis-chp}}(t) + V_{biogas_{dis-boiler}}(t) + V_{biogas_{dis-up}}(t) + V_{biogas_{dis-dryer}}(t) \tag{6.36}$$

$$0 \leq V_{biogas_{chp}}(t) + V_{syn_{chp}}(t) \leq V^{\max}_{chp_{unit}} \cdot n_{chp} \tag{6.37}$$

$$0 \leq V_{biogas_{boiler}}(t) + V_{gas_{boiler}}(t) + V_{syn_{boiler}}(t) \leq V^{\max}_{boiler_{unit}} \cdot n_{boiler} \tag{6.38}$$

Eq. (6.39) states the maximum volume of gas that can be used by the drying system.

$$0 \leq V_{biogas_{dryer}}(t) + V_{gas_{dryer}}(t) + V_{syn_{dryer}}(t) \leq V^{\max}_{dryer_{unit}} \cdot n_{dryer} \tag{6.39}$$

Eqs. (6.40), (6.41) and (6.42) are reformulated to consider the syngas produced in the sludge gasification process and its allocation to the CHP units and boilers. $c_{p_{syn}}$ denotes the calorific value of the syngas.

$$P_{chp}(t) = \frac{[V_{biogas_{chp}}(t) \cdot c_{p_{biogas}} + V_{syn_{chp}}(t) \cdot c_{p_{syn}}] \cdot \eta_{e_{chp}} \cdot k_{jw}}{\Delta t} \tag{6.40}$$

$$Q_{chp}(t) = \frac{[V_{biogas_{chp}}(t) \cdot c_{p_{biogas}} + V_{syn_{chp}}(t) \cdot c_{p_{syn}}] \cdot \eta_{th_{chp}} \cdot k_{jw}}{\Delta t} \tag{6.41}$$

$$Q_{boiler}(t) = \frac{[V_{biogas_{boiler}}(t) \cdot c_{p_{biogas}} + V_{gas_{boiler}}(t) \cdot c_{p_{gas}} + V_{syn_{boiler}}(t) \cdot c_{p_{syn}}] \cdot \eta_{th_{boiler}} \cdot k_{jw}}{\Delta t} \tag{6.42}$$

$$0 \leq V_{biogas_{up}}(t) \leq V_{up_{unit}}^{\max} \cdot n_{up} \tag{6.43}$$

Eq. (6.44) is updated to include the power consumed by the gasification process ($P_{gasi}(t)$) in the power balance equation.

$$\begin{aligned} P_{grid}(t) + P_{chp}(t) + P_{pv}(t) + P_{b_{dis}}(t) + P_{hyd}(t) = \\ P_{wwtp}(t) + P_{sold}(t) + P_{b_{ch}}(t) + P_{up}(t) + P_{dew}(t) + P_{gasi}(t) \end{aligned} \tag{6.44}$$

Eq. (6.45) is rewritten to account for the investment costs of the gasification and sludge drying systems in Case 2, where $c_{gasi_{unit}}$ and $c_{dryer_{unit}}$ represent the costs of a single unit of gasification and a single unit of sludge drying, respectively.

$$\begin{aligned} f_{inv} = c_{pv_{unit}} \cdot n_{pv} + c_{chp_{unit}} \cdot n_{chp} + c_{b_{unit}} \cdot n_b + c_{hyd_{unit}} \cdot n_{hyd} + c_{boiler_{unit}} \cdot n_{boiler} \\ + c_{up_{unit}} \cdot n_{up} + c_{storage_{unit}} \cdot n_{storage} + c_{gasi_{unit}} \cdot n_{gasi} + c_{dryer_{unit}} \cdot n_{dryer} \end{aligned} \tag{6.45}$$

Since the gasification and sludge drying systems of sewage sludge are considered in this case, the 1-year OPEX function is reformulated, as defined in (6.46), to incorporate the volume of dried sludge ($V_{dss_{dry}}(t)$) designated for disposal.

$$\begin{aligned} f_{op_{1y}} = \sum_t \Bigg\{ \Bigg[& P_{grid}(t) \cdot \lambda_{dlf} \cdot \big(c_{ele_{imp}}(t) + c_{ele_{use}}(t) + c_{ele_{other}}(t)\big) \\ & + P_{wwtp_{cap}}(t) \cdot c_{ele_{cap}}(t) - P_{sold}(t) \cdot c_{ele_{exp}}(t) \Bigg] \cdot \Delta t \\ + \Bigg[& V_{gas_{grid}}(t) \cdot \big(c_{gas_{imp}}(t) + c_{gas_{use}}(t)\big) \\ & - V_{biomet}(t) \cdot c_{gas_{exp}}(t) + V_{dss_{dry}}(t) \cdot c_{ss_{disp}} \Bigg] \Bigg\} \end{aligned} \tag{6.46}$$

Table 6.4 summarises the results of the planning model, including the microgrid configuration, payback period, and CAPEX for Case 2. The microgrid comprises a boiler with a capacity of 1.6 MW, a CHP unit of 1.78 MWe, a gasifier of 280 kW, and a sludge dryer of 4.07 MW. The biogas storage and upgrading capacities are 100 m^3 and 170 $m^3\,h^{-1}$, respectively, whereas PV,

micro-hydro, and BESS systems were not included in this configuration. The total CAPEX is estimated at $17.24 million, with a projected payback period of 5.7 years

Table 6.4: Proposed microgrid configuration - Case 2 (Planning model)

Boiler (kW)	**CHP (kWe)**	**Gasifier (kW)**	**Dryer (kW)**	**Biogas storage (m^3)**	**Biogas upgrade ($m^3\,h^{-1}$)**	**CAPEX ($ M)**	**Payback period (y)**
1,610	1,780	280	4,070	100	170	17.24	5.7

Table 6.5 illustrates the results for the WWTP 1-year operation, including the biogas generation and utilisation, natural gas importation, microgrid generation, power imported and exported to the grid, and 1-year OPEX. Over the 1-year operation, the WWTP produced approximately 11.75 million m^3 of biogas, of which 37% was used in the CHP, 9% in the boiler, 49% in the dryer, and 5% was upgraded to biomethane. Syngas production reached 8.65 million m^3, with 58% used in the CHP, 8% in the boiler, and 33% in the dryer. Natural gas importation accounted for less than 1% of total gas use. The CHP and boiler supplied 15.61 GWh and 7.58 GWh of thermal energy, respectively, to meet the WWTP's thermal needs for the anaerobic digester, which required approximately 22.75 GWh, while the dryer generated 27.14 GWh for the sludge drying process. The WWTP consumed 26.80 GWh of electricity, with 49% generated by the CHP and 51% imported from the grid; no electricity was exported. The 1-year OPEX accounted for $3.44 million, with gas costs offsetting approximately $31,530, indicating a minimal revenue generation from biomethane sales. Compared to Case 1, sludge disposal costs dropped significantly from $4 million to $1.1 million due to the implementation of sludge dryers, while electricity costs increased to $2.37 million.

Table 6.5: Result summary for 1-year operation - Case 2 (Planning model)

Biogas production (m^3)	11,746,008
Biogas used in the CHP (m^3)	4,379,985
Biogas used in the boiler (m^3)	986,981
Biogas used in the dryer (m^3)	5,778,304
Biogas upgraded to biomethane (m^3)	600,738
Biomethane sold (m^3)	411,032
Biogas stored (m^3)	13,700
Biogas discharged (m^3)	13,700
Total syngas production (m^3)	8,649,966
Syngas used in the CHP (m^3)	5,043,757
Syngas used in the boiler (m^3)	733,477
Syngas used in the dryer (m^3)	2,872,732
Natural gas imported (m^3)	90,533
CHP thermal generation (kWh)	15,611,380
Boiler thermal generation (kWh)	7,584,524
Thermal energy required in the AD (kWh)	22,750,097
Dryer thermal generation (kWh)	27,141,284
WWTP consumption (kWh)	26,801,045
CHP electricity generation (kWh)	13,146,426
Electricity imported from the grid (kWh)	16,591,284
Electricity exported to the grid (kWh)	0

Sludge dewatering consumption (kWh)	882,650
Biogas upgrading system consumption (kWh)	210,258
Gasifier consumption (kWh)	1,843,757
Electricity costs ($)	2,367,301
Gas costs ($)	-31,530
Sludge disposal costs ($)	1,103,312
1-year OPEX ($)	3,439,083

c. Case 3

This Case 3 considers water electrolysis and fuel cells as part of the microgrid system. In addition, the co-digestion is adopted, with assumptions consistent with those defined in Sections 4.4.2 and 5.4.2.

Figure 6.4 illustrates the schematic diagram of the microgrid system.

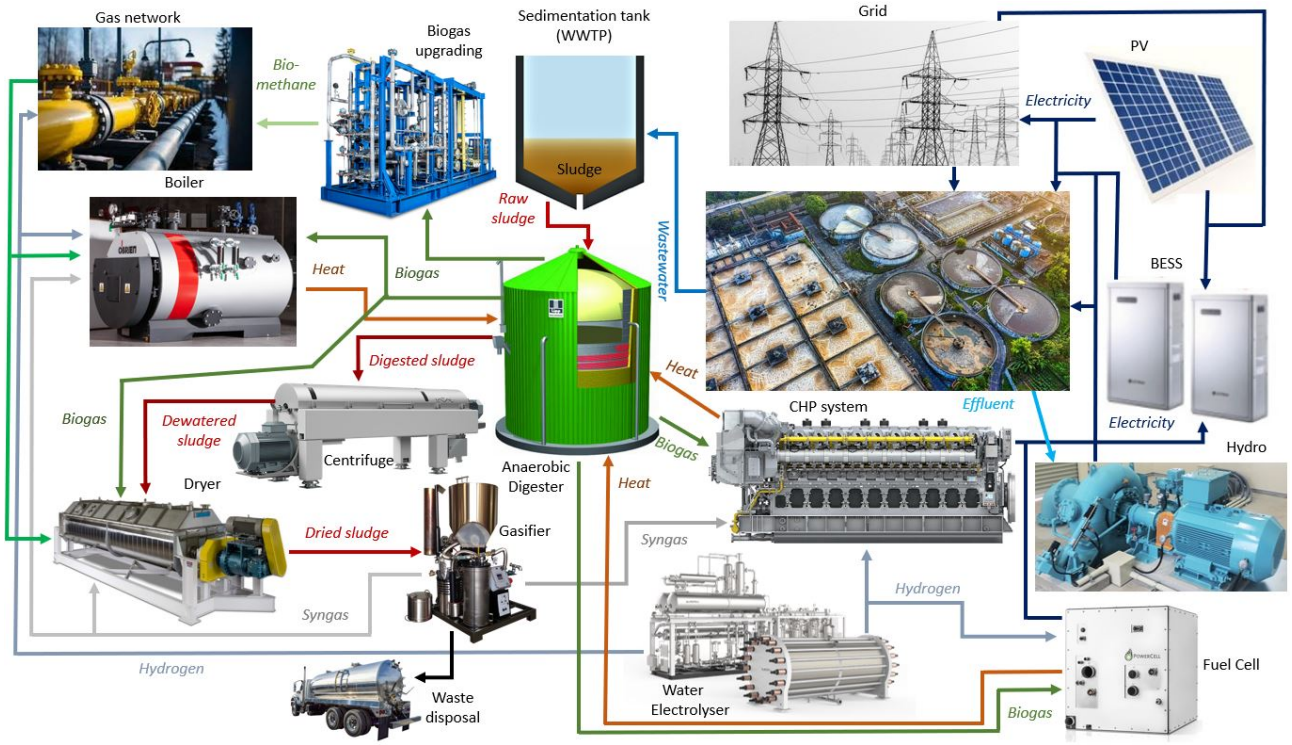

Figure 6.4: Microgrid configuration (Case 3 - Planning model)

Eqs. (6.47) and (6.48) express the hydrogen volume generated by the water electrolyser system ($V_{h2}(t)$) and its allocation components, respectively. Constraint (6.49) limits the maximum hydrogen production of the water electrolyser system. $V_{h2o}(t)$ and $k_{h2o_{h2}}$ represent the water volume consumed by the electrolysers and the conversion factor from water to hydrogen, respectively. $V_{h2_{chp}}(t)$, $V_{h2_{boiler}}(t)$, $V_{h2_{fc}}(t)$, $V_{h2_{dryer}}(t)$ and $V_{h2_{sold}}(t)$ correspond to hydrogen components used in the CHP, boilers, fuel cells, drying system and sold to the gas grid, respectively. $V_{h2_{unit}}^{\max}$ and n_{we} denote the maximum output of a single electrolyser unit and the total number of water electrolyser units, respectively. Eq. (6.50) defines the upper limit of water that can be supplied to the the water electrolysis system ($V_{h2o}^{\max}$).

$$V_{h2}(t) = V_{h2o}(t) \cdot k_{h2o_{h2}} \tag{6.47}$$

$$V_{h2}(t) = V_{h2_{chp}}(t) + V_{h2_{boiler}}(t) + V_{h2_{sold}}(t) + V_{h2_{fc}}(t) + V_{h2_{dryer}}(t) \tag{6.48}$$

$$0 \leq V_{h2}(t) \leq V_{h2_{unit}}^{\max} \cdot n_{we} \tag{6.49}$$

$$0 \leq V_{h2o}(t) \leq V_{h2o}^{\max} \tag{6.50}$$

In Case 3, it is assumed that the converted biomethane can either be exported to the gas grid ($V_{biomet_{sold}}(t)$) or used in the fuel cell system ($V_{biomet_{fc}}(t)$), as defined in (6.51) and illustrated in Figure 6.5.

$$V_{biomet}(t) = V_{biomet_{sold}}(t) + V_{biomet_{fc}}(t) \tag{6.51}$$

Figure 6.5 illustrates the gas utilisation considered in Case 3.

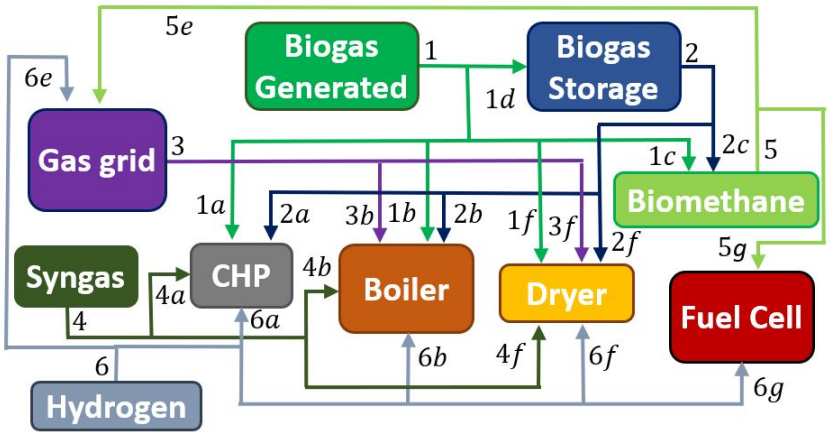

Figure 6.5: Biogas, biomethane, hydrogen and natural gas components (Case 3 - Planning model)

Eq. (6.52) defines the electrical power ($P_{we}(t)$) consumed by the water electrolyser system, while Constraint (6.53) limits its maximum power. r_{we} is the power consumption rate of electrolyser, $P_{we_{unit}}^{\max}$ is the maximum power consumption of a single electrolyser, and n_{we} denotes the total number of water electrolysis units.

$$P_{we}(t) = V_{h2o}(t) \cdot r_{we}(t) \tag{6.52}$$

$$0 \leq P_{we}(t) \leq P_{we_{unit}}^{\max} \cdot n_{we} \tag{6.53}$$

Eqs. (6.54) and (6.55) define the thermal ($Q_{fc}(t)$) and electrical ($P_{fc}(t)$) power generated by the fuel cell system. Constraints (6.56) and (6.57) limit the maximum thermal and electrical

power output from the fuel cell system, respectively. $Q^{\max}_{fc_{unit}}$ and $P^{\max}_{fc_{unit}}$ maximum thermal and electrical power outputs of a single fuel cell unit, and n_{fc} is the number of fuel cells units. $\eta_{th_{fc}}$ and $\eta_{e_{fc}}$ denote the thermal and electrical efficiencies of the fuel cell, while $c_{p_{biomet}}$ and $c_{p_{h2}}$ represent the calorific values for biomethane and hydrogen, respectively.

$$Q_{fc}(t) = \frac{[V_{h2_{fc}}(t) \cdot c_{p_{h2}} + V_{biomet_{fc}}(t) \cdot c_{p_{biomet}}] \cdot \eta_{th_{fc}} \cdot k_{jw}}{\Delta t} \tag{6.54}$$

$$P_{fc}(t) = \frac{[V_{h2_{fc}}(t) \cdot c_{p_{h2}} + V_{biomet_{fc}}(t) \cdot c_{p_{biomet}}] \cdot \eta_{e_{fc}} \cdot k_{jw}}{\Delta t} \tag{6.55}$$

$$0 \leq Q_{fc}(t) \leq Q^{\max}_{fc_{unit}} \cdot n_{fc} \tag{6.56}$$

$$0 \leq P_{fc}(t) \leq P^{\max}_{fc_{unit}} \cdot n_{fc} \tag{6.57}$$

Eqs. (6.58) and (6.59) represent the hydrogen constraints. x_{h2} defines the maximum percentage of hydrogen allowed to be blended with biomethane for injection into the gas network. According to AEMO, hydrogen injection into the existing gas network is limited to a maximum of 10% when blended with biomethane or natural gas.

$$V_{h2_{sold}}(t) \leq V_{biomet_{sold}}(t) \cdot x_{h2}(t) \tag{6.58}$$

$$0 \leq V_{h2_{sold}}(t) \leq V^{\max}_{h2_{sold}} \cdot [1 - u_{gas}(t)] \tag{6.59}$$

Eqs. (6.60 - 6.65) are updated to consider the hydrogen component. $V_{h2_{chp}}(t)$, $V_{h2_{boiler}}(t)$ and denote the volumes of hydrogen used in the CHP and boilers, respectively, while $c_{p_{h2}}$ represents the calorific value of hydrogen.

$$0 \leq V_{biogas_{chp}}(t) + V_{syn_{chp}}(t) + V_{h2_{chp}}(t) \leq V^{\max}_{chp_{unit}} \cdot n_{chp}(t) \tag{6.60}$$

$$0 \leq V_{gas_{boiler}}(t) + V_{biogas_{boiler}}(t) + V_{syn_{boiler}}(t) + V_{h2_{boiler}}(t) \leq V^{\max}_{boiler_{unit}} \cdot n_{boiler}(t) \tag{6.61}$$

$$0 \leq V_{h2_{sold}}(t) + V_{biomet_{sold}}(t) \leq V^{\max}_{gas_{inj}} \cdot [1 - u_{gas}(t)] \tag{6.62}$$

$$P_{chp}(t) = \left[V_{biogas_{chp}}(t) \cdot c_{p_{biogas}} + V_{syn_{chp}}(t) \cdot c_{p_{syn}} + V_{h2_{chp}}(t) \cdot c_{p_{h2}} \right] \cdot \eta_{e_{chp}} \cdot k_{jw} \tag{6.63}$$

$$Q_{chp}(t) = \left[V_{biogas_{chp}}(t) \cdot c_{p_{biogas}} + V_{syn_{chp}}(t) \cdot c_{p_{syn}} + V_{h2_{chp}}(t) \cdot c_{p_{h2}} \right] \cdot \eta_{th_{chp}} \cdot k_{jw} \tag{6.64}$$

$$Q_{boiler}(t) = \Big[V_{gas_{boiler}}(t) \cdot c_{p_{gas}} + V_{biogas_{boiler}}(t) \cdot c_{p_{biogas}} + V_{syn_{boiler}}(t) \cdot c_{p_{syn}} + V_{h2_{boiler}}(t) \cdot c_{p_{h2}} \Big] \cdot \eta_{th_{boiler}} \cdot k_{jw} \tag{6.65}$$

Eq. (6.66) is updated to include the hydrogen component for the drying system.

$$Q_{dryer}(t) = \Big[V_{gas_{dryer}}(t) \cdot c_{p_{gas}} + V_{biogas_{dryer}}(t) \cdot c_{p_{biogas}} + V_{syn_{dryer}}(t) \cdot c_{p_{syn}} + V_{h2_{dryer}}(t) \cdot c_{p_{h2}} \Big] \cdot \eta_{th_{dryer}} \cdot k_{jw} \tag{6.66}$$

Eq. (6.67) is revised to account for the total natural gas import, which can supply both the boilers and the sludge drying system.

$$V_{gas_{grid}}(t) = V_{gas_{boiler}}(t) + V_{gas_{dryer}}(t) \tag{6.67}$$

Eq. (6.68) incorporates the power generated by the fuel cell system ($P_{fc}(t)$) and the power consumed by the water electrolyser units ($P_{we}(t)$). Eq. (6.69) is updated to include the thermal energy contribution of the fuel cell system.

$$\begin{aligned} P_{grid}(t) + P_{chp}(t) + P_{pv}(t) + P_{b_{dis}}(t) + P_{hyd}(t) + P_{fc}(t) = \\ P_{wwtp}(t) + P_{sold}(t) + P_{b_{ch}}(t) + P_{up}(t) + P_{dew}(t) + P_{gasi}(t) + P_{we}(t) \end{aligned} \tag{6.68}$$

$$Q_{ad}(t) \leq Q_{chp}(t) + Q_{boiler}(t) + Q_{fc}(t) \tag{6.69}$$

Eq. (6.70) is rewritten to consider the investment costs of the water electrolysis and fuel cell systems in the model, where $c_{we_{unit}}$ and $c_{fc_{unit}}$ denote the costs of individual water electrolysis and fuel cell units, respectively.

$$\begin{aligned} f_{inv} = c_{pv_{unit}} \cdot n_{pv} + c_{chp_{unit}} \cdot n_{chp} + c_{b_{unit}} \cdot n_b + c_{hyd_{unit}} \cdot n_{hyd} + \\ c_{boiler_{unit}} \cdot n_{boiler} + c_{storage_{unit}} \cdot n_{storage} + c_{up_{unit}} \cdot n_{up} + \\ c_{gasi_{unit}} \cdot n_{gasi} + c_{dryer_{unit}} \cdot n_{dryer} + c_{fc_{unit}} \cdot n_{fc} + c_{we_{unit}} \cdot n_{we} \end{aligned} \tag{6.70}$$

The 1-year OPEX function is updated as defined in (6.71).

$$
\begin{aligned}
f_{op_{1y}} = \sum_t \Bigg\{ \Bigg[& P_{grid}(t) \cdot \lambda_{dlf} \cdot \left(c_{ele_{imp}}(t) + c_{ele_{use}}(t) + c_{ele_{other}}(t) \right) \\
& + P_{wwtp_{cap}}(t) \cdot c_{ele_{cap}}(t) - P_{sold}(t) \cdot c_{ele_{exp}}(t) \Bigg] \cdot \Delta t \\
& + \Bigg[V_{gas_{grid}}(t) \cdot \left(c_{gas_{imp}}(t) + c_{gas_{use}}(t) \right) - \\
& [V_{biomet_{sold}}(t) + V_{h2_{sold}}(t)] \cdot c_{gas_{exp}}(t) \\
& + V_{dss_{dry}}(t) \cdot c_{ss_{disp}} + V_{fog}(t) \cdot c_{fog} \Bigg] \Bigg\}
\end{aligned}
\tag{6.71}
$$

Table 6.6 summarises the proposed microgrid configuration for Case 3 in the planning model. The system includes a CHP unit with a capacity of 3.28 MWe, a gasifier of 300 kW, and a sludge dryer of 4.28 MW. The biogas storage and upgrading capacities are 200 m^3 and 320 $m^3\,h^{-1}$, respectively. This configuration has the highest CAPEX among all scenarios, approximately $19.6 million, with a projected payback period of 6 years.

Table 6.6: Proposed microgrid configuration - Case 3 (Planning model)

CHP (kWe)	**Gasifier (kW)**	**Dryer (kW)**	**Biogas storage** (m^3)	**Biogas upgrade** ($m^3\,h^{-1}$)	**CAPEX ($ M)**	**Payback period (y)**
3,280	300	4,280	200	320	19.57	6

Table 6.7 summarises the 1-year operation results for Case 3. The WWTP produced approximately 17.95 million m^3 of biogas, of which 57% was used in the CHP, 33% in the dryer, and 10% upgraded to biomethane. Syngas production reached 9.08 million m^3, with 58% used in the CHP and 42% in the dryer. For this configuration, no boiler was selected; therefore, the CHP system was responsible for supplying all the thermal energy required by the WWTP (23.6 GWh required for the anaerobic digestion process), providing a total of 30.3 GWh. The WWTP consumed 26.8 GWh of electricity, while the biogas upgrading system, sludge dewatering and gasifiers consumed about 3.52 GWh, which 95% was supplied by the CHP and 5% imported from the grid. Negligible electricity was exported. The 1-year OPEX totaled $3.17 million, with gas costs offsetting nearly $624,000 reflecting revenue from biomethane sales and additional co-digestion costs of $1.77 million.

Table 6.7: Result summary for 1-year operation - Case 3 (Planning model)

Biogas production (m^3)	17,947,941
Biogas used in the CHP (m^3)	10,223,240
Biogas used in the dryer (m^3)	5,851,497
Biogas upgraded to biomethane (m^3)	1,873,204
Biomethane sold (m^3)	1,281,666
Biogas stored (m^3)	184,566
Biogas discharged (m^3)	184,566
Total syngas production (m^3)	9,082,464
Syngas used in the CHP (m^3)	5,307,208

Syngas used in the dryer (m^3)	3,775,257
Natural gas imported (m^3)	2,166
CHP thermal generation (kWh)	30,295,673
Thermal energy required in the AD (kWh)	23,720,267
Dryer thermal generation (kWh)	28,498,348
WWTP electricity consumption (kWh)	26,801,045
CHP electricity generation (kWh)	25,512,146
Electricity imported from the grid (kWh)	4,807,841
Electricity exported to the grid (kWh)	594
Biogas upgrading system consumption (kWh)	655,622
Gasifier consumption (kWh)	1,935,945
Sludge dewatering consumption (kWh)	926,782
Electricity costs ($)	865,706
Gas costs ($)	-624,344
Sludge disposal costs ($)	1,158,478
Co-digestion costs ($)	1,765,299
1-year OPEX ($)	3,165,138

6.5.3 Discussions

In this section, the results of the case studies are analysed to assess the performance of the proposed planning model under various technological configurations and resource integration strategies. The comparative analysis across these scenarios focused on the 3 main components: investment cost, operational costs and payback period to decide which mix generation technologies are more suitable for each scenario. These results underscore the importance of evaluating diverse configurations to fully understand the model's capabilities and to identify the most effective strategies for optimising energy and resource use in WWTPs.

In Case 1, the optimal configuration of the microgrid system for the WWTP included a 230 kW boiler, 2.95 MWe CHP, 40 kW BESS, 800 m^3 storage system and a biogas upgrading system capable of converting up to 190 $m^3\,h^{-1}$ per hour, with a total system CAPEX of $9.52 million. For this proposed system, the microgrid payback period was calculated to be 5.4 years, and the 1-year OPEX was $4.68 million. As shown in Table 6.2, the proposed system prioritises the CHP technology over other generating technologies, likely due to its ability to generate both electricity and thermal energy required by the plant. PV and micro-hydro systems were not selected in this Case 1 configuration. Regarding operational expenses, sludge disposal had a significant impact on the 1-year OPEX, accounting for $4 million. In Case 2, the optimal configuration of the microgrid system comprised a 1.6 MW boiler system, 1.78 MWe CHP system, 280 kW gasifier, a 4.1 MW drying system, 100 m^3 storage unit and a biogas upgrading system capable of converting up to 170 $m^3\,h^{-1}$ per hour. The CAPEX was $17.24 million, and the 1-year OPEX was approximately $3.44 million. The payback period of the entire system was 5.7 years. Compared with Case 1, the CAPEX cost increased by around 80%, but the annual OPEX was reduced by almost $1.25 million. The increase in CAPEX was primarily driven by investments in gasification and drying systems, aimed at reducing sludge management costs, which account for approximately $1.1 million of the OPEX, as seen in Table 6.5. The gasification and sludge drying systems consumed about 1.84 GWh and 27 GWh annually and generated approximately 8.6 million m^3 of syngas, which was utilised on-site. In Case 3, the

optimal configuration of the microgrid system was comprised of a 3.28 MWe CHP, 300 kW gasifier, 4.28 MW drying system, 200 m^3 storage unit and a biogas upgrading system capable of converting up to 320 $m^3\,h^{-1}$ of biomethane. The system's CAPEX was \$19.57 million, and the OPEX costs over the one year was approximately \$3.17 million, giving a payback period of the microgrid system of 6 years. Compared to Cases 1 and 2, Case 3 has the highest CAPEX among the microgrid configurations, but also the lowest OPEX. Although co-digestion increased the biogas production by around 53%, it had a high OPEX of nearly \$1.76 million.

The case studies result show that the optimisation engine mainly prioritised the CHP system for power and thermal generation for the microgrid system, despite the availability of other technologies in the model, such as PV, BESS, biogas upgrading system, water electrolysers, and fuel cells. This outcome is likely influenced by the ability that the CHP has to simultaneously generate both electricity and thermal energy to meet the WWTP's demand and use the free biogas available on-site. However, to ensure a comprehensive evaluation and identify potential future opportunities, it is essential to conduct sensitivity analysis on the CAPEX of each technology. Accurate CAPEX data is notoriously difficult to obtain due to a range of market variables, including technology brand, original equipment manufacturer (OEM), system size, and regional pricing differences. Therefore, adopting a range of CAPEX values in the analysis is a practical and robust approach to capture market uncertainty and provide a more nuanced understanding of each technology's economic viability within the microgrid context.

6.5.4 Sensitivity Analysis

Conducting a sensitivity analysis is essential in economic evaluation, as it helps assess how changes in key input parameters can impact the overall results and outcomes of the proposed model. In the context of complex systems such as microgrid planning, where multiple technologies and uncertain market conditions are involved, sensitivity analysis provides critical insights into the robustness of the chosen configuration. It allows decision-makers to identify which variables have the greatest influence on outcomes, evaluate risks, and test the resilience of the economic case under different scenarios. This is particularly important when data uncertainty is high, such as with unit cost estimation, which often vary widely depending on technology maturity, supplier, location, and project scale. By exploring a range of input values, sensitivity analysis enables a more informed and confident decision-making process, reducing the risk of costly errors and highlighting potential opportunities for future investment or optimisation.

In this section, sensitivity analysis is conducted on three key parameters: (a) unit costs for each generating technology, and (b) weighting factors (a_1, a_2 and a_3) applied to the single-objective function presented in (6.21). These parameters can directly influence the CAPEX, OPEX and the payback period of the proposed system, and most likely the final results. To conduct a comprehensive yet manageable sensitivity analysis, different scenarios are considered and evaluated to determine which component has the greatest impact on the outcome. To simplify, the sensitivity analysis is conducted for 2 case studies only, Case 1 and Case 3.

a. Impact of unit cost

In this section, the unit costs of the generation technologies in the microgrid system are varied to evaluate their impact on the overall outcomes.

Table 6.8 presents a range of unit costs for the technologies used in this study, based on market prices, including CSIRO GenCost 2024-25 report [287], and the costs of biogas upgrading system

was based on [288].

Table 6.8: Unit cost ranges for different technologies

Boiler ($/kW)	CHP ($/kWe)	PV ($/kW)	BESS ($/kW)	Hydro ($/kW)	Gasifier ($/kW)	Dryer ($/kW)	Electro-lyser ($/kW)	Fuel cell ($/kW)	Biogas upgrade ($/m^3/h)	Biogas storage ($/m^3)
1,200 ∼ 2,500	2,000 ∼ 3,500	850 ∼ 1,250	300 ∼ 800	3,500 ∼ 6,500	4,500 ∼ 7,500	1,200 ∼ 2,400	2,250 ∼ 4,750	4,000 ∼ 7,000	1,800 ∼ 4,500	150 ∼ 350

The weighting factors and the disposal cost of sludge were kept consistent with the previous values: a_1= 0.6, a_2= 0.2 and a_3= 0.2, and \$75/m^3 of sludge, respectively.

- Case 1

A sensitivity analysis was carried out, and the results were examined. In Case 1, the microgrid system can include the following components: CHP, boilers, PV, BESS, micro-hydro, biogas upgrading system, and biogas storage. Table 6.9 presents the microgrid configurations based on different unit costs for the generating technologies. Note that the costs for the CHP is given in \$/kWe and capacity in kWe, boiler, micro-hydro, PV and BESS system units are given in \$/kW and the system sizes in kW, while the unit costs of the biogas upgrading system is given in \$/m^3 h^{-1} and the size in m^3 h^{-1}, and biogas storage is in \$/m^3 and the size in m^3. Table 6.10 illustrates the associated values of total CAPEX, 1-year OPEX costs, and payback period for each scenario outlined in Table 6.9.

As shown Table 6.9, the CHP was proposed as the main generating source across all scenarios, with an average capacity of approximately 2.9 MWe. Boiler capacity varied between 260 kW and 300 kW, while the maximum size of the micro-hydro system was set at 70 kW. The biogas upgrading system was estimated to treat between 190 and 210 m^3 h^{-1}, and the biogas storage capacity ranged from 500 m^3 and 900 m^3 size. The PV and BESS systems contributed modestly, with capacities of up to 20 kW and 80 kW, respectively.

Table 6.9: Microgrid configuration - Case 1 scenarios (1a-1d)

	Boiler		CHP		Hydro		PV		BESS		Storage		Upgrade	
	Cost	Size	Cost	Size	Cost	Size	Cost	Size	Cost	Size	Cost	Size	Cost	Size
Unit	\$/kW	kW	\$/kWe	kWe	\$/kW	kW	\$/kW	kW	\$/kW	kW	\$/m^3	m^3	\$/m^3 h^{-1}	m^3 h^{-1}
1a	1,200	300	2,000	2,910	3,000	70	850	20	300	30	150	900	1,800	190
1b	1,525	260	2,375	2,920	3,875	0	950	0	425	0	200	500	2,475	210
1c	2,175	280	3,125	2,910	5,625		1,150	20	675	80	300	700	3,825	200
1d	2,500	260	3,500	2,920	6,500		1,250	0	800	0	350	500	4,500	210

Additionally, the microgrid CAPEX for scenarios 1a-1d ranged from \$6.9 million to \$12 million, with payback periods ranging from 3.7 years under the lowest unit cost assumptions to 6.8 years based on the highest. The annual OPEX remained stable across all scenarios (around \$4.6-\$4.7 million), as shown in Table 6.10.

Table 6.10: CAPEX, 1-year OPEX and payback period - Case 1 scenarios (1a-1d)

	1a	**1b**	**1c**	**1d**
Total CAPEX (\$ M)	6.89	7.95	10.75	11.99

1-year OPEX ($ M)	4.60	4.69	4.68	4.69
Payback period (y)	3.7	4.5	6.1	6.8

- Case 3

In Case 3, the microgrid system can include the technologies presented in Case 1, and also the following components: fuel cell, water electrolysis, gasifier and sludge drying system. The gasifier and drying systems are electrical and thermal loads, respectively, used in the WWTP, aiming to reduce the operating costs associated with sludge disposal.

Tables 6.11 and 6.12 present the unit costs for each technology and the results of the microgrid configurations based on different unit costs for the generation technologies, respectively. Similarly to Case 1, the CHP was proposed as the main generating source for all Case 3 scenarios (3a-3d), with a capacity of 3.27 MWe, as illustrated in Table 6.12. The gasifier and dryers were also fixed at 300 kW and 4.28 MW, respectively, while the maximum size of the micro-hydro system was set at 80 kW. The biogas upgrading system was estimated to treat up to 260 $m^3\,h^{-1}$, and the biogas storage capacity was set at 300 m^3. PV and BESS systems were not selected in this configuration, and the boiler capacity was minimal (10 kW).

Table 6.11: Unit costs of each tecnology - Case 3 scenarios (3a-3d)

	CHP	Boiler	Hydro	PV	BESS	Gasifier	Dryer	Electrolyser	Fuel cell	Storage	Upgrade
Unit	$/kWe	$/kW								$/$m^3$	$/$m^3\,h^{-1}$
3a	2,000	1,200	3,000	850	300	4,500	1,200	2,250	4,000	150	1,800
3b	2,375	1,525	3,875	950	425	5,250	1,500	2,875	4,750	200	2,475
3c	3,125	2,175	5,625	1,150	675	6,750	2,100	4,125	6,250	300	3,825
3d	3,500	2,500	6,500	1,250	800	7,500	2,400	4,750	7,000	350	4,500

Table 6.12: Microgrid configuration - Case 3 scenarios (3a-3d)

	CHP	Boiler	Hydro	PV	BESS	Gasifier	Dryer	Electrolyser	Fuel cell	Storage	Upgrade
Unit	kWe	kW								m^3	$m^3\,h^{-1}$
3a	3,270	10	80	0	0	300	4,280	0	0	300	260
3b											
3c			0								
3d											

As shown in Table 6.13, the microgrid CAPEX for scenarios 3a-3d ranged from $13.8 million to $25.3 million. The payback period varied accordingly, from 4.1 years in Scenario 3a (lowest unit cost assumption) to 7.7 years in Scenario 3d (highest unit cosst assumption). The OPEX remained almost constant across all scenarios, ranging between $3.1-$3.2 million per year.

Table 6.13: CAPEX, 1-year OPEX and payback period - Case 3 scenarios (3a-3d)

	3a	**3b**	**3c**	**3d**
Total CAPEX ($ M)	13.79	16.48	22.34	25.27
1-year OPEX ($ M)	3.09	3.17		
Payback period (y)	4.1	5.0	6.8	7.7

b. Impact of weighting factors

In this section, the weighting factors a_1, a_2 and a_3 applied into the single-objective function are varied to assess their influence on the CAPEX, OPEX and payback period of the proposed microgrid configuration. Four different sets of weighting factors, referred to as (*"sub-scenarios"*), were considered, including the baseline case (i):

(i) a_1=0.6, a_2=0.2, a_3=0.2;
(ii) a_1=0.3, a_2=0.3, a_3=0.4;
(iii) a_1=0.4, a_2=0.5, a_3=0.1; and
(iv) a_1=0.3, a_2=0.1, a_3=0.6;

The unit costs for the generation technologies were selected to be within the range of values presented in Table 6.8, and the costs of sludge management was assumed to be \$75/m^3 sludge.

- Case 1

Table 6.14 presents the microgrid configurations based on the different sets of weighting factors.

Table 6.14: Case 1 scenarios (1-1d) - Different weighting factors

		Boiler		CHP		Hydro		PV		BESS		Storage		Upgrade	
		Cost	Size	Cost	Size	Cost	Size	Cost	Size	Cost	Size	Cost	Size	Cost	Size
Unit		\$/kW	kW	\$/kWe	kWe	\$/kW	kW	\$/kW	kW	\$/kW	kW	\$/m^3	m^3	\$/m^3 h^{-1}	m^3 h^{-1}
1	**i**	1,800	230	2,800	2,950	3,800	0	1,000	0	500	40	200	800	3,500	190
	ii		470		2,740		110		4,850		1,500		100		290
	iii		700		3,210		110		5,000		1,080		700		540
	iv		320		2,870		0		10		10		500		220
1a	**i**	1,200	300	2,000	2,910	3,000	70	850	20	300	30	150	900	1,800	190
	ii		660		2,580		110		5,000		2,450		700		380
	iii		740		2,540		120		4,990		2,780		400		320
	iv		310		3,010		80		0		0		300		210
1b	**i**	1,525	260	2,375	2,920	3,875	0	950	0	425	0	200	500	2,475	210
	ii		550		2,770		100		5,000		1,650		800		240
	iii		580		2,650		110				2,220		700		340
	iv		260		2,920		0		0		0		500		210
1c	**i**	2,175	280	3,125	2,910	5,625	0	1,150	20	675	80	300	700	3,825	200
	ii		560		2,800		100		3,050		840		100		260
	iii		400						5,000		1,270		400		250
	iv		260		2,920		0		0		0		500		210
1d	**i**	2,500	260	3,500	2,920	6,500	0	1,250	0	800	0	350	500	4,500	210
	ii		340		2,860		90		1,480		0		700		210
	iii		360		2,840		100		4,100		690				270
	iv		430		2,780		0		0		0		100		280

As illustrated in Table 6.14 and Figure 6.6, the results for Case 1 scenarios (1 - 1d) under different weighting factors, a_1, a_2, a_3, reveal notable variations in technology deployment and associated costs.

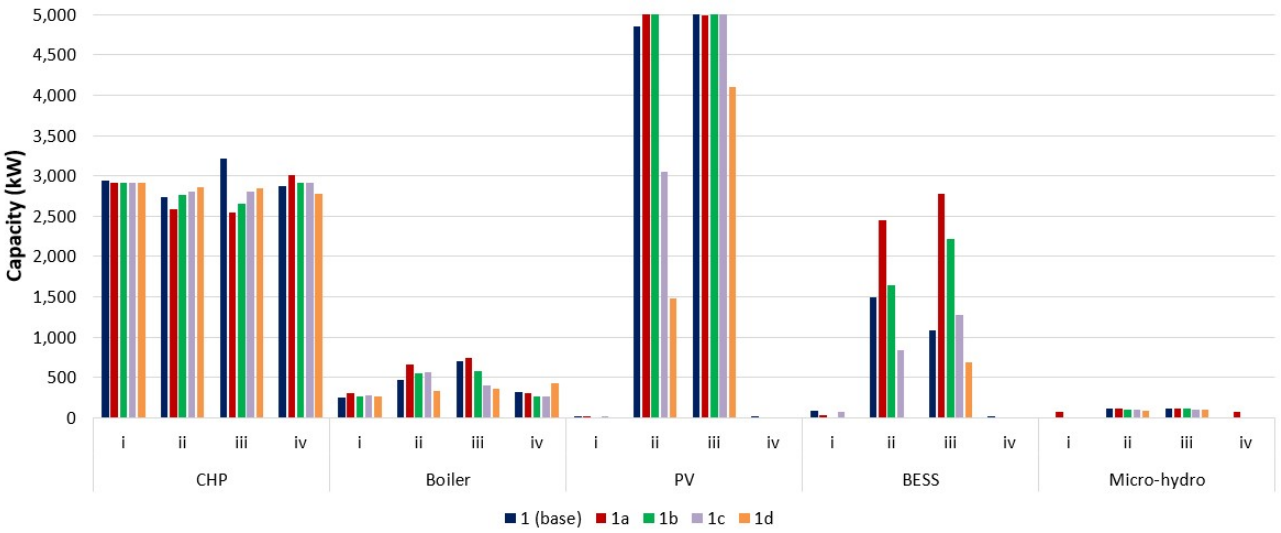

Figure 6.6: Microgrid capacity for different unit costs and weighting factors (Case 1 scenarios)

Across all scenarios, CHP was used in all cases, with installed capacities ranging from approximately 2.54 MWe to 3.2 MWe, while boiler sizes varied from 260 kW and 740 kW. The micro-hydro system, despite having a high unit cost of $6,500/kW in scenario 1d, reached a capacity of up to 100 kW. PV and BESS systems were also deployed, particularly in sub-scenarios ii and iii, with PV and BESS capacities ranging up to 5 MW and 2.78 MW, respectively. In sub-scenario iv across all scenarios (1 to 1d), PV, micro-hydro and BESS were generally absent (except in scenario 1, where PV capacity was minimal, and in scenario 1a, which included a 80 kW micro-hydro system). In addition, biogas storage capacities ranged between 100 m^3 and 800 m^3, while upgrading systems were sized between 210 $m^3\,h^{-1}$ and 540 $m^3\,h^{-1}$. Overall, the results presented in the Table 6.14 and illustrated in Figure 6.6 show that, depending on the unit costs and weighting factors considered, the microgrid configuration capacity, particularly the PV, BESS and biogas upgrading technologies, can vary significantly.

Table 6.15 summarises the total CAPEX, 1-year OPEX and payback period for the Case 1 scenarios under different weighting factors.

Table 6.15: CAPEX, 1-year OPEX and payback period (Scenarios 1–1d and Sub-scenarios i-iv)

	1				**1a**				**1b**				**1c**				**1d**			
	i	**ii**	**iii**	**iv**	**i**	**ii**	**iii**	**iv**	**i**	**ii**	**iii**	**iv**	**i**	**ii**	**iii**	**iv**	**i**	**ii**	**iii**	**iv**
CAPEX ($ M)	9.57	15.57	18.24	9.50	6.89	12.06	12.04	7.06	7.95	14.01	14.28	7.95	10.75	15.63	17.87	10.64	11.99	14.49	18.63	12.10
OPEX ($ M)	4.68	3.88	3.84	4.69	4.60	3.81		4.59	4.69	3.85	3.82	4.69	4.68	4.13	3.87	4.69		4.36	4.00	4.71
Payback (y)	5.4	6.1	7.0	5.4	3.7	4.6		3.8	4.5	5.4		4.5	6.1	6.7	6.9	6.0	6.8	6.9	7.6	6.9

As illustrated in Table 6.15 and Figure 6.7, the CAPEX values ranged from $7.06 million to $18.63 million, with scenario 1d sub-scenario iii exhibiting the highest value. Sub-scenario iv consistently resulted in lower CAPEX across all main scenarios, reflecting configurations with reduced or minimal PV, BESS, and micro-hydro components. The annual OPEX remained relatively stable across sub-scenarios, typically around $3.8–$4.7 million, whereas payback periods varied more significantly, from as low as 3.8 years in scenario 1a sub-scenario iv to as high as

7.6 years in scenario 1d sub-scenario iii. Notably, scenario 1a generally demonstrated the most cost-effective performance, with both low CAPEX and short payback times, while scenario 1d was the most capital-intensive with longer returns on investment.

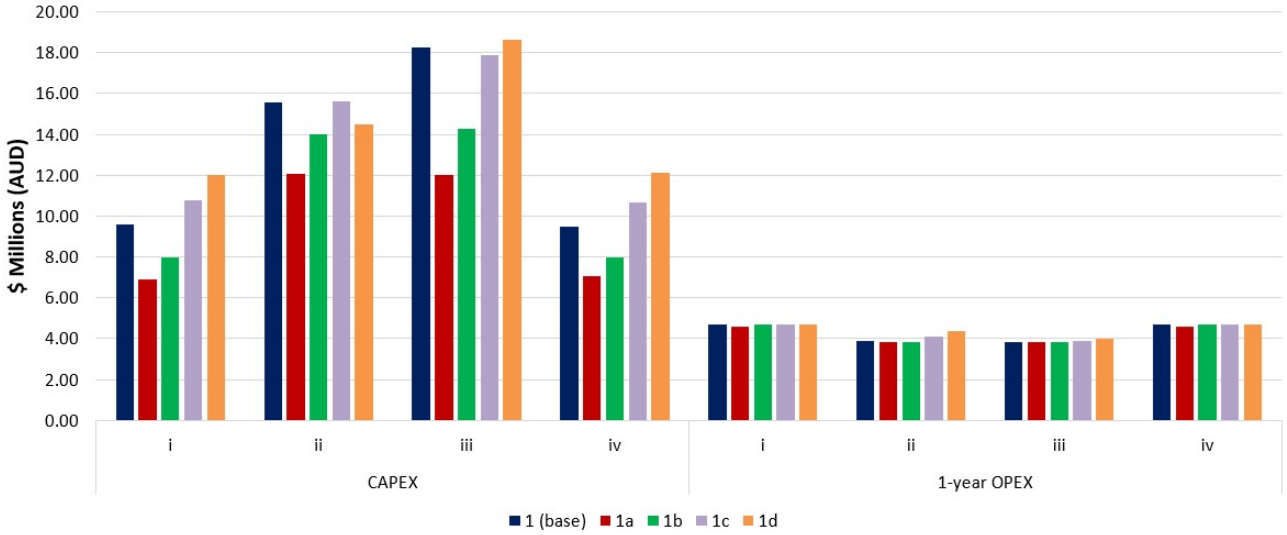

Figure 6.7: CAPEX and 1-year OPEX for different unit costs and weighting factors (Case 1 scenarios)

- *Case 3*

Table 6.16 presents the microgrid configurations based on the four sets of weighting factors for some of the scenarios presented in Table 6.12.

Table 6.16: Case 3 scenarios (3-3d) - Different weighting factors

		CHP	Boiler	Hydro	PV	BESS	Gasifier	Dryer	Electrolyser	Fuel cell	Storage	Upgrade
Unit		kWe	kW								m^3	$m^3\,h^{-1}$
3	**i**	3,280	0	0	0	0	300	4,280	0	0	200	320
	ii	3,100	210	110	4,280	1,290					100	340
	iii	3,080	330		5,000	1,620						560
	iv	3,280	0	0	0	0					600	240
3a	**i**	3,270	10	80	0	0	300	4,280	0	0	300	260
	ii	2,940	300	110	5,000	2,160					1,600	380
	iii	2,760	590			3,200				20	700	440
	iv	3,270	10	80	0	0				0	300	260
3b	**i**	3,270	10	0	0	0	300	4,280	0	0	300	260
	ii	3,070	250	100	5,000	1,620					1,000	360
	iii	3,210	80	110		1,610					100	460
	iv	3,270	10	0							300	260
3c	**i**	3,270	10	0	0	0	300	4,280	0	0	300	260
	ii	3,280	0	100	1,660	0					500	250
	iii	3,110	200		5,000	1,250					400	330
	iv	3,270	10	0	0	0					300	260
3d	**i**	3,270	10	0	0	0	300	4,280	0	0	300	260
	ii	3,280	0	90	1,190	0					500	250
	iii			100	3,230	170					400	280
	iv	3,270	10	0	0	0					300	260

Figure 6.8 shows the capacity of each generating technology across the weighting factors.

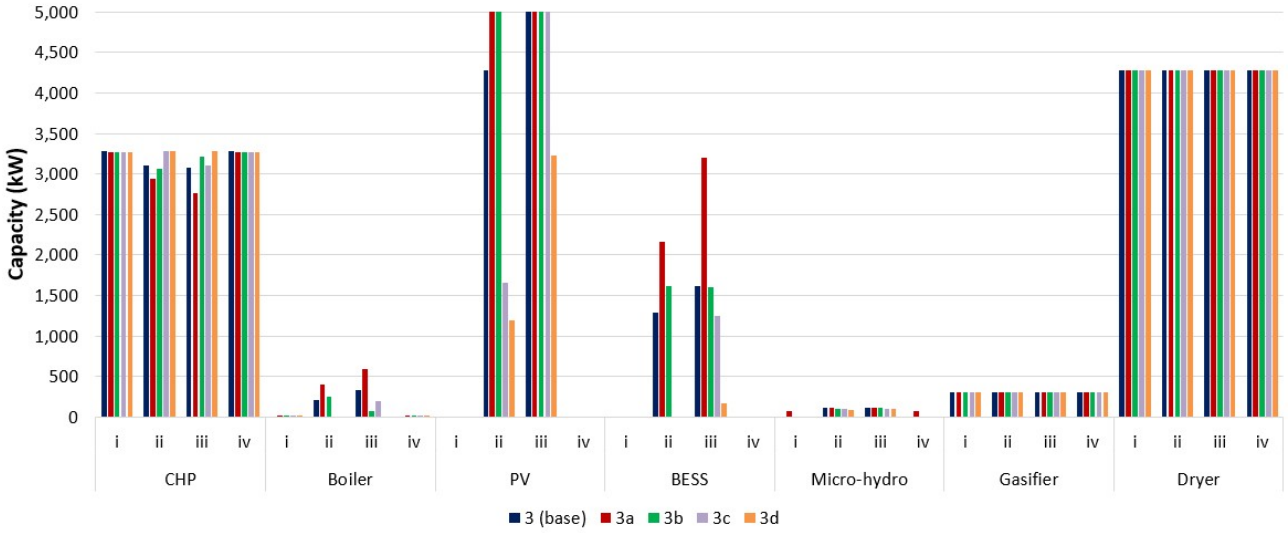

Figure 6.8: Microgrid capacity for different unit costs and weighting factors (Case 3 scenarios)

As reported in Table 6.16, the CHP system was implemented across all Case 3 scenarios, with installed capacities consistently around 3.1 MWe. Boiler capacities showed notable variation, reaching up to 590 kW, with the highest value observed in scenario 3a sub-scenario iii. Sub-scenario iv seems to not favour renewable and storage technologies, resulted in minimal (in scenario 3a) or zero capacities for PV, BESS, and hydro systems across all scenarios. In contrast, sub-scenario ii favoured more balanced configurations, often including PV and BESS capacities up to 5 MW and 2.16 MW. Scenario 3a–iii featured the most diverse setup, integrating a gasifier, dryer, 20 kW fuel cell, and the highest BESS capacity (3.2 MW). Biogas upgrading capacities ranged between 240 $m^3\,h^{-1}$ and 560 $m^3\,h^{-1}$, with the highest value observed in Scenario 3-iii. Water electrolyser and fuel cell systems were not selected in any scenario (expect in scenario 3a-iii, which included a small 20 kW fuel cell system). The gasifier and dryer system were kept constant at capacities of 300 kW and 4.28 MW, respectively. This consistent configuration was due to the sludge volume being the same across all scenarios. Across all configurations, sub-scenario iv consistently resulted in simplified system designs with reduced microgrid components.

Table 6.17 presents the total CAPEX, 1-year OPEX and payback period for the cases presented in Table 6.16. Figure 6.9 illustrates the CAPEX and annual OPEX for the same Case 3 scenarios.

Table 6.17: CAPEX, 1-year OPEX and payback period (Scenarios 3–3d and Sub-scenarios i-iv)

	3				**3a**				**3b**				**3c**				**3d**			
	i	**ii**	**iii**	**iv**	**i**	**ii**	**iii**	**iv**	**i**	**ii**	**iii**	**iv**	**i**	**ii**	**iii**	**iv**	**i**	**ii**	**iii**	**iv**
CAPEX ($ M)	19.57	24.84	26.66	19.37	13.79	19.00	19.23	13.79	16.48	22.58	22.76	16.48	22.34	24.84	29.70	22.34	25.27	27.37	30.22	25.27
OPEX ($ M)	3.17	2.45	2.33	3.17	3.09	2.31	2.29	3.09	3.17	2.34		3.17	2.82	2.37	3.17		2.89	2.63	3.17	
Payback (y)	6.0	6.2	6.5	5.9	4.1	4.6		4.1	5.0	5.5		5.0	6.8	6.8	7.3	6.8	7.7	7.7	7.9	7.7

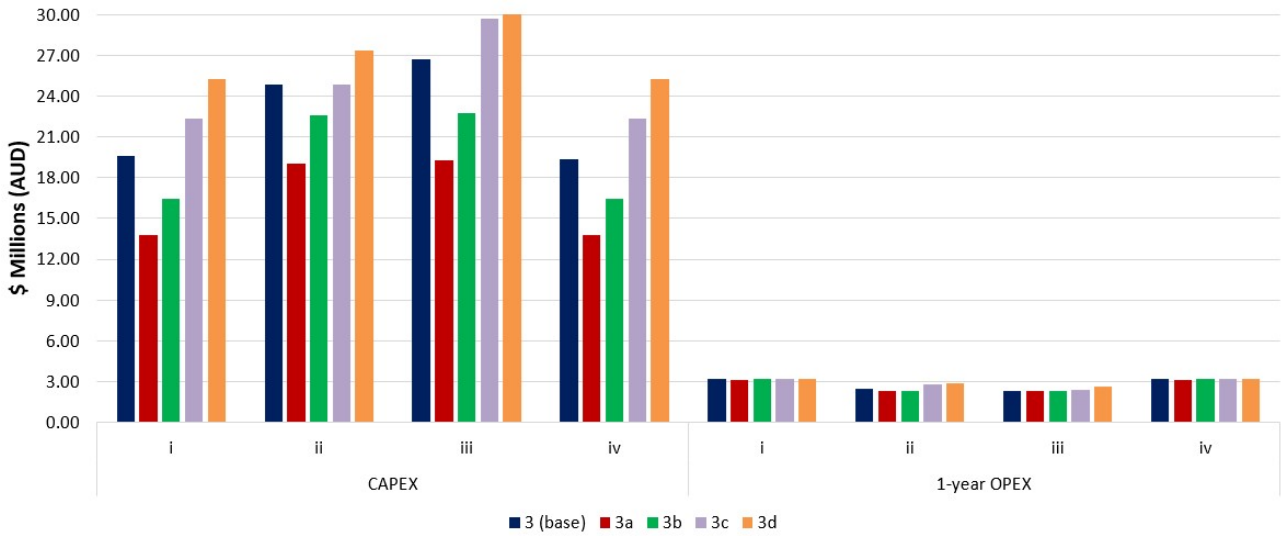

Figure 6.9: CAPEX and 1-year OPEX for different unit costs and weighting factors (Case 3 scenarios)

As illustrated, the CAPEX values varied significantly, ranging from \$13.79 million (3a–iv) to \$30.2 million (3d–iii), with sub-scenario iv generally yielding the lowest investment costs due to simplified system configurations, whereas 1-year OPEX remained relatively stable across all scenarios (between \$2.29 million and \$3.17 million), with the highest values consistently appearing under sub-scenario iv. Scenario 3a showed the most favourable economic performance, achieving the lowest CAPEX and shortest payback period—down to 4.1 years in sub-scenario iv. In contrast, scenario 3d–iii had the highest CAPEX and longest payback period of 7.9 years. Notably, payback periods tended to improve in scenarios where lower-cost configurations were adopted, especially under sub-scenarios ii and iii.

6.6 Summary

Municipal WWTPs are energy-intensive facilities, and reducing their energy consumption is critical for improving sustainability and decreasing operational costs. The adoption of microgrids can be one of the most effective strategies to achieve these goals. This study explored the planning problem of microgrid system optimisation aiming to reduce both the investment and operating costs of electricity, gas and sludge management in a WWTP. The analysis was conducted through four case scenarios, based on different scenarios and conditions, including co-digestion, biogas upgrading for biomethane injection into the gas grid, and multiple options of renewable energy technologies. The analysis was conducted through three case scenarios, based on different scenarios and conditions. Additionally, a sensitivity analysis was conducted in two scenarios (Case 1 and Case 3) to further evaluate how variations in CAPEX, sludge disposal costs, and multi-objective weighting factors (a_1, a_2, a_3) impact the performance of proposed microgrid configurations for two case studies.

The microgrid configuration in Case 1 consisted of a 3.05 MWe CHP system, 530 kW boiler, 90 kW micro-hydro, 200 m^3 biogas storage, and a 240 $m^3\,h^{-1}$ biogas upgrading system, with a CAPEX of \$11.36 million and a payback period of 6 years. CHP was prioritised due to its ability to meet both electrical and thermal demands, while PV and BESS were not selected. OPEX totalled \$4.56 million annually, with sludge disposal alone accounting for almost \$4 million. In Case 2, a more diversified system was implemented, including CHP, boiler, micro-hydro, gasifier, dryer, and 400 m^3 biogas storage unit, with a higher CAPEX of \$15.8 million,

but lower OPEX ($3.24 million/year), thanks to reduced sludge management costs by about 70%. In Case 3, the system included CHP, micro-hydro, electrolyser, and biogas upgrading (620 $m^3\,h^{-1}$), with a high CAPEX and OPEX of $25.3 million and $1.1 million, respectively. Although the co-digestion increased the biogas production, the costs of co-digestion accounted for almost $1.76 million making a significant impact on the costs.

In Section 6.5.4, sensitivity analysis was conducted to investigate the influence of two key parameters (unit costs of generating technology, weighting factors and sludge disposal costs) on the CAPEX, OPEX and payback period for Case 1 and Case 3. The results indicate that the variations in unit costs exert a substantial effect on both CAPEX and the payback period, whereas OPEX is not heavily impacted. This outcome may be attributed to the fact that the microgrid configuration capacity does not vary significantly despite changes in unit costs of the generating technologies. The analysis confirmed the critical role of unit cost assumptions, with lower costs leading to reduced CAPEX and shorter payback periods in both cases. In Case 1, CAPEX ranged from $6.9M to $12M and payback periods from 3.7 to 6.8 years, while Case 3 exhibited higher overall investment levels ($13.8M–$30.2M) and longer payback periods (4.1–7.9 years), due in part to more complex configurations (i.e., gasification and dryer systems). Across all scenarios, CHP was implemented in all cases, while the inclusion of technologies such as PV, BESS, and hydro varied significantly depending on cost assumptions and weighting factors. Varying the weighting factors (a_1, a_2 and a_3) further demonstrated their strong influence on system design. Sub-scenarios i and iv proposed microgrid configurations with lower CAPEX and shorter payback periods; however, they also incurred a higher OPEX. In constrast, sub-scenarios ii and iii promoted a more balanced microgrid system, characterised by higher CAPEX and longer payback period but lower OPEX, in both Cases 1 and 3. Notably, scenarios 3a-i and 3a-iv were identified as the most cost-effective, achieving the lowest CAPEX and shortest payback periods (as low 4.1 years). In contrast, scenario 3d–iii was the most capital-intensive, with payback periods extending up to 7.9 years. Overall, the analysis highlights the importance of carefully selecting economic parameters and objective priorities in microgrid planning, as they substantially impact both system configuration and financial viability.

Chapter 7

Conclusion

This chapter summarizes the current studied results and provides suggestions for further work.

7.1 Summary of Outcomes

The literature review of this thesis explored different types of renewable energy recovery technologies that can be used in WWTPs with the goal of improving energy efficiency, reducing operational costs, and enhancing sustainability. Anaerobic digestion (AD) remains the most widely adopted method for sewage sludge treatment due to its technological maturity, operational efficiency, low costs, and the added benefit of biogas production. Co-digestion and pre-treatment are commonly employed to enhance biogas yields and overall AD performance; however, given their additional costs, a thorough economic feasibility assessment is essential prior to implementation. Thermochemical processes, such as pyrolysis and gasification, are also mature technologies that can convert sludge into valuable by-products such as syngas and bio-oil, although further research is needed, particularly with sewage sludge as feedstock, to optimise conversion efficiencies, minimise emissions and reduce overall costs. The adoption of PV systems offers an attractive solution for WWTPs, especially due to their scalability, modularity, and declining costs. When combined with BESS, additional benefits can be achieved by offsetting grid electricity consumption, reducing grid reliance, and lowering operating costs. The applications of hydropower, particularly micro-hydro, are limited and are highly associated with site-specific and key parameters, such as net head and water flow. However, when conditions are favorable, they can offer unique advantages for energy recovery. Wind technology is identified as very limited due to uncertainties and variability in wind availability and site constraints. Emerging bioelectrochemical technologies, MFCs and MECs, show strong potential for both energy recovery and wastewater treatment, but they face significant challenges related to scalability, efficiency and technology maturity. The literature review also highlights several key barriers to the widespread adoption of renewable technologies in WWTPs, including the limited scope of existing studies (often small-scale or pilot-based projects), site-specific performance variability, early-stage development of emerging solutions and challenges. Additionally, challenges related to validation and implementation in full-scale plants persist, largely due to the complexity and non-stop operation of WWTPs, which can limit opportunities for real-world testing and integration.

Chapter 3 introduces a novel biogas production model for sewage sludge treatment that com-

bines the simplicity of steady-state models with the dynamic characteristics of semi-continuous feeding through the FIFO methodology. By capturing time-dependent retention times based on sludge inflow and maintaining a fixed digester volume, the model realistically simulates the continuous feeding operation of large-scale anaerobic digesters. Validation against three years of real data from a full-scale municipal WWTP in Sydney demonstrated that the model forecasts biogas production with strong accuracy, achieving an average error below 5%, despite real-world fluctuations and operational complexities. The model addresses challenges inherent to continuous processes, such as variability in feed composition, microbial washout, and the presence of inhibitory compounds, which can impact digestion efficiency and biogas yield. However, the assumption of no mixing between sludge parcels inside the digester—while enabling dynamic retention time modeling—represents a limitation that may affect the model's representation of microbial interactions and sludge homogenization. Overall, this work presents a significant step toward bridging the gap between theoretical batch models and real-world semi-continuous operations, providing a practical tool to enhance the prediction and management of biogas production in WWTPs.

Chapters 4 presents an optimal operation model for the power generation system of a large-scale WWTP, focusing on existing generating infrastructure, including CHP units, boilers and the plant's reliance on the main power grid. The primary objective of the proposed operation model is to minimise operational costs by optimising the use of on-site biogas, incorporating real operational constraints and performance data. Using a MILP framework and validated with historical data from a large-scale WWTP in Sydney, Australia, the model effectively identifies the optimal anaerobic digestion temperature and operation strategy to enhance energy efficiency and cost-effectiveness. The proposed operation model uses the ouput from the biogas forecasting from Chapther 3. Case studies assessment were conducted to evaluate the model's performance and explore alternative operational strategies. Overall, the proposed operation model offers a practical and scalable approach for improving energy efficiency, maximizing the utilisation of on-site biogas, and advancing toward more sustainable WWTP operations.

Chapter 5 explored the second part of the WWTP operation model, extending the previous work on Chapter 4, by incorporating a microgrid-based approach to enhance energy resilience and reduce dependency on external energy sources. The proposed optimisation model aims to minimise the total operating costs of the plant by coordinating the operation of multiple on-site energy technologies, including CHP units, PV, BESS, and micro-hydro turbines, while also considering the biogas utilisation and option of biomethane injection. Case studies were conducted to explore the system's response under different configurations and market conditions. The results demonstrate the model's flexibility and practical relevance, showing how the microgrid configuration and market strategies can significantly influence energy costs, operational stability, and renewable integration.

Chapter 6 proposes an optimal planning framework for integrating a microgrid system into a large-scale WWTP, aiming to reduce both investment and operational costs while enhancing energy self-sufficiency. The model incorporated various DERs, including PV, BESS, micro-hydro turbines, CHP units, biogas upgrading technologies, gasification, sludge dyring, water electrolysis and fuel cells, and assessments considered 3 case scenarios. A multi-objective optimisation approach was formulated to determine the most cost-effective and technically viable generation mix, accounting for investment, operational expenditures, and payback period. The planning model was validated using data from a full-scale WWTP in Sydney and assessed through multiple case studies to evaluate different configurations and resource recovery strategies. Simulation results revealed that, despite the inclusion of several advanced technologies in the microgrid

model, the optimisation engine consistently prioritised the CHP system for both power and thermal generation. This is largely due to its dual-output capability and the ability to use on-site biogas, making it the most cost-effective option under the assumed conditions. To better understand the economic viability of alternative technologies and capture uncertainties inherent to real-world planning, a detailed sensitivity analysis was conducted. This analysis evaluated the effects of key parameters, including CAPEX for generation technologies, the weighting factors used in the optimisation function, and sludge disposal costs. The results underscored the importance of accurate cost estimation, as well as the need to assess risks and variability when planning complex systems. The inclusion of sensitivity analysis provided critical insights into the robustness of the model's outcomes and highlighted which parameters most significantly influence the overall system performance. By doing so, it enables more informed, resilient, and confident decision-making in the context of long-term energy planning for WWTPs.

7.2 Recommendations and Future Work

This thesis proposes methodologies for both planning investment and operation optimisation for the microgrid-based MG in WWTPs. Additionally, a biogas model to forecast biogas production is proposed. Meanwhile, more recommendations are proposed below that would extend the current research. For Chapter 3, it includes:

1. Incorporate statistical analysis to evaluate the model's accuracy and benchmark its performance against other mathematical models.
2. Adopt artificial intelligence (AI) to enhance accuracy and predictability by analysing large volumes of data, identifying patterns, forecasting future events, and generating predictions quickly and efficiently.
3. Account for uncertainties to improve decision quality and ensure that models remain realistic and reliable, enabling more informed and robust planning, particularly under unpredictable conditions.
4. Conduct Lab experiments and compare the results with model predictions for validation and calibration.
5. Explore hybrid models that incorporate mixing dynamics and microbial kinetics to improve prediction accuracy, especially under co-digestion and variable sludge conditions.

For Chapters 4, 5 and 6, it includes:

1. Include the integration of other renewable energy resources, such as solar thermal, sludge pyrolysis, thermal treatment, wind and others. This would not only enhance energy resilience but also open up new revenue streams and cost-saving opportunities.
2. Integrate WWTP process optimisation with the proposed model and Demand Response strategies or provision of ancillary services to maximize benefits on both operation and planning models.
3. Incorporate demand-side management strategies, such as load shifting, flexible aeration control, or sludge dewatering schedules, to improve overall cost-effectiveness and reduce peak electricity consumption.

Bibliography

[1] BECA, "Opportunities for renewable energy in the australian water sector," ARENA, Report, 2015. [Online]. Available: https://arena.gov.au/assets/2016/01/Opportunities-for-renewable-energy-in-the-Australian-water-sector.pdf.

[2] N. Government, "Energy efficiency opportunities in wastewater treatment facilities," Report, 25 June 2019 2019. [Online]. Available: https://www.environment.nsw.gov.au/resources/business/wastewater-treatment-facilities-energy-efficiency-opportunities-190114.pdf.

[3] L. H. Moss, "Accelerating resource recovery: Biosolids innovations and opportunities," in *WEFTEC 2018*, Water Environment Federation, 2018, pp. 2128–2137.

[4] M. Maktabifard, E. Zaborowska, and J. Makinia, "Achieving energy neutrality in wastewater treatment plants through energy savings and enhancing renewable energy production," *Reviews in Environmental Science and Bio/Technology*, vol. 17, no. 4, pp. 655–689, 2018, ISSN: 1572-9826.

[5] N. S. Topare, S. Attar, and M. M. Manfe, "Sewage/wastewater treatment technologies: A review," *Sci. Revs. Chem. Commun*, vol. 1, no. 1, pp. 18–24, 2011.

[6] C. V. Andreoli, M. Von Sperling, and F. Fernandes, *Sludge treatment and disposal*. IWA publishing, 2007, ISBN: 184339166X.

[7] R. Riffat and T. Husnain, *Fundamentals of wastewater treatment and engineering*. Crc Press, 2013, ISBN: 1003134378.

[8] H. T. Nguyen, U. Safder, X. N. Nguyen, and C. Yoo, "Multi-objective decision-making and optimal sizing of a hybrid renewable energy system to meet the dynamic energy demands of a wastewater treatment plant," *Energy*, vol. 191, p. 116 570, 2020, ISSN: 0360-5442.

[9] Y. Gu, Y. Li, X. Li, *et al.*, "Energy self-sufficient wastewater treatment plants: Feasibilities and challenges," *Energy Procedia*, vol. 105, pp. 3741–3751, 2017, ISSN: 1876-6102.

[10] A. Strazzabosco, S. Kenway, and P. Lant, "Solar pv adoption in wastewater treatment plants: A review of practice in california," *Journal of environmental management*, vol. 248, p. 109 337, 2019, ISSN: 0301-4797.

[11] D. Lima, L. Li, and G. Appleby, "A review of renewable energy technologies in municipal wastewater treatment plants (wwtps)," *Energies*, vol. 17, no. 23, p. 6084, 2024, ISSN: 1996-1073.

[12] A. Strazzabosco, S. Kenway, and P. Lant, "Quantification of renewable electricity generation in the australian water industry," *Journal of Cleaner Production*, vol. 254, p. 120 119, 2020, ISSN: 0959-6526.

[13] M. Maktabifard, E. Zaborowska, and J. Makinia, "Energy neutrality versus carbon footprint minimization in municipal wastewater treatment plants," *Bioresource Technology*, vol. 300, p. 122 647, 2020, ISSN: 0960-8524.

[14] M. Gandiglio, A. Lanzini, A. Soto, P. Leone, and M. Santarelli, "Enhancing the energy efficiency of wastewater treatment plants through co-digestion and fuel cell systems," *Frontiers in Environmental Science*, vol. 5, p. 70, 2017, ISSN: 2296-665X.

[15] D. Lima, G. Appleby, and L. Li, "A scoping review of options for increasing biogas production from sewage sludge: Challenges and opportunities for enhancing energy self-sufficiency in wastewater treatment plants," *Energies*, vol. 16, no. 5, p. 2369, 2023, ISSN: 1996-1073.

[16] S. A. Saadabadi, A. T. Thattai, L. Fan, R. E. Lindeboom, H. Spanjers, and P. Aravind, "Solid oxide fuel cells fuelled with biogas: Potential and constraints," *Renewable Energy*, vol. 134, pp. 194–214, 2019, ISSN: 0960-1481.

[17] D. M. Riley, J. Tian, G. Güngör-Demirci, P. Phelan, J. R. Villalobos, and R. J. Milcarek, "Techno-economic assessment of chp systems in wastewater treatment plants," *Environments*, vol. 7, no. 10, p. 74, 2020.

[18] A. Ibrahim and H. Akilli, "Supercritical water gasification of wastewater sludge for hydrogen production," *International Journal of Hydrogen Energy*, vol. 44, no. 21, pp. 10 328–10 349, 2019, ISSN: 0360-3199.

[19] Y. Fan, U. Hornung, and N. Dahmen, "Hydrothermal liquefaction of sewage sludge for biofuel application: A review on fundamentals, current challenges and strategies," *Biomass and Bioenergy*, vol. 165, p. 106 570, 2022, ISSN: 0961-9534.

[20] N. Gao, K. Kamran, C. Quan, and P. T. Williams, "Thermochemical conversion of sewage sludge: A critical review," *Progress in Energy and Combustion Science*, vol. 79, p. 100 843, 2020, ISSN: 0360-1285.

[21] W. Ghoneim, A. Helal, and M. A. Wahab, "Renewable energy resources and recovery opportunities in wastewater treatment plants," in *2016 3rd International Conference on Renewable Energies for Developing Countries (REDEC)*, IEEE, pp. 1–8, ISBN: 1509018646.

[22] A. K. Islam, P. S. Dunlop, N. J. Hewitt, R. Lenihan, and C. Brandoni, "Bio-hydrogen production from wastewater: A comparative study of low energy intensive production processes," *Clean Technologies*, vol. 3, no. 1, pp. 156–182, 2021, ISSN: 2571-8797.

[23] A. Escapa, R. Mateos, E. Martínez, and J. Blanes, "Microbial electrolysis cells: An emerging technology for wastewater treatment and energy recovery. from laboratory to pilot plant and beyond," *Renewable and Sustainable Energy Reviews*, vol. 55, pp. 942–956, 2016, ISSN: 1364-0321.

[24] A. AlSayed, M. Soliman, and A. Eldyasti, "Microbial fuel cells for municipal wastewater treatment: From technology fundamentals to full-scale development," *Renewable and Sustainable Energy Reviews*, vol. 134, p. 110 367, 2020, ISSN: 1364-0321.

[25] X. Liu, F. Zhu, R. Zhang, L. Zhao, and J. Qi, "Recent progress on biodiesel production from municipal sewage sludge," *Renewable and Sustainable Energy Reviews*, vol. 135, p. 110 260, 2021, ISSN: 1364-0321.

[26] P. Do, C. W. Chow, R. Rameezdeen, and N. Gorjian, "Understanding the impact of spot market electricity price on wastewater asset management strategy," *Water Conservation Science and Engineering*, vol. 7, no. 2, pp. 101–117, 2022, ISSN: 2364-5687.

[27] I. V. Junior, R. de Almeida, and M. C. Cammarota, "A review of sludge pretreatment methods and co-digestion to boost biogas production and energy self-sufficiency in wastewater treatment plants," *Journal of Water Process Engineering*, vol. 40, p. 101 857, 2021, ISSN: 2214-7144.

[28] D. Elalami, H. Carrere, F. Monlau, K. Abdelouahdi, A. Oukarroum, and A. Barakat, "Pretreatment and co-digestion of wastewater sludge for biogas production: Recent research advances and trends," *Renewable and Sustainable Energy Reviews*, vol. 114, p. 109 287, 2019, ISSN: 1364-0321.

[29] L. N. Nguyen, J. Kumar, M. T. Vu, *et al.*, "Biomethane production from anaerobic co-digestion at wastewater treatment plants: A critical review on development and innovations in biogas upgrading techniques," *Science of the Total Environment*, vol. 765, p. 142 753, 2021, ISSN: 0048-9697.

[30] M. C. Chrispim, M. Scholz, and M. A. Nolasco, "Biogas recovery for sustainable cities: A critical review of enhancement techniques and key local conditions for implementation," *Sustainable Cities and Society*, vol. 72, p. 103 033, 2021, ISSN: 2210-6707.

[31] P. Neumann, S. Pesante, M. Venegas, and G. Vidal, "Developments in pre-treatment methods to improve anaerobic digestion of sewage sludge," *Reviews in Environmental Science and Bio/Technology*, vol. 15, no. 2, pp. 173–211, 2016, ISSN: 1572-9826.

[32] G.-C. Mitraka, K. N. Kontogiannopoulos, M. Batsioula, G. F. Banias, A. I. Zouboulis, and P. G. Kougias, "A comprehensive review on pretreatment methods for enhanced biogas production from sewage sludge," *Energies*, vol. 15, no. 18, p. 6536, 2022, ISSN: 1996-1073.

[33] D. Rusmanis, R. O'Shea, D. M. Wall, and J. D. Murphy, "Biological hydrogen methanation systems–an overview of design and efficiency," *Bioengineered*, vol. 10, no. 1, pp. 604–634, 2019, ISSN: 2165-5979.

[34] M. Tabatabaei, M. Aghbashlo, E. Valijanian, *et al.*, "A comprehensive review on recent biological innovations to improve biogas production, part 1: Upstream strategies," *Renewable Energy*, vol. 146, pp. 1204–1220, 2020, ISSN: 0960-1481.

[35] A. ARMCANZ, "Australian guidelines for sewerage systems—effluent management," in *Australian Government Publishing Service, Canberra*. 1997.

[36] M. Von Sperling, *Wastewater characteristics, treatment and disposal*. IWA publishing, 2007, ISBN: 1843391619.

[37] M. Kacprzak, E. Neczaj, K. Fijałkowski, *et al.*, "Sewage sludge disposal strategies for sustainable development," *Environmental research*, vol. 156, pp. 39–46, 2017, ISSN: 0013-9351.

[38] H. Kamyab, A. Yuzir, V. Ashokkumar, S. E. Hosseini, B. Balasubramanian, and I. Kirpichnikova, "Review of the application of gasification and combustion technology

and waste-to-energy technologies in sewage sludge treatment," *Fuel*, vol. 316, p. 123 199, 2022, ISSN: 0016-2361.

[39] W. C. Kuo-Dahab, P. Amirhor, M. Zona, D. Duest, and C. Park, "Investigating anaerobic co-digestion of sewage sludge and food waste using a bench-scale pilot study," in *WEFTEC 2014*, Water Environment Federation, ISBN: 1938-6478.

[40] R. Azarmanesh, M. H. Zonoozi, and H. Ghiasinejad, "Characterization of food waste and sewage sludge mesophilic anaerobic co-digestion under different mixing ratios of primary sludge, secondary sludge and food waste," *Biomass and Bioenergy*, vol. 139, p. 105 610, 2020.

[41] M. S. Prabhu and S. Mutnuri, "Anaerobic co-digestion of sewage sludge and food waste," *Waste management research*, vol. 34, no. 4, pp. 307–315, 2016, ISSN: 0734-242X.

[42] L. Pastor, L. Ruiz, A. Pascual, and B. Ruiz, "Co-digestion of used oils and urban landfill leachates with sewage sludge and the effect on the biogas production," *Applied energy*, vol. 107, pp. 438–445, 2013, ISSN: 0306-2619.

[43] A. Grosser, E. Neczaj, B. Singh, Å. Almås, H. Brattebø, and M. Kacprzak, "Anaerobic digestion of sewage sludge with grease trap sludge and municipal solid waste as co-substrates," *Environmental Research*, vol. 155, pp. 249–260, 2017, ISSN: 0013-9351.

[44] S. Yalcinkaya and J. F. Malina, "Anaerobic co-digestion of municipal wastewater sludge and un-dewatered grease trap waste for assessing direct feed of grease trap waste in municipal digesters," *International Biodeterioration Biodegradation*, vol. 104, pp. 490–497, 2015, ISSN: 0964-8305.

[45] R. M. Alqaralleh, K. Kennedy, R. Delatolla, and M. Sartaj, "Thermophilic and hyperthermophilic co-digestion of waste activated sludge and fat, oil and grease: Evaluating and modeling methane production," *Journal of environmental management*, vol. 183, pp. 551–561, 2016, ISSN: 0301-4797.

[46] M. Tandukar and S. G. Pavlostathis, "Anaerobic co-digestion of municipal sludge with fat-oil-grease (fog) enhances the destruction of sludge solids," *Chemosphere*, vol. 292, p. 133 530, 2022, ISSN: 0045-6535.

[47] I. R. Alves, C. F. Mahler, L. B. Oliveira, M. M. Reis, and J. P. Bassin, "Investigating the effect of crude glycerol from biodiesel industry on the anaerobic co-digestion of sewage sludge and food waste in ternary mixtures," *Energy*, vol. 241, p. 122 818, 2022, ISSN: 0360-5442.

[48] G. Silvestre, B. Fernández, and A. Bonmatí, "Addition of crude glycerine as strategy to balance the c/n ratio on sewage sludge thermophilic and mesophilic anaerobic co-digestion," *Bioresource Technology*, vol. 193, pp. 377–385, 2015, ISSN: 0960-8524.

[49] X. Bai and Y.-C. Chen, "Synergistic effect and supernatant nitrogen reduction from anaerobic co-digestion of sewage sludge and pig manure," *Bioresource Technology Reports*, vol. 10, p. 100 424, 2020, ISSN: 2589-014X.

[50] S. Borowski, J. Domański, and L. Weatherley, "Anaerobic co-digestion of swine and poultry manure with municipal sewage sludge," *Waste Management*, vol. 34, no. 2, pp. 513–521, 2014, ISSN: 0956-053X.

[51] C. Beltrán, D. Jeison, F. G. Fermoso, and R. Borja, "Batch anaerobic co-digestion of waste activated sludge and microalgae (chlorella sorokiniana) at mesophilic tempera-

ture," *Journal of Environmental Science and Health, Part A*, vol. 51, no. 10, pp. 847–850, 2016, ISSN: 1093-4529.

[52] E. Ortega-Martinez, I. Sapkaite, F. Fdz-Polanco, and A. Donoso-Bravo, "From pretreatment toward inter-treatment. getting some clues from sewage sludge biomethanation," *Bioresource technology*, vol. 212, pp. 227–235, 2016, ISSN: 0960-8524.

[53] J.-M. Choi, S.-K. Han, and C.-Y. Lee, "Enhancement of methane production in anaerobic digestion of sewage sludge by thermal hydrolysis pretreatment," *Bioresource technology*, vol. 259, pp. 207–213, 2018, ISSN: 0960-8524.

[54] X. Liu, Q. Xu, D. Wang, *et al.*, "Improved methane production from waste activated sludge by combining free ammonia with heat pretreatment: Performance, mechanisms and applications," *Bioresource technology*, vol. 268, pp. 230–236, 2018, ISSN: 0960-8524.

[55] J. Liu, M. Yang, J. Zhang, *et al.*, "A comprehensive insight into the effects of microwave-h2o2 pretreatment on concentrated sewage sludge anaerobic digestion based on semi-continuous operation," *Bioresource technology*, vol. 256, pp. 118–127, 2018, ISSN: 0960-8524.

[56] A. Serrano, J. Siles, M. Martín, A. Chica, F. Estévez-Pastor, and E. Toro-Baptista, "Improvement of anaerobic digestion of sewage sludge through microwave pre-treatment," *Journal of Environmental Management*, vol. 177, pp. 231–239, 2016, ISSN: 0301-4797.

[57] E. Martínez, M. Gil, J. Rosas, *et al.*, "Application of thermal analysis for evaluating the digestion of microwave pre-treated sewage sludge," *Journal of Thermal Analysis and Calorimetry*, vol. 127, no. 2, pp. 1209–1219, 2017, ISSN: 1588-2926.

[58] P. Neumann, Z. González, and G. Vidal, "Sequential ultrasound and low-temperature thermal pretreatment: Process optimization and influence on sewage sludge solubilization, enzyme activity and anaerobic digestion," *Bioresource technology*, vol. 234, pp. 178–187, 2017, ISSN: 0960-8524.

[59] S. Houtmeyers, J. Degrève, K. Willems, R. Dewil, and L. Appels, "Comparing the influence of low power ultrasonic and microwave pre-treatments on the solubilisation and semi-continuous anaerobic digestion of waste activated sludge," *Bioresource Technology*, vol. 171, pp. 44–49, 2014, ISSN: 0960-8524.

[60] A. C. Lizama, C. C. Figueiras, R. R. Herrera, A. Z. Pedreguera, and J. E. R. Espinoza, "Effects of ultrasonic pretreatment on the solubilization and kinetic study of biogas production from anaerobic digestion of waste activated sludge," *International Biodeterioration Biodegradation*, vol. 123, pp. 1–9, 2017, ISSN: 0964-8305.

[61] A. Serrano, J. Á. Siles, M. d. C. Gutiérrez, and M. d. l. Á. Martín, "Comparison of pre-treatment technologies to improve sewage sludge biomethanization," *Applied Biochemistry and Biotechnology*, vol. 193, no. 3, pp. 777–790, 2021, ISSN: 1559-0291.

[62] X. Tian, C. Wang, A. P. Trzcinski, L. Lin, and W. J. Ng, "Interpreting the synergistic effect in combined ultrasonication–ozonation sewage sludge pre-treatment," *Chemosphere*, vol. 140, pp. 63–71, 2015, ISSN: 0045-6535.

[63] A. P. Trzcinski, X. Tian, C. Wang, L. L. Lin, and W. J. Ng, "Combined ultrasonication and thermal pre-treatment of sewage sludge for increasing methane production," *Journal of Environmental Science and Health, Part A*, vol. 50, no. 2, pp. 213–223, 2015, ISSN: 1093-4529.

[64] R. Lukoševičius, S. Rimkevičius, and R. Pabarčius, "Presumptions for the integration of green hydrogen and biomethane production in wastewater treatment plants," *Applied Sciences*, vol. 15, no. 13, p. 7417, 2025.

[65] I. U. Khan, M. H. D. Othman, H. Hashim, *et al.*, "Biogas as a renewable energy fuel – a review of biogas upgrading, utilisation and storage," *Energy Conversion and Management*, vol. 150, pp. 277–294, 2017, ISSN: 0196-8904.

[66] Y. Shen, J. L. Linville, M. Urgun-Demirtas, M. M. Mintz, and S. W. Snyder, "An overview of biogas production and utilization at full-scale wastewater treatment plants (wwtps) in the united states: Challenges and opportunities towards energy-neutral wwtps," *Renewable and Sustainable Energy Reviews*, vol. 50, pp. 346–362, 2015, ISSN: 1364-0321.

[67] AEMO, "Gas quality guidelines," AEMO (Australian Energy Market Operator), Report, Jan. 2017.

[68] L. Atkins, "Aemo gas quality guidelines," 2017.

[69] H. Treloar, "Gas quality guidelines-operating procedure (april 2014)," 2014.

[70] M. Gustafsson, J. Ammenberg, and J. D. Murphy, "Iea bioenergy task 37 - a perspective on the state of the biogas industry from selected member countries," Report, 2022.

[71] M. Hu, H. Hu, Z. Ye, *et al.*, "A review on turning sewage sludge to value-added energy and materials via thermochemical conversion towards carbon neutrality," *Journal of Cleaner Production*, vol. 379, p. 134 657, 2022, ISSN: 0959-6526.

[72] G. Jiang, D. Xu, B. Hao, L. Liu, S. Wang, and Z. Wu, "Thermochemical methods for the treatment of municipal sludge," *Journal of Cleaner Production*, vol. 311, p. 127 811, 2021, ISSN: 0959-6526.

[73] E. Adar, B. Karatop, M. İnce, and M. S. Bilgili, "Comparison of methods for sustainable energy management with sewage sludge in turkey based on swot-fahp analysis," *Renewable and sustainable energy reviews*, vol. 62, pp. 429–440, 2016, ISSN: 1364-0321.

[74] L. Swann, D. Downs, and M. Waye, "Waste to energy solution–the sludge treatment facility in tuen mun, hong kong," *Energy Procedia*, vol. 143, pp. 500–505, 2017, ISSN: 1876-6102.

[75] N. L. Enebe, C. B. Chigor, K. Obileke, M. S. Lawal, and M. C. Enebe, "Biogas and syngas production from sewage sludge: A sustainable source of energy generation," *Methane*, vol. 2, no. 2, pp. 192–217, 2023, ISSN: 2674-0389.

[76] M. Campoy, A. Gómez-Barea, P. Ollero, and S. Nilsson, "Gasification of wastes in a pilot fluidized bed gasifier," *Fuel Processing Technology*, vol. 121, pp. 63–69, 2014, ISSN: 0378-3820.

[77] T. P. Thomsen, Z. Sárossy, B. Gøbel, *et al.*, "Low temperature circulating fluidized bed gasification and co-gasification of municipal sewage sludge. part 1: Process performance and gas product characterization," *Waste Management*, vol. 66, pp. 123–133, 2017, ISSN: 0956-053X.

[78] K.-Y. Chiang, C.-H. Lu, C.-K. Liao, and R. H.-R. Ger, "Characteristics of hydrogen energy yield by co-gasified of sewage sludge and paper-mill sludge in a commercial scale plant," *International Journal of Hydrogen Energy*, vol. 41, no. 46, pp. 21 641–21 648, 2016, ISSN: 0360-3199.

[79] M. Schmid, M. Beirow, D. Schweitzer, G. Waizmann, R. Spörl, and G. Scheffknecht, "Product gas composition for steam-oxygen fluidized bed gasification of dried sewage sludge, straw pellets and wood pellets and the influence of limestone as bed material," *Biomass and Bioenergy*, vol. 117, pp. 71–77, 2018, ISSN: 0961-9534.

[80] A. Ayol, O. T. Yurdakos, and A. Gurgen, "Investigation of municipal sludge gasification potential: Gasification characteristics of dried sludge in a pilot-scale downdraft fixed bed gasifier," *International Journal of Hydrogen Energy*, vol. 44, no. 32, pp. 17 397–17 410, 2019, ISSN: 0360-3199.

[81] D. Schweitzer, A. Gredinger, M. Schmid, *et al.*, "Steam gasification of wood pellets, sewage sludge and manure: Gasification performance and concentration of impurities," *Biomass and Bioenergy*, vol. 111, pp. 308–319, 2018, ISSN: 0961-9534.

[82] J. Ma, M. Chen, T. Yang, *et al.*, "Gasification performance of the hydrochar derived from co-hydrothermal carbonization of sewage sludge and sawdust," *Energy*, vol. 173, pp. 732–739, 2019, ISSN: 0360-5442.

[83] C. Freda, G. Cornacchia, A. Romanelli, V. Valerio, and M. Grieco, "Sewage sludge gasification in a bench scale rotary kiln," *Fuel*, vol. 212, pp. 88–94, 2018, ISSN: 0016-2361.

[84] Y.-K. Choi, J.-H. Ko, and J.-S. Kim, "Gasification of dried sewage sludge using an innovative three-stage gasifier: Clean and h2-rich gas production using condensers as the only secondary tar removal apparatus," *Fuel*, vol. 216, pp. 810–817, 2018, ISSN: 0016-2361.

[85] E. Roche, J. M. De Andrés, A. Narros, and M. E. Rodríguez, "Air and air-steam gasification of sewage sludge. the influence of dolomite and throughput in tar production and composition," *Fuel*, vol. 115, pp. 54–61, 2014, ISSN: 0016-2361.

[86] Y.-K. Choi, M.-H. Cho, and J.-S. Kim, "Steam/oxygen gasification of dried sewage sludge in a two-stage gasifier: Effects of the steam to fuel ratio and ash of the activated carbon on the production of hydrogen and tar removal," *Energy*, vol. 91, pp. 160–167, 2015, ISSN: 0360-5442.

[87] Y.-S. Jeong, Y.-K. Choi, K.-B. Park, and J.-S. Kim, "Air co-gasification of coal and dried sewage sludge in a two-stage gasifier: Effect of blending ratio on the producer gas composition and tar removal," *Energy*, vol. 185, pp. 708–716, 2019, ISSN: 0360-5442.

[88] T.-Y. Mun, M.-H. Cho, and J.-S. Kim, "Air gasification of dried sewage sludge in a two-stage gasifier. part 3: Application of olivine as a bed material and nickel coated distributor for the production of a clean hydrogen-rich producer gas," *international journal of hydrogen energy*, vol. 39, no. 11, pp. 5634–5643, 2014, ISSN: 0360-3199.

[89] Y.-K. Choi, M.-H. Cho, and J.-S. Kim, "Air gasification of dried sewage sludge in a two-stage gasifier. part 4: Application of additives including ni-impregnated activated carbon for the production of a tar-free and h2-rich producer gas with a low nh3 content," *International Journal of Hydrogen Energy*, vol. 41, no. 3, pp. 1460–1467, 2016, ISSN: 0360-3199.

[90] M. Haghighat, N. Majidian, and A. Hallajisani, "Production of bio-oil from sewage sludge: A review on the thermal and catalytic conversion by pyrolysis," *Sustainable Energy Technologies and Assessments*, vol. 42, p. 100 870, 2020, ISSN: 2213-1388.

[91] A. Al-Rumaihi, M. Shahbaz, G. Mckay, H. Mackey, and T. Al-Ansari, "A review of pyrolysis technologies and feedstock: A blending approach for plastic and biomass towards optimum biochar yield," *Renewable and Sustainable Energy Reviews*, vol. 167, p. 112 715, 2022, ISSN: 1364-0321.

[92] A. Jaramillo-Arango, I. Fonts, F. Chejne, and J. Arauzo, "Product compositions from sewage sludge pyrolysis in a fluidized bed and correlations with temperature," *Journal of analytical and applied pyrolysis*, vol. 121, pp. 287–296, 2016, ISSN: 0165-2370.

[93] F. Huang, Y. Yu, and H. Huang, "Temperature influence and distribution of bio-oil from pyrolysis of granular sewage sludge," *Journal of Analytical and Applied Pyrolysis*, vol. 130, pp. 36–42, 2018, ISSN: 0165-2370.

[94] R. O. Arazo, D. A. D. Genuino, M. D. G. de Luna, and S. C. Capareda, "Bio-oil production from dry sewage sludge by fast pyrolysis in an electrically-heated fluidized bed reactor," *Sustainable Environment Research*, vol. 27, no. 1, pp. 7–14, 2017, ISSN: 2468-2039.

[95] J. Alvarez, M. Amutio, G. Lopez, I. Barbarias, J. Bilbao, and M. Olazar, "Sewage sludge valorization by flash pyrolysis in a conical spouted bed reactor," *Chemical Engineering Journal*, vol. 273, pp. 173–183, 2015, ISSN: 1385-8947.

[96] J. Alvarez, M. Amutio, G. Lopez, J. Bilbao, and M. Olazar, "Fast co-pyrolysis of sewage sludge and lignocellulosic biomass in a conical spouted bed reactor," *Fuel*, vol. 159, pp. 810–818, 2015, ISSN: 0016-2361.

[97] J. Zhou, S. Liu, N. Zhou, *et al.*, "Development and application of a continuous fast microwave pyrolysis system for sewage sludge utilization," *Bioresource technology*, vol. 256, pp. 295–301, 2018, ISSN: 0960-8524.

[98] Q. Xie, P. Peng, S. Liu, *et al.*, "Fast microwave-assisted catalytic pyrolysis of sewage sludge for bio-oil production," *Bioresource technology*, vol. 172, pp. 162–168, 2014, ISSN: 0960-8524.

[99] S. Deng, H. Tan, X. Wang, *et al.*, "Investigation on the fast co-pyrolysis of sewage sludge with biomass and the combustion reactivity of residual char," *Bioresource technology*, vol. 239, pp. 302–310, 2017, ISSN: 0960-8524.

[100] N. Ruiz-Gómez, V. Quispe, J. Ábrego, M. Atienza-Martínez, M. B. Murillo, and G. Gea, "Co-pyrolysis of sewage sludge and manure," *Waste management*, vol. 59, pp. 211–221, 2017, ISSN: 0956-053X.

[101] Y. Zhou, Y. Liu, W. Jiang, L. Shao, L. Zhang, and L. Feng, "Effects of pyrolysis temperature and addition proportions of corncob on the distribution of products and potential energy recovery during the preparation of sludge activated carbon," *Chemosphere*, vol. 221, pp. 175–183, 2019, ISSN: 0045-6535.

[102] J. Zhu, Y. Yang, L. Yang, and Y. Zhu, "High quality syngas produced from the co-pyrolysis of wet sewage sludge with sawdust," *International Journal of Hydrogen Energy*, vol. 43, no. 11, pp. 5463–5472, 2018, ISSN: 0360-3199.

[103] S. Patel, S. Kundu, J. Paz-Ferreiro, *et al.*, "Transformation of biosolids to biochar: A case study," *Environmental Progress Sustainable Energy*, vol. 38, no. 4, p. 13 113, 2019, ISSN: 1944-7442.

[104] C. He, K. Wang, A. Giannis, Y. Yang, and J.-Y. Wang, "Products evolution during hydrothermal conversion of dewatered sewage sludge in sub-and near-critical water: Effects of reaction conditions and calcium oxide additive," *International journal of hydrogen energy*, vol. 40, no. 17, pp. 5776–5787, 2015, ISSN: 0360-3199.

[105] Y. Su, D. Liu, M. Gong, W. Zhu, Y. Yu, and H. Gu, "Investigation on the decomposition of chemical compositions during hydrothermal conversion of dewatered sewage sludge," *International Journal of Hydrogen Energy*, vol. 44, no. 49, pp. 26 933–26 942, 2019, ISSN: 0360-3199.

[106] D. Kim, K. Lee, and K. Y. Park, "Hydrothermal carbonization of anaerobically digested sludge for solid fuel production and energy recovery," *Fuel*, vol. 130, pp. 120–125, 2014, ISSN: 0016-2361.

[107] P. Zhao, Y. Shen, S. Ge, and K. Yoshikawa, "Energy recycling from sewage sludge by producing solid biofuel with hydrothermal carbonization," *Energy conversion and management*, vol. 78, pp. 815–821, 2014, ISSN: 0196-8904.

[108] C. Peng, Y. Zhai, Y. Zhu, *et al.*, "Production of char from sewage sludge employing hydrothermal carbonization: Char properties, combustion behavior and thermal characteristics," *Fuel*, vol. 176, pp. 110–118, 2016, ISSN: 0016-2361.

[109] R. D. V. K. Silva, Z. Lei, K. Shimizu, and Z. Zhang, "Hydrothermal treatment of sewage sludge to produce solid biofuel: Focus on fuel characteristics," *Bioresource Technology Reports*, vol. 11, p. 100 453, 2020, ISSN: 2589-014X.

[110] R. Z. Gaur, O. Khoury, M. Zohar, *et al.*, "Hydrothermal carbonization of sewage sludge coupled with anaerobic digestion: Integrated approach for sludge management and energy recycling," *Energy conversion and management*, vol. 224, p. 113 353, 2020, ISSN: 0196-8904.

[111] J. Zhao, C. Liu, T. Hou, *et al.*, "Conversion of biomass waste to solid fuel via hydrothermal co-carbonization of distillers grains and sewage sludge," *Bioresource Technology*, vol. 345, p. 126 545, 2022, ISSN: 0960-8524.

[112] J. Lee, D. Sohn, K. Lee, and K. Y. Park, "Solid fuel production through hydrothermal carbonization of sewage sludge and microalgae chlorella sp. from wastewater treatment plant," *Chemosphere*, vol. 230, pp. 157–163, 2019, ISSN: 0045-6535.

[113] L. Nazari, Z. Yuan, M. B. Ray, and C. C. Xu, "Co-conversion of waste activated sludge and sawdust through hydrothermal liquefaction: Optimization of reaction parameters using response surface methodology," *Applied energy*, vol. 203, pp. 1–10, 2017, ISSN: 0306-2619.

[114] K. Anastasakis, P. Biller, R. B. Madsen, M. Glasius, and I. Johannsen, "Continuous hydrothermal liquefaction of biomass in a novel pilot plant with heat recovery and hydraulic oscillation," *Energies*, vol. 11, no. 10, p. 2695, 2018, ISSN: 1996-1073.

[115] P. Biller, I. Johannsen, J. S. Dos Passos, and L. D. M. Ottosen, "Primary sewage sludge filtration using biomass filter aids and subsequent hydrothermal co-liquefaction," *Water research*, vol. 130, pp. 58–68, 2018, ISSN: 0043-1354.

[116] K. Malins, V. Kampars, J. Brinks, I. Neibolte, R. Murnieks, and R. Kampare, "Bio-oil from thermo-chemical hydro-liquefaction of wet sewage sludge," *Bioresource Technology*, vol. 187, pp. 23–29, 2015, ISSN: 0960-8524.

[117] A. A. Shah, S. S. Toor, F. Conti, A. H. Nielsen, and L. A. Rosendahl, "Hydrothermal liquefaction of high ash containing sewage sludge at sub and supercritical conditions," *Biomass and Bioenergy*, vol. 135, p. 105 504, 2020, ISSN: 0961-9534.

[118] D. Xu, G. Lin, L. Liu, Y. Wang, Z. Jing, and S. Wang, "Comprehensive evaluation on product characteristics of fast hydrothermal liquefaction of sewage sludge at different temperatures," *Energy*, vol. 159, pp. 686–695, 2018, ISSN: 0360-5442.

[119] L. Qian, S. Wang, and P. E. Savage, "Hydrothermal liquefaction of sewage sludge under isothermal and fast conditions," *Bioresource technology*, vol. 232, pp. 27–34, 2017, ISSN: 0960-8524.

[120] R. Liu, W. Tian, S. Kong, Y. Meng, H. Wang, and J. Zhang, "Effects of inorganic and organic acid pretreatments on the hydrothermal liquefaction of municipal secondary sludge," *Energy conversion and management*, vol. 174, pp. 661–667, 2018, ISSN: 0196-8904.

[121] W. Wang, Q. Yu, H. Meng, W. Han, J. Li, and J. Zhang, "Catalytic liquefaction of municipal sewage sludge over transition metal catalysts in ethanol-water co-solvent," *Bioresource technology*, vol. 249, pp. 361–367, 2018, ISSN: 0960-8524.

[122] Y. Zhai, H. Chen, B. Xu, *et al.*, "Influence of sewage sludge-based activated carbon and temperature on the liquefaction of sewage sludge: Yield and composition of bio-oil, immobilization and risk assessment of heavy metals," *Bioresource Technology*, vol. 159, pp. 72–79, 2014, ISSN: 0960-8524.

[123] P. Das, S. Khan, M. AbdulQuadir, *et al.*, "Energy recovery and nutrients recycling from municipal sewage sludge," *Science of The Total Environment*, vol. 715, p. 136 775, 2020, ISSN: 0048-9697.

[124] T. Rahman, H. Jahromi, P. Roy, S. Adhikari, E. Hassani, and T.-S. Oh, "Hydrothermal liquefaction of municipal sewage sludge: Effect of red mud catalyst in ethylene and inert ambiences," *Energy Conversion and Management*, vol. 245, p. 114 615, 2021, ISSN: 0196-8904.

[125] T. Yang, X. Liu, R. Li, B. Li, and X. Kai, "Hydrothermal liquefaction of sewage sludge to produce bio-oil: Effect of co-pretreatment with subcritical water and mixed surfactants," *The Journal of Supercritical Fluids*, vol. 144, pp. 28–38, 2019, ISSN: 0896-8446.

[126] S. Wang, D. Xu, Y. Guo, *et al.*, *Supercritical water processing technologies for environment, energy and nanomaterial applications*. Springer, 2020, ISBN: 9811393265.

[127] E. Adar, M. İnce, and M. S. Bilgili, "Evaluation of development in supercritical water oxidation technology," *Desalin. Water Treat*, vol. 161, pp. 243–253, 2019.

[128] L. Qian, S. Wang, D. Xu, Y. Guo, X. Tang, and L. Wang, "Treatment of municipal sewage sludge in supercritical water: A review," *Water research*, vol. 89, pp. 118–131, 2016, ISSN: 0043-1354.

[129] M. Gong, W. Zhu, Y. Fan, H. Zhang, and Y. Su, "Influence of the reactant carbon–hydrogen–oxygen composition on the key products of the direct gasification of dewatered sewage sludge in supercritical water," *Bioresource technology*, vol. 208, pp. 81–86, 2016, ISSN: 0960-8524.

[130] Y. Chen, L. Yi, W. Wei, H. Jin, and L. Guo, "Hydrogen production by sewage sludge gasification in supercritical water with high heating rate batch reactor," *Energy*, vol. 238, p. 121 740, 2022, ISSN: 0360-5442.

[131] G. Weijin, Z. Zizheng, L. Yue, W. Qingyu, and G. Lina, "Hydrogen production and phosphorus recovery via supercritical water gasification of sewage sludge in a batch reactor," *Waste Management*, vol. 96, pp. 198–205, 2019, ISSN: 0956-053X.

[132] M. Gong, W. Zhu, H. Zhang, Q. Ma, Y. Su, and Y. Fan, "Influence of naoh and ni catalysts on hydrogen production from the supercritical water gasification of dewatered sewage sludge," *international journal of hydrogen energy*, vol. 39, no. 35, pp. 19 947–19 954, 2014, ISSN: 0360-3199.

[133] C. Wang, W. Zhu, M. Gong, Y. Su, and Y. Fan, "Influence of h2o2 and ni catalysts on hydrogen production and pahs inhibition from the supercritical water gasification of dewatered sewage sludge," *The Journal of Supercritical Fluids*, vol. 130, pp. 183–188, 2017, ISSN: 0896-8446.

[134] Y. Fan, W. Zhu, M. Gong, Y. Su, H. Zhang, and J. Zeng, "Catalytic gasification of dewatered sewage sludge in supercritical water: Influences of formic acid on hydrogen production," *International Journal of Hydrogen Energy*, vol. 41, no. 7, pp. 4366–4373, 2016, ISSN: 0360-3199.

[135] A. Amrullah and Y. Matsumura, "Supercritical water gasification of sewage sludge in continuous reactor," *Bioresource technology*, vol. 249, pp. 276–283, 2018, ISSN: 0960-8524.

[136] O. Sawai, T. Nunoura, and K. Yamamoto, "Supercritical water gasification of sewage sludge using bench-scale batch reactor: Advantages and drawbacks," *Journal of Material Cycles and Waste Management*, vol. 16, pp. 82–92, 2014, ISSN: 1438-4957.

[137] C. Wang, W. Zhu, C. Chen, H. Zhang, N. Lin, and Y. Su, "Influence of reaction conditions on the catalytic activity of a nickel during the supercritical water gasification of dewatered sewage sludge," *The Journal of Supercritical Fluids*, vol. 140, pp. 356–363, 2018, ISSN: 0896-8446.

[138] D. Hantoko, E. Kanchanatip, M. Yan, Z. Weng, Z. Gao, and Y. Zhong, "Assessment of sewage sludge gasification in supercritical water for h2-rich syngas production," *Process Safety and Environmental Protection*, vol. 131, pp. 63–72, 2019, ISSN: 0957-5820.

[139] E. Adar, M. Ince, and M. S. Bilgili, "Supercritical water gasification of sewage sludge by continuous flow tubular reactor: A pilot scale study," *Chemical Engineering Journal*, vol. 391, p. 123 499, 2020, ISSN: 1385-8947.

[140] L. Qian, S. Wang, D. Xu, Y. Guo, X. Tang, and L. Wang, "Treatment of sewage sludge in supercritical water and evaluation of the combined process of supercritical water gasification and oxidation," *Bioresource Technology*, vol. 176, pp. 218–224, 2015, ISSN: 0960-8524.

[141] P. Bharathi and M. Pennarasi, "Production of biodiesel from municipal sewage sludge by transesterification process," *Biomass Valorization to Bioenergy*, pp. 97–111, 2020, ISSN: 9811504091.

[142] A. G. Capodaglio, A. Callegari, and D. Dondi, "Microwave-induced pyrolysis for production of sustainable biodiesel from waste sludges," *Waste and biomass valorization*, vol. 7, pp. 703–709, 2016, ISSN: 1877-2641.

[143] R. O. Arazo, M. D. G. de Luna, and S. C. Capareda, "Assessing biodiesel production from sewage sludge-derived bio-oil," *Biocatalysis and agricultural biotechnology*, vol. 10, pp. 189–196, 2017, ISSN: 1878-8181.

[144] J. Qi, F. Zhu, X. Wei, *et al.*, "Comparison of biodiesel production from sewage sludge obtained from the a2/o and mbr processes by in situ transesterification," *Waste management*, vol. 49, pp. 212–220, 2016, ISSN: 0956-053X.

[145] J. Melero, R. Sánchez-Vázquez, I. Vasiliadou, *et al.*, "Municipal sewage sludge to biodiesel by simultaneous extraction and conversion of lipids," *Energy conversion and management*, vol. 103, pp. 111–118, 2015, ISSN: 0196-8904.

[146] O. Choi, J. Song, D. Cha, and J. Lee, "Biodiesel production from wet municipal sludge: Evaluation of in situ transesterification using xylene as a cosolvent," *Bioresource technology*, vol. 166, pp. 51–56, 2014, ISSN: 0960-8524.

[147] Y. Patiño, L. G. Mantecón, S. Polo, L. Faba, E. Díaz, and S. Ordóñez, "Effect of sludge features and extraction-esterification technology on the synthesis of biodiesel from secondary wastewater treatment sludges," *Bioresource technology*, vol. 247, pp. 209–216, 2018, ISSN: 0960-8524.

[148] Y. Patiño, L. Faba, E. Díaz, and S. Ordóñez, "Effect of pretreatments and catalytic route in the quality and productivity of biodiesel obtained from secondary sludge," *Biomass and Bioenergy*, vol. 152, p. 106 195, 2021, ISSN: 0961-9534.

[149] P. Supaporn and S. H. Yeom, "Optimization of a two-step biodiesel production process comprised of lipid extraction from blended sewage sludge and subsequent lipid transesterification," *Biotechnology and Bioprocess Engineering*, vol. 21, pp. 551–560, 2016, ISSN: 1226-8372.

[150] X. Wu, F. Zhu, J. Qi, L. Zhao, F. Yan, and C. Li, "Challenge of biodiesel production from sewage sludge catalyzed by koh, koh/activated carbon, and koh/cao," *Frontiers of Environmental Science Engineering*, vol. 11, pp. 1–11, 2017, ISSN: 2095-2201.

[151] R. Zhang, F. Zhu, Y. Dong, *et al.*, "Function promotion of so42/al2o3–sno2 catalyst for biodiesel production from sewage sludge," *Renewable energy*, vol. 147, pp. 275–283, 2020, ISSN: 0960-1481.

[152] S. Jung, M. Kim, Y.-H. Kim, *et al.*, "Use of sewage sludge biochar as a catalyst in production of biodiesel through thermally induced transesterification," *Biochar*, vol. 4, no. 1, p. 67, 2022, ISSN: 2524-7972.

[153] K. P. Katuri, M. Ali, and P. E. Saikaly, "The role of microbial electrolysis cell in urban wastewater treatment: Integration options, challenges, and prospects," *Current Opinion in Biotechnology*, vol. 57, pp. 101–110, 2019, ISSN: 0958-1669.

[154] E. S. Heidrich, S. R. Edwards, J. Dolfing, S. E. Cotterill, and T. P. Curtis, "Performance of a pilot scale microbial electrolysis cell fed on domestic wastewater at ambient temperatures for a 12 month period," *Bioresource technology*, vol. 173, pp. 87–95, 2014, ISSN: 0960-8524.

[155] J. A. Baeza, À. Martínez-Miró, J. Guerrero, Y. Ruiz, and A. Guisasola, "Bioelectrochemical hydrogen production from urban wastewater on a pilot scale," *Journal of Power Sources*, vol. 356, pp. 500–509, 2017, ISSN: 0378-7753.

[156] S. Cotterill, J. Dolfing, C. Jones, T. Curtis, and E. Heidrich, "Low temperature domestic wastewater treatment in a microbial electrolysis cell with 1 m2 anodes: Towards system scale-up," *Fuel Cells*, vol. 17, no. 5, pp. 584–592, 2017, ISSN: 1615-6846.

[157] B. S. Zakaria, L. Lin, and B. R. Dhar, "Shift of biofilm and suspended bacterial communities with changes in anode potential in a microbial electrolysis cell treating primary sludge," *Science of the total environment*, vol. 689, pp. 691–699, 2019, ISSN: 0048-9697.

[158] Y. Ahn, S. Im, and J.-W. Chung, "Optimizing the operating temperature for microbial electrolysis cell treating sewage sludge," *International Journal of Hydrogen Energy*, vol. 42, no. 45, pp. 27 784–27 791, 2017, ISSN: 0360-3199.

[159] R. Moreno, M. San-Martín, A. Escapa, and A. Morán, "Domestic wastewater treatment in parallel with methane production in a microbial electrolysis cell," *Renewable Energy*, vol. 93, pp. 442–448, 2016, ISSN: 0960-1481.

[160] Z. Ge and Z. He, "Long-term performance of a 200 liter modularized microbial fuel cell system treating municipal wastewater: Treatment, energy, and cost," *Environmental Science: Water Research Technology*, vol. 2, no. 2, pp. 274–281, 2016.

[161] H. Hiegemann, D. Herzer, E. Nettmann, *et al.*, "An integrated 45 l pilot microbial fuel cell system at a full-scale wastewater treatment plant," *Bioresource technology*, vol. 218, pp. 115–122, 2016, ISSN: 0960-8524.

[162] P. Liang, R. Duan, Y. Jiang, X. Zhang, Y. Qiu, and X. Huang, "One-year operation of 1000-l modularized microbial fuel cell for municipal wastewater treatment," *Water Research*, vol. 141, pp. 1–8, 2018, ISSN: 0043-1354.

[163] R. Rossi, D. Jones, J. Myung, *et al.*, "Evaluating a multi-panel air cathode through electrochemical and biotic tests," *Water research*, vol. 148, pp. 51–59, 2019, ISSN: 0043-1354.

[164] W. He, X. Zhang, J. Liu, X. Zhu, Y. Feng, and B. E. Logan, "Microbial fuel cells with an integrated spacer and separate anode and cathode modules," *Environmental Science: Water Research Technology*, vol. 2, no. 1, pp. 186–195, 2016.

[165] Y. Park, S. Park, J. Yu, C. I. Torres, B. E. Rittmann, and T. Lee, "Complete nitrogen removal by simultaneous nitrification and denitrification in flat-panel air-cathode microbial fuel cells treating domestic wastewater," *Chemical Engineering Journal*, vol. 316, pp. 673–679, 2017, ISSN: 1385-8947.

[166] M. Blatter, L. Delabays, C. Furrer, G. Huguenin, C. P. Cachelin, and F. Fischer, "Stretched 1000-l microbial fuel cell," *Journal of Power Sources*, vol. 483, p. 229 130, 2021, ISSN: 0378-7753.

[167] J. M. Sonawane, E. Marsili, and P. C. Ghosh, "Treatment of domestic and distillery wastewater in high surface microbial fuel cells," *International journal of hydrogen energy*, vol. 39, no. 36, pp. 21 819–21 827, 2014, ISSN: 0360-3199.

[168] A. E.-H. Ali, O. M. Gomaa, R. Fathey, H. Abd El Kareem, and M. Abou Zaid, "Optimization of double chamber microbial fuel cell for domestic wastewater treatment and electricity production," *Journal of fuel chemistry and technology*, vol. 43, no. 9, pp. 1092–1099, 2015, ISSN: 1872-5813.

[169] W. He, Y. Dong, C. Li, *et al.*, "Field tests of cubic-meter scale microbial electrochemical system in a municipal wastewater treatment plant," *Water research*, vol. 155, pp. 372–380, 2019, ISSN: 0043-1354.

[170] A. I. Abbas, M. D. Qandil, M. R. Al-Haddad, M. S. Saravani, and R. S. Amano, "Utilization of hydroturbines in wastewater treatment plants," *Journal of Energy Resources Technology*, vol. 141, no. 6, 2019, ISSN: 0195-0738.

[171] R. M. Llácer-Iglesias, P. A. López-Jiménez, and M. Pérez-Sánchez, "Hydropower technology for sustainable energy generation in wastewater systems: Learning from the experience," *Water*, vol. 13, no. 22, p. 3259, 2021, ISSN: 2073-4441.

[172] C. Bousquet, I. Samora, P. Manso, L. Rossi, P. Heller, and A. J. Schleiss, "Assessment of hydropower potential in wastewater systems and application to switzerland," *Renewable energy*, vol. 113, pp. 64–73, 2017, ISSN: 0960-1481.

[173] I. Loots, M. Van Dijk, B. Barta, S. Van Vuuren, and J. Bhagwan, "A review of low head hydropower technologies and applications in a south african context," *Renewable and Sustainable Energy Reviews*, vol. 50, pp. 1254–1268, 2015, ISSN: 1364-0321.

[174] K. Kusakana, "Hydropower energy recovery from wastewater treatment plant: Case of zeekoegat plant," in *2019 IEEE PES Asia-Pacific Power and Energy Engineering Conference (APPEEC)*, IEEE, pp. 1–5, ISBN: 1728108136.

[175] C. Power, A. McNabola, and P. Coughlan, "Development of an evaluation method for hydropower energy recovery in wastewater treatment plants: Case studies in ireland and the uk," *Sustainable Energy Technologies and Assessments*, vol. 7, pp. 166–177, 2014, ISSN: 2213-1388.

[176] P. Tomczyk, K. Mastalerek, M. Wiatkowski, A. Kuriqi, and J. Jurasz, "Assessment of a francis micro hydro turbine performance installed in a wastewater treatment plant," *Energies*, vol. 16, no. 20, p. 7214, 2023, ISSN: 1996-1073.

[177] C. Power, P. Coughlan, and A. McNabola, "Microhydropower energy recovery at wastewater-treatment plants: Turbine selection and optimization," *Journal of Energy Engineering*, vol. 143, no. 1, p. 04 016 036, 2017, ISSN: 0733-9402.

[178] K.-J. Chae, I.-S. Kim, X. Ren, and K.-H. Cheon, "Reliable energy recovery in an existing municipal wastewater treatment plant with a flow-variable micro-hydropower system," *Energy Conversion and Management*, vol. 101, pp. 681–688, 2015, ISSN: 0196-8904.

[179] A. M. Durrani, O. Mujahid, and M. Uzair, "Micro hydro power plant using sewage water of hayatabad peshawar," in *2019 15th International Conference on Emerging Technologies (ICET)*, IEEE, pp. 1–5, ISBN: 1728154030.

[180] A. Hasan, A. R. Salem, A. A. Hadi, M. Qandil, R. S. Amano, and A. Alkhalidi, "The power reclamation of utilizing micro-hydro turbines in the aeration basins of wastewater treatment plants," *Journal of Energy Resources Technology*, vol. 143, no. 8, 2021, ISSN: 0195-0738.

[181] M. Ak, E. Kentel, and S. Kucukali, "A fuzzy logic tool to evaluate low-head hydropower technologies at the outlet of wastewater treatment plants," *Renewable and Sustainable Energy Reviews*, vol. 68, pp. 727–737, 2017, ISSN: 1364-0321.

[182] V. Petran, W. Fernandes, H. Topiwala, *et al.*, "The power of wastewater-micro hydro turbine at the clarkson wastewater treatment plant," *Proceedings of the Water Environment Federation*, vol. 2015, no. 13, pp. 4271–4285, 2015, ISSN: 1938-6478.

[183] S. G. Simoes, J. Catarino, A. Picado, *et al.*, "Water availability and water usage solutions for electrolysis in hydrogen production," *Journal of Cleaner Production*, vol. 315, p. 128 124, 2021, ISSN: 0959-6526.

[184] P. Zawadzki, B. Kończak, and A. Smoliński, "Municipal wastewater reclamation: Reclaimed water for hydrogen production by electrolysis–a case study," *Measurement*, vol. 216, p. 112 928, 2023, ISSN: 0263-2241.

[185] O. Gretzschel, M. Schäfer, H. Steinmetz, E. Pick, K. Kanitz, and S. Krieger, "Advanced wastewater treatment to eliminate organic micropollutants in wastewater treatment plants in combination with energy-efficient electrolysis at wwtp mainz," *Energies*, vol. 13, no. 14, p. 3599, 2020, ISSN: 1996-1073.

[186] D. Chauhan and Y.-H. Ahn, "Alkaline electrolysis of wastewater and low-quality water," *Journal of Cleaner Production*, vol. 397, p. 136 613, 2023, ISSN: 0959-6526.

[187] Z. Guo, Y. Sun, S.-Y. Pan, and P.-C. Chiang, "Integration of green energy and advanced energy-efficient technologies for municipal wastewater treatment plants," *International journal of environmental research and public health*, vol. 16, no. 7, p. 1282, 2019.

[188] I. Ali, L. Abdelkader, B. El Houssayne, K. Mohamed, and L. El Khadir, "Solar convective drying in thin layers and modeling of municipal waste at three temperatures," *Applied Thermal Engineering*, vol. 108, pp. 41–47, 2016, ISSN: 1359-4311.

[189] A. Khanlari, A. D. Tuncer, A. Sözen, C. Şirin, and A. Gungor, "Energetic, environmental and economic analysis of drying municipal sewage sludge with a modified sustainable solar drying system," *Solar Energy*, vol. 208, pp. 787–799, 2020, ISSN: 0038-092X.

[190] P. Wang, D. Mohammed, P. Zhou, Z. Lou, P. Qian, and Q. Zhou, "Roof solar drying processes for sewage sludge within sandwich-like chamber bed," *Renewable Energy*, vol. 136, pp. 1071–1081, 2019, ISSN: 0960-1481.

[191] Y. Huang, M. Chen, and L. Jia, "Assessment on thermal behavior of municipal sewage sludge thin-layer during hot air forced convective drying," *Applied Thermal Engineering*, vol. 96, pp. 209–216, 2016, ISSN: 1359-4311.

[192] A. Khanlari, A. Sözen, F. Afshari, C. Şirin, A. D. Tuncer, and A. Gungor, "Drying municipal sewage sludge with v-groove triple-pass and quadruple-pass solar air heaters along with testing of a solar absorber drying chamber," *Science of The Total Environment*, vol. 709, p. 136 198, 2020, ISSN: 0048-9697.

[193] P. Hochloff and M. Braun, "Optimizing biogas plants with excess power unit and storage capacity in electricity and control reserve markets," *Biomass and bioenergy*, vol. 65, pp. 125–135, 2014, ISSN: 0961-9534.

[194] V. Piergrossi, M. De Sanctis, S. Chimienti, and C. Di Iaconi, "Energy recovery capacity evaluation within innovative biological wastewater treatment process," *Energy Conversion and Management*, vol. 172, pp. 529–539, 2018, ISSN: 0196-8904.

[195] D. F. Quintero Pulido, C. M. Barreto, M. V. Ten Kortenaar, R. R. Balda, J. L. Hurink, and G. J. Smit, "Simulation of sizing of energy storage for off-grid decentralized wastewater treatment units: A case study in the netherlands," *Water Practice Technology*, vol. 13, no. 4, pp. 771–779, 2018, ISSN: 1751-231X.

[196] A. H. A. Mbarga, K. Rainwater, L. Song, T. Cleveland, and W. R. Williams, "Economic analyses of the seadrift wind-aided wastewater treatment plant operations," *Texas Water Journal*, vol. 12, no. 1, pp. 42–57, 2021, ISSN: 2160-5319.

[197] P. T. Duarte, E. A. Duarte, and J. Murta-Pina, "Increasing self-sufficiency of a wastewater treatment plant with integrated implementation of anaerobic co-digestion and photovoltaics," in *2018 International Young Engineers Forum (YEF-ECE)*, IEEE, pp. 103–108, ISBN: 1538615045.

[198] A. del Moral and F. Petrakopoulou, "Evaluation of the coupling of a hybrid power plant with a water generation system," *Applied Sciences*, vol. 9, no. 23, p. 4989, 2019.

[199] H. Andrei, C. A. Badea, P. Andrei, and F. Spertino, "Energetic-environmental-economic feasibility and impact assessment of grid-connected photovoltaic system in wastewater treatment plant: Case study," *Energies*, vol. 14, no. 1, p. 100, 2020, ISSN: 1996-1073.

[200] R. Jacob, M. Short, M. Belusko, and F. Bruno, "Maximising renewable gas export opportunities at wastewater treatment plants through the integration of alternate energy generation and storage options," *Science of The Total Environment*, vol. 742, p. 140 580, 2020, ISSN: 0048-9697.

[201] A. K. Islam, "Hydropower coupled with hydrogen production from wastewater: Integration of micro-hydropower plant (mhp) and microbial electrolysis cell (mec)," *International Journal of Hydrogen Energy*, vol. 49, pp. 1–14, 2024, ISSN: 0360-3199.

[202] A. Mehr, M. Gandiglio, M. MosayebNezhad, *et al.*, "Solar-assisted integrated biogas solid oxide fuel cell (sofc) installation in wastewater treatment plant: Energy and economic analysis," *Applied energy*, vol. 191, pp. 620–638, 2017, ISSN: 0306-2619.

[203] M. Gandiglio, A. S. Mehr, M. MosayebNezhad, A. Lanzini, and M. Santarelli, "Solutions for improving the energy efficiency in wastewater treatment plants based on solid oxide fuel cell technology," *Journal of Cleaner Production*, vol. 247, p. 119 080, 2020, ISSN: 0959-6526.

[204] Web Page, 2011. [Online]. Available: `https://travel.sygic.com/en/poi/acua-wastewater-treatment-facility-poi:12844`.

[205] Web Page, 2015. [Online]. Available: `https://www.tpomag.com/editorial/2015/02/wind_turbines_from_goldwind_usa_help_the_fields_point_treatment_plant_save`.

[206] Web Page, 2011. [Online]. Available: `https://www.environmental-expert.com/news/city-of-pueblo-colo-recognized-for-using-solar-power-at-wastewater-treatment-facility-258583`.

[207] Web Page, 2017. [Online]. Available: `https://www.bv.com/perspectives/water-facilities-generate-their-own-power`.

[208] Web Page. [Online]. Available: `https://www.emwd.org/post/energy-efficiency-programs`.

[209] Web Page, 2011. [Online]. Available: `https://www.biocycle.net/directed-biogas-to-power-fuel-cells/`.

[210] Web Page, 2016. [Online]. Available: `https://www.globenewswire.com/news-release/2016/03/15/1695810/0/en/Sustainable-sewage-sludge-incineration-for-Z%C3%BCrich-canton.html`.

[211] Web Page, 2012. [Online]. Available: https://www.metso.com/corporate/media/news/2012/11/outotec-to-build-the-largest-and-most-advanced-sewage-sludge-thermal-treatment-plant-in-switzerland/.

[212] D. o. E. Resources, "Renewable energy case study: Deer island wastewater treatment plant, mass. water resources authority," Massachusetts Department of Energy Resources, Report, 2017. [Online]. Available: https://www.mass.gov/doc/renewable-energy-installations-at-deer-island/download.

[213] Web Page, 2019. [Online]. Available: https://www.mwra.com/03sewer/html/renewableenergydi.htm#:~:text=MWRA%20%2D%20Renewable%20Energy%20at%20Deer%20Island&text=The%20MWRA's%20Deer%20Island%20Wastewater,electricity%20users%20in%20the%20Northeast..

[214] Web Page. [Online]. Available: https://www.hunterwater.com.au/community/major-projects-in-your-area/renewables.

[215] M. Water, "Melbourne water annual report 2020/21," Report, 2021. [Online]. Available: https://www.melbournewater.com.au/about/strategies-and-reports/annual-report.

[216] Web Page. [Online]. Available: https://www.iconwater.com.au/water-education/sustainability-and-environment/sustainability-and-environment-programs/carbon-and-energy.

[217] Web Page. [Online]. Available: https://www.iconwater.com.au/Water-education/Our-projects/Mt-Stromlo-Mini-Hydro.

[218] Web Page, 2020. [Online]. Available: https://arena.gov.au/blog/sewage-treatment-plants-turn-sludge-into-liquid-fuel/.

[219] Web Page, 2018. [Online]. Available: https://arena.gov.au/blog/sewage-sludge-to-jet-fuel/.

[220] Web Page, 2019. [Online]. Available: https://arena.gov.au/blog/logan-gasification-sewage-treatment-plant/.

[221] Web Page. [Online]. Available: https://www.sawater.com.au/water-and-the-environment/recycling-and-the-environment/energy-management-and-climate.

[222] Web Page. [Online]. Available: https://www.sydneywater.com.au/water-the-environment/what-we-are-doing/energy-management-climate-change.html.

[223] W. Corporation, "Annual report 2021," Water Corporation, Report, 2021. [Online]. Available: https://pw-cdn.watercorporation.com.au/-/media/WaterCorp/Documents/About-us/Our-performance/Annual-Reports/2021-Annual-Report/Water_Corporation_Annual_Report_2021.pdf?rev=06dffd8387764bf6ad20708d7abab6ed&hash=319404485B22EBA7C62A3E80ABDBE5F1.

[224] Web Page, 2022. [Online]. Available: https://www.watercorporation.com.au/About-us/Media-releases/2020/February-2020/Water-Corporation-commits-30-million-to-solar-energy.

[225] I. Abdin and E. Zio, "Optimal planning of electric power systems," in *Optimization in large scale problems*. Springer, 2019, pp. 53–65.

[226] P. Kehrein, M. Van Loosdrecht, P. Osseweijer, M. Garfí, J. Dewulf, and J. Posada, "A critical review of resource recovery from municipal wastewater treatment plants–market

supply potentials, technologies and bottlenecks," *Environmental Science: Water Research Technology*, vol. 6, no. 4, pp. 877–910, 2020.

[227] E. Ranieri, S. Giuliano, and A. C. Ranieri, "Energy consumption in anaerobic and aerobic based wastewater treatment plants in italy," *Water Practice Technology*, vol. 16, no. 3, pp. 851–863, 2021, ISSN: 1751-231X.

[228] D. Lima, L. Li, and J. Zhang, "Minimizing electricity costs using biogas generated from food waste," in *2021 31st Australasian Universities Power Engineering Conference (AUPEC)*, IEEE, pp. 1–6, ISBN: 1665434511.

[229] L. Deng, Y. Liu, and W. Wang, *Biogas technology*. Springer, 2020, ISBN: 9811549397.

[230] R. Chowdhury and D. Fulford, "Batch and semi-continuous anaerobic digestion systems," *Renewable energy*, vol. 2, no. 4-5, pp. 391–400, 1992.

[231] N. Balagurusamy and A. K. Chandel, *Biogas production*. Springer, 2020, ISBN: 3030588270.

[232] F. R. Spellman, *Handbook of water and wastewater treatment plant operations*. CRC press, 2008, ISBN: 0429141653.

[233] H. Akbaş, B. Bilgen, and A. M. Turhan, "An integrated prediction and optimization model of biogas production system at a wastewater treatment facility," *Bioresource technology*, vol. 196, pp. 566–576, 2015, ISSN: 0960-8524.

[234] A. M. Enitan, J. Adeyemo, F. M. Swalaha, S. Kumari, and F. Bux, "Optimization of biogas generation using anaerobic digestion models and computational intelligence approaches," *Reviews in Chemical Engineering*, vol. 33, no. 3, pp. 309–335, 2017, ISSN: 2191-0235.

[235] K. R. Manchala, Y. Sun, D. Zhang, and Z.-W. Wang, "Anaerobic digestion modelling," in *Advances in bioenergy*. Elsevier, 2017, vol. 2, pp. 69–141, ISBN: 2468-0125.

[236] EPA, "Anaerobic digester/biogas system operator guidebook," United States Environmental Protection Agency (EPA), Report, Nov. 2020. [Online]. Available: `https://www.epa.gov/sites/default/files/2020-11/documents/agstar-operator-guidebook.pdf`.

[237] S. Emebu, J. Pecha, and D. Janáčová, "Review on anaerobic digestion models: Model classification elaboration of process phenomena," *Renewable and Sustainable Energy Reviews*, vol. 160, p. 112 288, 2022, ISSN: 1364-0321.

[238] M. M. Otuzalti and N. A. Perendeci, "Modeling of real scale waste activated sludge anaerobic digestion process by anaerobic digestion model 1 (adm1)," *International Journal of Green Energy*, vol. 15, no. 7, pp. 454–464, 2018, ISSN: 1543-5075.

[239] A. Rosa, L. Lobato, and C. Chernicharo, "Mathematical model to predict the energy potential of uasb-based sewage treatment plants," *Brazilian Journal of Chemical Engineering*, vol. 37, pp. 73–87, 2020, ISSN: 0104-6632.

[240] X. Wei and A. Kusiak, "Optimization of biogas production process in a wastewater treatment plant," in *IIE Annual Conference. Proceedings*, Citeseer, p. 1.

[241] S. Sotemann, N. Ristow, M. Wentzel, and G. Ekama, "A steady state model for anaerobic digestion of sewage sludges," *Water SA*, vol. 31, no. 4, pp. 511–528, 2005, ISSN: 0378-4738.

[242] C. A. de Lemos Chernicharo, *Anaerobic reactors*. IWA publishing, 2007, ISBN: 1843391643.

[243] H. Siegrist, D. Renggli, and W. Gujer, "Mathematical modelling of anaerobic mesophilic sewage sludge treatment," *Water Science and Technology*, vol. 27, no. 2, pp. 25–36, 1993, ISSN: 0273-1223.

[244] L. Lobato, C. Chernicharo, and C. Souza, "Estimates of methane loss and energy recovery potential in anaerobic reactors treating domestic wastewater," *Water Science and Technology*, vol. 66, no. 12, pp. 2745–2753, 2012, ISSN: 0273-1223.

[245] J. M. Zepter, J. Engelhardt, T. Gabderakhmanova, and M. Marinelli, "Empirical validation of a biogas plant simulation model and analysis of biogas upgrading potentials," *Energies*, vol. 14, no. 9, p. 2424, 2021, ISSN: 1996-1073.

[246] D. J. Batstone, J. Keller, I. Angelidaki, *et al.*, "The iwa anaerobic digestion model no 1 (adm1)," *Water Science and technology*, vol. 45, no. 10, pp. 65–73, 2002.

[247] H. Ozgun, "Anaerobic digestion model no. 1 (adm1) for mathematical modeling of full-scale sludge digester performance in a municipal wastewater treatment plant," *Biodegradation*, vol. 30, no. 1, pp. 27–36, 2019, ISSN: 0923-9820.

[248] A. C. Sembiring, J. Tampubolon, D. Sitanggang, and M. Turnip, "Improvement of inventory system using first in first out (fifo) method," in *Journal of Physics: Conference Series*, vol. 1361, IOP Publishing, p. 012 070, ISBN: 1742-6596.

[249] E. Castillo, J. M. Menendez, M. Nogal, P. Jimenez, and S. Sanchez-Cambronero, "A fifo rule consistent model for the continuous dynamic network loading problem," *IEEE Transactions on Intelligent Transportation Systems*, vol. 13, no. 1, pp. 264–283, 2011, ISSN: 1524-9050.

[250] M. C. Wentzel, G. Ekama, and S. Sotemann, "Mass balance-based plant-wide wastewater treatment plant models-part 1: Biodegradability of wastewater organics under anaerobic conditions," *Water Sa*, vol. 32, no. 3, pp. 269–275, 2006, ISSN: 0378-4738.

[251] S. Ramdasi and D. K. Shinde, "Effect of fifo strategy implementation on warehouse inventory management in the furniture manufacturing industry,"

[252] L. A. Kerr and D. R. Goethel, "Simulation modeling as a tool for synthesis of stock identification information," in *Stock identification methods*. Elsevier, 2014, pp. 501–533.

[253] F. Pianosi, K. Beven, J. Freer, *et al.*, "Sensitivity analysis of environmental models: A systematic review with practical workflow," *Environmental Modelling Software*, vol. 79, pp. 214–232, 2016, ISSN: 1364-8152.

[254] H. Thakur, A. Dhar, and S. Powar, "Biogas production from anaerobic co-digestion of sewage sludge and food waste in continuously stirred tank reactor," *Results in Engineering*, vol. 16, p. 100 617, 2022, ISSN: 2590-1230.

[255] K. Koch, M. Plabst, A. Schmidt, B. Helmreich, and J. E. Drewes, "Co-digestion of food waste in a municipal wastewater treatment plant: Comparison of batch tests and full-scale experiences," *Waste Management*, vol. 47, pp. 28–33, 2016, ISSN: 0956-053X.

[256] Y. Yuan, L. Zhang, Y. Zhang, and Y. Liu, "The impact of semi-continuous and alternating microbial feeding patterns on methane yield from uasb reactors," *Chemical Engineering Journal*, vol. 472, p. 144 747, 2023.

[257] H. Zhou and Z. Wen, "Solid-state anaerobic digestion for waste management and biogas production," *solid state fermentation: research and industrial applications*, pp. 147–168, 2019.

[258] R. Wang, Y. Zhang, S. Jia, *et al.*, "Comparison of batch and fed-batch solid-state anaerobic digestion of on-farm organic residues: Reactor performance and economic evaluation," *Environmental Technology & Innovation*, vol. 24, p. 101 977, 2021.

[259] Y. Yuan, L. Zhang, Y. Zhang, and Y. Liu, "The impact of semi-continuous and alternating microbial feeding patterns on methane yield from uasb reactors," *Chemical Engineering Journal*, vol. 472, p. 144 747, 2023.

[260] T. Amani, M. Nosrati, and T. Sreekrishnan, "Anaerobic digestion from the viewpoint of microbiological, chemical, and operational aspects—a review," *Environmental Reviews*, vol. 18, no. NA, pp. 255–278, 2010.

[261] I. Rocamora, S. T. Wagland, M. R. Casado, *et al.*, "Managing full-scale dry anaerobic digestion: Semi-continuous and batch operation," *Journal of Environmental Chemical Engineering*, vol. 10, no. 4, p. 108 154, 2022.

[262] Y. Qi, N. Beecher, and M. Finn, "Biogas production and use at water resource recovery facilities in the united states," *Water Environment Federation, Alexandria, VA, National Biosolids Partnership*, 2013.

[263] D. Dominguez and W. Gujer, "Evolution of a wastewater treatment plant challenges traditional design concepts," *Water Research*, vol. 40, no. 7, pp. 1389–1396, 2006.

[264] NRC-CNRC, "Wastewater treatment plant optimization," Federation of Canadian Municipalities and National Research Council, Report, Nov. 2003.

[265] D. Lima, L. Li, and G. Appleby, "Biogas production modelling based on a semi-continuous feeding operation in a municipal wastewater treatment plant," *Energies*, vol. 18, no. 5, p. 1065, 2025.

[266] G. D. Gebreeyessus and P. Jenicek, "Thermophilic versus mesophilic anaerobic digestion of sewage sludge: A comparative review," *Bioengineering*, vol. 3, no. 2, p. 15, 2016.

[267] M. Kim, Y.-H. Ahn, and R. Speece, "Comparative process stability and efficiency of anaerobic digestion; mesophilic vs. thermophilic," *Water research*, vol. 36, no. 17, pp. 4369–4385, 2002.

[268] K. Gao, T. Wang, C. Han, J. Xie, Y. Ma, and R. Peng, "A review of optimization of microgrid operation," *Energies*, vol. 14, no. 10, p. 2842, 2021.

[269] P. Ray and M. Biswal, *Microgrid: operation, control, monitoring and protection*. Springer, 2020.

[270] G. Gust, T. Brandt, S. Mashayekh, *et al.*, "Strategies for microgrid operation under real-world conditions," *European Journal of Operational Research*, vol. 292, no. 1, pp. 339–352, 2021.

[271] S. Di Fraia, N. Massarotti, L. Vanoli, and M. Costa, "Thermo-economic analysis of a novel cogeneration system for sewage sludge treatment," *Energy*, vol. 115, pp. 1560–1571, 2016, ISSN: 0360-5442.

[272] AEMO. "Gas supply hub – data dashboard." Accessed: 02/05/2025. (2025), [Online]. Available: `https://www.aemo.com.au/energy-systems/gas/gas-supply-hub-gsh/data-gsh/data-dashboard`.

[273] D. Kirchem, M. Á. Lynch, V. Bertsch, and E. Casey, "Modelling demand response with process models and energy systems models: Potential applications for wastewater treatment within the energy-water nexus," *Applied Energy*, vol. 260, p. 114 321, 2020.

[274] I. Shizas and D. M. Bagley, "Experimental determination of energy content of unknown organics in municipal wastewater streams," *Journal of energy engineering*, vol. 130, no. 2, pp. 45–53, 2004, ISSN: 0733-9402.

[275] A. G. Capodaglio and G. Olsson, "Energy issues in sustainable urban wastewater management: Use, demand reduction and recovery in the urban water cycle," *Sustainability*, vol. 12, no. 1, p. 266, 2019, ISSN: 2071-1050.

[276] A. Khodaei, S. Bahramirad, and M. Shahidehpour, "Microgrid planning under uncertainty," *IEEE Transactions on Power Systems*, vol. 30, no. 5, pp. 2417–2425, 2014, ISSN: 0885-8950.

[277] R. Hemmati, R.-A. Hooshmand, and A. Khodabakhshian, "Comprehensive review of generation and transmission expansion planning," *IET Generation, Transmission Distribution*, vol. 7, no. 9, pp. 955–964, 2013, ISSN: 1751-8687.

[278] L. Water, "Delivering the design for australia's first biosolids gasification facility," Logan Water, Report, 2022. [Online]. Available: `https://arena.gov.au/assets/2022/06/delivering-the-design-for-australias-first-biosolids-gasification-facility.pdf`.

[279] A. Chebabhi, I. Tegani, A. D. Benhamadouche, and O. Kraa, "Optimal design and sizing of renewable energies in microgrids based on financial considerations a case study of biskra, algeria," *Energy Conversion and Management*, vol. 291, p. 117 270, 2023.

[280] D. Fioriti, S. Pintus, G. Lutzemberger, and D. Poli, "Economic multi-objective approach to design off-grid microgrids: A support for business decision making," *Renewable Energy*, vol. 159, pp. 693–704, 2020.

[281] P. Ziółkowski, J. Badur, H. Pawlak-Kruczek, *et al.*, "Mathematical modelling of gasification process of sewage sludge in reactor of negative co2 emission power plant," *Energy*, vol. 244, p. 122 601, 2022.

[282] F. Kokalj, B. Arbiter, and N. Samec, "Sewage sludge gasification as an alternative energy storage model," *Energy Conversion and Management*, vol. 149, pp. 738–747, 2017, ISSN: 0196-8904.

[283] S. Werle and S. Sobek, "Gasification of sewage sludge within a circular economy perspective: A polish case study," *Environmental Science and Pollution Research*, vol. 26, pp. 35 422–35 432, 2019, ISSN: 0944-1344.

[284] I. B. Matveev, S. I. Serbin, and N. V. Washchilenko, "Sewage sludge-to-power," *IEEE Transactions on Plasma Science*, vol. 42, no. 12, pp. 3876–3880, 2014, ISSN: 0093-3813.

[285] Y. Zhang, A. Zhou, Z. Li, *et al.*, "Numerical simulation analysis of biomass gasification and rich-h2 production process in a downdraft gasifier," *Journal of the Energy Institute*, vol. 114, p. 101 596, 2024.

[286] L. C. Council, "Technical report loganholme wastewater treatment plant: Biosolids gasification demonstration project (pbe-075)," 2021.

[287] P. Graham, J. Hayward, and J. Foster, *Gencost 2024-25: Final report*, 2025.

[288] P. Kaparaju, E. Conde, L. Nghiem, *et al.*, *Anaerobic digestion for electricity, transport and gas: Final report of opportunity assessment for research theme b5 prepared for race for 2030 crc*, 2023.